2007

Stability And Preservation Properties Of Multisymplectic Integrators

Tomasz Wlodarczyk
University of Central Florida

STABILITY AND PRESERVATION PROPERTIES OF MULTISYMPLECTIC INTEGRATORS

by

TOMASZ H. WLODARCZYK
M.S. Silesian University of Technology, 2002
M.S. University of Central Florida, 2005

A dissertation submitted in partial fulfillment of the requirements
for the degree of Doctor of Philosophy
in the Department of Mathematics
in the College of Sciences
at the University of Central Florida
Orlando, Florida

Summer Term
2007

Major Professor: Constance M. Schober

ABSTRACT

This dissertation presents results of the study on symplectic and multisymplectic numerical methods for solving linear and nonlinear Hamiltonian wave equations. The emphasis is put on the second order space and time discretizations of the linear wave, the Klein–Gordon and the sine–Gordon equations. For those equations we develop two multisymplectic (MS) integrators and compare their performance to other popular symplectic and non-symplectic numerical methods. Tools used in the linear analysis are related to the Fourier transform and consist of the dispersion relationship and the power spectrum of the numerical solution. Nonlinear analysis, in turn, is closely connected to the temporal evolution of the total energy (Hamiltonian) and can be viewed from the topological perspective as preservation of the phase space structures. Using both linear and nonlinear diagnostics we find qualitative differences between MS and non-MS methods. The first difference can be noted in simulations of the linear wave equation solved for broad spectrum Gaussian initial data. Initial wave profiles of this type immediately split into an oscillatory wave-train with the high modes traveling faster (MS schemes), or slower (non-MS methods), than the analytic group velocity. This result is confirmed by an analysis of the dispersion relationship, which also indicates improved qualitative agreement of the dispersive curves for MS methods over non-MS ones. Moreover, observations of the convergence patterns in the wave profile obtained for the sine–Gordon equation for the initial data corresponding to the double-pole soliton and the temporal evolution of the Hamiltonian functional computed for solutions obtained from different discretizations suggest a change of the geometry of the phase space. Finally, we

present some theoretical considerations concerning wave action. Lagrangian formulation of linear partial differential equations (PDEs) with slowly varying solutions is capable of linking the wave action conservation law with the dispersion relationship thus suggesting the possibility to extend this connection to multisymplectic PDEs.

I dedicate this work to Sabina, my beloved wife.

ACKNOWLEDGMENTS

I would like to thank my adviser, Dr. Constance Schober, for help and support in this research. I also thank Dr. Alvaro Islas for his help with implementations of numerical schemes. This work was partially supported by National Science Foundation grants number DMS 0438154 and DMS 0608693.

TABLE OF CONTENTS

LIST OF FIGURES

LIST OF TABLES

CHAPTER ONE: INTRODUCTION

In the past years certain level of sophistication has been achieved in numerical integration of ordinary differential equations (ODEs). In the process of development of various numerical methods researchers realized that it is not practical to forever increase the order of numerical schemes and that in many cases there is not enough computational resources available to decrease time step in simulations. It turned out that there is another possibility for improving quality of numerical solutions, namely use of so called geometric, or structure preserving, integrators. The motivation for developing such algorithms for special classes of problems came from different research areas like astronomy, molecular dynamics, mechanics, theoretical physics, numerical analysis and other areas of pure and applied mathematics. Preservation of geometric properties of problems arising in these areas not only produced an improved qualitative behavior of the solution, but also permitted accurate long-time integration without using impractically small time step. An extensive presentation of various geometric integrators can be found in [15, 16, 17, 32].

The natural extension of ideas related to geometric integration of ODEs is the notion of structure preserving algorithms for partial differential equations (PDEs). It is a developing branch of numerical analysis and there still exist many open problems. Numerical methods for some special classes of PDEs are a good starting point for such a research. In the last couple of years numerical analysts became interested in the, so called, multisymplectic integrators. Multisymplectic integrators are numerical schemes which exactly preserve a discrete space-time symplectic structure of Hamiltonian PDEs. To date much of the liter-

ature has been devoted to establishing that various discretization methods have subclasses which are multisymplectic. However, a thorough analysis of the local and global properties of multisymplectic integrators has yet to be carried out. Preservation of the multisymplectic structure by a numerical scheme does not imply preservation of other dynamical invariants of the system such as the local conservation laws or of global invariants which determine the phase space structure.

The focal point of this work is the centered-cell (multisymplectic) box scheme in two forms, called MS–1 and MS–2, obtained from two different multisymplectic formulations of the sine–Gordon equation. Multisymplectic box scheme is a finite difference method having second order accuracy in both space and time. It is therefore most appropriate to compare its performance with other second order (symplectic and non-symplectic), Hamiltonian finite difference approximations of the sine–Gordon equation. These methods include (explicit) Störmer/Verlet scheme (MS–3), implicit midpoint rule (MS–4), and the explicit Runge–Kutta of order two (ERK). We will occasionally refer to the MS–3 scheme as a leap-frog and we typically call MS–3 and MS–4 symplectic schemes although these are in fact multisymplectic discretizations. The reason for that distinction between methods designated MS–1,2 and MS–3,4 is that MS–1,2 methods were derived as discretizations of the PDEs expressed in the multisymplectic form, while integrators designated MS–3,4 are symplectic time discretizations of the second order, centered-cell Hamiltonian spatial semi-discretization of the sine–Gordon equation. The comparison will be conducted by means of conserved quantities – energy and momentum – in their various forms, the dispersion relationship and the error in the wave propagation speed. In the course of this dissertation we will also look at other

discretizations as well as at the box scheme for other than the sine–Gordon equations, like the linear wave equation, the variable coefficient Klein–Gordon equation and the nonlinear Schrödinger equation.

The centered cell box scheme was first developed by Preissmann and Keller for the turbulent boundary layer equations [25, 31]. It is unconditionally stable and of second order accuracy. It is also A–stable (i.e. if the exact solution decays in time so does the numerical one, with the approximately the same rate). As shown in [11], when applied to the multisymplectic system of PDEs, the box scheme preserves a discrete version of a multisymplectic conservation law (multisymplecticness of the scheme). Another interesting feature of this method is presented in [6], namely that the box scheme qualitatively preserves the dispersion relationship of any first order, linear system of PDEs expressed in multisymplectic form.

There are two ways of implementing the box scheme, either by directly simulating the system of first order PDEs or by first eliminating variables introduced to the equation in order to put the equation in a multisymplectic form and than solving the resulting equation. The first approach has a significant drawback. Iterative solver of the system of nonlinear equations is non-convergent for almost all numerical meshes (cf. [39]). The second approach is sometimes called a reduced box scheme, however we will simply refer to it as the reduced box scheme. The functional iteration solver for the modified box scheme does not indicate nonconvergence issue and this is the scheme implemented in the numerical simulations here. Simulations show that, among the two (reduced) multisymplectic box schemes emerging from different multisymplectic forms of the sine–Gordon equation, the MS–2 possesses superior convergence properties.

It is well known that the error in the propagation speed can destroy the numerical solution. For instance, according to [36], while solving a linear, first order wave equation by means of the Crank–Nicolson scheme one notices the unwanted oscillations behind the computed wave after a very short time. Moreover, when carrying the simulation out to longer times, all of the character of the true solution is lost. The errors for the solution are due to both damping and the error in the dispersion relationship. Following [6, 19, 36], we investigate the preservation of the dispersion relationship and the error in the phase velocity (wave propagation speed) as well as its influence on the numerical solutions. The symbol of a numerical scheme in section 5.2.1 allows one to determine the stability of the scheme as well as its dispersive properties. The modulus of a symbol gives the dissipation/growth rate of the scheme thus addressing the stability of the scheme. As expected, all the symplectic and multisymplectic schemes are non-dissipative and stable. The multisymplectic box scheme preserves the numerical dispersion best and the only scheme indicating growth is the non-symplectic explicit RK, having a long–term growth in the Hamiltonian.

Numerical studies on a multisymplectic finite–difference discretization of the nonlinear Schrödinger (NLS) equation demonstrated that the local energy and momentum conservation laws are preserved far better than expected, given the order of the schemes [22]. In addition, several global invariants are preserved within roundoff by multisymplectic integrators. Robustness of the box scheme for the Kortweg–deVries (KdV) equation was examined by McLachlan and Ascher [6]. They also found that the dispersion relation for linear Hamiltonian PDEs is preserved by the multisymplectic box schemes well. We have used the sine–Gordon equation as a benchmark equations for several reasons. The first and foremost

is an attempt to generalize numerical results obtained in [6] and [22] to another equation. The second reason is the importance of the preservation of dispersion relationship by the numerical scheme and questions related, through the symbol of a scheme, to the dispersive and dissipative properties of the discrete linearized sine–Gordon equation. The last reason is that the sine–Gordon equation possess a rich structure of the phase space for periodic boundary conditions on a finite interval, which makes it somewhat a challenging problem to work with. The choice of this equation provides us with the material for further study on the nonlinear stability of symplectic and multisymplectic integrators.

Simulations were performed for initial data close to a homoclinic orbit of the unstable state $\bar{u} \equiv \pi$. An interesting phenomenon is observed here. After relatively short time ($t \approx 30$) the wave profile undertakes a series of jumps which can be interpreted as homoclinic crossings. They are caused by numerical errors and are described in [1]. Analysis of an infinite-line boundary value problem associated with this equation is also presented. This problem possess stable solutions called solitons. Three types of solitons, the breather, the kink–antikink and the double–pole soliton, were examined. The third type is a limiting case between the first two types (cf. [4]) and, as a bifurcation state, presents some difficulties in numerically capturing the wave profile. For the choice of the initial data corresponding to the double–pole soliton one can observe two different types of convergence patterns. Symplectic and non-symplectic (also a pseudo-spectral method as reported in [1]) converges to the correct wave profile from the parameter regime associated with the kink–antikink solution, that is by the decrease in the wave propagation speed as the numerical mesh is refined. On the other hand, the multisymplectic box schemes converge to the analytic solution from the parameter

regime related to the breather soliton. In this case, as the numerical mesh is refined, one notices an increase in the period of the temporal, breather, oscillations. A remark has to be made here. Although the choice of the particular equation is important, one of the goals of this thesis is to examine the consequences of the property of multisymplecticness on the preservation of the energy, momentum and dispersion relation by numerical schemes.

Conservation of wave action under multisymplectic discretization is the most current direction of research in numerical analysis of structure preserving discretizations of PDEs (cf. [13]). We summarize existing results on the wave action in Lagrangian formulation and its relations to adiabatic invariants, i.e. quantities that remain constant to the leading order in the slow-time. Average Lagrangian formulation for slowly varying linear waves gives a common ground for both the dispersion relationship and the wave action conservation law [5, 8, 18, 40]. This interesting property of average Lagrangian for linear wave equations, after proper generalization, might provide a connection between seemingly different areas discussed in this dissertation. In this dissertation we discuss the wave action conservation for the multisymplectic formulation of continuous problems in physical as well as in the Fourier spectral spaces. Understanding of methods used in derivations of continuous wave action provides us with methods of addressing the issue of preservation of the wave action under various discretizations, with special emphasis on multisymplectic ones. We will show analytically and verify numerically that the multisymplectic box scheme exactly preserves a discrete analog of the wave action. We will then attempt to extend results of [13] toward numerical methods based on spectral and pseudo-spectral spatial semi-discretizations.

This paper is organized as follows. Chapter two introduces a concept of a symplectic

discretization of Hamiltonian ODEs and provides illustrations of consequences of preserving the symplectic structure by means of discretizations of two dimensional systems of ODEs. In the third chapter fundamental definitions and theorems concerning Hamiltonian and multisymplectic forms of PDEs are recalled and local conservation laws associated with the multisymplectic formulation are defined. The fourth chapter is devoted to the derivation of numerical schemes as well as the description of some practical aspects of their implementations. In the fifth chapter linearizations of certain equations and associated dispersion relationships are given and an analysis of dispersive properties of numerical schemes derived in chapter four is performed. We study the error in the dispersion introduced by the discretization and use the error in the wave propagation speed and the group velocity dispersion to compare numerical schemes under investigation. In the sixth chapter a presentation and discussion of results of numerical simulations is shown. This chapter is divided into four sections. The first one is an illustrations of dispersive and dissipative properties of discretizations and a confirmation of analytic results of chapter five. Second section of the sixth chapter presents various diagnostics computed for numerical solutions for soliton and space-periodic initial data and illustrates preservation of conserved quantities under multisymplectic discretizations. We also show the change to the geometry of the phase space introduced by the discretization. Last section of this chapter contains series of plots presenting numerical simulations in more details. Final chapter presents the concept of wave action. We review previous results of the wave action conservation law in physical space and extend it to the case of the Fourier spectral space. We also analytically investigate preservation of the discrete analog of wave action under various discretizations and find that the MS box

scheme exactly preserves discrete wave action. Appendices contain additional theoretical information about symplectic integrators of Runge–Kutta type with detailed proof of their symplecticness (Appendix A). We also list some of the classical analytic solutions (solitons) that were used in the assessment of numerical schemes (Appendix B).

CHAPTER TWO: HAMILTONIAN ORDINARY DIFFERENTIAL EQUATIONS

Geometric integration is a branch of numerical analysis aiming at constructing numerical methods capable of reproducing qualitative features of the solution of a differential equation under discretization and a particular emphasis is placed on preserving its geometric properties. In geometric integration these properties are built into the numerical scheme giving the method an improved qualitative behavior and allowing for a significantly more accurate long-time integration than with general-purpose methods. In addition to the construction of new numerical algorithms, an important aspect of geometric integration is the explanation of the relationship between preservation of the geometric properties of a numerical method and the observed error propagation in long-time integration.

In this introductory chapter we would like to present some properties of Hamiltonian ordinary differential equations (ODEs) and their discretizations. The emphasis is placed on the notion of symplecticness of the flow of a Hamiltonian system as its most fundamental feature. We begin with definitions and some simple, one-degree-of-freedom examples and than generalize to higher-dimensional systems by presenting a series of theorems characterizing the flow of every Hamiltonian ODE. Next we illustrate these theorems by comparing two first order discretizations of the pendulum equation and prove, via backward error analysis (BEA), that the integrator with superior behavior generates a (discrete) map that is itself symplectic. As a consequence we observe excellent energy conservation of such a scheme. Finally, in the section closing this chapter, we compare two symplectic, second-order schemes.

We observe that the distortion of the original phase space may lead to qualitative changes in the behavior of the solution depending on the discretization applied. This phenomenon is observed for initial data corresponding to some special (separatrix) solutions of the continuous system. It is very important to be able to identify such cases as they are present in discrete systems obtained for partial differential equations (PDEs) as well.

We would like to remark, that the idea of geometric integration of ODEs has been around for at least 30 years. This chapter is intended to be a brief introduction to the concepts underlying this vast area of research and its presentation very closely follows [5, 15, 16, 17, 27, 32, 34].

2.1 The Idea of a Symplectic Map

Consider a nonempty, open, connected set $\mathcal{U} \subset \mathbb{R}^{2d}$, for some $d \in \mathbb{N}$, and an open interval $I \subset \mathbb{R}$. Let $\mathbf{z}^T = [\mathbf{p}^T, \mathbf{q}^T] = [p_1, \ldots, p_d, q_1, \ldots, q_d] \in D$ and let $H = H(\mathbf{z}, t) = H(\mathbf{p}, \mathbf{q}, t)$ be a sufficiently smooth, real-valued function defined on $\mathcal{U} \times I$. The system of differential equations of the form

$$J_d \frac{\mathrm{d}}{\mathrm{d}t}\mathbf{z} = \nabla_{\mathbf{z}} H \tag{2.1}$$

is called Hamiltonian. The matrix $J_d \in \mathcal{M}_{2d\times 2d}(\mathbb{R})$,

$$J_d = \begin{bmatrix} 0 & I_d \\ -I_d & 0 \end{bmatrix},$$

where $I_d \in \mathcal{M}_{d\times d}(\mathbb{R})$ is the identity matrix, is said to define a symplectic structure on $\mathcal{U}$. It is sometimes convenient to use the fact that the matrix J_d is invertible and express (2.1) as

$$\mathbf{z}_t = J_d^{-1} \nabla_{\mathbf{z}} H \stackrel{\mathrm{df}}{=} \mathbf{g}(\mathbf{z}). \tag{2.2}$$

We understand the operator $\nabla_{\mathbf{z}}$, the gradient, as a symbolic vector

$$\nabla_{\mathbf{z}} = \Big[\frac{\partial}{\partial p_1}, \ldots, \frac{\partial}{\partial p_d}, \frac{\partial}{\partial q_1}, \ldots, \frac{\partial}{\partial q_d}\Big]^T.$$

With this notation, the system (2.2) takes the form

$$\frac{\mathrm{d}}{\mathrm{d}t}p_i = -\frac{\partial H}{\partial q_i}, \qquad \frac{\mathrm{d}}{\mathrm{d}t}q_i = \frac{\partial H}{\partial p_i}, \qquad i \in \{1, \ldots, d\}. \tag{2.3}$$

The integer d is called the number of degrees of freedom and $\mathcal{U}$ is the phase space. The set $\mathcal{U} \times I$ is called the extended phase space.

Associated with (2.3) is the system of variational equations

$$\frac{\mathrm{d}}{\mathrm{d}t}\mathrm{d}p_i = -H_{q_ip_i}\mathrm{d}p_i - H_{q_iq_i}\mathrm{d}q_i, \qquad \frac{\mathrm{d}}{\mathrm{d}t}\mathrm{d}p_i = H_{p_ip_i}\mathrm{d}p_i - H_{p_iq_i}\mathrm{d}q_i, \tag{2.4}$$

or in vector form

$$(\mathrm{d}\mathbf{z})_t = J_d^{-1}H_{\mathbf{zz}}\mathrm{d}\mathbf{z}, \tag{2.5}$$

where the $H_{\mathbf{zz}} = H_{\mathbf{zz}}(\mathbf{z})$, $H_{\mathbf{zz}} \in \mathcal{M}_{2d\times 2d}(\mathbb{R})$ is a symmetric matrix (the Hessian matrix of H)

$$H_{\mathbf{zz}} = \begin{bmatrix} H_{\mathbf{pp}} & H_{\mathbf{pq}} \\ H_{\mathbf{qp}} & H_{\mathbf{qq}} \end{bmatrix}.$$

We will denote a set of twice continuously differentiable functions on $\mathbb{R}$ by $\mathcal{C}^2(\mathbb{R})$ and assume that $H \in \mathcal{C}^2(\mathbb{R})$, so that $H_{\mathbf{pq}} = H_{\mathbf{qp}}^T$. $H_{\mathbf{pq}}$ is understood as

$$H_{\mathbf{pq}} = \left[\frac{\partial^2 H}{\partial p_i \partial q_j}\right]_{i,j\in\{1,\ldots,d\}} \in \mathcal{M}_{d\times d}(\mathbb{R}).$$

Additionally, $H_{\mathbf{pp}} = H_{\mathbf{pp}}^T$ and $H_{\mathbf{qq}} = H_{\mathbf{qq}}^T$, with

$$H_{\mathbf{pp}} = \left[\frac{\partial^2 H}{\partial p_i \partial p_j}\right]_{i,j\in\{1,\ldots,d\}} \in \mathcal{M}_{d\times d}(\mathbb{R})$$

and an analogous definition for $H_{\mathbf{qq}}$. In terms of the Jacobian matrix $\mathrm{d}\mathbf{g} = \mathrm{d}\mathbf{g}(\mathbf{z})$, $\mathrm{d}\mathbf{g} \in \mathcal{M}_{2d\times 2d}(\mathbb{R})$, the variational equation (2.5) is

$$(\mathrm{d}\mathbf{z})_t = \mathrm{d}\mathbf{g}(\mathbf{z})$$

and it is an immediate conclusion of (2.2) and (2.5) that

$$\mathrm{d}\mathbf{g} = J_d^{-1} H_{\mathbf{zz}} = \begin{bmatrix} -H_{\mathbf{pp}} & -H_{\mathbf{pq}} \\ H_{\mathbf{qp}} & H_{\mathbf{qq}} \end{bmatrix}.$$

Using elementary row operations, equation (2.5) can be written as

$$(\mathrm{d}\tilde{\mathbf{z}})_t = (I_d \otimes J^{-1}) H_{\tilde{\mathbf{z}}\tilde{\mathbf{z}}} \mathrm{d}\tilde{\mathbf{z}},$$

where $\tilde{\mathbf{z}}^T = [p_1, q_1, \ldots, p_d, q_d]$ and

$$J \stackrel{\mathrm{df}}{=} J_1 = \begin{bmatrix} 0 & 1 \\ -1 & 0 \end{bmatrix}. \tag{2.6}$$

For brevity of notation we use the Kronecker's product of matrices defined as follows.

Definition 1 *Given two matrices $A \in \mathcal{M}_{m\times n}(\mathbb{R})$ and $B \in \mathcal{M}_{p\times q}(\mathbb{R})$, their direct product $C = A \otimes B$, also called the Kronecker product, is a matrix $C \in \mathcal{M}_{mp\times nq}(\mathbb{R})$ with elements defined by*

$$c_{\alpha\beta} = a_{ij} b_{kl},$$

where $\alpha = p(i-1) + k$ and $\beta = q(j-1) + l$.

For instance, the matrix direct product of the 2×2 identity matrix I_2 and a 3×2 matrix A

is given by the following matrix $C \in \mathcal{M}_{6\times 4}(\mathbb{R})$.

$$C = I_2 \otimes A = \begin{bmatrix} 1\cdot A & 0\cdot A \\ 0\cdot A & 1\cdot A \end{bmatrix} = \left[\begin{array}{cc|cc} 1\cdot a_{11} & 1\cdot a_{12} & 0\cdot a_{11} & 0\cdot a_{12} \\ 1\cdot a_{21} & 1\cdot a_{22} & 0\cdot a_{23} & 0\cdot a_{22} \\ 1\cdot a_{31} & 1\cdot a_{32} & 0\cdot a_{31} & 0\cdot a_{32} \\ \hline 0\cdot a_{11} & 0\cdot a_{12} & 1\cdot a_{11} & 1\cdot a_{12} \\ 0\cdot a_{21} & 0\cdot a_{22} & 1\cdot a_{23} & 1\cdot a_{22} \\ 0\cdot a_{31} & 0\cdot a_{32} & 1\cdot a_{31} & 1\cdot a_{32} \end{array}\right]$$

The Kronecker's product is bilinear and associative and, with respect to transpositions, it satisfies $(A \otimes B)^T = A^T \otimes B^T$. Moreover, if matrices A and B are invertible such is their Kronecker product and $(A \otimes B)^{-1} = A^{-1} \otimes B^{-1}$.

The following property is fundamental for (2.2). For matrix $L = (I_d \otimes J_1^{-1})H_{\tilde{\mathbf{z}}\tilde{\mathbf{z}}}$, treated as a function of t, it can be shown (see [17, 32, 34]) that

$$\frac{\partial}{\partial t}|L| = \frac{\partial}{\partial t}\sum_{i=1}^{d} \det \begin{bmatrix} -H_{p_ip_i} & -H_{p_iq_i} \\ H_{q_ip_i} & H_{q_iq_i} \end{bmatrix} = \frac{\partial}{\partial t}\sum_{i=1}^{d}(H_{p_iq_i}^2 - H_{p_ip_i}H_{q_iq_i}) \equiv 0.$$

This identity means that the sum of oriented areas of projections onto the (p_i, q_i)–coordinate planes is conserved by the flow of the linearized system (2.5) and is referred to as symplecticness of the flow map defined by the variational equations. In the sections that follow we will elaborate on the concept of symplecticness and present its applications to discrete systems arising in the numerical analysis of Hamiltonian ODEs.

Definition 2 *We say that the linear mapping $\mathcal{L} : \mathbb{R}^{2d} \to \mathbb{R}^{2d}$ is symplectic if $\mathcal{L}^T J_d \mathcal{L} = J_d$, i.e. if*

$$\Omega(\mathcal{L}\boldsymbol{\xi}, \mathcal{L}\boldsymbol{\eta}) = \Omega(\boldsymbol{\xi}, \boldsymbol{\eta}), \text{ for all } \boldsymbol{\xi}, \boldsymbol{\eta} \in \mathbb{R}^{2d},$$

where

$$\Omega(\boldsymbol{\xi},\boldsymbol{\eta}) = \sum_{i=1}^{d} \det \begin{bmatrix} \xi_i^p & \eta_i^p \\ \xi_i^q & \eta_i^q \end{bmatrix} = \boldsymbol{\xi}^T J_d \boldsymbol{\eta}.$$

In case of nonlinear, differentiable maps we consider local approximations by a linear mapping according to

Definition 3 *Let $\mathcal{U} \subset \mathbb{R}^{2d}$ be an open set. A differentiable map $\mathbf{g} : \mathcal{U} \to \mathbb{R}^{2d}$ is called symplectic if its Jacobian matrix $\mathcal{L} = \mathrm{d}\mathbf{g}(\mathbf{p},\mathbf{q})$ is symplectic.*

We are now in the position to rephrase the notion of symplecticness in terms of a flow map. Recall that the flow $\varphi_{t\to t^*}\colon \mathcal{U} \to \mathbb{R}^{2d}$ of a Hamiltonian system is the mapping that advances the solution by time t, i.e.

$$\mathbf{z}^* = \varphi_{t\to t^*}(\mathbf{z}),$$

where $\mathbf{z}^*$ is the solution of the system at time t^* corresponding to initial values $\mathbf{z}$, i.e. the solution at some time $t < t^*$.

Theorem 1 (Poincaré, 1899) *Let $H(\mathbf{p},\mathbf{q})$ be twice continuously differentiable function on $\mathcal{U} \subset \mathbb{R}^{2d}$. Then, for each fixed t, the flow $\varphi_{t\to t^*}$ is a symplectic transformation wherever it is defined.*

For two-dimensional systems (i.e. for $d = 1$), Theorem 1 can also be stated (see [32]) in the form of the identity

$$\frac{\partial p^*}{\partial p}\frac{\partial q^*}{\partial q} - \frac{\partial q^*}{\partial p}\frac{\partial p^*}{\partial q} \equiv 1,$$

which is equivalent (see [34]) to the statement, that

$$\det \begin{bmatrix} H_{qp} & H_{qq} \\ -H_{pp} & -H_{pq} \end{bmatrix} = H_{pp}H_{qq} - (H_{pq})^2 \equiv 1. \tag{2.7}$$

We will use equation (2.7) to establish an important property of a class of discretizations of one-degree-of-freedom Hamiltonian ODEs.

2.1.1 Summary of Area-Preservation

The most fundamental (characteristic) property of Hamiltonian systems is that they are area-preserving. That is, a system of ODEs has an area-preserving property if and only if it is Hamiltonian. For simplicity we present the agrumentation for two-dimensional (i.e. for $d = 1$) systems.

From the assumption that $H \in \mathcal{C}^2(\mathbb{R})$ and the equation (2.2)

$$\frac{\partial}{\partial p}\Big(-\frac{\partial H}{\partial q}\Big) + \frac{\partial}{\partial q}\Big(\frac{\partial H}{\partial p}\Big) = 0$$

i.e. the vector field $[-H_q, H_p]^T$ is divergence-free. As a consequence, for each fixed $t, t^* \in I$, the flow $\varphi_{t\to t^*}$ is an area-preserving transformation on $\mathcal{U}$. By the area-preserving we mean that for every bounded set D, $D \subset \mathcal{U}$, the area of D is the same as the area of $\varphi_{t\to t^*}(D)$ and the orientation of D is preserved as well. On the other hand, if $\varphi_{t\to t^*}$ is an area-preserving solution operator for the system

$$\frac{\mathrm{d}}{\mathrm{d}t}p = f(p, q, t), \qquad \frac{\mathrm{d}}{\mathrm{d}t}q = g(p, q, t),$$

then, by Liouvile's theorem (see, for instance, [5]), for each fixed $t, t^* \in I$, the vector field

$[f, g]^T$ is divergence-free, i.e.

$$\frac{\partial f}{\partial p} + \frac{\partial g}{\partial q} = 0,$$

which is a necessary and sufficient condition for the field $[g, -f]^T$ to be the gradient of a scalar function H (assuming that $\mathcal{U}$ is simply connected).

2.2 Symplecticness Formalized

In the presentation of the concept of symplecticness presented in this section we closely follow the treatment of [5] and use the "odd-dimensional" approach to Hamiltonian phase flow. We begin by stating a hydrodynamical lemma in three-dimensional spaces. Let $\mathbf{v}$ be a vector field in three-dimensional oriented euclidean space $\mathbb{R}^3$, and $\mathbf{r} = \text{curl } \mathbf{v}$ its curl. The integral curves of $\mathbf{r}$ are called vortex lines. If γ_1 is any closed curve in $\mathbb{R}^3$, the vortex lines passing through the points of γ_1 form a tube called a vortex tube. Let γ_2 be another curve encircling the same vortex tube, then

Lemma 1 (Stokes) *The field* $\mathbf{v}$ *has equal circulation along the curves* γ_1 *and* γ_2*, i.e.*

$$\oint_{\gamma_1} \mathbf{v}\ \mathrm{d}\mathbf{l} = \oint_{\gamma_2} \mathbf{v}\ \mathrm{d}\mathbf{l}$$

It turns out that Stokes' lemma generalizes to the case of any odd-dimensional manifold M^{2d+1} (in place of $\mathbb{R}^3$). The formulation of such a generalization is usually stated in terms of differential forms, as the circulation of a vector field $\mathbf{v}$ is the integral of the 1-form ω and to the curl of $\mathbf{v}$ there corresponds the 2-form $\Omega = \mathrm{d}\omega$. A detailed treatment can be found in [5].

Theorem 2 (Arnold) *The vortex lines of the form* $\omega = \mathbf{p}\ \mathrm{d}\mathbf{q} - H\ \mathrm{d}t$ *on the* $(2d+1)$*–dimensional extended phase space* $(\mathbf{p},\ \mathbf{q},\ t)$ *have a one-to-one projection onto the* t*-axis, i.e. they are given by functions* $\mathbf{p} = \mathbf{p}(t)$ *and* $\mathbf{q} = \mathbf{q}(t)$*. These functions satisfy the system of canonical differential equations with Hamiltonian function* H

$$\frac{\mathrm{d}\mathbf{p}}{\mathrm{d}t} = -\frac{\partial H}{\partial \mathbf{q}}, \qquad \frac{\mathrm{d}\mathbf{q}}{\mathrm{d}t} = \frac{\partial H}{\partial \mathbf{p}}. \tag{2.8}$$

In other words the vortex lines of the form $\mathbf{p}\ \mathrm{d}\mathbf{q} - H\ \mathrm{d}t$ are the trajectories of the phase flow in the extended phase space, i.e. the integral curves of the canonical equations (2.8). When the Stokes' theorem is applied to the differential form ω one obtains a fundamental

Theorem 3 (Arnold) *Suppose that the two curves* γ_1 *and* γ_2 *encircle the same tube of phase trajectories of (2.8). Then the integrals of the form* $\mathbf{p}\ \mathrm{d}\mathbf{q} - H\ \mathrm{d}t$ *along them are the same, i.e.*

$$\oint_{\gamma_1} \mathbf{p}\ \mathrm{d}\mathbf{q} - H\ \mathrm{d}t = \oint_{\gamma_2} \mathbf{p}\ \mathrm{d}\mathbf{q} - H\ \mathrm{d}t.$$

The form $\mathbf{p}\ \mathrm{d}\mathbf{q} - H\ \mathrm{d}t$ is called the *integral invariant of Poincaré–Cartan*. It is now an immediate corollary, that if the curves γ_i consist of simultaneous states, i.e. every curve γ_i lies on the plane $t = t_i = \text{const}$ then, since $\mathrm{d}t = 0$ one has that

$$\oint_{\gamma_1} \mathbf{p}\ \mathrm{d}\mathbf{q} = \oint_{\gamma_2} \mathbf{p}\ \mathrm{d}\mathbf{q}.$$

This means that the phase flow preserves the integral of $\mathbf{p}\ \mathrm{d}\mathbf{q}$, since we can always choose $\gamma_2 = \varphi_{t_1 \to t_2}(\gamma_1)$. The form $\mathbf{p}\ \mathrm{d}\mathbf{q}$ is called *Poincaré's relative integral invariant* and has a simple geometric interpretation. Let D be a subset of the extended phase space such that

$\gamma = \partial D$, then, by Stoke's formula, we find that

$$\oint_{\gamma} \mathbf{p}\ \mathrm{d}\mathbf{q} = \iint_{D} \mathrm{d}\mathbf{p} \wedge \mathrm{d}\mathbf{q}.$$

Thus we have proved the important

Theorem 4 (Arnold) *The phase flow preserves the sum of oriented areas of the projections of a surface onto the d coordinate planes (p_i, q_i), i.e. that*

$$\iint_{D} \mathrm{d}\mathbf{p} \wedge \mathrm{d}\mathbf{q} = \iint_{\varphi_{t\to t^*}(D)} \mathrm{d}\mathbf{p} \wedge \mathrm{d}\mathbf{q}. \tag{2.9}$$

In other words, Theorem 4 states, that the 2-form $\Omega = \mathrm{d}\mathbf{p} \wedge \mathrm{d}\mathbf{q}$ is an absolute integral invariant of the phase flow. This property of the phase flow is very often called symplecticness of the Hamiltonian phase flow. An alternative, direct proof of symplecticness of the flow of Hamiltonian system can be found in [15].

Conservation of symplecticness is sometimes stated in the context of preservation of the oriented area of infinitesimally small parallelograms. In such a case, Theorem 4 is equivalent to the statement that

$$\frac{\partial}{\partial t}\Omega = \frac{\partial}{\partial t}(\mathrm{d}\mathbf{z} \wedge J_d\, \mathrm{d}\mathbf{z}) = \frac{\partial}{\partial t}(\mathrm{d}\mathbf{p} \wedge \mathrm{d}\mathbf{q}) = 0. \tag{2.10}$$

For $d = 1$, the 2-form $\Omega = \mathrm{d}p \wedge \mathrm{d}q$, an exterior product of a pair of 1-forms $\mathrm{d}p$ and $\mathrm{d}q$, is a bilinear, skew-symmetric map acting on two vectors

$$\Omega(\xi_1, \xi_2) = (\mathrm{d}p \wedge \mathrm{d}q)(\xi_1, \xi_2) = \det \begin{bmatrix} \mathrm{d}p(\xi_1) & \mathrm{d}p(\xi_2) \\ \mathrm{d}q(\xi_1) & \mathrm{d}q(\xi_2) \end{bmatrix} = \mathrm{d}p(\xi_1)\mathrm{d}q(\xi_2) - \mathrm{d}p(\xi_2)\mathrm{d}q(\xi_1).$$

The vector wedge product $\mathrm{d}\mathbf{p} \wedge \mathrm{d}\mathbf{q}$ is understood as

$$\mathrm{d}\mathbf{p} \wedge \mathrm{d}\mathbf{q} = \sum_{i=1}^{d} \mathrm{d}p_i \wedge \mathrm{d}q_i.$$

It is now an immediate observation that the 2-form Ω represents the sum of oriented areas of the projections of infinitesimal parallelogram $\mathrm{d}\mathbf{p} \wedge \mathrm{d}\mathbf{q}$ onto the d coordinate planes (p_i, q_i).

Theorem 5 *The wedge product has the following properties:*

(i) linearity, i.e. $\forall_{\lambda_1,\lambda_2}\ (\lambda_1 \mathrm{d}p + \lambda_2 \mathrm{d}q) \wedge \mathrm{d}s = \lambda_1 \mathrm{d}p \wedge \mathrm{d}s + \lambda_2 \mathrm{d}q \wedge \mathrm{d}s$,

(ii) skew–symmetry, i.e. $\mathrm{d}p \wedge \mathrm{d}q = -\mathrm{d}q \wedge \mathrm{d}p$,

(iii) $\mathrm{d}p \wedge \mathrm{d}p = 0$.

For more details concerning differential forms see for instance [5, 33].

2.2.1 Example: Linear Pendulum

As an illustration, let's consider one of the simplest examples of a Hamiltonian system of ODEs, the linear pendulum equation

$$\dot{p} = -kq, \qquad \dot{q} = p/m,$$

with Hamiltonian function

$$H = \frac{1}{2m}p^2 + \frac{k}{2}q^2,$$

$m, k > 0$ are constants. The general solution of this system has the form

$$q(t) = C_1 \sin(\omega t + C_2), \qquad p(t) = m\omega C_1 \cos(\omega t + C_2).$$

For given initial data, the solution can be written as

$$\begin{bmatrix} p(t) \\ q(t) \end{bmatrix} = \begin{bmatrix} \cos(\omega t) & -m\omega \sin(\omega t) \\ \sin(\omega t)/(\omega t) & \cos(\omega t) \end{bmatrix} \begin{bmatrix} p(0) \\ q(0) \end{bmatrix},$$

so that the solution operator can be decomposed as follows

$$\varphi_{t_0\to t} = \begin{bmatrix} 1 & 0 \\ 0 & m\omega \end{bmatrix} \begin{bmatrix} \cos(\omega t) & -\sin(\omega t) \\ \sin(\omega t) & \cos(\omega t) \end{bmatrix} \begin{bmatrix} 1 & 0 \\ 0 & 1/(m\omega) \end{bmatrix} \tag{2.11}$$

and we note that $\varphi_{t_0\to t}$ is area-preserving since $\det \varphi_{t_0\to t} = 1$. A graphical representation of the area-preserving property of $\varphi_{t_0\to t}$ given by the equation (2.11) for $\omega = 1$, $t = \pi/2$ and $m = 2$ is presented in Figure 2.1. A set of initial data D is transformed to the set $D_3 = \varphi_{t_0\to t}(D)$ and the area of D is the same as the area of D_3. Operations due to the decomposition of the operator $\varphi_{t_0\to t}$ are depicted as sets D_1 and D_2.

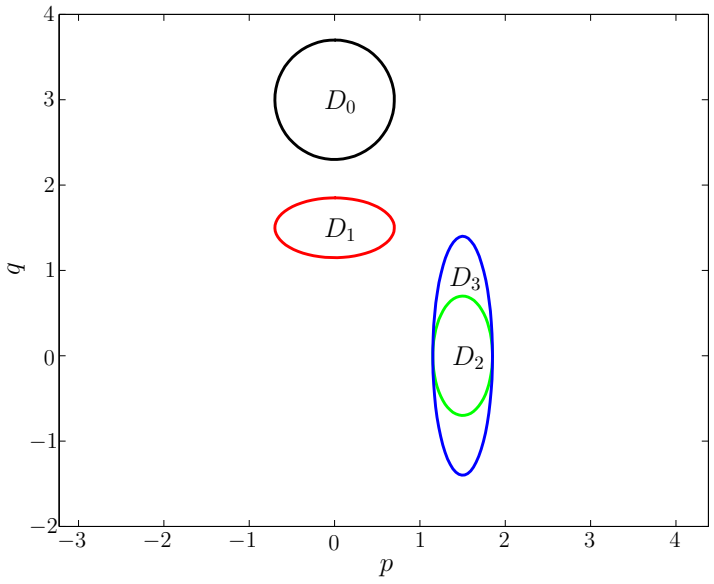

Figure 2.1: Preservation of the area by the flow of the harmonic oscillator (from [32]).

2.2.2 Example: Mathematical Pendulum

Our second example of a Hamiltonian ODE is a mathematical pendulum

$$p' = \sin q, \qquad q' = p, \tag{2.12}$$

for which the Hamiltonian function is

$$H = \frac{1}{2}p^2 + \cos q. \tag{2.13}$$

The phase portrait of the system described by equation (2.12) is presented on Figure 2.2. The plot was generated as a contour plot of the Hamiltonian function (2.13). The system under consideration is autonomous and therefore its critical points are centers and saddles. Later in this chapter we use this fact to illustrate the change to the topology of level curves introduced by various discretizations.

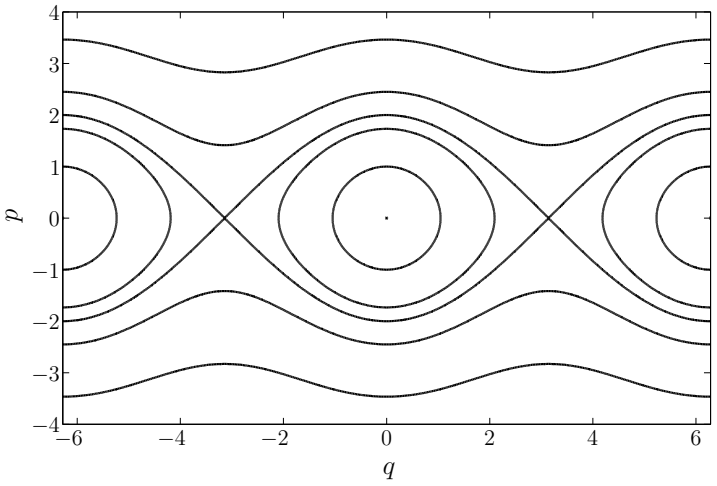

Figure 2.2: Phase Portrait of the Pendulum Equation.

2.3 Discretizations of 2D Hamiltonian ODEs

This section illustrates some of the consequences that symplecticness of the flow has on numerical solutions of Hamiltonian ODEs. Symplecticness of a numerical scheme is typically established in terms of the wedge product on differential forms in essentially the same way

as for continuous cases described in previous section. The procedure is illustrated on a simple example of the first-order method called symplectic Euler's method and compared with the standard explicit Euler's method. We are able to observe that the oriented area of an infinitesimal parallelogram is preserved by the discrete flow generated by the symplectic Euler's scheme while it increases in time for the regular explicit Euler's scheme. We illustrate these phenomena in the extended phase space in much the same way as in theorems 2 to 4.

2.3.1 Symplectic vs. Non-Symplectic Discretizations

For the general 2D Hamiltonian system

$$p' = -H_q(p,q), \qquad q' = H_p(p,q), \tag{2.14}$$

the following two methods are symplectic. The first reads

$$p_1 = p_0 - hH_q(p_0,q_1), \qquad q_1 = q_0 + hH_p(p_0,q_1), \tag{2.15}$$

and the method adjoint to it is

$$p_1 = p_0 - hH_q(p_1,q_0), \qquad q_1 = q_0 + hH_p(p_1,q_0). \tag{2.16}$$

Here we use standard notation that $u_0 = u(t_n)$ and $u_1 = u(t_n + h)$. These are called symplectic Euler's methods.

In order to prove that these methods are symplectic, consider the following system of variational equation

$$\mathrm{d}p_1 = \mathrm{d}p_0 - hH_{qp}\mathrm{d}p_0 - hH_{qq}\mathrm{d}q_1, \tag{2.17a}$$

$$\mathrm{d}q_1 = \mathrm{d}q_0 + hH_{pp}\mathrm{d}p_0 + hH_{pq}\mathrm{d}q_1. \tag{2.17b}$$

Taking the wedge product of equations (2.17) we obtain

$$\begin{aligned}
\mathrm{d}p_1 \wedge \mathrm{d}q_1 &= \mathrm{d}p_0 \wedge \mathrm{d}q_0 + \mathrm{d}p_0 \wedge (hH_{pp}\mathrm{d}p_0) + \mathrm{d}p_0 \wedge (hH_{pq}\mathrm{d}q_1) \\
&\quad -(hH_{qp}\mathrm{d}p_0) \wedge \mathrm{d}q_0 - (hH_{qp}\mathrm{d}p_0) \wedge (hH_{pp}\mathrm{d}p_0) - (hH_{qp}\mathrm{d}p_0) \wedge (hH_{pq}\mathrm{d}q_1) \\
&\quad -(hH_{qq}\mathrm{d}q_1) \wedge \mathrm{d}q_0 - (hH_{qq}\mathrm{d}q_1) \wedge (hH_{pp}\mathrm{d}p_0) - (hH_{qq}\mathrm{d}q_1) \wedge (hH_{pq}\mathrm{d}q_1).
\end{aligned}$$

Using properties of the wedge product given by the Theorem 5, we arrive at

$$\begin{aligned}
\mathrm{d}p_1 \wedge \mathrm{d}q_1 &= \mathrm{d}p_0 \wedge \mathrm{d}q_0 + hH_{pq}\mathrm{d}p_0 \wedge \mathrm{d}q_1 - hH_{qp}\mathrm{d}p_0 \wedge \mathrm{d}q_0 - hH_{qq}\mathrm{d}q_1 \wedge \mathrm{d}q_0 \\
&\quad -h^2 H_{qp}H_{pq}\mathrm{d}p_0 \wedge \mathrm{d}q_1 - h^2 H_{qq}H_{pp}\mathrm{d}q_1 \wedge \mathrm{d}p_0. \\
&= \mathrm{d}p_0 \wedge \mathrm{d}q_0 - h^2 H_{qp}H_{pq}\mathrm{d}p_0 \wedge \mathrm{d}q_1 + hH_{pq}\mathrm{d}p_0 \wedge (\mathrm{d}q_1 - \mathrm{d}q_0) \\
&\quad -hH_{qq}\mathrm{d}q_1 \wedge (\mathrm{d}q_0 + hH_{pp}\mathrm{d}p_0).
\end{aligned}$$

Noticing that $H_{pq} = H_{qp}$,

$$\mathrm{d}q_1 - \mathrm{d}q_0 = hH_{pp}\mathrm{d}p_0 + hH_{pq}\mathrm{d}q_1$$

and

$$\mathrm{d}q_1 - hH_{pq}\mathrm{d}q_1 = \mathrm{d}q_0 + hH_{pp}\mathrm{d}p_0,$$

we arrive at

$$\begin{aligned}
\mathrm{d}p_1 \wedge \mathrm{d}q_1 &= \mathrm{d}p_0 \wedge \mathrm{d}q_0 - h^2 H_{pq}H_{pq}\mathrm{d}p_0 \wedge \mathrm{d}q_1 + hH_{pq}\mathrm{d}p_0 \wedge \Big(hH_{pp}\mathrm{d}p_0 + hH_{pq}\mathrm{d}q_1\Big) \\
&\quad -hH_{qq}\mathrm{d}q_1 \wedge \Big(\mathrm{d}q_1 - hH_{pq}\mathrm{d}q_1\Big) \\
&= \mathrm{d}p_0 \wedge \mathrm{d}q_0,
\end{aligned}$$

which proves symplecticness of the scheme.

If we repeat the same procedure for the explicit Euler's method we obtain the following. Since the explicit Euler's method reads

$$p_1 = p_0 - hH_q(p_0, q_0), \qquad q_1 = q_0 + hH_p(p_0, q_0), \tag{2.18}$$

in order to show the difference between symplectic and explicit Euler's methods, consider the variational equation constructed for (2.18)

$$\mathrm{d}p_1 = \mathrm{d}p_0 - hH_{qp}\mathrm{d}p_0 - hH_{qq}\mathrm{d}q_0, \tag{2.19a}$$

$$\mathrm{d}q_1 = \mathrm{d}q_0 + hH_{pp}\mathrm{d}p_0 + hH_{pq}\mathrm{d}q_0. \tag{2.19b}$$

Taking the wedge product of equations (2.19) we obtain

$$\begin{aligned}\mathrm{d}p_1 \wedge \mathrm{d}q_1 = {} & \mathrm{d}p_0 \wedge \mathrm{d}q_0 + \mathrm{d}p_0 \wedge (hH_{pp}\mathrm{d}p_0) + \mathrm{d}p_0 \wedge (hH_{pq}\mathrm{d}q_0) \\ & -(hH_{qp}\mathrm{d}p_0) \wedge \mathrm{d}q_0 - (hH_{qp}\mathrm{d}p_0) \wedge (hH_{pp}\mathrm{d}p_0) - (hH_{qp}\mathrm{d}p_0) \wedge (hH_{pq}\mathrm{d}q_0) \\ & -(hH_{qq}\mathrm{d}q_0) \wedge \mathrm{d}q_0 - (hH_{qq}\mathrm{d}q_0) \wedge (hH_{pp}\mathrm{d}p_0) - (hH_{qq}\mathrm{d}q_0) \wedge (hH_{pq}\mathrm{d}q_0)\end{aligned}$$

Using properties of the wedge product given by the Theorem 5, we arrive at

$$\begin{aligned}\mathrm{d}p_1 \wedge \mathrm{d}q_1 = {} & \mathrm{d}p_0 \wedge \mathrm{d}q_0 + \mathrm{d}p_0 \wedge (hH_{pq}\mathrm{d}q_0) - (hH_{qp}\mathrm{d}p_0) \wedge \mathrm{d}q_0 \\ & -(hH_{qp}\mathrm{d}p_0) \wedge (hH_{pq}\mathrm{d}q_0) - (hH_{qq}\mathrm{d}q_0) \wedge (hH_{pp}\mathrm{d}p_0).\end{aligned}$$

Now, since $H_{pq} = H_{qp}$ we have that

$$\mathrm{d}p_1 \wedge \mathrm{d}q_1 = \Big(1 + h^2(H_{pp}H_{qq} - (H_{pq})^2)\Big)(\mathrm{d}p_0 \wedge \mathrm{d}q_0)$$

and thus, from (2.7), for the explicit Euler scheme

$$\mathrm{d}p_1 \wedge \mathrm{d}q_1 = (1 + h^2)(\mathrm{d}p_0 \wedge \mathrm{d}q_0),$$

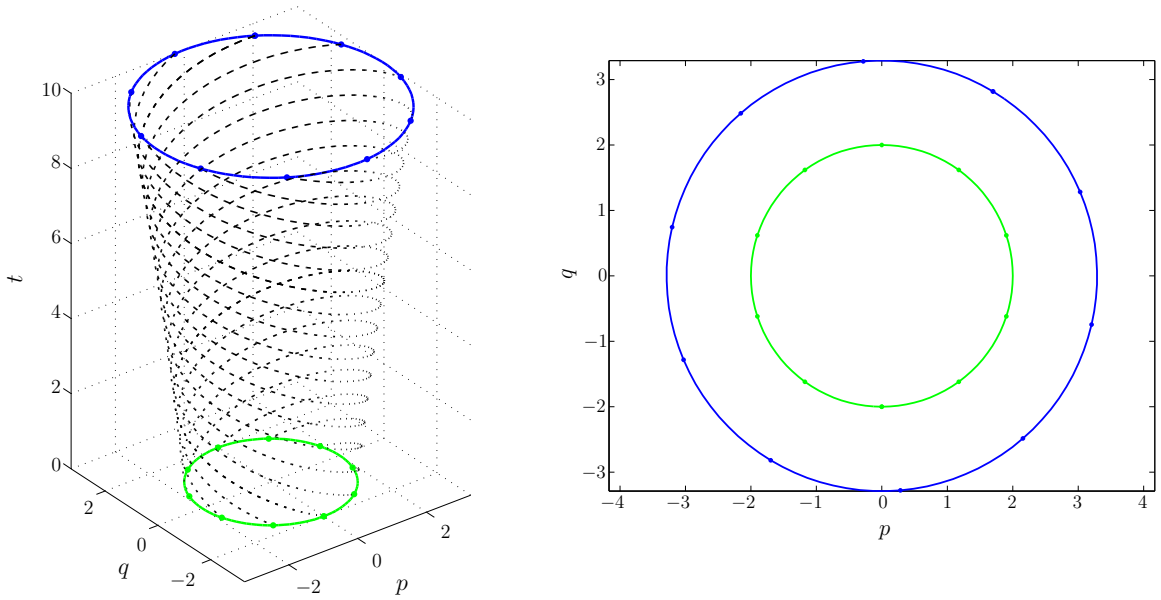

Figure 2.3: Explicit Euler – linear pendulum. $h = 0.1$.

indicating growth in time $(1 + h^2 > 1)$.

We would like to show what happens to the set of initial data under the action of a discrete-time flow. As an example, consider two first order discretizations of the pendulum equation (2.12). The first one is an explicit Euler's method

$$p_{n+1} = p_n - hq_n, \qquad q_{n+1} = q_n + hp_n$$

and the second one is its modification called the symplectic Euler's method

$$p_{n+1} = p_n - hq_n, \qquad q_{n+1} = q_n + hp_{n+1},$$

where we use standard notation that $u_n = u(t_n)$ and $u_{n+1} = u(t_n + h)$ and h is the time-step of integration. Figures 2.3 and 2.5 present a vortex tube of (discrete) trajectories obtained by the explicit Euler's method. It is not difficult to note that the area of the original set

increases under the discrete flow. In turn, Figures 2.4 and 2.6 present an analogous case, but now the trajectories were computed by the symplectic Euler's method. The area of the initial set is conserved and one observes only a slight change in its shape. Figures 2.3 to 2.6, where an initial set (a green circle) is evolved under two different, first order discretizations of the linear pendulum equation, can be considered an illustration to the discrete analog of Theorem 4.

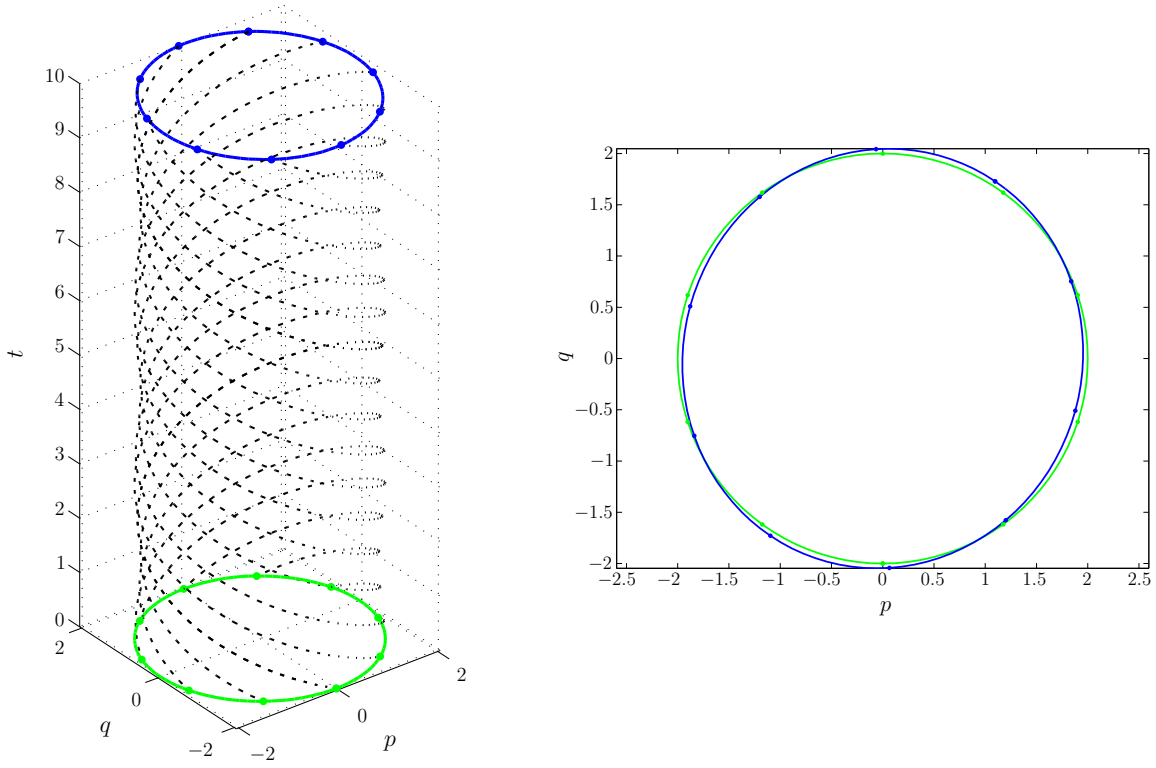

Figure 2.4: Symplectic Euler – linear pendulum. $h = 0.1$.

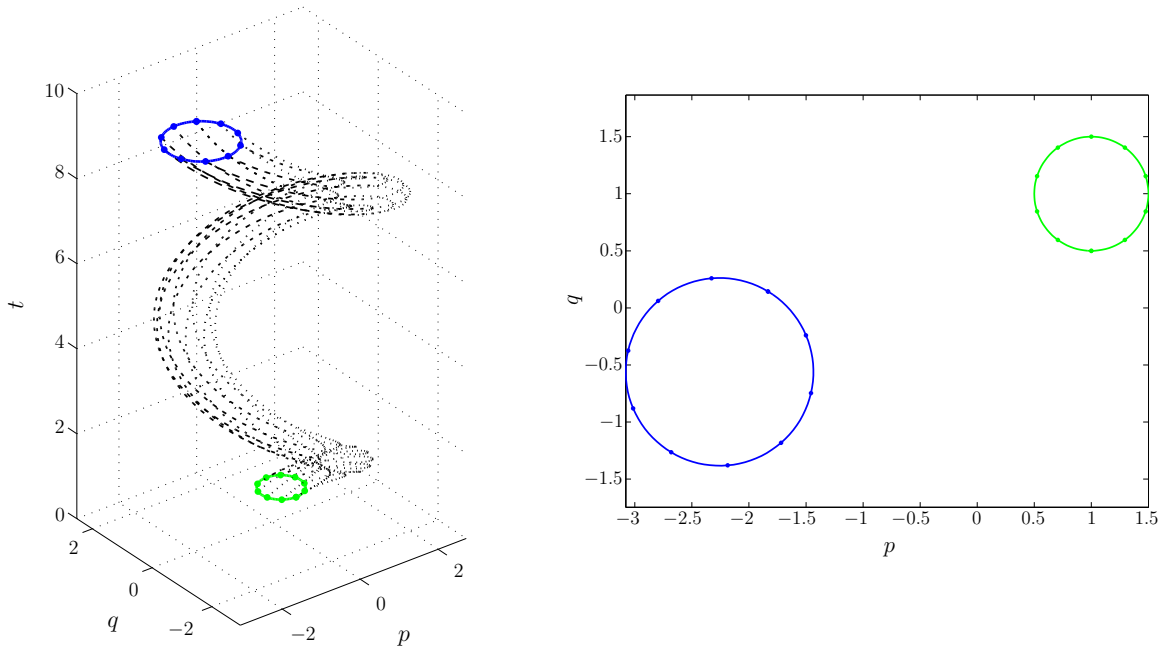

Figure 2.5: Explicit Euler – linear pendulum. $h = 0.1$.

2.4 Backward Error Analysis

A forward error analysis consists of the study of the errors $y_1 - \tilde{\varphi}_h(y_0)$ (local error) and $y_n - \tilde{\varphi}_{nh}(y_0)$ (global error) in the solution space. The idea of backward error analysis is to search for a *modified differential equation* $\frac{\mathrm{d}}{\mathrm{d}t}\tilde{y} = \tilde{f}_h(\tilde{y})$ of the form

$$\frac{\mathrm{d}}{\mathrm{d}t}\tilde{y} = \tilde{f}_0(\tilde{y}) + h\tilde{f}_1(\tilde{y}) + h^2\tilde{f}_2(\tilde{y}) + \cdots ,$$

such that $y_n = \tilde{y}(nh)$, and studying the difference of vector fields $f(y)$ and $\tilde{f}_h(y)$.

We illustrate the idea of BEA on the previous example of two first order discretizations of a general 2D Hamiltonian system of equations (2.14). For such a system, using Taylor

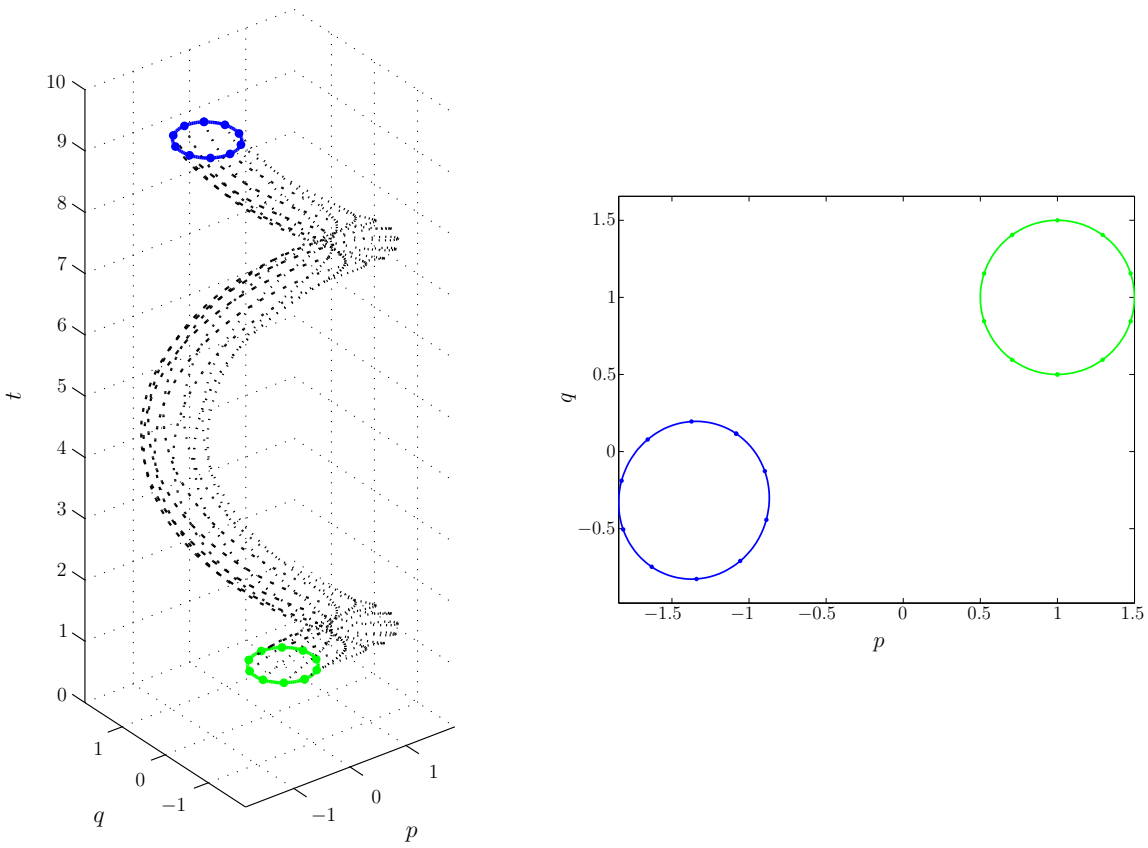

Figure 2.6: Symplectic Euler – linear pendulum. $h = 0.1$.

series expansion, one finds the following

$$\begin{aligned} p'' &= -(p'H_{pq} + q'H_{qq}) = H_q H_{pq} - H_p H_{qq}, \\ q'' &= p'H_{pp} + q'H_{pq} = H_p H_{pq} - H_q H_{pp}, \end{aligned}$$

so that, since

$$f(x+h) = f(x) + hf'(x) + \frac{h^2}{2} f''(x) + \mathcal{O}(h^3),$$

one writes

$$\begin{aligned} p_1 &= p_0 + hp_0' + \frac{h^2}{2}p_0'' + \mathcal{O}(h^3), \\ q_1 &= q_0 + hq_0' + \frac{h^2}{2}q_0'' + \mathcal{O}(h^3). \end{aligned}$$

If p and q satisfies the system of Hamiltonian equations on obtains

$$p_1 = p_0 - hH_q + \frac{h^2}{2}(H_qH_{pq} - H_pH_{qq}) + \mathcal{O}(h^3) = p_0 + \widetilde{h},$$

where lower index 0 indicates that the function is evaluated at (p_0, q_0). Similarly

$$q_1 = q_0 + hH_p + \frac{h^2}{2}(H_pH_{pq} - H_qH_{pp}) + \mathcal{O}(h^3) = q_0 + \widetilde{k}.$$

We use this technique repeatedly for various, more specific systems in order to obtain a Hamiltonian function of a modified system, so we established some general formulas and notations to be used later throughout this section.

2.4.1 System of Modified Equations

As was mentioned before, the idea behind the BEA is to construct a modified Hamiltonian system in such a way that the numerical solution will satisfy it exactly, i.e. to every order in h. Assume that the modified systme is given by

$$p' = -\widetilde{H}_q(p,q) \qquad q' = \widetilde{H}_p(p,q), \tag{2.20}$$

where

$$\widetilde{H} = H + hH^{(1)} + h^2H^{(2)} + \mathcal{O}(h^3).$$

Clearly then

$$
\begin{aligned}
\widetilde{H}_p &= H_p + h(H^{(1)})_p + h^2(H^{(2)})_p + \mathcal{O}(h^3), \\
\widetilde{H}_q &= H_q + h(H^{(1)})_q + h^2(H^{(2)})_q + \mathcal{O}(h^3)
\end{aligned}
$$

and so

$$
\begin{aligned}
\widetilde{H}_p\widetilde{H}_{pq} &= H_pH_{pq} + h(H_p(H^{(1)})_{pq} + (H^{(1)})_pH_{pq}) \\
&\quad + h^2\Big(H_p(H^{(2)})_{pq} + (H^{(1)})_p(H^{(1)})_{pq} + (H^{(2)})_pH_{pq}\Big) + \mathcal{O}(h^3), \\
\widetilde{H}_p\widetilde{H}_{qq} &= H_pH_{qq} + h(H_p(H^{(1)})_{qq} + (H^{(1)})_pH_{qq}) \\
&\quad + h^2\Big(H_p(H^{(2)})_{qq} + (H^{(1)})_p(H^{(1)})_{qq} + (H^{(2)})_pH_{qq}\Big) + \mathcal{O}(h^3), \\
\widetilde{H}_q\widetilde{H}_{pq} &= H_qH_{pq} + h(H_q(H^{(1)})_{pq} + (H^{(1)})_qH_{pq}) \\
&\quad + h^2\Big(H_q(H^{(2)})_{pq} + (H^{(1)})_q(H^{(1)})_{pq} + (H^{(2)})_qH_{pq}\Big) + \mathcal{O}(h^3), \\
\widetilde{H}_q\widetilde{H}_{pp} &= H_qH_{pp} + h(H_q(H^{(1)})_{pp} + (H^{(1)})_qH_{pp}) \\
&\quad + h^2\Big(H_q(H^{(2)})_{pp} + (H^{(1)})_q(H^{(1)})_{pp} + (H^{(2)})_qH_{pp}\Big) + \mathcal{O}(h^3).
\end{aligned}
$$

For the modified Hamiltonian we have the following

$$
\begin{aligned}
p_1 &= p_0 - h\widetilde{H}_q + \frac{h^2}{2}(\widetilde{H}_q\widetilde{H}_{pq} - \widetilde{H}_p\widetilde{H}_{qq}) + \mathcal{O}(h^3) \\
&= p_0 - h\Big(H_q + h(H^{(1)})_q\Big) + \frac{h^2}{2}\Big(H_qH_{pq} - H_pH_{qq}\Big) + \mathcal{O}(h^3)
\end{aligned}
$$

and

$$
\begin{aligned}
q_1 &= q_0 + h\widetilde{H}_p + \frac{h^2}{2}(\widetilde{H}_p\widetilde{H}_{pq} - \widetilde{H}_q\widetilde{H}_{pp}) + \mathcal{O}(h^3) \\
&= q_0 + h\Big(H_p + h(H^{(1)})_p\Big) + \frac{h^2}{2}\Big(H_pH_{pq} - H_qH_{pp}\Big) + \mathcal{O}(h^3).
\end{aligned}
$$

Our task is now reduced to finding specific expressions of $H^{(i)}$ corresponding to a particular discretization. We illustrate this procedure by finding expressions of $H^{(1)}$ for symplectic and explicit Euler's methods.

2.4.2 Symplectic Euler's Method

Consider the method

$$p_1 = p_0 - hH_q(p_0, q_1), \qquad q_1 = q_0 + hH_p(p_0, q_1)$$

and observe that if

$$\widetilde{k} = hH_p + \frac{h^2}{2}(H_pH_{pq} - H_qH_{pp}) + \mathcal{O}(h^3),$$

we have that

$$\widetilde{k}^2 = h^2(H_p)^2 + \mathcal{O}(h^3).$$

Expanding,

$$\begin{aligned} H_q(p_0, q_1) &= H_q(p_0, q_0 + \widetilde{k}) = H_q + \widetilde{k}H_{qq} + \frac{\widetilde{k}^2}{2}H_{qqq} + \mathcal{O}(\widetilde{k}^3) \\ &= H_q + \Big(hH_p + \frac{h^2}{2}(H_pH_{pq} - H_qH_{pp})\Big)H_{qq} + \frac{h^2}{2}(H_p)^2H_{qqq} + \mathcal{O}(h^3) \end{aligned}$$

and

$$\begin{aligned} H_p(p_0, q_1) &= H_p(p_0, q_0 + \widetilde{k}) = H_p + \widetilde{k}H_{pq} + \frac{\widetilde{k}^2}{2}H_{pqq} + \mathcal{O}(\widetilde{k}^3) \\ &= H_p + \Big(hH_p + \frac{h^2}{2}(H_pH_{pq} - H_qH_{pp})\Big)H_{pq} + \frac{h^2}{2}(H_p)^2H_{pqq} + \mathcal{O}(h^3). \end{aligned}$$

Comparing $\mathcal{O}(h^2)$ terms we obtain

$$\begin{aligned} -(H^{(1)})_q + \frac{1}{2}(H_qH_{pq} - H_pH_{qq}) &= -H_pH_{qq}, \\ (H^{(1)})_p + \frac{1}{2}(H_pH_{pq} - H_qH_{pp}) &= H_pH_{pq}, \end{aligned}$$

that is

$$\begin{aligned}(H^{(1)})_p &= \frac{1}{2}(H_pH_{pq} + H_qH_{pp}),\\ (H^{(1)})_q &= \frac{1}{2}(H_qH_{pq} + H_pH_{qq}),\end{aligned}$$

so finally, since the integrability condition $(H^{(1)})_{qp} = (H^{(1)})_{pq}$ is satisfied,

$$H^{(1)} = \frac{1}{2}H_pH_q.$$

For a symplectic numerical method this procedure can be carried to any order, which implies that the numerical solution is an exact solution to a Hamiltonian system.

2.4.3 Explicit Euler's Method

If we try to repeat the same procedure for the explicit Euler's discretization

$$p_1 = p_0 - hH_q(p_0, q_0), \qquad q_1 = q_0 + hH_p(p_0, q_0)$$

we obtain, from the expansion of the modified equations (2.20), that

$$\begin{aligned}p_1 &= p_0 - hH_q - h^2(H^{(1)})_q + \frac{h^2}{2}\Big(H_qH_{pq} - H_pH_{qq}\Big) + \mathcal{O}(h^3),\\ q_1 &= q_0 + hH_p + h^2(H^{(1)})_p + \frac{h^2}{2}\Big(H_pH_{pq} - H_qH_{pp}\Big) + \mathcal{O}(h^3).\end{aligned}$$

At $\mathcal{O}(h^2)$ we therefore obtain

$$\begin{aligned}(H^{(1)})_q &= \frac{1}{2}\Big(H_qH_{pq} - H_pH_{qq}\Big),\\ (H^{(1)})_p &= \frac{1}{2}\Big(H_qH_{pp} - H_pH_{pq}\Big).\end{aligned}$$

We have to check integrability condition. Computing mixed derivatives we have

$$\begin{aligned}(H^{(1)})_{qp} &= \frac{1}{2}\Big(H_{qp}H_{pq} + H_qH_{pqp} - H_{pp}H_{qq} - H_pH_{qqp}\Big),\\ (H^{(1)})_{pq} &= \frac{1}{2}\Big(H_{qq}H_{pp} + H_qH_{ppq} - H_{pq}H_{pq} - H_pH_{pqq}\Big)\end{aligned}$$

and so

$$(H^{(1)})_{pq} - (H^{(1)})_{qp} = H_{pp}H_{qq} - H_{pq}^2 \equiv 1,$$

by (2.7). Clearly, it is not possible to construct a modified Hamiltonian, thus the discrete flow is not symplectic.

2.4.4 Conservation of Energy

An immediate question occurs. What is the relation between preservation of symplecticness and preservation of energy? In order to answer this question let's first recall that the energy (Hamiltonian) is a conserved quantity only for autonomous Hamiltonian systems. Let $\mathbf{z} = \mathbf{z}(t)$ be a solution to (2.2). Then

$$\frac{\mathrm{d}}{\mathrm{d}t}H(\mathbf{z}(t),t) = (\nabla_{\mathbf{z}}H)^T\frac{\mathrm{d}}{\mathrm{d}t}\mathbf{z} + \frac{\partial}{\partial t}H = (\nabla_{\mathbf{z}}H)^T J_d(\nabla_{\mathbf{z}}H)\mathbf{z} + \frac{\partial}{\partial t}H = \frac{\partial H}{\partial t},$$

by the skew-symmetry property of the matrix J_d. In particular, if the system (2.2) is autonomous ($\partial_t H \equiv 0$), then

$$\frac{\mathrm{d}}{\mathrm{d}t}H \equiv 0,$$

which means that the Hamiltonian is a constant of motion. This fact is often interpreted as conservation of energy by the flow of the system. From the backward error analysis (BEA) we know that an approximated solution obtained from the symplectic discretization can be viewed as an exact solution to a (nearby) Hamiltonian system. One concludes that for any choice of initial condition the numerical solution will lay on the level curve of a modified Hamiltonian corresponding to a certain value $\widetilde{H}_c$ which will not be significantly different

from an original one H_c. The distinction between energy-conserving discretizations and symplectic ones is discussed in more detail in [30].

The notion of symplecticness of discrete autonomous Hamiltonian systems is very often illustrated by presenting a comparison as in Figure 2.7. We computed numerical solution using the explicit Euler's method

$$p_{n+1} = p_n + h \sin q_n, \qquad q_{n+1} = q_n + hp_n$$

and its modification called the symplectic Euler's method

$$p_{n+1} = p_n + h \sin q_n, \qquad q_{n+1} = q_n + hp_{n+1},$$

where again $u_n = u(t_n)$ and $u_{n+1} = u(t_n + h)$ and h is the time-step of integration. Figure 2.7(a) shows a numerical solution of the pendulum equation (2.12) obtained by the explicit Euler's method (blue dots) for initial data $(p_0, q_0) = (2, 0)$ corresponding to a periodic solution of the original system (solid line). the numerical trajectory is an (unstable) spiral – qualitative properties of the original solution are destroyed by the discretization. On the other hand, in Figure 2.7(b) presented is a numerical solution obtained, for the same system and the same initial data, by the symplectic Euler's method. The solution much more closely resembles the original one, even for significantly larger time steps. From the BEA we know that the numerical solution is a level curve of a modified Hamiltonian that is autonomous and, as such, is a closed curve. However, a non-symplectic discretization causes the topology of the phase space to be destroyed.

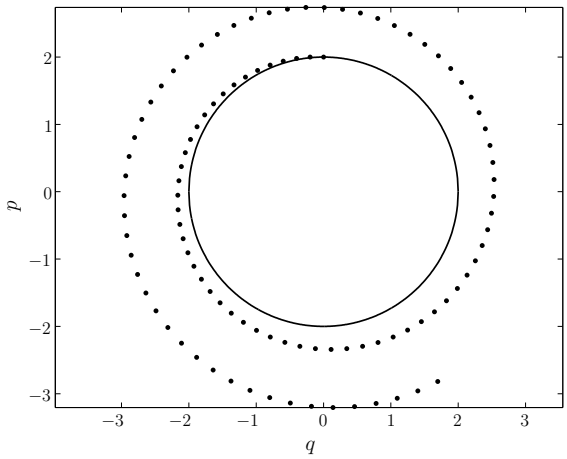

(a) Forward Euler's Method, time step $h = 0.1$, simulation carried up to $T = 10$.

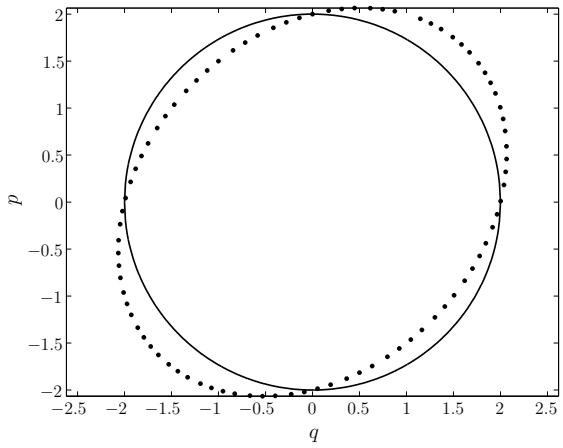

(b) Symplectic Euler's Method, time step $h = 0.5$, simulation carried up to $T = 42$.

Figure 2.7: Numerical solutions of the linear pendulum equation.

2.5 Nonlinear Stability of Symplectic Integrators

In the previous section we showed differences between symplectic and non-symplectic discretizations. It should be clear by now, that the preferred methods of numerically solving Hamiltonian ODEs are symplectic ones. The question now is about differences between symplectic methods. In the paper on nonlinear stability [27], McLachlan, Perlmutter and Quispel gave examples of what happens if the initial data are closed to some special orbits, like separatrix, or homo-, or hetero-clinic orbits. It turns out that the change of the phase space geometry under the discretization may cause numerical solutions obtained by some integrators to become unstable, while some integrators produce over-stabilized solutions. A simple example is an implicit midpoint and the leap-frog discretizations of the following

Hamiltonian system of equations

$$p' = q - 3q^2, \qquad q' = p, \tag{2.21}$$

with Hamiltonian function

$$H = \frac{1}{2}p^2 - \frac{1}{2}q^2 + q^3. \tag{2.22}$$

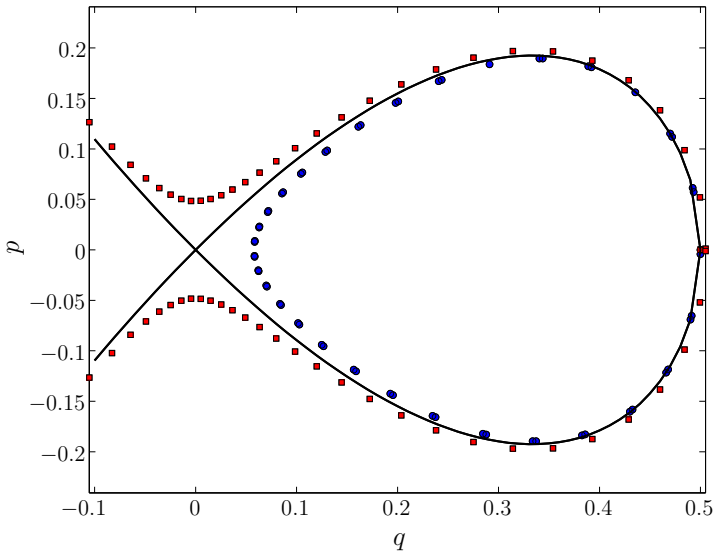

Figure 2.8: Critical energy set (homoclinic orbit) of the cubic oscillator together with two different numerical solutions obtained by the leap-frog method (red squares) and the implicit midpoint rule (blue dots). The leap-frog solution was computed for $h = 0.6$ and carried until $T = 6$, while the midpoint was computed for $h = 0.85$ and until $T = 50$ with solver tolerance $\epsilon = 10^{-11}$.

Figure 2.8 presents a comparison of two numerical solutions obtained for this system by the leap-frog method (red squares) with time-step $h = 0.05$ and the implicit midpoint method (blue dots) with time-step $h = 0.8$, with the homoclinic orbit plotted as the appropriate level curve of the Hamiltonian (2.22). Initial data for both numerical solutions are located on this

homoclinic orbit at the point $(p, q) = (0, 1/2)$. We computed numerical solutions using the leap-frog method

$$p_{n+2} = p_n + h(q_n - 3(q_n)^2), \qquad q_{n+2} = q_n + hp_n$$

and the implicit midpoint rule

$$p_{n+1} = p_n + h\Big(\frac{1}{2}(q_{n+1} + q_n) - \frac{3}{4}(q_{n+1} + q_n)^2\Big), \qquad q_{n+1} = q_n + \frac{h}{2}(p_{n+1} + p_n).$$

The leap-frog, as a multi-step method requires initialization, i.e. initial one-step advancement of the solution by some other method. For this purpose we used the midpoint rule, as both methods are second order accurate and symplectic.

We observe (Figure 2.8) that the change of the geometry of the phase space under the discretization changes. This phenomenon influences qualitative features of numerical solutions depending on the discretization. The implicit midpoint discretization (blue dots) expands the original phase space, so that the discrete orbit is located in the interior of the modified homoclinic orbit. In this case the discretization over-stabilizes the solution. In the case of the leap-frog method the phase space is expanded in one direction (along the q–axis) and at the same time contracted along the other direction (p–axis). This causes the numerical orbit (red squares) to be in the exterior if the modified homoclinic orbit (for the leap-frog method this modified homoclinic orbit is different than for the midpoint), thus destabilizing the solution. We will return to this phenomenon in Chapter 6, where we present numerical evidences that the change in the geometry of the phase space of partial differential equations influences qualitative features of the numerical solution in a very similar manner.

CHAPTER THREE: MULTISYMPLECTIC PARTIAL DIFFERENTIAL EQUATIONS

In many cases of wave propagation, particularly the equations governing ocean waves and atmospheric flow, a conservative model is accurate and when studying conservative partial differential equations it is natural to appeal to the powerful geometric methods of Lagrangian and Hamiltonian mechanics. The Lagrangian formulation and the Hamiltonian formulation for a conservative system are usually considered to be dually related through the Legendre transform and, in finite dimensions, when the Legendre transform is non-degenerate, the duality is exact. However, according to Bridges [10], in infinite dimensions, particularly for systems governing wave propagation where one or more spatial directions is infinite, the Lagrange – Hamiltonian duality is no longer uniquely defined. Formally taking the Legendre transform of the Lagrange density results in a Hamiltonian formulation

$$J\frac{\partial}{\partial t}\begin{bmatrix} u \\ \\ v \end{bmatrix} = \begin{bmatrix} \delta\mathscr{H}/\delta u \\ \\ \delta\mathscr{H}/\delta v \end{bmatrix}, \tag{3.1}$$

where $\mathscr{H}$ is typically an integral functional and matrix J is defined by the equation (2.6)(cf. [4, 10, 24, 28]).

An advantage of the formulation (3.1) is that the system is an evolution equation in time and so one can easily obtain existence results for the initial value problem. Another advantage is the organizing structure provided by the symplectic operator. The necessity to consider a space of functions for which the integral functional $\mathscr{H}$ is well defined might be thought as a disadvantage. Therefore such a Hamiltonian formulation is most useful when

the spatial domain is finite or when one is interested in a wave with a particular spatial variation.

One of the most important results presented in [10] is a complete Legendre transform that eliminates the x–derivatives in the Lagrangian density. Such a formulation is called multisymplectic. The multisymplectic form (3.2) discussed in this chapter organizes each facet of the model equation. All time derivatives appear in the term $L\mathbf{z}_t$, all space derivatives appear in the term $K\mathbf{z}_x$ and the gradient of $S(\mathbf{z})$ is defined with respect to an inner product on the phase space $\mathcal{H}$ which in this case is $\mathbb{R}^d$. We recollect fundamental definitions and theorems concerning Hamiltonian and multisymplectic forms of PDEs in physical and Fourier spectral space and statet local conservation laws associated with the multisymplectic formulation. We list various equations, their multisymplectic forms and conservation laws as examples. We also give linearizations of certain equations about some special solutions and associated dispersion relationships. Background material presented here will be used in later chapters to construct and analyze properties of various discretization.

3.1 Multisymplectic Formulation

It is well known [32] that the flow of a Hamiltonian ODE preserves the sum of the oriented areas of the projections of parallelograms, as described in Chapter 2. A Hamiltonian structure generalizing a classical Hamiltonian structure of a Hamiltonian evolution equation is derived by assigning a distinct symplectic operator for each unbounded space direction and time. This generalization, called multisymplectic structures, is natural for dispersive wave propagation problems [10]. For Hamiltonian PDEs we have the following

Definition 4 *A Hamiltonian PDE (in the "$1+1$" case) is said to be* multisymplectic *if it can be written as*

$$L\mathbf{z}_t + K\mathbf{z}_x = \nabla_{\mathbf{z}} S, \qquad \mathbf{z} \in \mathbb{R}^d, \tag{3.2}$$

where $L, K \in \mathcal{M}_{d\times d}(\mathbb{R})$ are $d \times d$, skew-symmetric matrices, and $S : \mathbb{R}^d \to \mathbb{R}$ is a smooth function of the state variable $\mathbf{z}$.

In justifying the direction in which the Hamiltonian form (3.1) was generalized to obtain (3.2) let's resort to the original paper of Bridges [10]. The system (3.2) is a Hamiltonian formulation of a wave model equation on a multi-symplectic structure which means that, instead of a single symplectic form (2.10) as in (3.1), there are two pre-symplectic operators L and K. These operators are skew-symmetric and can be identified with closed two forms that define a generalized symplectic structure for the system. However operators L and K do not have to be represented by invertible matrices and do not have to be unique as will be shown later in this chapter using the nonlinear wave equation as an example. In the partial Legendre transform used to obtain (3.1) one defines a new set of variables (u, v), generates a Hamiltonian functional $\mathscr{H}(u, v)$ and creates an action density. The action density in this case is vu_t and the gradient of action (with respect to an inner product that includes integration over t) results in the left-hand side of (3.1) and hence is responsible for generating the single symplectic operator in the system. In the multisymplectic formulation, in addition to new variables, the complete Legendre transform defines a family of action densities and creates a family of symplectic operators and a new Hamiltonian functional. The derivation of a multisymplectic form in [10] concludes with the statement that a partial Legendre transform

and a complete Legendre transform lead to non-trivially different symplectic structures and Hamiltonian systems and that the Hamiltonian formulation on a multi-symplectic structure is a natural framework for analyzing and proving particular properties of dispersive wave propagation in conservative systems.

In contrast to Hamiltonian ODEs, where symplecticness is a global property, an important aspect of the multisymplectic structure is that symplecticness is now a local property – it varies both in time and in space. This local feature is expressed through the multisymplectic conservation law.

Theorem 6 *Multisymplectic formulation of any PDE satisfies the multisymplectic conservation law*

$$\partial_t \Omega^{(t)} + \partial_x \Omega^{(x)} = 0, \tag{3.3}$$

where

$$\Omega^{(t)} = \frac{1}{2}(\mathrm{d}\mathbf{z} \wedge L\mathrm{d}\mathbf{z}), \tag{3.4a}$$

$$\Omega^{(x)} = \frac{1}{2}(\mathrm{d}\mathbf{z} \wedge K\mathrm{d}\mathbf{z}), \tag{3.4b}$$

are differential two–forms defining a space–time symplectic (multisymplectic) structure.

Remark 1 *Differential two–forms (3.4) are scalar functions of the form*

$$\Omega^{(t)} = \frac{1}{2}\sum_{i=1}^{d}\Big[\mathrm{d}z^i \wedge \Big(\sum_{j=1}^{d} L^{ij}\mathrm{d}z^j\Big)\Big], \qquad \Omega^{(x)} = \frac{1}{2}\sum_{i=1}^{d}\Big[\mathrm{d}z^i \wedge \Big(\sum_{j=1}^{d} K^{ij}\mathrm{d}z^j\Big)\Big],$$

where $\wedge$ denotes the wedge product, which properties are given by Theorem 5.

Proof: Let's first note the following

Lemma 2 *For any matrix* $L \in \mathcal{M}_{d\times d}(\mathbb{R})$

$$\mathrm{d}\mathbf{p} \wedge L\mathrm{d}\mathbf{q} = L^T\mathrm{d}\mathbf{p} \wedge \mathrm{d}\mathbf{q}. \tag{3.5}$$

Proof: Directly from remark 1 we have that

$$\begin{aligned}
\mathrm{d}\mathbf{p} \wedge L\mathrm{d}\mathbf{q} &= \sum_{i=1}^{d} \mathrm{d}p^i \wedge \sum_{j=1}^{d} L^{ij}\mathrm{d}q^j = \sum_{i=1}^{d}\sum_{j=1}^{d} \mathrm{d}p^i \wedge L^{ij}\mathrm{d}q^j \\
&= \sum_{j=1}^{d} \Big(\sum_{i=1}^{d} ((L^T)^{ji})\mathrm{d}p^i \Big) \wedge \mathrm{d}q^j = L^T\mathrm{d}\mathbf{p} \wedge \mathrm{d}\mathbf{q},
\end{aligned}$$

which completes the proof of Lemma 2. ■

From Lemma 2 we immediately conclude that for skew-symmetric matrices L and K, i.e. for such matrices that matrices $L = -L^T$ and $K = -K^T$, the following is true

$$\mathrm{d}\mathbf{p} \wedge L\mathrm{d}\mathbf{q} = -L\mathrm{d}\mathbf{p} \wedge \mathrm{d}\mathbf{q}, \quad \mathrm{d}\mathbf{p} \wedge K\mathrm{d}\mathbf{q} = -K\mathrm{d}\mathbf{p} \wedge \mathrm{d}\mathbf{q}$$

and therefore

$$\begin{aligned}
2\Omega_t^{(t)} + 2\Omega_x^{(x)} &= (\mathrm{d}\mathbf{z} \wedge L\mathrm{d}\mathbf{z})_t + (\mathrm{d}\mathbf{z} \wedge K\mathrm{d}\mathbf{z})_x \\
&= (\mathrm{d}\mathbf{z}_t \wedge L\mathrm{d}\mathbf{z} + \mathrm{d}\mathbf{z} \wedge L\mathrm{d}\mathbf{z}_t) + (\mathrm{d}\mathbf{z}_x \wedge K\mathrm{d}\mathbf{z} + \mathrm{d}\mathbf{z} \wedge K\mathrm{d}\mathbf{z}_x) \\
&= (-L\mathrm{d}\mathbf{z}_t \wedge \mathrm{d}\mathbf{z} + \mathrm{d}\mathbf{z} \wedge L\mathrm{d}\mathbf{z}_t) + (-K\mathrm{d}\mathbf{z}_x \wedge \mathrm{d}\mathbf{z} + \mathrm{d}\mathbf{z} \wedge K\mathrm{d}\mathbf{z}_x) \\
&= -2(L\mathrm{d}\mathbf{z}_t + K\mathrm{d}\mathbf{z}_x) \wedge \mathrm{d}\mathbf{z} \\
&= -2(S_{\mathbf{zz}}\mathrm{d}\mathbf{z}) \wedge \mathrm{d}\mathbf{z} = 0
\end{aligned}$$

since $S_{\mathbf{zz}}$, a Hessian matrix, is symmetric and the variational equation

$$L\mathrm{d}\mathbf{z}_t + K\mathrm{d}\mathbf{z}_x = S_{\mathbf{zz}}\mathrm{d}\mathbf{z}$$

holds. The symmetry of the Hessian matrix $S_{\mathbf{zz}}$ and the skew-symmetry of the wedge product implies that

$$(S_{\mathbf{zz}}\mathrm{d}\mathbf{z}) \wedge \mathrm{d}\mathbf{z} = -\mathrm{d}\mathbf{z} \wedge (S_{\mathbf{zz}}\mathrm{d}\mathbf{z}) = (S_{\mathbf{zz}}\mathrm{d}\mathbf{z}) \wedge \mathrm{d}\mathbf{z}$$

which is only possible if $(S_{\mathbf{zz}}\mathrm{d}\mathbf{z}) \wedge \mathrm{d}\mathbf{z} = 0$. ■

Differential two–forms $\Omega^{(t)}$ and $\Omega^{(x)}$ are called pre-symplectic and the pair $(\Omega^{(t)}, \Omega^{(x)})$ is sometimes referred to as the bi-symplectic structure on the phase space $\mathcal{H}$.

Aside from the differential form of the multisymplectic conservation law (3.3), especially in derivations of finite–element multisymplectic discretizations the following equivalent form is useful [11]. Consider (3.3) integrated over a closed, simply–connected region R of the plane (x, t)

$$\iint_R \partial_t \Omega^{(t)} + \partial_x \Omega^{(x)} \mathrm{d}A = 0.$$

Using Green's theorem it can be transformed into the integral form

$$\oint_{\partial R} \Big(\Omega^{(t)} \mathrm{d}x - \Omega^{(x)} \mathrm{d}t \Big) = 0.$$

An important consequence of the multisymplectic structure is the fact that when the Hamiltonian $S(\mathbf{z})$ is independent of t, equation (3.2) has local energy conservation law (LECL) and if $S(\mathbf{z})$ is independent of x, equation (3.2) has local momentum conservation law (LMCL).

Theorem 7 *Assume that $S(\mathbf{z})$ is independent of t and x. Then*

$$\partial_t \mathscr{E} + \partial_x \mathscr{F} = 0, \qquad \mathscr{E} = S(\mathbf{z}) + \frac{1}{2}\mathbf{z}_x^T K \mathbf{z}, \quad \mathscr{F} = -\frac{1}{2}\mathbf{z}_t^T K \mathbf{z}, \tag{3.6a}$$

$$\partial_t \mathscr{I} + \partial_x \mathscr{G} = 0, \qquad \mathscr{G} = S(\mathbf{z}) + \frac{1}{2}\mathbf{z}_t^T L \mathbf{z}, \quad \mathscr{I} = -\frac{1}{2}\mathbf{z}_x^T L \mathbf{z}, \tag{3.6b}$$

Moreover, if equation (3.2) is furnished with periodic boundary conditions

$$u(x+\ell,t) = u(x,t), \tag{3.7}$$

local conservation laws (3.6) can be integrated in x to obtain global conservation of energy (GE) and momentum (GM).

PROOF: Clearly if $f = \mathbf{u}^T\mathbf{v}$ than $f' = (\mathbf{u}')^T\mathbf{v} + \mathbf{u}^T\mathbf{v}'$. Now the proof is straightforward since

$$\mathscr{E}_t = \frac{\partial}{\partial t}S(\mathbf{z}) + \frac{1}{2}\mathbf{z}_{xt}^T K\mathbf{z} + \frac{1}{2}\mathbf{z}_x^T K\mathbf{z}_t \qquad \mathscr{F}_x = -\frac{1}{2}\mathbf{z}_{tx}^T K\mathbf{z} - \frac{1}{2}\mathbf{z}_t^T K\mathbf{z}_x \tag{3.8a}$$

$$\mathscr{G}_x = \frac{\partial}{\partial x}S(\mathbf{z}) + \frac{1}{2}\mathbf{z}_{tx}^T L\mathbf{z} + \frac{1}{2}\mathbf{z}_t^T L\mathbf{z}_x \qquad \mathscr{I}_t = -\frac{1}{2}\mathbf{z}_{xt}^T L\mathbf{z} - \frac{1}{2}\mathbf{z}_x^T L\mathbf{z}_t \tag{3.8b}$$

and thus

$$\begin{aligned}
\mathscr{E}_t + \mathscr{F}_x &= \frac{\partial}{\partial t}S(\mathbf{z}) + \frac{1}{2}\mathbf{z}_x^T K\mathbf{z}_t - \frac{1}{2}\mathbf{z}_t^T K\mathbf{z}_x, \\
\mathscr{I}_t + \mathscr{G}_x &= \frac{\partial}{\partial x}S(\mathbf{z}) + \frac{1}{2}\mathbf{z}_t^T L\mathbf{z}_x - \frac{1}{2}\mathbf{z}_x^T L\mathbf{z}_t.
\end{aligned}$$

Notice also, that $\mathbf{z}_x^T K\mathbf{z}_t$ is a scalar quantity, so $\mathbf{z}_x^T K\mathbf{z}_t = (\mathbf{z}_x^T K\mathbf{z}_t)^T = -\mathbf{z}_t^T K\mathbf{z}_x$, by the skew-symmetricity of the matrix K. Now, we have

$$\begin{aligned}
\mathscr{E}_t + \mathscr{F}_x &= \mathbf{z}_t^T\nabla_{\mathbf{z}}S(\mathbf{z}) - \frac{1}{2}(\mathbf{z}_t^T K\mathbf{z}_x + \mathbf{z}_t^T K\mathbf{z}_x) = \mathbf{z}_t^T\Big(\nabla_{\mathbf{z}}S(\mathbf{z}) - K\mathbf{z}_x\Big) = \mathbf{z}_t^T L\mathbf{z}_t = 0 \\
\mathscr{I}_t + \mathscr{G}_x &= \mathbf{z}_x^T\nabla_{\mathbf{z}}S(\mathbf{z}) - \frac{1}{2}(\mathbf{z}_x^T L\mathbf{z}_t - \mathbf{z}_x^T L\mathbf{z}_t) = \mathbf{z}_x^T\Big(\nabla_{\mathbf{z}}S(\mathbf{z}) - L\mathbf{z}_t\Big) = \mathbf{z}_x^T K\mathbf{z}_x = 0
\end{aligned}$$

since $0 = \mathbf{z}_x^T K\mathbf{z}_x - (\mathbf{z}_x^T K\mathbf{z}_x)^T = \mathbf{z}_x^T K\mathbf{z}_x + \mathbf{z}_x^T K\mathbf{z}_x = 2\mathbf{z}_x^T K\mathbf{z}_x$. Similar arguments proves the case with matrix L.

Now it only remains to show that integration of the local conservation laws in x yields global conservation of energy (GE) and momentum (GM). Clearly,

$$0 = \int_0^\ell (\mathscr{E}_t + \mathscr{F}_x)\,\mathrm{d}x = \frac{\partial}{\partial t}\int_0^\ell \mathscr{E}\,\mathrm{d}x,$$

since by periodic boundary conditions (3.7)

$$\int_o^\ell \mathscr{F}_x \,\mathrm{d}x = \mathscr{F}\Big|_0^\ell = 0.$$

Similarly we can show that

$$\frac{\partial}{\partial t}\int_0^\ell \mathscr{I} = 0,$$

which completes the proof. ■

Additional possibility exists for solutions of (3.2) periodic in time, namely that when the local conservation laws are integrated over the multiplicity of the period, one obtains a spatial conserved quantities. Observe that

$$0 = \int_0^{mT} (\mathscr{E}_t + \mathscr{F}_x) \,\mathrm{d}t = \frac{\partial}{\partial x}\int_0^{mT} \mathscr{F} \,\mathrm{d}t, \qquad m \in \mathbb{Z},$$

since by the periodicity of the solution

$$\int_0^{mT} \mathscr{E}_t \,\mathrm{d}t = \mathscr{E}\Big|_0^{mT} = 0.$$

This is so called spatial conservation of energy (spatial GE). Similarly we can show that

$$\frac{\partial}{\partial x}\int_0^{mT} \mathscr{G} = 0,$$

which is called spatial conservation of momentum (spatial GM).

3.1.1 Example: The Klein–Gordon Equation

A central point of this work is a particular class of finite difference discretizations of the equation

$$u_{tt} - u_{xx} + \chi \sin u = 0, \qquad \chi \in \{0, 1\} \tag{3.9}$$

called, for $\chi = 1$, the sine–Gordon equation and, for $\chi = 1$, the linear wave equation. Parameter χ is an "on–off" parameter for the nonlinearity and is introduced to allow more general approach to the dispersion analysis of numerical schemes. Equation (3.9) is a special case of the so called nonlinear Klein–Gordon equation

$$u_{tt} - u_{xx} + V'(u) = 0. \tag{3.10}$$

One may also find interesting to analyze variable coefficient Klein–Gordon equation. This equation ma be thought of as describing a wave propagation through medium which properties change in space as well as in time. Commonly, variable coefficient Klein–Gordon equation is written as

$$u_{tt} = \Big((\alpha(x,t))^2 u_x\Big)_x - (\beta(x,t))^2 u. \tag{3.11}$$

All the results presented here follows for this more general form and thus we will concentrate on the sine–Gordon equation.

Hamiltonian Formulation Hamiltonian equations constitute an important and interesting class of ordinary differential equations (ODEs). They describe energy–conserving systems, for instance, in celestial and molecular dynamics. A natural question arises then about possible generalizations toward partial differential equations. Let's define some terms first.

Definition 5 *Variational derivatives of the functional*

$$\mathscr{H}(p,q) = \int_a^b h(p,q)\mathrm{d}x$$

with respect to functions p and q are given by

$$\frac{\delta \mathscr{H}}{\delta p} = \sum_{n=0}^{\infty} (-1)^n \frac{\partial^n}{\partial x^n} \frac{\partial h}{\partial p_n}, \qquad \frac{\delta \mathscr{H}}{\delta q} = \sum_{n=0}^{\infty} (-1)^n \frac{\partial^n}{\partial x^n} \frac{\partial h}{\partial q_n},$$

where

$$p_n = \frac{\partial^n p}{\partial x^n}, \qquad q_n = \frac{\partial^n q}{\partial x^n}.$$

Definition 6 *An evolution partial differential equation is called Hamiltonian if it can be expressed in the form*

$$p_t = -\frac{\delta \mathscr{H}}{\delta q}, \qquad q_t = \frac{\delta \mathscr{H}}{\delta p},$$

for some functional $\mathscr{H}$. Variables p and q are then said to be canonically conjugated.

Theorem 8 *Equation (3.9) is a Hamiltonian PDE with canonically conjugated variables $q = u$ and $p = u_t$ and Hamiltonian functional*

$$\mathscr{H}(p, q) = \int_0^{\ell} \Big(\frac{1}{2} p^2 + \frac{1}{2} (q_x)^2 + \chi(1 - \cos q) \Big) \mathrm{d}x. \tag{3.12}$$

Proof: Indeed, using Definition 5

$$q_t = \frac{\delta \mathscr{H}}{\delta p} = \frac{\partial h}{\partial p} - \frac{\partial}{\partial x} \frac{\partial h}{\partial p_x} + \cdots = \frac{\partial h}{\partial p} = p \tag{3.13a}$$

$$p_t = -\frac{\delta \mathscr{H}}{\delta q} = -\frac{\partial h}{\partial q} + \frac{\partial}{\partial x} \frac{\partial h}{\partial q_x} = q_{xx} - \chi \sin q \tag{3.13b}$$

thus $p_t = u_{tt} = u_{xx} - \chi \sin u$, that is equation (3.9) is Hamiltonian. ■

Constants of Motion An important feature of equation (3.9) is existence of the so called integrals (constants) of motion. It can be shown that momentum $\mathscr{C}_1$ and Hamiltonian

(energy) functionals $\mathscr{C}_2$

$$\mathscr{C}_1 = \int_0^\ell u_x u_t \mathrm{d}x \tag{3.14a}$$

$$\mathscr{C}_2 = \int_0^\ell \Big(\frac{1}{2}(u_t)^2 + \frac{1}{2}(u_x)^2 + \chi(1-\cos u)\Big)\mathrm{d}x \tag{3.14b}$$

are constant along the flow of the system. Indeed, if equation (3.9) is furnished with periodic boundary conditions on the interval $x \in [-\ell, \ell)$, i.e. assuming (3.7), the following holds

$$\begin{aligned}
\frac{\mathrm{d}}{\mathrm{d}t}\mathscr{C}_1 &= \int_0^\ell \frac{\partial}{\partial t}(u_x u_t)\mathrm{d}x = \int_0^\ell (u_x u_{tt} + u_t u_{xt})\mathrm{d}x = \int_0^\ell (u_x[u_{xx} - \chi\sin u] + u_t u_{xt})\mathrm{d}x \\
&= \int_0^\ell \frac{\partial}{\partial x}\Big(\frac{1}{2}(u_t)^2 + \frac{1}{2}(u_x)^2 + \chi\cos u\Big)\mathrm{d}x = \Big(\frac{1}{2}(u_t)^2 + \frac{1}{2}(u_x)^2 + \chi\cos u\Big)\Big|_0^\ell \equiv 0, \\
\frac{\mathrm{d}}{\mathrm{d}t}\mathscr{C}_2 &= \int_0^\ell \frac{\partial}{\partial t}\Big(\frac{1}{2}(u_t)^2 + \frac{1}{2}(u_x)^2 + \chi(1-\cos u)\Big)\mathrm{d}x \\
&= \int_0^\ell u_t u_{tt} + u_x u_{xt} + \chi u_t \sin u \mathrm{d}x = \int_0^\ell u_t(u_{tt} - u_{xx} + \chi\sin u)\mathrm{d}x \equiv 0.
\end{aligned}$$

Conclusion follows since

$$\int_0^\ell u_x u_{xt}\mathrm{d}x = u_x u_t\Big|_{x=0}^\ell - \int_0^\ell u_t u_{xx}\mathrm{d}x = -\int_0^\ell u_t u_{xx}\mathrm{d}x.$$

Chapter 6 is devoted to analysis of the numerical schemes and presents an investigation of an extent to which these quantities are preserved by discretizations thus constructing diagnostic tools measuring performance of numerical integrators.

MS–1 Formulation We now would like to establish the multisymplectic structure of (3.9). By introducing new variables $u_t = v$ and $u_x = -w$ one can write the equation as a system of the first order PDEs [22]

$$\begin{array}{rcccl}
v_t & + & w_x & = & -\chi\sin u \\
- \; u_t & & & = & -v \\
& - & u_x & = & w
\end{array}$$

that is multisymplectic structure is given by matrices

$$L_1 = \begin{bmatrix} 0 & 1 & 0 \\ -1 & 0 & 0 \\ 0 & 0 & 0 \end{bmatrix} \quad \text{and} \quad K_1 = \begin{bmatrix} 0 & 0 & 1 \\ 0 & 0 & 0 \\ -1 & 0 & 0 \end{bmatrix} \tag{3.15}$$

with $\mathbf{z} = [u,\ v,\ w]^T$ and thus

$$S = S(\mathbf{z}) = \frac{1}{2}(w^2 - v^2) + \chi \cos u \tag{3.16}$$

Local conserved quantities (3.6) may be simplified since

$$\begin{aligned}
\mathbf{z}_x^T K_1 \mathbf{z}_t &= [u_x\ v_x\ w_x] \begin{bmatrix} 0 & 0 & 1 \\ 0 & 0 & 0 \\ -1 & 0 & 0 \end{bmatrix} \begin{bmatrix} u_t \\ v_t \\ w_t \end{bmatrix} = [u_x\ v_x\ w_x] \begin{bmatrix} w_t \\ 0 \\ -u_t \end{bmatrix} = u_x w_t - w_x u_t \\
\mathbf{z}_t^T K_1 \mathbf{z}_x &= u_t w_x - w_t u_x \\
\mathbf{z}_x^T L_1 \mathbf{z}_t &= [u_x\ v_x\ w_x] \begin{bmatrix} 0 & 1 & 0 \\ -1 & 0 & 0 \\ 0 & 0 & 0 \end{bmatrix} \begin{bmatrix} u_t \\ v_t \\ w_t \end{bmatrix} = [u_x\ v_x\ w_x] \begin{bmatrix} v_t \\ -u_t \\ 0 \end{bmatrix} = u_x v_t - v_x u_t \\
\mathbf{z}_t^T L_1 \mathbf{z}_x &= u_t v_x - v_t u_x
\end{aligned}$$

and so

$$\begin{aligned}
0 &= \mathscr{E}_t + \mathscr{F}_x = \frac{\partial}{\partial t} S(\mathbf{z}) + \frac{1}{2}(u_x w_t - w_x u_t) - \frac{1}{2}(u_t w_x - w_t u_x) \\
&= w w_t - v v_t - \chi u_t \sin u - w w_t - w_x v = -w w_t - v v_t - \chi u_t \sin u - w v_x - w_x v \\
&= -\frac{\partial}{\partial t}\Big(\frac{1}{2}(v^2 + w^2) - \chi \cos u\Big) - \frac{\partial}{\partial x}(vw).
\end{aligned}$$

Thus, upon defining

$$\tilde{\mathscr{E}} = \frac{1}{2}(v^2 + w^2) - \chi \cos u, \qquad \tilde{\mathscr{F}} = vw \tag{3.17}$$

we obtain local energy conservation law (LECL)

$$\tilde{\mathscr{E}}_t + \tilde{\mathscr{F}}_x = 0. \tag{3.18}$$

Similarly, since

$$\begin{aligned} 0 &= \mathscr{I}_t + \mathscr{G}_x = \frac{\partial}{\partial x} S(\mathbf{z}) + \frac{1}{2}(u_t v_x - v_t u_x) - \frac{1}{2}(u_x v_t - v_x u_t) \\ &= w w_x - v v_x - \chi u_x \sin u + u_t v_x - v_t u_x = w w_x + v v_x - \chi u_x \sin u + v w_t + v_t w \\ &= \frac{\partial}{\partial x}\Big(\frac{1}{2}(v^2 + w^2) + \chi \cos u\Big) + \frac{\partial}{\partial x}(vw), \end{aligned}$$

upon defining

$$\tilde{\mathscr{I}} = vw, \qquad \tilde{\mathscr{G}} = \frac{1}{2}(v^2 + w^2) + \chi \cos u, \tag{3.19}$$

we obtain local momentum conservation law (LMCL)

$$\tilde{\mathscr{I}}_t + \tilde{\mathscr{G}}_x = 0. \tag{3.20}$$

If the sine–Gordon equation is furnished with the periodic boundary conditions (3.7) one shows that global conserved quantities (3.14) follow from the local ones by integration in x, as mentioned before. For the sine–Gordon equation in the multisymplectic form (3.15) and (3.21) we can write that

$$\begin{aligned} \mathscr{C}_1 = \int_0^\ell \tilde{\mathscr{I}}\ \mathrm{d}x &= \int_0^\ell vw\ \mathrm{d}x, \\ \mathscr{C}_2 = \int_0^\ell \tilde{\mathscr{E}}\ \mathrm{d}x &= \int_0^\ell \frac{1}{2}(v^2 + w^2) - \chi \cos u\ \mathrm{d}x. \end{aligned}$$

Note that the same property holds if we take $\tilde{\mathscr{E}} + C$, for any constant C. If variables u and v are renamed as $u = q$ and $v = p$, and one take $C = \chi$, functional $\mathscr{C}_2$ yields a Hamiltonian functional (3.14b).

MS–2 Formulation Structure in (3.15) may be improved [7, 22] by observing that v and w satisfy the constraint $w_t + v_x = -u_{xt} + u_{tx} = 0$ and introducing Lagrange multiplier p. Multisymplectic canonical form

$$\begin{array}{rcccc} & v_t & + & w_x & = & -\chi \sin u \\ - & u_t & - & p_x & = & -v \\ & p_t & - & u_x & = & w \\ - & w_t & - & v_x & = & 0 \end{array}$$

or in matrix notation

$$L_2 = \begin{bmatrix} 0 & 1 & 0 & 0 \\ -1 & 0 & 0 & 0 \\ 0 & 0 & 0 & 1 \\ 0 & 0 & -1 & 0 \end{bmatrix} \quad \text{and} \quad K_2 = \begin{bmatrix} 0 & 0 & 1 & 0 \\ 0 & 0 & 0 & 1 \\ -1 & 0 & 0 & 0 \\ 0 & -1 & 0 & 0 \end{bmatrix} \tag{3.21}$$

Function $S(\mathbf{z})$ is given by (3.16) and $\mathbf{z} = [u,\ v,\ w,\ p]^T$. By the exact analogy, observing that $p_x = v - u_t = 0$ and $p_t = w + u_x = 0$, we can derive the local conserved quantities for the MS–2 formulation. They are identical to those of the MS–1 formulation.

3.1.2 Alternate Formulation via Operator Splitting

Multisymplpectic conservation law (3.3) can be simplified by considering the following splitting of pre-symplectic matrices L and K. Let

$$L = L^+ + L^-, \qquad (K^+)^T = -K^-, \tag{3.22a}$$

$$K = K^+ + K^-, \qquad (L^+)^T = -L^-. \tag{3.22b}$$

Since, by (3.5) and properties of the wedge product given in Theorem 5,

$$\mathrm{d}\mathbf{z} \wedge L^{+}\mathrm{d}\mathbf{z} = (L^{+})^{T}\mathrm{d}\mathbf{z} \wedge \mathrm{d}\mathbf{z} = -L^{-}\mathrm{d}\mathbf{z} \wedge \mathrm{d}\mathbf{z} = \mathrm{d}\mathbf{z} \wedge L^{-}\mathrm{d}\mathbf{z}.$$

and identical properties holds for matrix K, i.e. $\mathrm{d}\mathbf{z}\wedge K^{+}\mathrm{d}\mathbf{z} = \mathrm{d}\mathbf{z}\wedge K^{-}\mathrm{d}\mathbf{z}$, differential 2–forms (3.4) can be written as

$$\Omega^{(t)} = \mathrm{d}\mathbf{z} \wedge L^{+}\mathrm{d}\mathbf{z}, \tag{3.23a}$$

$$\Omega^{(x)} = \mathrm{d}\mathbf{z} \wedge K^{+}\mathrm{d}\mathbf{z}. \tag{3.23b}$$

This splitting, originally introduced in [29], due to its non-uniqueness, is helpful in constructing various explicit multisymplectic integrators which will be presented in Section 4.4.

3.1.3 Example: The Nonlinear Schrödinger Equation

Results analogous to those obtained in the first part of this chapter of variants of the Klein–Gordon equations can also be obtained for the, so called, focusing one-dimensional nonlinear Schrödinger equation (NLS)

$$\imath u_t + u_{xx} + 2|u|^2 u = 0. \tag{3.24}$$

Equation (3.24) can be written in multisymplectic form by letting $u = p + \imath q$ and introducing new variables $v = p_x$ and $w = q_x$ [21, 22]. Separating (3.24) into real and imaginary parts, we obtain the system

$$\begin{aligned} q_t - v_x &= 2(p^2+q^2)p, \\ -p_t - w_x &= 2(p^2+q^2)q, \\ p_x &= v, \\ q_x &= w, \end{aligned}$$

which is equivalent to the multisymplectic form (3.2) with $\mathbf{z} = [p,\ q,\ v,\ w]^T$ and

$$L_{NLS} = \begin{bmatrix} 0 & 1 & 0 & 0 \\ -1 & 0 & 0 & 0 \\ 0 & 0 & 0 & 0 \\ 0 & 0 & 0 & 0 \end{bmatrix}, \qquad K_{NLS} = \begin{bmatrix} 0 & 0 & -1 & 0 \\ 0 & 0 & 0 & -1 \\ 1 & 0 & 0 & 0 \\ 0 & 1 & 0 & 0 \end{bmatrix}, \tag{3.25}$$

and Hamiltonian $S = \frac{1}{2}[(p^2+q^2)^2 + v^2 + w^2]$. For this particular equation relations (3.6) can be expressed as

$$\begin{aligned} \partial_t \mathscr{E} + \partial_x \mathscr{F} &= 0, \qquad \mathscr{E} = \frac{1}{2}\Big((p^2+q^2)^2 - v^2 - w^2\Big), \quad \mathscr{F} = vp_t + wq_t, \\ \partial_t \mathscr{I} + \partial_x \mathscr{G} &= 0, \qquad \mathscr{G} = (p^2+q^2)^2 + v^2 + w^2 - (pq_t - p_t q), \quad \mathscr{I} = pw - qv. \end{aligned}$$

Additionally, we have a norm conservation law for the NLS equation

$$\partial_t \mathscr{N} + \partial_x \mathscr{M}_x = 0, \qquad \mathscr{N} = \frac{1}{2}(p^2+q^2), \quad \mathscr{M} = qv - pw.$$

These three equations, when integrated with respect to x, yield the classical global conservation of energy (the Hamiltonian), the momentum and the norm defined as

$$\begin{aligned} &\frac{\mathrm{d}}{\mathrm{d}t}\int_0^\ell \mathscr{E}(\mathbf{z})\ \mathrm{d}x = 0, \\ &\frac{\mathrm{d}}{\mathrm{d}t}\int_0^\ell \mathscr{I}(\mathbf{z})\ \mathrm{d}x = 0, \\ &\frac{\mathrm{d}}{\mathrm{d}t}\int_0^\ell \mathscr{N}(\mathbf{z})\ \mathrm{d}x = 0. \end{aligned}$$

In the Chapter 5 we linearize equation (3.24) about the plain wave solution to obtain a real, second order in time, fourth order in space equation which we prove is also multisymplectic. We than use box scheme discretization of this linearized NLS to derive numerical dispersion relationships associated with it.

3.2 Multisymplecticness in Fourier Space

It is known (cf. [1, 2, 3, 24]) that finite difference discretizations may not be able to resolve spatial structures of the solution in sensitive regimes. Finite difference discretization are of polynomial accuracy so for such challenging problems more accurate approaches were developed – Fourier spectral discretizations that are exponentially accurate. Spectral discretizations have proven to be highly effective methods for solving problems with simple boundary conditions. Before we present Fourier spectral discretizations (in Chapter 4) we have to develop the underlying "continuous" theory. In this section we use the Fourier series expansion to transform equation (3.2) and obtain an infinite-dimensional system of ODEs having multisymplectic structure. In order to achieve this, similarly to the approach of [22], consider a multisymplectic PDE in the form (3.2). Using Fourier series expansion

$$\mathbf{z}(x,t) = \sum_{k=-\infty}^{\infty} \hat{\mathbf{z}}_k(t) e^{\imath k\nu x}, \tag{3.26a}$$

$$\hat{\mathbf{z}}_k = \frac{1}{\ell}\int_{-\ell/2}^{\ell/2} \mathbf{z}(x,t) e^{-\imath k\nu x} \mathrm{d}x, \tag{3.26b}$$

where

$$\nu = 2\pi/\ell, \tag{3.27}$$

to transform x–dependence of $\mathbf{z}$ to k–dependence in the interval $x \in [-\ell/2, \ell/2)$. Transformation (3.26a) applied to equation (3.2) gives

$$L\partial_t\Big(\sum_{k=-\infty}^{\infty} \hat{\mathbf{z}}_k(t) e^{\imath k\nu x}\Big) + K\partial_x\Big(\sum_{k=-\infty}^{\infty} \hat{\mathbf{z}}_k(t) e^{\imath k\nu x}\Big) = \nabla_{\mathbf{z}} S\Big(\sum_{k=-\infty}^{\infty} \hat{\mathbf{z}}_k(t) e^{\imath k\nu x}\Big).$$

Multiplying by $e^{-\imath m\nu x}$, for some $m \in \mathbb{Z}$, and integrating over $x \in [-\ell/2, \ell/2)$ we have

$$L\partial_t \int_{-\ell/2}^{\ell/2} \Big(\sum_{k=-\infty}^{\infty} \hat{\mathbf{z}}_k(t) e^{\imath k\nu x} \Big) e^{-\imath m\nu x} \mathrm{d}x + K \int_{-\ell/2}^{\ell/2} \partial_x \Big(\sum_{k=-\infty}^{\infty} \hat{\mathbf{z}}_k(t) e^{\imath k\nu x} \Big) e^{-\imath m\nu x} \mathrm{d}x$$
$$= \int_{-\ell/2}^{\ell/2} \nabla_{\mathbf{z}} S \Big(\sum_{k=-\infty}^{\infty} \hat{\mathbf{z}}_k(t) e^{\imath k\nu x} \Big) e^{-\imath m\nu x} \mathrm{d}x.$$

Integration by parts yields

$$\begin{aligned} \int_{-\ell/2}^{\ell/2} \partial_x \Big(\sum_{k=-\infty}^{\infty} \hat{\mathbf{z}}_k(t) e^{\imath k\nu x} \Big) e^{-\imath m\nu x} \mathrm{d}x &= \mathbf{z}(x,t) e^{-\imath m\nu x} \Big|_{-\ell/2}^{\ell/2} \\ &\quad - \int_{-\ell/2}^{\ell/2} \Big(\sum_{k=-\infty}^{\infty} \hat{\mathbf{z}}_k(t) e^{\imath k\nu x} \Big) (-\imath m\nu) e^{-\imath m\nu x} \mathrm{d}x \end{aligned}$$

and thus, by periodicity in x, $\mathbf{z}(-\ell/2, t) = \mathbf{z}(\ell/2, t)$,

$$\mathbf{z}(x,t) e^{-\imath m\nu x} \Big|_{-\ell/2}^{\ell/2} = 0.$$

Denoting $\vartheta_m = -\imath m\nu$ we have

$$L\partial_t \int_{-\ell/2}^{\ell/2} \Big(\sum_{k=-\infty}^{\infty} \hat{\mathbf{z}}_k(t) e^{\imath k\nu x} \Big) e^{-\imath m\nu x} \mathrm{d}x + K\vartheta_m \int_{-\ell/2}^{\ell/2} \Big(\sum_{k=-\infty}^{\infty} \hat{\mathbf{z}}_k(t) e^{\imath k\nu x} \Big) e^{-\imath m\nu x} \mathrm{d}x$$
$$= \int_{-\ell/2}^{\ell/2} \nabla_{\mathbf{z}} S \Big(\sum_{k=-\infty}^{\infty} \hat{\mathbf{z}}_k(t) e^{\imath k\nu x} \Big) e^{-\imath m\nu x} \mathrm{d}x.$$

which, by definition (3.26b) of Fourier series coefficient, can be written as

$$L\partial_t \hat{\mathbf{z}}_m(t) + K\vartheta_m \hat{\mathbf{z}}_m(t) = \frac{1}{\ell} \int_{-\ell/2}^{\ell/2} \nabla_{\mathbf{z}} S \Big(\sum_{k=-\infty}^{\infty} \hat{\mathbf{z}}_k(t) e^{\imath k\nu x} \Big) e^{-\imath m\nu x} \mathrm{d}x.$$

Note also, that the following change of variables $x = -x$ and $k = -k$ allows us to write that

$$\begin{aligned} \frac{1}{\ell} \int_{-\ell/2}^{\ell/2} \nabla_{\mathbf{z}} S \Big(\sum_{k=-\infty}^{\infty} \hat{\mathbf{z}}_k(t) e^{\imath k\nu x} \Big) e^{-\imath m\nu x} \mathrm{d}x &= \frac{1}{\ell} \int_{-\ell/2}^{\ell/2} \nabla_{\mathbf{z}} S \Big(\sum_{k=-\infty}^{\infty} \hat{\mathbf{z}}_k(t) e^{\imath k\nu x} \Big) e^{\imath m\nu x} \mathrm{d}x \\ &= \frac{1}{\ell} \int_{-\ell/2}^{\ell/2} \nabla_{\mathbf{z}} S \Big(\sum_{k=-\infty}^{\infty} \hat{\mathbf{z}}_k(t) e^{\imath k\nu x} \Big) \frac{\partial \mathbf{z}}{\partial \hat{\mathbf{z}}_m} \mathrm{d}x \\ &= \nabla_{\hat{\mathbf{z}}_m} \hat{S}(\hat{\mathbf{Z}}), \end{aligned}$$

where

$$\hat{S}(\hat{\mathbf{Z}}) = \frac{1}{\ell}\int_{-\ell/2}^{\ell/2} S\Big(\sum_{k=-\infty}^{\infty} \hat{\mathbf{z}}_k(t)e^{\imath k\nu x}\Big)\mathrm{d}x.$$

The equation holds since from (3.26)

$$\frac{\partial \mathbf{z}}{\partial \hat{\mathbf{z}}_m} = e^{\imath m\nu x},$$

which means that for every $m \in \mathbb{Z}$ we have obtained multisymplectic-like equation

$$L\partial_t \hat{\mathbf{z}}_m(t) + K\vartheta_m \hat{\mathbf{z}}_m(t) = \nabla_{\hat{\mathbf{z}}_m}\hat{S}(\hat{\mathbf{Z}}). \tag{3.28}$$

System of equations of the form (3.28) for $m \in \mathbb{Z}$, in fact represents an infinite system of ODEs which we will be calling, following [9, 22], a multisymplectic spectral PDE and typically write as

$$\mathbf{L}\partial_t \hat{\mathbf{Z}}(t) + \mathbf{K}\boldsymbol{\Theta}\hat{\mathbf{Z}}(t) = \nabla_{\hat{\mathbf{Z}}}\hat{S}(\hat{\mathbf{Z}}), \tag{3.29}$$

where $\hat{\mathbf{Z}} = [\ldots,\ \hat{\mathbf{z}}_m^T,\ \ldots]^T$, $\hat{\mathbf{z}}_m = [\hat{z}_m^1, \ldots,\ \hat{z}_m^d]^T$, matrices $\mathbf{L}$ and $\mathbf{K}$ are given in terms of the Kronecker's product (see Definition 1 in Chapter 1) $\mathbf{L} = I_\infty \otimes L$, $\mathbf{K} = I_\infty \otimes K$ with I_∞ being matrix representation of the identity operator acting on infinite sequences. Note that $\mathbf{L}^T = (I_\infty \otimes L)^T = I_\infty^T \otimes L^T = -(I_\infty \otimes L) = -\mathbf{L}$, and the same property holds for the matrix $\mathbf{K}$. Moreover, we define

$$\boldsymbol{\Theta} = \begin{bmatrix} \ddots & & \\ & \Theta_m & \\ & & \ddots \end{bmatrix}$$

with $\Theta_m = \vartheta_m I_d$ and $I_d \in \mathcal{M}_{d\times d}(\mathbb{R})$ being the identity matrix.

Theorem 9 *Equation (3.29) satisfies the following (spectral) multisymplectic conservation law*

$$\partial_t \hat{\Omega}^{(t)} + \hat{\Omega}^{(x)} = 0, \tag{3.30}$$

with

$$\hat{\Omega}^{(t)} = \frac{1}{2} \mathrm{d}\hat{\mathbf{Z}} \wedge \mathbf{L} \mathrm{d}\hat{\mathbf{Z}}, \tag{3.31a}$$

$$\hat{\Omega}^{(x)} = \frac{1}{2} (\mathbf{\Theta} \mathrm{d}\hat{\mathbf{Z}}) \wedge (\mathbf{K} \mathrm{d}\hat{\mathbf{Z}}) + \frac{1}{2} \mathrm{d}\hat{\mathbf{Z}} \wedge (\mathbf{K}\mathbf{\Theta} \mathrm{d}\hat{\mathbf{Z}}). \tag{3.31b}$$

Proof: Indeed, since the variational equation associated with (3.29) is

$$\mathbf{L}\partial_t \mathrm{d}\hat{\mathbf{Z}} + \mathbf{K}\mathbf{\Theta} \mathrm{d}\hat{\mathbf{Z}} = \hat{S}_{\hat{\mathbf{Z}}\hat{\mathbf{Z}}} \mathrm{d}\hat{\mathbf{Z}},$$

taking the wedge product of both sides of the variational equation with $\mathrm{d}\hat{\mathbf{Z}}$, one obtains

$$\mathrm{d}\hat{\mathbf{Z}} \wedge \mathbf{L} \mathrm{d}\hat{\mathbf{Z}}_t + \mathrm{d}\hat{\mathbf{Z}} \wedge \mathbf{K}\mathbf{\Theta} \mathrm{d}\hat{\mathbf{Z}} = \mathrm{d}\hat{\mathbf{Z}} \wedge (\hat{S}_{\hat{\mathbf{Z}}\hat{\mathbf{Z}}} \mathrm{d}\hat{\mathbf{Z}}).$$

Since $\hat{S}_{\hat{\mathbf{Z}}\hat{\mathbf{Z}}}$, the Hessian matrix, is symmetric we have that

$$\mathrm{d}\hat{\mathbf{Z}} \wedge (\hat{S}_{\hat{\mathbf{Z}}\hat{\mathbf{Z}}} \mathrm{d}\hat{\mathbf{Z}}) = (\hat{S}_{\hat{\mathbf{Z}}\hat{\mathbf{Z}}} \mathrm{d}\hat{\mathbf{Z}}) \wedge \mathrm{d}\hat{\mathbf{Z}} = -\mathrm{d}\hat{\mathbf{Z}} \wedge (\hat{S}_{\hat{\mathbf{Z}}\hat{\mathbf{Z}}} \mathrm{d}\hat{\mathbf{Z}}),$$

by the skew-symmetry of the wedge product. Clearly now

$$\begin{aligned} 0 &= \mathrm{d}\hat{\mathbf{Z}} \wedge \mathbf{L} \mathrm{d}\hat{\mathbf{Z}}_t + \mathrm{d}\hat{\mathbf{Z}} \wedge \mathbf{K}\mathbf{\Theta} \mathrm{d}\hat{\mathbf{Z}} \\ &= \partial_t (\mathrm{d}\hat{\mathbf{Z}} \wedge \mathbf{L} \mathrm{d}\hat{\mathbf{Z}}) + \mathbf{L}(\mathrm{d}\hat{\mathbf{Z}})_t \wedge \mathrm{d}\hat{\mathbf{Z}} \\ &\quad + \mathrm{d}\hat{\mathbf{Z}} \wedge (\mathbf{K}\mathbf{\Theta} \mathrm{d}\hat{\mathbf{Z}}) + (\mathbf{\Theta} \mathrm{d}\hat{\mathbf{Z}}) \wedge (\mathbf{K} \mathrm{d}\hat{\mathbf{Z}}) + (\mathbf{K}\mathbf{\Theta} \mathrm{d}\hat{\mathbf{Z}}) \wedge \mathrm{d}\hat{\mathbf{Z}}. \end{aligned} \tag{3.32}$$

Distributivity (linearity) of the wedge product guarantees that

$$\mathbf{L}(\mathrm{d}\hat{\mathbf{Z}})_t \wedge \mathrm{d}\hat{\mathbf{Z}} + (\mathbf{\Theta}\mathbf{K} \mathrm{d}\hat{\mathbf{Z}}) \wedge \mathrm{d}\hat{\mathbf{Z}} = (\mathbf{L} \mathrm{d}\hat{\mathbf{Z}}_t + \mathbf{K}\mathbf{\Theta} \mathrm{d}\hat{\mathbf{Z}}) \wedge \mathrm{d}\hat{\mathbf{Z}} = (\hat{S}_{\hat{\mathbf{Z}}\hat{\mathbf{Z}}} \mathrm{d}\hat{\mathbf{Z}}) \wedge \mathrm{d}\hat{\mathbf{Z}} = 0,$$

which guarantees the existence of the spectral multisymplectic conservation law. ■

Additionally, a multisymplectic spectral PDE has the local energy conservation law associated with it. This law takes the form

$$\partial_t \hat{\mathscr{E}} + \hat{\mathscr{F}} = 0, \tag{3.33}$$

with

$$\hat{\mathscr{E}} = \hat{S}(\hat{\mathbf{Z}}) + \langle \mathbf{L}\hat{\mathbf{Z}}, \mathbf{\Theta}\hat{\mathbf{Z}} \rangle, \tag{3.34a}$$

$$\hat{\mathscr{F}} = \frac{1}{2}\langle \mathbf{K}\mathbf{\Theta}\hat{\mathbf{Z}}, \hat{\mathbf{Z}}_t \rangle + \frac{1}{2}\langle \mathbf{K}\hat{\mathbf{Z}}, \mathbf{\Theta}\hat{\mathbf{Z}}_t \rangle. \tag{3.34b}$$

where $\langle \mathbf{u}, \mathbf{v} \rangle = \mathbf{v}^* \mathbf{u}$ denotes a standard complex inner product. It is more convenient to derive (3.33) in the framework of the wave action conservation law. We defer the proof till Chapter 7 (see section 7.4.1) and summarize this section with the following

Theorem 10 *Solution of the spectral multisymplectic equation (3.29) satisfies spectral multisymplectic conservation law (3.30) (sMSCL), as well as the so called spectral local energy conservation law (sLECL) (3.33).*

CHAPTER FOUR: MULTISYMPLECTIC DISCRETIZATIONS

Emergence of multiymplectic formulation for Hamiltonian PDEs clarified the theory of such systems in many respects thus permitting analysis of local properties and the study of stability for traveling wave solutions. It has also become very useful for the study of discretizations for such systems by making the extension from symplectic integration to multisymplectic integration simple. Multisymplectic integration has been presented by Marsden, Patrick and Shkoller [26] who use the multisymplectic structure of wave equations. Their approach derives a numerical scheme from the Lagrangian formulation in first-order field theory using a discrete variational principle. Approach to multisymplectic integration presented in this thesis was suggested by Bridges and Reich [9, 11] and elaborated by others (cf. [6, 14, 21, 22, 23, 28, 29, 35, 38, 39, 41]), and is based on the multisymplectic structure of the equations. This approach uses the application of a symplectic method to each independent variable (concatenation of symplectic discretozations), and defines multisymplectic integrators as methods that preserve a discrete version of a multisymplectic conservation law.

In the first part this chapter we derive two multisymplectic finite-difference integrators and discuss their implementation. In the second part we give three other numerical methods based on a second order, Hamiltonian spatial semi-discretization of the sine–Gordon equation. Those numerical methods are symplectic (MS–3 and MS–4) and non-symplectic (ERK) time integrators of second order. It turns out that method designated MS–3 and MS–4 are multisymplectic and we refer to them as "symplectic" to indicate that their derivation is

based on symplectic time discretization of a Hamiltonian spatial semi-discretization. We also discuss MS Euler scheme obtained by using alternate form the multisymplectic PDE formulated via operator splitting.

4.1 Multisymplectic Finite Difference Schemes

Symplectic discretizations discussed in Chapter 2 are designed to preserve the symplectic structure of the equation. This is achieved by requiring that the discrete differential two-form associated with the integrator be invariant under the flow of the (discrete) system. Multisymplectic discretizations are numerical schemes for approximating (3.2) which preserve a discrete version of the multisymplectic conservation law (3.3) exactly, i.e. up to the round-off error. That is, if the discretization of the multisymplectic PDE and its conservation law are written schematically as

$$L \cdot \partial_t^{j,n} \mathbf{z}_j^n + K \cdot \tilde{\partial}_x^{j,n} \mathbf{z}_j^n = \left(\nabla_z S(\mathbf{z}_j^n) \right)_j^n \tag{4.1}$$

and

$$\partial_t^{j,n} (\Omega^{(t)})_j^n + \tilde{\partial}_x^{j,n} (\Omega^{(x)})_j^n = 0, \tag{4.2}$$

where $\partial_t^{j,n}$ and $\tilde{\partial}_x^{j,n}$ are discretizations of the corresponding derivatives ∂_t and ∂_x, the numerical scheme (4.1) is said to be multisymplectic if (4.2) is a discrete conservation law of (4.1) [11, 9, 22, 24, 28].

4.2 Multisymplectic Box Scheme

4.2.1 Integral Equation Approach

In many cases, a finite difference numerical scheme may be derived in a very elegant and efficient way by integrating the original differential equation over the domain of interest. Integrating both sides of equation (3.2) over the square chosen to be a single mesh element, presented in Figure 4.1, one obtains

$$\int_{t_n}^{t_{n+1}} \int_{x_j}^{x_{j+1}} L\mathbf{z}_t + K\mathbf{z}_x \, \mathrm{d}t \, \mathrm{d}x = \int_{t_n}^{t_{n+1}} \int_{x_j}^{x_{j+1}} \nabla_{\mathbf{z}} S \, \mathrm{d}t \, \mathrm{d}x,$$

which, by the Fundamental Theorem of Calculus, becomes

$$\begin{aligned} L \int_{x_j}^{x_{j+1}} \mathbf{z}(t_{n+1}, x) - \mathbf{z}(t_n, x) \, \mathrm{d}x \quad &+ \quad K \int_{t_n}^{t_{n+1}} \mathbf{z}(t, x_{j+1}) - \mathbf{z}(t, x_j) \, \mathrm{d}t \\ &= \int_{t_n}^{t_{n+1}} \int_{x_j}^{x_{j+1}} \nabla_{\mathbf{z}} S \, \mathrm{d}t \, \mathrm{d}x. \end{aligned} \tag{4.3}$$

Choosing a midpoint approximation (linear approximation of the integrand between mesh nodes) to the integrals in (4.3), one have the box scheme.

4.2.2 Semi–discretization Approach

Another possibility leading to the box scheme is to first obtain semi-discretization for ∂_t operator. Let's fix x and write (3.15) as

$$L\frac{\mathrm{d}\mathbf{z}}{\mathrm{d}t} = f(\mathbf{z}(t)) = \nabla_{\mathbf{z}} S(\mathbf{z}) - K\partial_x \mathbf{z}.$$

Applying implicit midpoint rule to the time derivative, we get

$$L\frac{\mathbf{z}(t+\Delta t, x) - \mathbf{z}(t, x)}{\Delta t} = f\Big(\mathbf{z}(t + \frac{\Delta t}{2}, x)\Big).$$

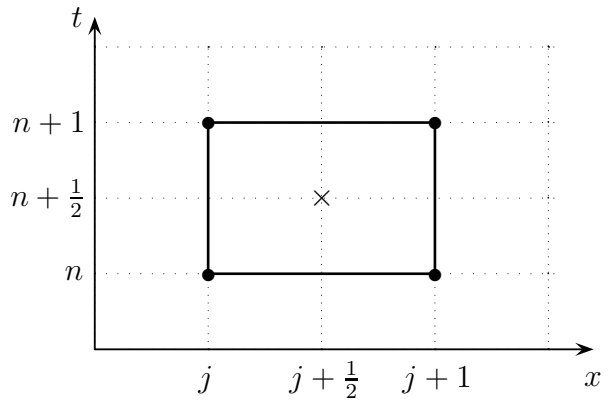

Figure 4.1: A single element of a general finite difference numerical mesh and the index notation used in discretizations.

By the same token, when we now fix t, we have

$$K\frac{\mathrm{d}}{\mathrm{d}x}\mathbf{z}(t+\frac{\Delta t}{2},x) = \nabla_{\mathbf{z}}S(\mathbf{z}(t+\frac{\Delta t}{2},x)) - L\frac{\mathbf{z}(t+\Delta t,x)-\mathbf{z}(t,x)}{\Delta t} = g\Big(\mathbf{z}(t+\frac{\Delta t}{2},x)\Big)$$

and upon application of the implicit midpoint rule to the x–derivative, we get

$$K\frac{\mathbf{z}(t+\frac{\Delta t}{2},x+\Delta x)-\mathbf{z}(t+\frac{\Delta t}{2},x)}{\Delta x} = g\Big(\mathbf{z}(t+\frac{\Delta t}{2},x+\frac{\Delta x}{2})\Big)$$

Finally

$$K\frac{\mathbf{z}(t+\frac{\Delta t}{2},x+\Delta x)-\mathbf{z}(t+\frac{\Delta t}{2},x)}{\Delta x} + L\frac{\mathbf{z}(t+\Delta t,x+\frac{\Delta x}{2})-\mathbf{z}(t,x+\frac{\Delta x}{2})}{\Delta t} = \nabla_{\mathbf{z}}S\Big(\mathbf{z}(t+\frac{\Delta t}{2},x+\frac{\Delta x}{2})\Big)$$

If we furthermore introduce the following approximations

$$\begin{aligned}
\mathbf{z}(t+\frac{\Delta t}{2},x) &\approx \frac{1}{2}\Big(\mathbf{z}(t,x)+\mathbf{z}(t+\Delta t,x)\Big),\\
\mathbf{z}(t+\frac{\Delta t}{2},x+\Delta x) &\approx \frac{1}{2}\Big(\mathbf{z}(t,x+\Delta x)+\mathbf{z}(t+\Delta t,x+\Delta x)\Big),\\
\mathbf{z}(t,x+\frac{\Delta x}{2}) &\approx \frac{1}{2}\Big(\mathbf{z}(t,x)+\mathbf{z}(t,x+\Delta x)\Big),\\
\mathbf{z}(t+\Delta t,x+\frac{\Delta x}{2}) &\approx \frac{1}{2}\Big(\mathbf{z}(t+\Delta t,x)+\mathbf{z}(t+\Delta t,x+\Delta x)\Big),\\
\mathbf{z}(t+\frac{\Delta t}{2},x+\frac{\Delta x}{2}) &\approx \frac{1}{4}\Big(\mathbf{z}(t,x)+\mathbf{z}(t+\Delta t,x)+\mathbf{z}(t,x+\Delta x)+\mathbf{z}(t+\Delta t,x+\Delta x)\Big),
\end{aligned}$$

we get

$$\begin{aligned}
&K\frac{\mathbf{z}(t+\Delta t,x+\Delta x)-\mathbf{z}(t+\Delta t,x)+\mathbf{z}(t,x+\Delta x)-\mathbf{z}(t,x)}{2\Delta x}\\
&\quad +L\frac{\mathbf{z}(t+\Delta t,x+\Delta x)+\mathbf{z}(t+\Delta t,x)-\mathbf{z}(t,x+\Delta x)-\mathbf{z}(t,x)}{2\Delta t}\\
&=\nabla_{\mathbf{z}}S\Big(\frac{1}{4}(\mathbf{z}(t+\Delta t,x+\Delta x)+\mathbf{z}(t+\Delta t,x)+\mathbf{z}(t,x+\Delta x)+\mathbf{z}(t,x))\Big). \qquad (4.4)
\end{aligned}$$

Introduce index notation

$$\mathbf{z}(t_n,x_j)=\mathbf{z}_j^n, \qquad j\in\{1,\dots,J\}, n\in\{1,\dots,N\},$$

for some J and N, where $t_{n+1}=t_0+n\Delta t$ and $x_{j+1}=x_0+j\Delta x$. Let's also introduce difference operator notation [6]

$$\begin{aligned}
\mathsf{D}_x[\mathbf{z}](t,x) &= \frac{\mathbf{z}(t,x+\Delta x)-\mathbf{z}(t,x)}{\Delta x} \qquad & \mathsf{D}_t[\mathbf{z}](t,x) &= \frac{\mathbf{z}(t+\Delta t,x)-\mathbf{z}(t,x)}{\Delta t}\\
\mathsf{M}_x[\mathbf{z}](t,x) &= \frac{\mathbf{z}(t,x+\Delta x)+\mathbf{z}(t,x)}{2} \qquad & \mathsf{M}_t[\mathbf{z}](t,x) &= \frac{\mathbf{z}(t+\Delta t,x)+\mathbf{z}(t,x)}{2}
\end{aligned}$$

Now (4.4) has an equivalent form

$$K\cdot\mathsf{M}_t\mathsf{D}_x[\mathbf{z}](t,x)+L\cdot\mathsf{M}_x\mathsf{D}_t[\mathbf{z}](t,x)=\nabla_{\mathbf{z}}S(\mathsf{M}_t\mathsf{M}_x[\mathbf{z}](t,x)). \qquad (4.5)$$

Before proceeding to the fully discrete case let's state the following

Lemma 3 *Operators* D_x, D_t, M_x, M_t *are linear and commutative with respect to the standard operation of composition of functions.*

PROOF: It suffices to prove one case of each – all the rest follows by the exact same argument. We decided to show linearity of D_t and commutativity of $\mathsf{M}_x \circ \mathsf{M}_t$. For the proof consider then

$$\begin{aligned}
\mathsf{D}_t[\mathbf{u}+\alpha\mathbf{v}](t,x) &= \frac{(\mathbf{u}+\alpha\mathbf{v})(t,x+\Delta x)-(\mathbf{u}+\alpha\mathbf{v})(t,x)}{\Delta x} \\
&= \frac{(\mathbf{u}(t,x+\Delta x)+\alpha\mathbf{v}(t,x+\Delta x))-(\mathbf{u}(t,x)+\alpha\mathbf{v}(t,x))}{\Delta x} \\
&= \mathsf{D}_t[\mathbf{u}](t,x)+\alpha\mathsf{D}_t[\mathbf{v}](t,x),
\end{aligned}$$

which proves linearity of D_t. Moreover

$$\begin{aligned}
\mathsf{M}_x\mathsf{M}_t[\mathbf{z}](t,x) &= \mathsf{M}_x\left[\frac{\mathbf{z}(t+\Delta t,x)+\mathbf{z}(t,x)}{2}\right] = \frac{\mathsf{M}_x[\mathbf{z}(t+\Delta t,x)]+\mathsf{M}_x[\mathbf{z}(t,x)]}{2} \\
&= \frac{1}{4}(\mathbf{z}(t+\Delta t,x+\Delta x)+\mathbf{z}(t+\Delta t,x)+\mathbf{z}(t,x+\Delta x)+\mathbf{z}(t,x))
\end{aligned}$$

and

$$\begin{aligned}
\mathsf{M}_t\mathsf{M}_x[\mathbf{z}](t,x) &= \mathsf{M}_t\left[\frac{\mathbf{z}(t,x+\Delta x)+\mathbf{z}(t,x)}{2}\right] = \frac{\mathsf{M}_t[\mathbf{z}(t,x+\Delta x)]+\mathsf{M}_t[\mathbf{z}(t,x)]}{2} \\
&= \frac{1}{4}(\mathbf{z}(t+\Delta t,x+\Delta x)+\mathbf{z}(t,x+\Delta x)+\mathbf{z}(t+\Delta t,x)+\mathbf{z}(t,x))
\end{aligned}$$

therefore

$$\mathsf{M}_x\mathsf{M}_t[\mathbf{z}](t,x) = \mathsf{M}_t\mathsf{M}_x[\mathbf{z}](t,x)$$

and the proof is completed. ■

4.2.3 Multisymplecticness of the Box Scheme

Let's introduce the following index notation for the discrete form of operators (4.4)

$$D_x \mathbf{z}_j^n = \frac{\mathbf{z}_{j+1}^n - \mathbf{z}_j^n}{\Delta x} \qquad D_t \mathbf{z}_j^n = \frac{\mathbf{z}_j^{n+1} - \mathbf{z}_j^n}{\Delta t} \tag{4.6a}$$

$$M_x \mathbf{z}_j^n = \frac{\mathbf{z}_{j+1}^n + \mathbf{z}_j^n}{2} \qquad M_t \mathbf{z}_j^n = \frac{\mathbf{z}_j^{n+1} + \mathbf{z}_j^n}{2} \tag{4.6b}$$

Operators defined by (4.6) has the same properties as the ones stated in the Lemma 3, i.e. these operators are linear and commute with each other. We use this properties to establish that the box scheme is a multisymplectic discretization.

Box scheme discretization (4.5), with notation introduced in (4.6),takes the form

$$K \cdot M_t D_x \mathbf{z}_j^n + L \cdot M_x D_t \mathbf{z}_j^n = \nabla_{\mathbf{z}} S(M_t M_x \mathbf{z}_j^n). \tag{4.7}$$

Associated with equation (4.7) is the following discrete variational equation

$$L \cdot D_t M_x \mathrm{d}\mathbf{z}_j^n + K \cdot D_x M_t \mathrm{d}\mathbf{z}_j^n = S_{\mathbf{zz}} M_t M_x \mathrm{d}\mathbf{z}_j^n. \tag{4.8}$$

Taking the wedge product of $M_t M_x \mathrm{d}\mathbf{z}_j^n$ with the equation (4.8) one can directly show the discrete multisymplectic conservation law associated with this discretization. Claearly

$$M_t M_x \mathrm{d}\mathbf{z}_j^n \wedge L \cdot D_t M_x \mathrm{d}\mathbf{z}_j^n + M_t M_x \mathrm{d}\mathbf{z}_j^n \wedge K \cdot D_x M_t \mathrm{d}\mathbf{z}_j^n = M_t M_x \mathrm{d}\mathbf{z}_j^n \wedge S_{\mathbf{zz}} M_t M_x \mathrm{d}\mathbf{z}_j^n$$

and one notes that the right-hand side is zero since $S_{\mathbf{zz}}$ (the Hessian matrix) is symmetric. Indeed

$$\begin{aligned} 8 M_t M_x \mathrm{d}\mathbf{z}_j^n \wedge S_{\mathbf{zz}} M_t M_x \mathrm{d}\mathbf{z}_j^n \;&=\; (\mathrm{d}\mathbf{z}_{j+1}^{n+1} + \mathrm{d}\mathbf{z}_j^{n+1} + \mathrm{d}\mathbf{z}_{j+1}^n + \mathrm{d}\mathbf{z}_j^n) \\ &\quad \wedge S_{\mathbf{zz}} (\mathrm{d}\mathbf{z}_{j+1}^{n+1} + \mathrm{d}\mathbf{z}_j^{n+1} + \mathrm{d}\mathbf{z}_{j+1}^n + \mathrm{d}\mathbf{z}_j^n) \end{aligned}$$

and by Theorem 5 (bi-linearity) the right-hand side of the previous equation reads

$$
\begin{aligned}
&\mathrm{d}\mathbf{z}_{j+1}^{n+1} \wedge S_{\mathbf{zz}}(\mathrm{d}\mathbf{z}_{j+1}^{n+1} + \mathrm{d}\mathbf{z}_{j}^{n+1} + \mathrm{d}\mathbf{z}_{j+1}^{n} + \mathrm{d}\mathbf{z}_{j}^{n}) \\
&\quad + \mathrm{d}\mathbf{z}_{j}^{n+1} \wedge S_{\mathbf{zz}}(\mathrm{d}\mathbf{z}_{j+1}^{n+1} + \mathrm{d}\mathbf{z}_{j}^{n+1} + \mathrm{d}\mathbf{z}_{j+1}^{n} + \mathrm{d}\mathbf{z}_{j}^{n}) \\
&\quad + \mathrm{d}\mathbf{z}_{j+1}^{n} \wedge S_{\mathbf{zz}}(\mathrm{d}\mathbf{z}_{j+1}^{n+1} + \mathrm{d}\mathbf{z}_{j}^{n+1} + \mathrm{d}\mathbf{z}_{j+1}^{n} + \mathrm{d}\mathbf{z}_{j}^{n}) \\
&\quad + \mathrm{d}\mathbf{z}_{j}^{n} \wedge S_{\mathbf{zz}}(\mathrm{d}\mathbf{z}_{j+1}^{n+1} + \mathrm{d}\mathbf{z}_{j}^{n+1} + \mathrm{d}\mathbf{z}_{j+1}^{n} + \mathrm{d}\mathbf{z}_{j}^{n}) \\
&= \mathrm{d}\mathbf{z}_{j+1}^{n+1} \wedge S_{\mathbf{zz}}(\mathrm{d}\mathbf{z}_{j}^{n+1} + \mathrm{d}\mathbf{z}_{j+1}^{n} + \mathrm{d}\mathbf{z}_{j}^{n}) + \mathrm{d}\mathbf{z}_{j}^{n+1} \wedge S_{\mathbf{zz}}(\mathrm{d}\mathbf{z}_{j+1}^{n+1} + \mathrm{d}\mathbf{z}_{j+1}^{n} + \mathrm{d}\mathbf{z}_{j}^{n}) \\
&\quad + \mathrm{d}\mathbf{z}_{j+1}^{n} \wedge S_{\mathbf{zz}}(\mathrm{d}\mathbf{z}_{j+1}^{n+1} + \mathrm{d}\mathbf{z}_{j}^{n+1} + \mathrm{d}\mathbf{z}_{j}^{n}) + \mathrm{d}\mathbf{z}_{j}^{n} \wedge S_{\mathbf{zz}}(\mathrm{d}\mathbf{z}_{j+1}^{n+1} + \mathrm{d}\mathbf{z}_{j}^{n+1} + \mathrm{d}\mathbf{z}_{j+1}^{n}).
\end{aligned}
$$

The simplification is now straightforward. For instance, we note that by the skew-symmetry property from the Theorem 5),

$$
\mathrm{d}\mathbf{z}_{j+1}^{n+1} \wedge S_{\mathbf{zz}}\mathrm{d}\mathbf{z}_{j}^{n+1} + \mathrm{d}\mathbf{z}_{j}^{n+1} \wedge S_{\mathbf{zz}}\mathrm{d}\mathbf{z}_{j+1}^{n+1} = \mathrm{d}\mathbf{z}_{j+1}^{n+1} \wedge S_{\mathbf{zz}}\mathrm{d}\mathbf{z}_{j}^{n+1} - (S_{\mathbf{zz}}\mathrm{d}\mathbf{z}_{j+1}^{n+1}) \wedge \mathrm{d}\mathbf{z}_{j}^{n+1} = 0
$$

and all the remaining terms simplify in the analogous manner leading to the conclusion that

$$
M_t M_x \mathrm{d}\mathbf{z}_{j}^{n} \wedge S_{\mathbf{zz}} M_t M_x \mathrm{d}\mathbf{z}_{j}^{n} = 0.
$$

To complete the derivation of the discrete multisymplectic conservation law for the box scheme discretization, it remains to show that

$$
\frac{1}{2} D_t (M_x \mathrm{d}\mathbf{z}_{j}^{n} \wedge L M_x \mathrm{d}\mathbf{z}_{j}^{n}) + \frac{1}{2} D_x (M_t \mathrm{d}\mathbf{z}_{j}^{n} \wedge K M_t \mathrm{d}\mathbf{z}_{j}^{n}) = 0. \tag{4.9}
$$

We have that

$$\begin{aligned}
0 &= M_t M_x \mathrm{d}\mathbf{z}_j^n \wedge L D_t M_x \mathrm{d}\mathbf{z}_j^n + M_t M_x \mathrm{d}\mathbf{z}_j^n \wedge K D_x M_t \mathrm{d}\mathbf{z}_j^n \\
&= \frac{1}{2(\Delta t)}(M_x \mathrm{d}\mathbf{z}_j^{n+1} + M_x \mathrm{d}\mathbf{z}_j^n) \wedge L(M_x \mathrm{d}\mathbf{z}_j^{n+1} - M_x \mathrm{d}\mathbf{z}_j^n) \\
&\qquad + \frac{1}{2(\Delta x)}(M_t \mathrm{d}\mathbf{z}_{j+1}^n + M_t \mathrm{d}\mathbf{z}_j^n) \wedge K(M_t \mathrm{d}\mathbf{z}_{j+1}^n - M_t \mathrm{d}\mathbf{z}_j^n) \\
&= \frac{1}{2} D_t(M_x \mathrm{d}\mathbf{z}_j^n \wedge L M_x \mathrm{d}\mathbf{z}_j^n) + \frac{1}{2} D_x(M_t \mathrm{d}\mathbf{z}_j^n \wedge K M_t \mathrm{d}\mathbf{z}_j^n) \\
&\qquad + \frac{1}{2(\Delta t)}\Big(M_x \mathrm{d}\mathbf{z}_j^n \wedge L M_x \mathrm{d}\mathbf{z}_j^{n+1} - M_x \mathrm{d}\mathbf{z}_j^{n+1} \wedge L M_x \mathrm{d}\mathbf{z}_j^n\Big) \\
&\qquad + \frac{1}{2(\Delta x)}\Big(M_t \mathrm{d}\mathbf{z}_j^n \wedge K M_t \mathrm{d}\mathbf{z}_{j+1}^n - M_t \mathrm{d}\mathbf{z}_{j+1}^n \wedge K M_t \mathrm{d}\mathbf{z}_j^n\Big).
\end{aligned}$$

The result (4.9) follows, since by the skew-symmetry property of both, the wedge product and matrices L and K, we have that

$$M_x \mathrm{d}\mathbf{z}_j^{n+1} \wedge L M_x \mathrm{d}\mathbf{z}_j^n = M_x \mathrm{d}\mathbf{z}_j^n \wedge L M_x \mathrm{d}\mathbf{z}_j^{n+1}$$

and

$$M_t \mathrm{d}\mathbf{z}_{j+1}^n \wedge K M_t \mathrm{d}\mathbf{z}_j^n = M_t \mathrm{d}\mathbf{z}_j^n \wedge K M_t \mathrm{d}\mathbf{z}_{j+1}^n.$$

Equation (4.9) is a discrete multisymplectic conservation law. It is sometimes written as

$$D_t(\Omega^{(t)})_{1/2}^n + D_x(\Omega^{(x)})_j^{1/2} = 0, \tag{4.10}$$

where we understand

$$(\Omega^{(t)})_{1/2}^n = \frac{1}{2}(M_x \mathrm{d}\mathbf{z}_j^n \wedge L M_x \mathrm{d}\mathbf{z}_j^n) = \frac{1}{2}(\mathrm{d}\mathbf{z}_{1/2}^n \wedge L \mathrm{d}\mathbf{z}_{1/2}^n), \tag{4.11a}$$

$$(\Omega^{(x)})_j^{1/2} = \frac{1}{2}(M_t \mathrm{d}\mathbf{z}_j^n \wedge K M_t \mathrm{d}\mathbf{z}_j^n) = \frac{1}{2}(\mathrm{d}\mathbf{z}_j^{1/2} \wedge K \mathrm{d}\mathbf{z}_j^{1/2}). \tag{4.11b}$$

4.3 Box Scheme for the sine–Gordon Equation

We now derive two versions of what will be called reduced box scheme for the sine–Gordon equation. Using multisymplectic form of the equation (3.9) and the centered cell box discretization (4.7) for the two formulations MS–1 and MS–2, described in sections 3.1.1 and 3.1.1, one can obtain two algorithms also denoted MS–1 and MS–2 and described below. Some authors refer to what we call "reduced box scheme" as "modified box scheme".

4.3.1 MS–1 Formulation

The sine–Gordon equation in multisymplectic form (3.15) discretized by the box scheme is

$$D_t M_x v_j^n + D_x M_t w_j^n = -\chi \sin(M_t M_x u_j^n) \tag{4.12a}$$

$$D_t M_x u_j^n = M_t M_x v_j^n \tag{4.12b}$$

$$D_x M_t u_j^n = -M_t M_x w_j^n. \tag{4.12c}$$

One has now two options. Either numerically solve the entire system or eliminate all the variables except u and working with the reduced box scheme. In this work we will concentrate on reduced schemes for two main reasons. The first one is of computational nature as it take much more resources to solve complete discrete system as opposed to just solving single discrete equation. Second reason is of implementational nature. Iterative process (functional iterations) obtained for the entire system is not converge for majority of numerical mesh choices. There are two possible solutions to this problem. The first approach requires introducing some artificial boundary conditions [39]. Another solution would be to implement more sophisticated iterative solvers, like Newton's method, and investigate convergence of

such a system. In this thesis we decided to work with reduced box scheme obtained via elimination of the variables corresponding to the derivatives, i.e. by eliminating v and w (and p in MS–2 formulation).

One proceeds as follows. Applying M_t to (4.12a) and D_t to (4.12b) and eliminating v_j^n term through application of M_x operator one gets

$$D_t^2 M_x^2 u_j^n + M_x D_x M_t^2 w_j^n = -\chi M_t M_x \sin(M_t M_x u_j^n)$$

noticing that

$$-D_x^2 M_t^2 u_j^n = D_x M_t^2 M_x w_j^n$$

one finally have a box scheme in MS–1 form

$$D_x^2 M_t^2 u_j^n - D_t^2 M_x^2 u_j^n = \chi M_t M_x \sin(M_t M_x u_j^n) \tag{4.13}$$

4.3.2 MS–2 Formulation

Similar approach applied to the multisymplectic form (3.21), in terms of discrete operators (4.6), yields

$$\begin{aligned} -D_t M_x v_j^n - D_x M_t w_j^n &= \chi \sin(M_x M_t u_j^n) && \text{(4.14a)} \\ D_t M_x u_j^n - D_x M_t p_j^n &= M_x M_t v_j^v && \text{(4.14b)} \\ -D_t M_x p_j^n + D_x M_t u_j^n &= -M_x M_t w_j^n && \text{(4.14c)} \\ D_t M_x w_j^n + D_x M_t v_j^n &= 0 && \text{(4.14d)} \end{aligned}$$

Our goal, as previously, is to eliminate v, w and p in order to find expression depending only upon u. Notice, that applying $D_x M_t$ operator to (4.14d) and $D_t M_x$ to (4.14a) and

eliminating terms involving w_j^n one gets

$$-D_t^2 M_x^2 v_j^n + D_x^2 M_t^2 v_j^n = \chi D_t M_x \sin(M_t M_x u_j^n). \tag{4.15}$$

Clearly, by applying D_t to (4.14c), M_t to (4.14d) and eliminating w_j^n term one obtains

$$D_x M_t^2 v_j^n = D_t D_x M_t u_j^n - D_t^2 M_x p_j^n \tag{4.16}$$

Applying M_t to (4.15), $D_t^2 M_x$ to (4.14b) and using (4.16), with additional $D_x M_t$ operator applied to it, one has

$$(D_t^2 D_x M_t M_x p_j^n - D_t^3 M_x^2 u_j^n) + M_t(D_t D_x^2 M_t u_j^n - D_t^2 D_x M_x p_j^n) = \chi D_t M_t M_x \sin(M_t M_x u_j^n)$$

and thus finally

$$D_t D_x^2 M_t^2 u_j^n - D_t^3 M_x^2 u_j^n = \chi D_t M_t M_x \sin(M_t M_x u_j^n) \tag{4.17}$$

One should note that (4.17) can be obtained from (4.13) by additional application of the operator D_t. Numerical schemes (4.13) and (4.17) are not equivalent though, since D_t is not invertible [6].

4.3.3 Implementation

Notation introduced by (4.6) is very convenient in derivation of reduced schemes, but for implementations and in order to investigate discrete dispersion relationships one needs to explicitly express dependencies on indices. In this section we want to present all the details needed for computer implementation. We decided not to include either pseudo-code nor the actual MATLAB procedures as only a minimal programming knowledge is necessary to reproduce numerical algorithms from information provided in this section.

MS–1 Formulation In order to reformulate equation (4.13) in terms of indices one notes the following

$$D_t M_x u_j^n = \frac{1}{2\Delta t}(u_{j+1}^{n+1} + u_j^{n+1} - u_{j+1}^n - u_j^n), \tag{4.18a}$$

$$D_x M_t u_j^n = \frac{1}{2\Delta x}(u_{j+1}^{n+1} - u_j^{n+1} + u_{j+1}^n - u_j^n), \tag{4.18b}$$

$$M_t M_x u_j^n = \frac{1}{4}(u_{j+1}^{n+1} + u_j^{n+1} + u_{j+1}^n + u_j^n), \tag{4.18c}$$

as well as, by linearity of difference operators (4.6), the following

$$D_t^2 u_j^n = \frac{1}{(\Delta t)^2}(u_j^{n+2} - 2u_j^{n+1} + u_j^n), \tag{4.19a}$$

$$D_x^2 u_j^n = \frac{1}{(\Delta x)^2}(u_{j+2}^n - 2u_{j+1}^n + u_j^n), \tag{4.19b}$$

$$M_t^2 u_j^n = \frac{1}{4}(u_j^{n+2} + 2u_j^{n+1} + u_j^n), \tag{4.19c}$$

$$M_x^2 u_j^n = \frac{1}{4}(u_{j+2}^n + 2u_{j+1}^n + u_j^n). \tag{4.19d}$$

Moreover

$$\begin{aligned} D_x^2 M_t^2 u_j^n = {} & \frac{1}{4(\Delta x)^2}[(u_{j+2}^{n+2} - 2u_{j+1}^{n+2} + u_j^{n+2}) + 2(u_{j+2}^{n+1} - 2u_{j+1}^{n+1} + u_j^{n+1}) \\ & + (u_{j+2}^n - 2u_{j+1}^n + u_j^n)], \end{aligned} \tag{4.20a}$$

$$\begin{aligned} D_t^2 M_x^2 u_j^n = {} & \frac{1}{4(\Delta t)^2}[(u_{j+2}^{n+2} + 2u_{j+1}^{n+2} + u_j^{n+2}) - 2(u_{j+2}^{n+1} + 2u_{j+1}^{n+1} + u_j^{n+1}) \\ & + (u_{j+2}^n + 2u_{j+1}^n + u_j^n)] \end{aligned} \tag{4.20b}$$

and

$$M_x M_t s_j^n = \frac{1}{4}(s_{j+1}^{n+1} + s_j^{n+1} + s_{j+1}^n + s_j^n), \tag{4.21}$$

where

$$s_j^n = \sin(M_x M_t u_j^n) = \sin\left(\frac{1}{4}(u_{j+1}^{n+1} + u_j^{n+1} + u_{j+1}^n + u_j^n)\right). \tag{4.22}$$

Using the so called stencil notation one can write reduced box scheme for the sine–Gordon equation as

$$a\begin{bmatrix} 1 & -2 & 1 \\ 2 & -4 & 2 \\ 1 & -2 & 1 \end{bmatrix}\mathbf{u} - b\begin{bmatrix} 1 & 2 & 1 \\ -2 & -4 & -2 \\ 1 & 2 & 1 \end{bmatrix}\mathbf{u} = \chi\frac{1}{4}\begin{bmatrix} 1 & 1 \\ 1 & 1 \end{bmatrix}\sin\Big(\frac{1}{4}\begin{bmatrix} 1 & 1 \\ 1 & 1 \end{bmatrix}\mathbf{u}\Big),$$

where

$$a = \frac{1}{4(\Delta x)^2}, \qquad b = \frac{1}{4(\Delta t)^2}. \tag{4.23}$$

If one furthermore introduce the following notation

$$\nu^2 = \frac{b}{a} = \left(\frac{\Delta x}{\Delta t}\right)^2 \tag{4.24}$$

and let

$$A = \begin{bmatrix} -2 & 1 & & & 1 \\ 1 & -2 & 1 & & \\ & \ddots & \ddots & \ddots & \\ & & 1 & -2 & 1 \\ 1 & & & 1 & -2 \end{bmatrix}, \qquad B = \begin{bmatrix} 2 & 1 & & & 1 \\ 1 & 2 & 1 & & \\ & \ddots & \ddots & \ddots & \\ & & 1 & 2 & 1 \\ 1 & & & 1 & 2 \end{bmatrix}, \tag{4.25}$$

then the numerical scheme (4.13) can be written as

$$(aA - bB)\mathbf{u}^{n+2} + 2(aA + bB)\mathbf{u}^{n+1} + (aA - bB)\mathbf{u}^n = \chi\frac{1}{4}\mathbf{F}(\mathbf{u}^{n+2}, \mathbf{u}^{n+1}, \mathbf{u}^n) \tag{4.26}$$

or equivalently, upon division by a, as

$$(A - \nu^2 B)\mathbf{u}^{n+2} + 2(A + \nu^2 B)\mathbf{u}^{n+1} + (A - \nu^2 B)\mathbf{u}^n = \chi\frac{1}{4a}\mathbf{F}(\mathbf{u}^{n+2}, \mathbf{u}^{n+1}, \mathbf{u}^n). \tag{4.27}$$

Here $\mathbf{u}^n = [u_1^n, \ldots, u_J^n]^T$. In constructing equations (4.26) and (4.27) we let

$$\begin{aligned}\mathbf{F}(\mathbf{u}^{n+2}, \mathbf{u}^{n+1}, \mathbf{u}^n) &= \sin\Big(\frac{1}{4}X(\mathbf{u}^{n+2} + \mathbf{u}^{n+1})\Big) + \sin\Big(\frac{1}{4}Y(\mathbf{u}^{n+2} + \mathbf{u}^{n+1})\Big) \\ &\quad + \sin\Big(\frac{1}{4}X(\mathbf{u}^{n+1} + \mathbf{u}^{n})\Big) + \sin\Big(\frac{1}{4}Y(\mathbf{u}^{n+1} + \mathbf{u}^{n})\Big)\end{aligned}$$

with

$$X = \begin{bmatrix} 1 & 1 & & & & \\ & 1 & 1 & & & \\ & & \ddots & \ddots & & \\ & & & & 1 & 1 \\ 1 & & & & & 1 \end{bmatrix}, \qquad Y = \begin{bmatrix} 1 & & & & & 1 \\ 1 & 1 & & & & \\ & 1 & 1 & & & \\ & & \ddots & \ddots & & \\ & & & & 1 & 1 \end{bmatrix}. \tag{4.28}$$

In order to obtained a closed system of algebraic equations, i.e. a system for which the number of equations is the same as the number of unknowns, we assumed that equation (3.9) was furnished with periodic boundary conditions (3.7). Numerically, these boundary conditions are typically written as

$$u_0^n = u_J^n, \quad u_{J+1}^n = u_1^n, \quad \text{for any } n \in \{1, \ldots, N\} \tag{4.29}$$

which causes matrices describing system of algebraic equations to have the, so called, circulant form. It is convenient to express numerical schemes in vector–matrix form as MATLAB is designed to treat all variables as matrices. This approach significantly reduces length of all numerical procedures and programming effort, as it essentially does not involve loops.

We may also reformulate scheme (4.26) by dividing (4.26) by b to obtain

$$(\lambda^2 A - B)\mathbf{u}^{n+2} + 2(\lambda^2 A + B)\mathbf{u}^{n+1} + (\lambda^2 A - B)\mathbf{u}^n = \chi\frac{1}{4b}\mathbf{F}(\mathbf{u}^{n+2}, \mathbf{u}^{n+1}, \mathbf{u}^n), \tag{4.30}$$

where

$$\lambda^2 = \frac{a}{b} = \Big(\frac{\Delta t}{\Delta x}\Big)^2. \tag{4.31}$$

Simulations performed on (4.30) were not successful as we encountered non-convergence of functional iterations solver of the system of nonlinear algebraic equations. All the results of numerical experiments presented in Chapter 6 were therefore obtained by using (4.27) instead. More specifically, these solutions were obtained by solving

$$\mathbf{u}^{n+2} = P^{-1}\Big(\chi(\Delta x)^2\mathbf{F}(\mathbf{u}^{n+2}, \mathbf{u}^{n+1}, \mathbf{u}^n) - Q\mathbf{u}^{n+1}\Big) - \mathbf{u}^n \tag{4.32}$$

iteratively, through the method of functional iterations. For more details on this method one may wish to consult [20] or [12]. In formulating equation (4.32) one assumes that $P \in \mathcal{M}_{J\times J}(\mathbb{R})$, $P = (A - \nu^2 B)$ is invertible and denotes $Q = 2(A + \nu^2 B)$.

Initial Conditions – Implementation We also have to implement initial conditions. To do so, let's consider an IVP (3.9) with initial conditions

$$u(0, x) = \phi(x), \tag{4.33a}$$

$$u_t(0, x) = \psi(x), \tag{4.33b}$$

where functions ϕ and ψ are given. Applying $D_t M_x$ operator to condition (4.33b) we get

$$u^2_{j+1} + u^2_j = (\Delta t)(\psi_{j+1} + \psi_j) + (u^1_{j+1} + u^1_j),$$

or equivalently in matrix formulation

$$X\mathbf{u}^2 = X\Big(\mathbf{u}^1 + (\Delta t)\boldsymbol{\psi}\Big). \tag{4.34}$$

For invertible matrix X (4.34) becomes

$$\mathbf{u}^2 = \mathbf{u}^1 + (\Delta t)\boldsymbol{\psi}, \tag{4.35}$$

where $\boldsymbol{\psi} = [\psi_1, \ldots, \psi_J]^T$.

Lemma 4 *Matrix $X \in \mathcal{M}_{J\times J}(\mathbb{R})$ defined by (4.28) is invertible iff $J = 2i - 1$ for some $i \in \mathbb{N}$.*

PROOF: Computing the determinant of X one has that

$$\begin{aligned}
\det(X) &= (-1)^2 \cdot 1 \cdot \det \begin{bmatrix} 1 & 1 & & & \\ & \ddots & \ddots & & \\ & & & 1 & 1 \\ & & & & 1 \end{bmatrix} + (-1)^{J+1} \cdot 1 \cdot \det \begin{bmatrix} 1 & & & & \\ 1 & 1 & & & \\ & \ddots & \ddots & & \\ & & & 1 & 1 \end{bmatrix} \\
&= 1 + (-1)^{J+1} = \begin{cases} 2 & \text{if} \quad J+1 = 2i, \\ 0 & \text{if} \quad J+1 = 2i-1. \end{cases}
\end{aligned}$$

That is $\det(X) \neq 0$, i.e. matrix X is invertible, for any $J = 2i - 1$, $i \in \mathbb{N}$. ■

In numerical simulations we will be using (4.35) as the initial conditions regardless of the invertibility condition for the matrix X, i.e. regardless of the number of spatial mesh points.

MS–2 Formulation Applying D_t operator to (4.20a), (4.20b) and (4.18c), one gets

$$\begin{aligned}
D_t D_x^2 M_t^2 u_j^n &= \frac{1}{4\Delta t(\Delta x)^2}[(u_{j+2}^{n+3} - 2u_{j+1}^{n+3} + u_j^{n+3}) + (u_{j+2}^{n+2} - 2u_{j+1}^{n+2} + u_j^{n+2}) \\
&\quad -(u_{j+2}^{n+1} - 2u_{j+1}^{n+1} + u_j^{n+1}) - (u_{j+2}^{n} - 2u_{j+1}^{n} + u_j^{n})], \\
D_t^3 M_x^2 u_j^n &= \frac{1}{4(\Delta t)^3}[(u_{j+2}^{n+3} + 2u_{j+1}^{n+3} + u_j^{n+3}) - 3(u_{j+2}^{n+2} + 2u_{j+1}^{n+2} + u_j^{n+2}) \\
&\quad +3(u_{j+2}^{n+1} + 2u_{j+1}^{n+1} + u_j^{n+1}) - (u_{j+2}^{n} + 2u_{j+1}^{n} + u_j^{n})], \\
D_t M_x M_t s_j^n &= \frac{1}{4\Delta t}(s_{j+1}^{n+2} + s_j^{n+2} - s_{j+1}^{n} - s_j^{n}),
\end{aligned}$$

respectively. Using notation (4.22) one arrives at

$$D_t M_x M_t s_j^n = \frac{1}{4\Delta t}(s_{j+1}^{n+2} + s_j^{n+2} - s_{j+1}^{n} - s_j^{n}), \tag{4.36}$$

so that the scheme in the stencil notation is

$$a \begin{bmatrix} 1 & -2 & 1 \\ 1 & -2 & 1 \\ -1 & 2 & -1 \\ -1 & 2 & -1 \end{bmatrix} \mathbf{u} - b \begin{bmatrix} 1 & 2 & 1 \\ -3 & -6 & -3 \\ 3 & 6 & 3 \\ -1 & -2 & -1 \end{bmatrix} \mathbf{u} = \chi \frac{1}{4} \begin{bmatrix} 1 & 1 \\ 0 & 0 \\ -1 & -1 \end{bmatrix} \sin\Big(\frac{1}{4} \begin{bmatrix} 1 & 1 \\ 1 & 1 \end{bmatrix} \mathbf{u}\Big)$$

and we have used notation (4.23). The MS–2 scheme (4.17) can thus be written, using notation introduced in (4.25) and periodic boundary conditions (4.29), as

$$\begin{aligned}
&(A - \nu^2 B)\mathbf{u}^{n+3} + (A + 3\nu^2 B)\mathbf{u}^{n+2} - (A + 3\nu^2 B)\mathbf{u}^{n+1} - (A - \nu^2 B)\mathbf{u}^{n} \\
&\qquad = \chi \frac{1}{4a} \mathbf{G}(\mathbf{u}^{n+3}, \mathbf{u}^{n+2}, \mathbf{u}^{n+1}, \mathbf{u}^{n}),
\end{aligned} \tag{4.37}$$

where

$$\begin{aligned}
\mathbf{G}(\mathbf{u}^{n+3}, \mathbf{u}^{n+2}, \mathbf{u}^{n+1}, \mathbf{u}^{n}) &= \sin\Big(\frac{1}{4}X(\mathbf{u}^{n+3} + \mathbf{u}^{n+2})\Big) + \sin\Big(\frac{1}{4}Y(\mathbf{u}^{n+3} + \mathbf{u}^{n+2})\Big) \\
&\quad - \sin\Big(\frac{1}{4}X(\mathbf{u}^{n+1} + \mathbf{u}^{n})\Big) - \sin\Big(\frac{1}{4}Y(\mathbf{u}^{n+1} + \mathbf{u}^{n})\Big).
\end{aligned}$$

Assuming that $P = (A - \nu^2 B)$ is an invertible matrix one rewrites (4.37) in the form

$$\mathbf{u}^{n+3} = P^{-1}\Big(\chi(\Delta x)^2 \mathbf{G}(\mathbf{u}^{n+3}, \mathbf{u}^{n+2}, \mathbf{u}^{n+1}, \mathbf{u}^n) - Q(\mathbf{u}^{n+2} - \mathbf{u}^{n+1})\Big) + \mathbf{u}^n, \tag{4.38}$$

where $Q = (A + 3\nu^2 B)$.

Initial Conditions Note that MS–2 formulation is a multi-step method requiring $\mathbf{u}^0$, $\mathbf{u}^1$ and $\mathbf{u}^2$ as initial data. One obtains $\mathbf{u}^2$ by advancing the solution on step using (4.27).

4.4 Multisymplectic Euler's Scheme

There exists another possibility to construct a multisymplectic discretization. It is described in [29] and relies on splitting of pre-symplectic matrices L and K described in Section 3.1.2. Consider a (non–unique) splitting of these matrices described in (3.22) and define the following discretization of (3.2)

$$L^+ D_t \mathbf{z}_j^n + L^- D_t \mathbf{z}_j^{n-1} + K^+ D_x \mathbf{z}_j^n + K^- D_x \mathbf{z}_{j-1}^n = \nabla_{\mathbf{z}} S(\mathbf{z}_j^n). \tag{4.39}$$

It can be shown that (4.39) satisfies the discrete multisymplecticnes conservation law (4.2) with

$$(\Omega^{(t)})_j^n = \mathrm{d}\mathbf{z}_{j-1}^n \wedge L^+ \mathrm{d}\mathbf{z}_j^n, \qquad (\Omega^{(x)})_j^n = \mathrm{d}\mathbf{z}_j^{n-1} \wedge K^+ \mathrm{d}\mathbf{z}_j^n.$$

4.4.1 Examples

One possible splitting is defined, for any $i, j \in \{1, \ldots, d\}$, as

$$K_{ij}^+ = \begin{cases} K_{ij} & \text{for} \quad j > i \\ 0 & \text{for} \quad j < i \end{cases}$$

and L^+ by analogy. Matrices L^- and K^- are chosen to satisfy their definition. In another words, we defined K^+ to be an upper triangular matrix obtained from K by setting all the elements under the diagonal to be 0 and for K^- taking K with all the elements above the diagonal set to 0, and doing the same for L. This an approach used in [13, 29].

Example 1 *For the sine–Gordon equation in MS–1 (3.15) form we therefore have the following*

$$L_1^+ = \begin{bmatrix} 0 & 1 & 0 \\ 0 & 0 & 0 \\ 0 & 0 & 0 \end{bmatrix} \quad \text{and} \quad K_1^+ = \begin{bmatrix} 0 & 0 & 1 \\ 0 & 0 & 0 \\ 0 & 0 & 0 \end{bmatrix} \tag{4.40}$$

Discretization (4.39) has the form

$$D_t v_j^n + D_x w_j^n = -\chi \sin u_j^n \tag{4.41a}$$

$$D_t u_j^{n-1} = v_j^n \tag{4.41b}$$

$$D_x u_{j-1}^n = -w_j^n \tag{4.41c}$$

It is an immediate conclusion, that a reduced form of (4.41) has the form

$$D_t^2 u_j^{n-1} - D_x^2 u_{j-1}^n + \chi \sin u_j^n = 0$$

which is precisely MS–3 discretization (4.44). This proves that, in fact, MS–3 is an explicit, multisymplectic integrator.

Example 2 *Second illustration of this type of a discretization is the following discretization*

of the variable coefficient Klein–Gordon equation (3.11) analyzed in [13]

$$D_t v_j^n + D_x w_j^n = -(\beta_j^n)^2 u_j^n \tag{4.42a}$$

$$D_t u_j^{n-1} = v_j^n \tag{4.42b}$$

$$D_x u_{j-1}^n = -(\alpha_j^n)^{-2} w_j^n \tag{4.42c}$$

that is, in reduced form,

$$D_t^2 u_j^{n-1} - D_x\Big((\alpha_j^n)^2 D_x u_{j-1}^n\Big) + (\beta_j^n)^2 u_j^n = 0. \tag{4.43}$$

Example 3 *Another option would be to take* $K^+ = K^- = (1/2)K$ *and* $L^+ = L^- = (1/2)L$. *In this case (4.39) for the MS–1 form of the sine–Gordon (3.15) becomes*

$$\frac{1}{2}L\Big(D_t\mathbf{z}_j^n + D_t\mathbf{z}_j^{n-1}\Big) + \frac{1}{2}K\Big(D_x\mathbf{z}_j^n + D_x\mathbf{z}_{j-1}^n\Big) = \nabla_{\mathbf{z}} S(\mathbf{z}_j^n),$$

i.e.

$$L\frac{1}{2(\Delta t)}\Big(\mathbf{z}_j^{n+1} - \mathbf{z}_j^{n-1}\Big) + K\frac{1}{2(\Delta x)}\Big(\mathbf{z}_{j+1}^n - \mathbf{z}_{j-1}^n\Big) = \nabla_{\mathbf{z}} S(\mathbf{z}_j^n),$$

It is not difficult to note that for (3.15) form of the sine–Gordon equation we have the following reduced form

$$u_j^{n+2} - 2u_j^n + u_j^{n-2} - \lambda^2(u_{j+2}^n - 2u_j^n + u_{j-2}^n) + 4\chi(\Delta t)^2 \sin u_j^n = 0.$$

4.5 Leap–frog Scheme (MS–3)

As we have mentioned in the introduction, the main goal of the paper is to investigate multi-symplectic integrators in comparison to other, symplectic and nonsymplectic, schemes. Box schemes discussed before are second order accurate in both space and time so we decided to

compare thir properties with other second order time integrators applied to the second order, Hamiltonian spatial semidiscretization of the sine–Gordon equation. The first integrator is an explicit, symplectic method called a leap–frog method, while the second and the third belong to the class of Runge–Kutta methods.

Staggered version of the leap–frog approximation of second order wave equation is obtained by writing the equation $u_{tt} - c^2 u_{xx} = 0$ in the form of the first order system of PDEs

$$\begin{aligned} u_t + cv_x &= 0, \\ v_t + cu_x &= 0. \end{aligned}$$

This system can be discretized as

$$\begin{aligned} D_t u_j^n + cD_x v_{j-1/2}^{n+1/2} &= 0, \\ D_t v_{j+1/2}^{n+1/2} + cD_x u_j^{n+1} &= 0, \end{aligned}$$

where we use notation introduced by (4.6a). Applying D_t to the first equation and D_x to the second one and shifting indices so that the derivatives are approximated at (t_n, x_j) we arrive at

$$D_t^2 u_{j+1}^n - c^2 D_x^2 u_j^{n+1} = 0.$$

We are now at the position to write the diectrtization of the sine–Gordon equation ($c = 1$) in the form

$$D_t^2 u_j^{n-1} - D_x^2 u_{j-1}^n + \chi \sin u_j^n = 0. \tag{4.44}$$

Multiplying by $(\Delta t)^2$, using (4.31) and solving for u_j^{n+1} we obtain

$$u_j^{n+1} = 2(1-\lambda^2)u_j^n + \lambda^2(u_{j+1}^n + u_{j-1}^n) - u_j^{n-1} - \chi(\Delta t)^2 \sin u_j^n.$$

Equivalently in the vector–matrix form

$$\mathbf{u}^{n+1} = (\lambda^2 A + 2I_J)\mathbf{u}^n - \mathbf{u}^{n-1} - \chi(\Delta t)^2 \sin \mathbf{u}^n,$$

where matrix A is given by (4.25) and $I_J \in \mathcal{M}_{J\times J}(\mathbb{R})$ is an identity matrix. It will be shown in a later section (Section 4.4) that (4.44) is a multisymplectic method.

4.6 Hamiltonian Semi-discretization

Consider now a spatial semi-discretization of (3.9). It is obtained directly from equations (3.13) by using a second order central difference discretization

$$\dot{p}_j = D_x^2 q_{j-1} - \chi \sin q_j \tag{4.45a}$$

$$\dot{q}_j = p_j \tag{4.45b}$$

Notice that the resulting system of ODEs is Hamiltionian with Hamiltonian function

$$\begin{aligned} \widetilde{H}(\mathbf{p},\mathbf{q}) &= \sum_{j=1}^{J} \Big[\frac{1}{2}p_j^2 + \frac{1}{2}(D_x q_j)^2 - \chi\cos q_j\Big] \\ &= \sum_{j=1}^{J} \Big[\frac{1}{2}p_j^2 + \frac{1}{(\Delta x)^2}(q_j^2 - q_{j+1}q_j) - \chi\cos q_j\Big]. \end{aligned} \tag{4.46}$$

The result holds since, by periodic boundary conditions (4.29),

$$\sum_{j=1}^{J} q_{j+1}^2 = \sum_{j=1}^{J} q_j^2.$$

We can also write a matrix form for the spatial discretization

$$\dot{\mathbf{p}} = \frac{1}{(\Delta x)^2} A\mathbf{q} - \chi \sin \mathbf{q} \tag{4.47a}$$

$$\dot{\mathbf{q}} = \mathbf{p} \tag{4.47b}$$

where $\mathbf{p} = [p_1, \ldots, p_J]^T$, $\mathbf{q} = [q_1, \ldots, q_J]^T$, matrix A is defined in (4.25) and the sin function is applied elementwise to the vector $\mathbf{q}$. The Hamiltonian can also be expressed in vector–matrix form

$$\widetilde{H}(\mathbf{p}, \mathbf{q}) = \frac{1}{2}\mathbf{p}^T\mathbf{p} + \frac{1}{(\Delta x)^2}\mathbf{q}^T U \mathbf{q} - \chi \mathbf{1}^T \cos \mathbf{q}$$

by introducing matrix $U \in \mathcal{M}_{J\times J}(\mathbb{R})$,

$$U = \begin{bmatrix} 1 & -1 & & & \\ & \ddots & \ddots & & \\ & & & 1 & -1 \\ -1 & & & & 1 \end{bmatrix}. \tag{4.48}$$

For simplicity we have chosen to implement (4.46) in its equivalent vector–matrix form

$$\widetilde{H}(\mathbf{p}, \mathbf{q}) = \mathbf{1}^T \Big[\frac{1}{2}\mathbf{p}^2 + \frac{1}{2(\Delta x)^2}(U\mathbf{q})^2 - \chi \cos \mathbf{q}\Big].$$

Standard convention for powers and the cosine function of vectors, as element-wise operations, is used. The $\mathbf{1} = [1, \ldots, 1]^T \in \mathcal{M}_{J\times 1}(\mathbb{R})$.

4.6.1 Implicit (MS–4) and Explicit (ERK) Runge–Kutta Methods

The remaining two schemes tested are second order Runge–Kutta (R–K) methods given by the Butcher's tableaux given by Table 4.1. Runge – Kutta method presented in Table 4.1a

is also called implicit Crank–Nicolson scheme (MS–4), while the one in Table 4.1b is the standard explicit Runge–Kutta method (ERK). It turns out that MS–4 is a symplectic time discretization of order two, while ERK is a nonsymplectic method of the same order (Appendix A).

Table 4.1: Butcher's tableaux for Runge – Kutta methods of order two.

(a) Implicit R–K method

1/2	1/2
	1

(b) Explicit R–K method

0	0	0
1/2	1/2	0
	0	1

ERK: For use in later section on dispersion analysis, let's express ERK explicitly. Equation (4.47) has the form

$$\dot{\mathbf{z}} = \mathbf{F}(\mathbf{z}), \quad \mathbf{z} = [\mathbf{p}, \mathbf{q}]^T$$

and so the scheme under consideration can be written as

$$\begin{aligned} \mathbf{k}_1 &= \mathbf{F}(\mathbf{z}^n) \\ \mathbf{k}_2 &= \mathbf{F}(\mathbf{z}^n + \frac{\Delta t}{2}\mathbf{k}_1) \\ \mathbf{z}^{n+1} &= \mathbf{z}^n + (\Delta t)\mathbf{k}_2 \end{aligned}$$

i.e.

$$\mathbf{z}^{n+1} = \mathbf{z}^n + \Delta t \mathbf{F}(\mathbf{z}^n + \frac{\Delta t}{2}\mathbf{F}(\mathbf{z}^n)).$$

Moreover, since

$$\mathbf{z}^n + \frac{\Delta t}{2}\mathbf{F}(\mathbf{z}^n) = \begin{bmatrix} \mathbf{p}^n \\ \mathbf{q}^n \end{bmatrix} + \frac{\Delta t}{2}\begin{bmatrix} \mathbf{f}(\mathbf{q}^n) \\ \mathbf{g}(\mathbf{p}^n) \end{bmatrix}$$

one has that

$$\begin{bmatrix} \mathbf{p}^{n+1} \\ \mathbf{q}^{n+1} \end{bmatrix} = \begin{bmatrix} \mathbf{p}^n \\ \mathbf{q}^n \end{bmatrix} + (\Delta t)\begin{bmatrix} \mathbf{f}(\mathbf{Q}^n) \\ \mathbf{g}(\mathbf{P}^n) \end{bmatrix} \tag{4.49}$$

where

$$\mathbf{P}^n = \mathbf{p}^n + \frac{\Delta t}{2}\mathbf{f}(\mathbf{q}^n) \tag{4.50a}$$

$$\mathbf{Q}^n = \mathbf{q}^n + \frac{\Delta t}{2}\mathbf{g}(\mathbf{p}^n) \tag{4.50b}$$

4.6.2 Additional Remarks on MS–3 and MS–4 Discretizations

MS–3 Derivation of the method (4.44) can also be performed by first considering a Hamiltonian system (4.45) and noticing that its Hamiltonian function can be expressed in the form $\widetilde{H} = T(p) + U(q)$ thus suggesting an application of the explicit symplectic integrator. The simplest choice would be the method known as Störmer (astronomy)/Verlet (molecular dynamics) method, which for the ODE in the form $\ddot{q} = f(q)$ takes the form

$$q^{n+1} - 2q^n + q^{n-1} = h^2 f(q^n) \tag{4.51}$$

that is a second order midpoint discretization. The following important theorem concerning Störmer/Verlet method is proved in [17].

Theorem 11 *The Störmer/Verlet scheme (4.51) is a symplectic method of order 2.*

Multisymplecticness of MS–3 and MS–4 Discretizations As we said in the introduction to this chapter, it turns out the discretizations designated MS–3 and MS–4 are multisymplectic. In order to show it we consider the second order Hamiltonian discretization

$$\dot{p}_j = D_x^2 qj - 1 - \chi \sin q_j, \quad \dot{q}_j = p_j, \qquad \mathscr{H}(\mathbf{p},\mathbf{q}) = \sum_{j=1}^{J} \Big[\frac{1}{2}p_j^2 + \frac{1}{2}(D_x q_j)^2 - \chi \cos q_j\Big],$$

where $\mathscr{H}(\mathbf{p},\mathbf{q})$ is the associated Hamiltonian. It actually corresponds to a leapfrog symplectic discretization in x and therefore it can be casted as a semi-discrete MS discretization

$$L\dot{\mathbf{z}}_j + K_1^+ D_x \mathbf{z}_j + K_1^- D_x \mathbf{z}_{j-1} = \nabla_{\mathbf{z}} S, \qquad K_1^+ = \begin{bmatrix} 0 & 0 & 1 \\ 0 & 0 & 0 \\ 0 & 0 & 0 \end{bmatrix}, \quad K_1^- = -(K^+)^T,$$

which can be combined with symplectic discretizations in time to produce additional MS discretizations.

If we use the leap-frog method in time too we obtain the MS discretization

$$L_1^+ D_t \mathbf{z}_j^n + L_1^- D_t \mathbf{z}_j^{n-1} + K_1^+ D_x \mathbf{z}_j^n + K_1^- D_x \mathbf{z}_{j-1}^n = \nabla_{\mathbf{z}} S(\mathbf{z}_j^n), \qquad L_1^+ = \begin{bmatrix} 0 & 1 & 0 \\ 0 & 0 & 0 \\ 0 & 0 & 0 \end{bmatrix}, \tag{4.52}$$

while using a midpoint discretization gives

$$L D_t M_x \mathbf{z}_j^n + K_1^+ D_x \mathbf{z}_j^n + K_1^- D_x \mathbf{z}_{j-1}^n = \nabla_{\mathbf{z}} S. \tag{4.53}$$

Applying MS discretizations (4.52) and (4.53) to the sine-Gordon equation yield the reduced equations

MS–3: $D_t^2 u_j^{n-1} - D_x^2 u_{j-1}^n + \chi \sin u_j^n = 0,$

MS–4: $D_t^2 u_j^n - D_x^2 M_t^2 u_{j-1}^n + \chi M_t \sin(M_t u_j^n) = 0.$

Related information concerning multisymplecticness of the leap-from method can be found in [11, 28].

4.7 Spectral Spatial Semi-discretization

In this section we would like to introduce the so called spectral semi-discretizations. The idea is to work in Fourier space to obtain high-accuracy discretizations of differentiation operators which are used to approximate spatial derivatives and obtain a finite-dimensional system of ODEs. Such a system is then integrated in time by some standard integrator. One of the most important features of this type of discretizations is the underlying assumption about periodicity of the solution with respect to the space-variable. We will follow similar paths to these established for in Section 3.2.

Consider a discrete Fourier transform

$$u(j,t) = \sum_{k=0}^{J-1} \hat{u}(k,t) e^{\imath 2\pi kj/J}, \tag{4.54a}$$

$$\hat{u}(k,t) = \frac{1}{J} \sum_{j=0}^{J-1} u(j,t) e^{-\imath 2\pi kj/J}. \tag{4.54b}$$

We should note the following properties of (4.54b). Firstly,

$$\begin{aligned} \hat{u}(J-k,t) &= \frac{1}{J} \sum_{j=0}^{J-1} u(j,t) e^{-\imath 2\pi (J-k)j/J} = \frac{1}{J} \sum_{j=0}^{J-1} u(j,t) e^{-\imath 2\pi (-k)j/J} e^{-\imath 2\pi j} \\ &= \hat{u}(-k,t) \end{aligned} \tag{4.55}$$

and secondly

$$\begin{aligned}\hat{u}(k-J,t) &= \frac{1}{J}\sum_{j=0}^{J-1} u(j,t)e^{-\imath 2\pi(k-J)j/J} = \frac{1}{J}\sum_{j=0}^{J-1} u(j,t)e^{\imath 2\pi(J-k)j/J} \\ &= \hat{u}^*(J-k,t) = \hat{u}^*(-k,t) = \hat{u}(k,t), \end{aligned} \tag{4.56}$$

by (4.55) applied to $\hat{u}^*$.

We are now at the position to reformulate (4.54a) and write it in a more convenient form. Notice first that

$$\begin{aligned}u(j,t) = \sum_{k=0}^{J-1} \hat{u}(k,t)e^{\imath 2\pi kj/J} &= \sum_{k=0}^{J/2-1} \hat{u}(k,t)e^{\imath 2\pi kj/J} + \Big(\hat{u}(k,t)e^{\imath 2\pi kj/J}\Big)\Big|_{k=J/2} \\ &\quad + \sum_{k=J/2+1}^{J-1} \hat{u}(k,t)e^{\imath 2\pi kj/J}\end{aligned}$$

and since

$$\sum_{k=J/2+1}^{J-1} \hat{u}(k,t)e^{\imath 2\pi kj/J} = \sum_{k=-J/2+1}^{-1} \hat{u}(k-J,t)e^{\imath 2\pi(k-J)j/J} = \sum_{k=-J/2+1}^{-1} \hat{u}(k,t)e^{\imath 2\pi kj/J}$$

we have that

$$u(j,t) = \sum_{k=-J/2+1}^{J/2-1} \hat{u}(k,t)e^{\imath 2\pi kj/J} + \hat{u}_{\pm J/2}\cos(\pi j), \tag{4.57}$$

where we used the fact that $\hat{u}(J/2,t) = \hat{u}(J/2-J,t) = \hat{u}(-J/2,t)$ to denote this quantity by $\hat{u}_{\pm J/2}$ and write

$$\Big(\hat{u}(k,t)e^{\imath 2\pi kj/J}\Big)\Big|_{k=J/2} = \hat{u}_{\pm J/2}\frac{1}{2}\Big(e^{\imath 2\pi(J/2)j/J} + e^{\imath 2\pi(-J/2)j/J}\Big).$$

Note that since $J = \ell/(\Delta x)$ equation (4.57) can be written as

$$u(j,t) = \sum_{k=-J/2+1}^{J/2-1} \hat{u}(k,t)e^{\vartheta_k j(\Delta x)} + \hat{u}_{\pm J/2}\cos(\pi j), \tag{4.58}$$

where

$$\vartheta_k = \frac{2\pi\imath k}{\ell}. \tag{4.59}$$

Considering now the continuous interpolating trigonometric polynomial and requiring it to take values $u(j,t)$ at the mesh-points $x_j = -\ell/2 + j(\Delta x)$, $j \in \{0, \ldots J-1\}$ leads to the following closed form

$$\widetilde{u}(x,t) = \sum_{k=-J/2+1}^{J/2-1} \hat{u}(k,t) e^{\vartheta_k (x+\ell/2)} + \hat{u}_{\pm J/2} \cos\Big(\frac{\pi J}{\ell}(x+\ell/2)\Big).$$

Thus, the first and second derivatives are given by

$$\widetilde{u}'(x,t) = \sum_{k=-J/2+1}^{J/2-1} \vartheta_k \hat{u}(k,t) e^{\vartheta_k (x+\ell/2)} - \hat{u}_{\pm J/2} \frac{\pi J}{\ell} \sin\Big(\frac{\pi J}{\ell}(x+\ell/2)\Big), \tag{4.60a}$$

$$\widetilde{u}''(x,t) = \sum_{k=-J/2+1}^{J/2-1} (\vartheta_k)^2 \hat{u}(k,t) e^{\vartheta_k (x+\ell/2)} - \hat{u}_{\pm J/2} \Big(\frac{\pi J}{\ell}\Big)^2 \cos\Big(\frac{\pi J}{\ell}(x+\ell/2)\Big). \tag{4.60b}$$

At the grid-points x_j, while the 0 and $\pm J/2$ modes do not contribute to the first derivative, the $\pm J/2$ mode does contribute to the second derivative. Therefore, the first and second partial derivatives with respect to x can be discretized as follows

$$\partial_x u(x,t) \approx F^{-1}\Big[\bar{\Theta} F[u](k,t)\Big](x,t), \tag{4.61a}$$

$$\partial_{xx} u(x,t) \approx F^{-1}\Big[\Theta^2 F[u](k,t)\Big](x,t), \tag{4.61b}$$

where $F[u](k,t)$ and $F^{-1}[\hat{u}](x,t)$ denote Fourier transform and its inverse. respectively. The diagonal matrix $\bar{\Theta}$ has the entries $\bar{\vartheta}_k$ defined by

$$\bar{\vartheta}_k = \begin{cases} \vartheta_k & \text{for } k \in \{0, \ldots, J/2-1\}, \\ 0 & \text{for } k = J/2, \\ \vartheta_{J-k} & \text{for } k \in \{J/2+1, \ldots, J-1\}, \end{cases}$$

with ϑ_k given by (4.59).

4.7.1 Implicit Midpoint Discretization in Time

We will close this chapter by presenting a fully discrete system based on the spectral semi-discretization and show that it satisfies discrete spectral multisymplectic conservation law. Let's consider the following spatial semi-discretization

$$L\partial_t\hat{\mathbf{Z}} + K\bar{\Theta}\hat{\mathbf{Z}} = \nabla_{\hat{\mathbf{Z}}}\hat{S}(\hat{\mathbf{Z}}),$$

where $\hat{\mathbf{Z}} = [\hat{Z}_0, \dots \hat{Z}_{J-1}]^T$ and $\bar{\Theta} = [\bar{\vartheta}_m] \in \mathcal{M}_{dJ\times dJ}(\mathbb{C})$. Forming an implicit midpoint time discrete system we have

$$LD_t\hat{\mathbf{Z}}^n + K(M_t\bar{\Theta}\hat{\mathbf{Z}}^n) = \nabla_{\hat{\mathbf{Z}}}\hat{S}(M_t\hat{\mathbf{Z}}^n). \tag{4.62}$$

We note first that this discretization is multisymplectic. To prove it consider associated variational equation

$$LD_t\mathrm{d}\hat{\mathbf{Z}}^n + K(\bar{\Theta}\mathrm{d}\hat{\mathbf{Z}}^{1/2}) = \hat{S}_{\hat{\mathbf{Z}}\hat{\mathbf{Z}}}\mathrm{d}\hat{\mathbf{Z}}^{1/2}. \tag{4.63}$$

Taking the wedge product with $\mathrm{d}\hat{\mathbf{Z}}^{1/2}$ we have

$$(\mathrm{d}\hat{\mathbf{Z}}^{1/2}) \wedge (LD_t\mathrm{d}\hat{\mathbf{Z}}^n) + (\mathrm{d}\hat{\mathbf{Z}}^{1/2}) \wedge (K\bar{\Theta}\mathrm{d}\hat{\mathbf{Z}}^{1/2}) = (\mathrm{d}\hat{\mathbf{Z}}^{1/2}) \wedge (\hat{S}_{\hat{\mathbf{Z}}\hat{\mathbf{Z}}}\mathrm{d}\hat{\mathbf{Z}}^{1/2}).$$

that is we have

$$\begin{aligned} 0 \;=\; & \frac{1}{2(\Delta t)}\Big((\mathrm{d}\hat{\mathbf{Z}}^{n+1} + \mathrm{d}\hat{\mathbf{Z}}^n) \wedge L(\mathrm{d}\hat{\mathbf{Z}}^{n+1} - \mathrm{d}\hat{\mathbf{Z}}^n)\Big) \\ & + \frac{1}{2}\Big((\mathrm{d}\hat{\mathbf{Z}}^{1/2}) \wedge K(\bar{\Theta}\mathrm{d}\hat{\mathbf{Z}}^{1/2}) + (\bar{\Theta}\mathrm{d}\hat{\mathbf{Z}}^{1/2}) \wedge K(\mathrm{d}\hat{\mathbf{Z}}^{1/2})\Big) \end{aligned} \tag{4.64}$$

It is clear that

$$\mathrm{d}\hat{\mathbf{Z}}^n \wedge L\mathrm{d}\hat{\mathbf{Z}}^{n+1} = -(L\mathrm{d}\hat{\mathbf{Z}}^{n+1}) \wedge \mathrm{d}\hat{\mathbf{Z}}^n = \mathrm{d}\hat{\mathbf{Z}}^{n+1} \wedge L\mathrm{d}\hat{\mathbf{Z}}^n$$

and that

$$\begin{aligned}&(\mathrm{d}\hat{\mathbf{Z}}^{1/2})\wedge K(\bar{\Theta}\mathrm{d}\hat{\mathbf{Z}}^{1/2})+(\bar{\Theta}\mathrm{d}\hat{\mathbf{Z}}^{1/2})\wedge K(\mathrm{d}\hat{\mathbf{Z}}^{1/2})\\ =\ &(\mathrm{d}\hat{\mathbf{Z}}^{1/2})\wedge K(\bar{\Theta}\mathrm{d}\hat{\mathbf{Z}}^{1/2})-K(\bar{\Theta}\mathrm{d}\hat{\mathbf{Z}}^{1/2})\wedge(\mathrm{d}\hat{\mathbf{Z}}^{1/2}) \quad = \quad 2(\mathrm{d}\hat{\mathbf{Z}}^{1/2})\wedge K(\bar{\Theta}\mathrm{d}\hat{\mathbf{Z}}^{1/2}).\end{aligned}$$

The spectral conservation law of multisymplecticness holds

$$\frac{1}{2}D_t(\mathrm{d}\hat{\mathbf{Z}}^n\wedge L\mathrm{d}\hat{\mathbf{Z}}^n)+\frac{1}{2}\Big(\mathrm{d}\hat{\mathbf{Z}}^{1/2}\wedge K(\bar{\Theta}\mathrm{d}\hat{\mathbf{Z}}^{1/2})+(\bar{\Theta}\mathrm{d}\hat{\mathbf{Z}}^{1/2})\wedge K\mathrm{d}\hat{\mathbf{Z}}^{1/2}\Big)=0.$$

For two complex-valued functions we understand the wedge product as $\mathrm{d}u\wedge\mathrm{d}v=\mathrm{d}u_R\wedge\mathrm{d}v_R+\imath(\mathrm{d}u_I\wedge\mathrm{d}v_I)$.

CHAPTER FIVE: DISCRETE DISPERSION RELATIONSHIPS

This chapter discusses dispersion–dissipation properties of numerical schemes derived in previous chapter. Information provided in this chapter is related to linear stability analysis of numerical schemes although it could be thought of as a byproduct of a method of deriving dispersion relationships of discretizations. In what follows we obtain results analogous to results of section 5.1.1 for the continuous case. It turns out that due to an error in preservation of numerical dispersion relationship qualitative properties of numerical solutions, particularly of linear wave equations, are destroyed. We will presents numerical evidence in the next chapter and now focus on more theoretical approach for which let's consider the discrete analog of the Fourier mode (5.6) which takes the form

$$u_j^n = \hat{u} e^{\imath(jk\Delta x + n\omega\Delta t)}. \tag{5.1}$$

It is convenient to introduce the following notation, let $k\Delta x = \bar{k}$ and $\bar{\omega} = \omega\Delta t$, then (5.1) becomes

$$u_j^n = \hat{u} e^{\imath(j\bar{k} + n\bar{\omega})} \tag{5.2}$$

and the analytic dispersion relationship (5.7) for $\bar{u} \equiv \pi$, after transformation to the $(\bar{k}, \bar{\omega})$–coordinates, takes the form

$$\Big(\frac{\bar{\omega}}{\Delta t}\Big)^2 - \Big(\frac{\bar{k}}{\Delta x}\Big)^2 + \chi = 0. \tag{5.3}$$

Note that if we consider a difference scheme for an initial–value problem and the Fourier transform, the part of the term (5.1) given by $e^{\imath j\bar{k}}$ corresponds to the $e^{\imath jk}$ in the finite Fourier

transform. Hence, by considering $0 \leq \bar{k} \leq \pi$ we obtain information on all the modes present in the finite Fourier transform representation of the solution.

5.1 Linearized PDEs

5.1.1 Linearization of the sine–Gordon Equation

Assume that $\epsilon : \mathbb{R}^2 \to \mathbb{R}$ is a twice continuously differentiable function, such that $|\epsilon(t,x)| \ll 1$ and let $u = \bar{u} + \epsilon(t,x)$, where u and $\bar{u}$ are solutions to (3.9). Clearly $u_{tt} = \bar{u}_{tt} + \epsilon_{tt}$ and $u_{xx} = \bar{u}_{xx} + \epsilon_{xx}$. Since $\sin(\bar{u}+\epsilon) = \sin\bar{u}\cos\epsilon + \cos\bar{u}\sin\epsilon \approx \sin\bar{u} + \epsilon\cos\bar{u}$, we have the following linearized sine–Gordon equation

$$\epsilon_{tt} - \epsilon_{xx} + \chi\epsilon\cos\bar{u} = 0 \tag{5.4}$$

Example 4 *Linearization about $\bar{u} \equiv \pi$ takes the form*

$$\epsilon_{tt} - \epsilon_{xx} - \epsilon = 0. \tag{5.5}$$

Linear Dispersion Relationship Similarly to [36] assume that the solution of the linearized equation (5.4) takes the form

$$u(x,t) = \hat{u}e^{\imath(\omega t + kx)} = \hat{u}e^{\imath\omega t}e^{\imath kx} \tag{5.6}$$

Clearly $u_{tt} = -\omega^2\hat{u}e^{\imath(\omega t+kx)} = -\omega^2 u$ and $u_{xx} = -k^2\hat{u}e^{\imath(\omega t+kx)} = -k^2 u$. Substituting it to the linearized equation (5.4) and simplifying, we obtain

$$\omega^2 - k^2 - \chi\cos\bar{u} = 0 \tag{5.7}$$

Example 5 *In case of $\bar{u} \equiv \pi$, the dispersion relation takes the form*

$$\omega^2 - k^2 + \chi = 0. \tag{5.8}$$

To conclude this section let's consider another form of (5.6), namely

$$u(x,t) = \hat{u}e^{\imath k(x \pm c_A t)}, \tag{5.9}$$

where

$$c_A = \frac{\omega}{k}$$

denotes the wave propagation speed (phase velocity) and for ω given by (5.7) is equal to

$$c_A = \pm \frac{\sqrt{k^2 + \chi \cos \bar{u}}}{k}. \tag{5.10}$$

5.1.2 Linearized NLS

Our purpose is to take a closer look at linearization of (3.24), its dispersion relationship and, in later section, at preservation of the dispersion relationship by the box scheme discretization. Let's begin, by observing that equation (3.24) assumes plain-wave solution

$$u = ae^{\imath \varphi t}$$

iff $-\varphi u + 2a^2 u = 0$, i.e. iff $\varphi = 2a^2$.

In order to linearize equation (3.24) assume that the solution is expanded in the following way:

$$\begin{aligned} u &= u_0 + \epsilon u_1 + \mathcal{O}(\epsilon^2) \\ u_0 &= ae^{2\imath a^2 t} \\ u_1 &= \alpha(x,t) u_0 \end{aligned}$$

Order equations becomes

$$\mathcal{O}(1): \quad \imath(u_0)_t + (u_0)_{xx} + 2|u_0|^2 u_0 = 0 \tag{5.11}$$

$$\mathcal{O}(\epsilon): \quad \imath(u_1)_t + (u_1)_{xx} + 4|u_0|^2 u_1 + 2u_0^2 u_1^* = 0 \tag{5.12}$$

where $*$ denotes (complex) conjugation. Clearly now

$$\mathcal{L}[\alpha] = (\imath\partial_t + \partial_{xx} + 2a^2)\alpha = -2a^2\alpha^* \tag{5.13}$$

and since

$$\mathcal{L}^*[\alpha^*] = (-\imath\partial_t + \partial_{xx} + 2a^2)\alpha^* = -2a^2\alpha \tag{5.14}$$

Applying $\mathcal{L}^*$ to both sides of (3.24) yields

$$\mathcal{L}^*\mathcal{L}[\alpha] = \mathcal{L}^*[-2a^2\alpha^*]$$

by linearity of $\mathcal{L}^*$ we finally have

$$\partial_{tt}\alpha + \partial_{xxxx}\alpha + 4a^2\partial_{xx}\alpha = 0 \tag{5.15}$$

Let's note that (5.15) has a multisymplectic form. It is derived by introducing new variables $v = u_t$, $w = u_x$, $p = u_{xx}$ and $q = u_{xxx}$. In doing so, we obtain

$$\begin{aligned} v_t + q_x + 4a^2 w_x &= 0 \\ -u_t &= -v \\ -4a^2 u_x - p_x &= -q - 4a^2 w \\ w_x &= p \\ -u_x &= -w \end{aligned} \tag{5.16}$$

that is a multisymplectic form of the NLS equation with Hamiltonian function

$$S(\mathbf{z}) = \frac{1}{2}v^2 - qw - 2a^2w^2 + \frac{1}{2}p^2, \qquad \mathbf{z} = [u, v, w, p, q]. \tag{5.17}$$

Linear Dispersion Relationship Dispersion relationship for (5.15) is obtained by assuming the following ansatz solution

$$\alpha = e^{\imath(kx+\omega t)}.$$

Clearly, $\alpha_t = \imath\omega\alpha$, $\alpha_{tt} = -\omega^2\alpha$ and $\alpha_x = \imath k\alpha$, $\alpha_{xx} = -k^2\alpha$ and $\alpha_{xxxx} = k^4\alpha$ so that

$$\omega^2 - k^2(k^2 - 4a^2) = 0, \tag{5.18}$$

which is a dispersion relationship for the linearization of the NLS equation (3.24) around the plain wave solution.

5.2 Discrete Dispersion Relationships

5.2.1 Multisymplectic Box Scheme

MS–1 Formulation Consider at first linearized sine–Gordon equation (5.5) and its discretization by the first multisymplectic scheme MS–1

$$D_t^2 M_x^2 u_j^n - D_x^2 M_t^2 u_j^n = \chi M_t^2 M_x^2 u_j^n. \tag{5.19}$$

Using (4.20) and the fact that

$$\begin{aligned} M_t^2 M_x^2 u_j^n &= \frac{1}{16}\Big[(u_{j+2}^{n+2} + 2u_{j+1}^{n+2} + u_j^{n+2}) + 2(u_{j+2}^{n+1} + 2u_{j+1}^{n+1} + u_j^{n+1}) \\ &\quad + (u_{j+2}^{n} + 2u_{j+1}^{n} + u_j^{n})\Big] \end{aligned}$$

one obtains the following form of equation (5.19)

$$\begin{aligned}
&\frac{1}{4(\Delta t)^2}[(u_{j+2}^{n+2}+2u_{j+1}^{n+2}+u_j^{n+2})-2(u_{j+2}^{n+1}+2u_{j+1}^{n+1}+u_j^{n+1})+(u_{j+2}^{n}+2u_{j+1}^{n}+u_j^{n})]\\
-&\frac{1}{4(\Delta x)^2}[(u_{j+2}^{n+2}-2u_{j+1}^{n+2}+u_j^{n+2})+2(u_{j+2}^{n+1}-2u_{j+1}^{n+1}+u_j^{n+1})+(u_{j+2}^{n}-2u_{j+1}^{n}+u_j^{n})]\\
-&\frac{\chi}{16}\Big[(u_{j+2}^{n+2}+2u_{j+1}^{n+2}+u_j^{n+2})+2(u_{j+2}^{n+1}+2u_{j+1}^{n+1}+u_j^{n+1})+(u_{j+2}^{n}+2u_{j+1}^{n}+u_j^{n})\Big]=0.
\end{aligned}$$

Substituting the discrete Fourier mode (5.1) and simplifying one arrives at

$$\begin{aligned}
&4(e^{\imath 2\bar{k}}+2e^{\imath\bar{k}}+1)\Big[e^{\imath 2\omega\Delta t}-2e^{\imath\omega\Delta t}+1\Big]\\
-&4\lambda^2(e^{\imath 2\bar{k}}-2e^{\imath\bar{k}}+1)\Big[e^{\imath 2\omega\Delta t}+2e^{\imath\omega\Delta t}+1\Big]\\
-&\chi(\Delta t)^2(e^{\imath 2\bar{k}}+2e^{\imath\bar{k}}+1)\Big[e^{\imath 2\omega\Delta t}+2e^{\imath\omega\Delta t}+1\Big] \;=\; 0,
\end{aligned} \tag{5.20}$$

where λ is defined in (4.31).

There are two ways to simplify the expression (5.20). First approach starts with an assumption, that $\bar{\omega}$ is a real–valued quantity. This assumption allows using trigonometric identities to obtain dispersion relationships. This approach is simpler, but the trade–off for simplicity is that it does not produce desired results for all the schemes, for instance it does not work for the explicit Runge–Kutta (ERK) discretization discussed here, neither provides linearized stability results. We will thus defer its presentation to the end of this chapter (Section 5.4) and focus on the, so called, dispersion–dissipation analysis used in [36]. From that point on we will be working with complex–valued $\bar{\omega}$. Thanks to allowing $\bar{\omega}$ to be complex–valued quantity one obtains information not only about dispersive properties of the numerical schemes, but also information about its dissipative/growth characteristics. In that sense, an assumption, that $\bar{\omega}$ is complex–valued, produces more general results giving the, so called, real and imaginary dispersion relations.

Multiplying equation (5.20) by $e^{-\imath\bar{k}}$ the following is established

$$4(e^{\imath\bar{k}/2}+e^{-\imath\bar{k}/2})^2(\rho^2-2\rho+1)-4\lambda^2(e^{\imath\bar{k}/2}-e^{-\imath\bar{k}/2})^2(\rho^2+2\rho+1)$$
$$-\chi(\Delta t)^2(e^{\imath\bar{k}/2}+e^{-\imath\bar{k}/2})^2(\rho^2+2\rho+1) = 0 \tag{5.21}$$

where we defined

$$\rho = e^{\imath\bar{\omega}}. \tag{5.22}$$

If now

$$\sigma = \cos^2(\bar{k}/2) \tag{5.23a}$$

$$\tau = \sin^2(\bar{k}/2) \tag{5.23b}$$

equation (5.21) can be expressed as

$$\rho^2 - 2\frac{c}{d}\rho + 1 = 0, \tag{5.24}$$

where

$$c = 4\sigma - 4\lambda^2\tau + \chi(\Delta t)^2\sigma, \tag{5.25a}$$

$$d = 4\sigma + 4\lambda^2\tau - \chi(\Delta t)^2\sigma. \tag{5.25b}$$

Notice also that $d = 0$ iff

$$\tan^2(\bar{k}/2) = \frac{\chi(\Delta t)^2 - 4}{4\lambda^2}.$$

For $\Delta t < 2$ the right hand side is negative which gives, since $\bar{k}$ is a real quantity, a contradictory statement. Therefore, for $\Delta t < 2$, one can assume that $d \neq 0$ thanks to which division by d is permissible. This immediately yields

$$\rho = \frac{1}{d}\Big[c \pm \sqrt{c^2 - d^2}\Big] \tag{5.26}$$

It is customary to call a solution $\rho = \rho(\bar{k})$ to equation (5.24), treated as a function of the Fourier mode $\bar{k}$, a symbol of the numerical scheme [36]. Moreover, one should note that, in general, for n–time level schemes the symbol is obtained as a solution to a polynomial equation of degree n in ρ.

One continues the analysis by observing that

$$c^2 - d^2 = 16\sigma\Big(\chi(\Delta t)^2\sigma - 4\lambda^2\tau\Big),$$

for which two cases are possible. First, assume that $c^2 - d^2 \geq 0$. This assumption implies that

$$\frac{4}{(\Delta x)^2}\tan^2(\bar{k}/2) - \chi \leq 0, \tag{5.27}$$

and, since both $\sigma,\ \tau \geq 0$ and $\tau/\sigma = \tan^2(\bar{k}/2)$, the solution to inequality (5.27) is of the form

$$|\bar{k}| \leq \bar{k}_0, \tag{5.28}$$

where

$$\bar{k}_0 = 2\arctan\Big(\frac{\chi\Delta x}{2}\Big). \tag{5.29}$$

Inequality (5.28) reflects natural symmetry of the dispersion curve.

Second possibility, namely that $c^2 - d^2 < 0$, leads to the expression of the discrete dispersion relationship. Assuming that

$$\bar{\omega} = \bar{\omega}_R + \imath\bar{\omega}_I \tag{5.30}$$

and writing (5.22) in the trigonometric form

$$\rho = e^{-\bar{\omega}_I} e^{\imath \bar{\omega}_R} = e^{-\bar{\omega}_I}[\cos(\bar{\omega}_R) + \imath \sin(\bar{\omega}_R)] \tag{5.31}$$

one arrives at

$$\rho = \frac{c}{d} \pm \imath \frac{\sqrt{d^2 - c^2}}{d}$$

and so

$$|\rho|^2 = e^{-2\bar{\omega}_I} = \frac{c^2}{d^2} + \frac{d^2 - c^2}{d^2} = 1$$

thus $\bar{\omega}_I = 0$ (stable, nondissipative scheme) and

$$\tan^2(\bar{\omega}_R) = \frac{d^2 - c^2}{c^2} = \frac{-16(\Delta t)^2}{[4 + \chi(\Delta t)^2]^2} \frac{\left[\chi - \frac{4\lambda^2}{(\Delta t)^2} \tan^2(\bar{k}/2)\right]}{\left[1 - \frac{4\lambda^2}{4 + \chi(\Delta t)^2} \tan^2(\bar{k}/2)\right]^2} \tag{5.32}$$

Upon expanding the denominator of (5.32) in Taylor series one obtains

$$(\bar{\omega}_R)^2 \approx \frac{16(\Delta t)^2}{[4 + \chi(\Delta t)^2]^2} \Big[\frac{4\lambda^2}{(\Delta t)^2} \tan^2(\bar{k}/2) - \chi\Big] \Big[1 + 2\frac{4\lambda^2}{4 + \chi(\Delta t)^2} \tan^2(\bar{k}/2)\Big] \tag{5.33}$$

and further simplifications yield

$$\omega_R^2 \approx -\frac{16}{[4 + \chi(\Delta t)^2]^2} \Big[\chi - \frac{4}{(\Delta t)^2} \Big(\frac{\Delta t}{\Delta x}\Big)^2 \frac{4 - \chi(\Delta t)^2}{4 + \chi(\Delta t)^2} \frac{(\bar{k})^2}{4}\Big]$$

Thus in the limit as $\Delta t \to 0$,

$$\omega^2 = \omega_R^2 \to k^2 - \chi$$

The following observation is necessary to determine the appropriate domain restriction of the tangent function. The singularity of the denominator in (5.32) occurs at

$$\bar{k} = \bar{k}_S = \pm 2 \arctan \frac{\sqrt{4 + \chi(\Delta t)^2}}{2\lambda}$$

where the denominator in (5.32) is zero. Moreover, since

$$|\tan(\bar{\omega}_R)| = \frac{4\sqrt{4\lambda^2\tan^2(\bar{k}/2) - \chi(\Delta t)^2}}{\left|4 + \chi(\Delta t)^2 - 4\lambda^2\tan^2(\bar{k}/2)\right|} \stackrel{\text{df}}{=} \Upsilon_1(\Delta x, \Delta t, \bar{k}) \tag{5.34}$$

by restricting the domain of tangent function to $(0, \pi/2) \cup (\pi/2, \pi)$ one obtains

$$\bar{\omega}_R = \begin{cases} \arctan(\Upsilon(\bar{k}; \Delta x, \Delta t)) & \text{for} \quad k \in (\bar{k}_0, \bar{k}_S), \\ \pi - \arctan(\Upsilon(\bar{k}; \Delta x, \Delta t)) & \text{for} \quad k \in (\bar{k}_S, \pi), \end{cases} \tag{5.35}$$

where $\Upsilon = \Upsilon_1$.

MS–2 Formulation Linearization of the MS–2 form yields

$$D_t D_x^2 M_t^2 u_j^n - D_t^3 M_x^2 u_j^n + \chi D_t M_t^2 M_x^2 u_j^n = 0 \tag{5.36}$$

Noticing that

$$\begin{aligned} D_t M_t^2 M_x^2 u_j^n &= \frac{1}{16\Delta t}\Big[(u_{j+2}^{n+3} + 2u_{j+1}^{n+3} + u_j^{n+3}) + (u_{j+2}^{n+2} + 2u_{j+1}^{n+2} + u_j^{n+2}) \\ &\qquad -(u_{j+2}^{n+1} + 2u_{j+1}^{n+1} + u_j^{n+1}) - (u_{j+2}^{n} + 2u_{j+1}^{n} + u_j^{n})\Big] \end{aligned}$$

equation (5.36) becomes

$$\begin{aligned} 0 &= \frac{1}{4\Delta t(\Delta x)^2}\Big[(u_{j+2}^{n+3} - 2u_{j+1}^{n+3} + u_j^{n+3}) + (u_{j+2}^{n+2} - 2u_{j+1}^{n+2} + u_j^{n+2}) \\ &\qquad -(u_{j+2}^{n+1} - 2u_{j+1}^{n+1} + u_j^{n+1}) - (u_{j+2}^{n} - 2u_{j+1}^{n} + u_j^{n})\Big] \\ &\quad -\frac{1}{4(\Delta t)^3}\Big[(u_{j+2}^{n+3} + 2u_{j+1}^{n+3} + u_j^{n+3}) - 3(u_{j+2}^{n+2} + 2u_{j+1}^{n+2} + u_j^{n+2}) \\ &\qquad +3(u_{j+2}^{n+1} + 2u_{j+1}^{n+1} + u_j^{n+1}) - (u_{j+2}^{n} + 2u_{j+1}^{n} + u_j^{n})\Big] \\ &\quad -\frac{\chi}{16\Delta t}\Big[(u_{j+2}^{n+3} + 2u_{j+1}^{n+3} + u_j^{n+3}) + (u_{j+2}^{n+2} + 2u_{j+1}^{n+2} + u_j^{n+2}) \\ &\qquad -(u_{j+2}^{n+1} + 2u_{j+1}^{n+1} + u_j^{n+1}) - (u_{j+2}^{n} + 2u_{j+1}^{n} + u_j^{n})\Big] \end{aligned}$$

and after substituting (5.1) and simplifying

$$\begin{aligned} 4\Big[(e^{\imath(2\bar{k})}+2e^{\imath\bar{k}}+1)(e^{\imath(3\omega\Delta t)}-3e^{\imath(2\omega\Delta t)}+3e^{\imath\omega\Delta t}-1)\Big] \\ -4\lambda^2\Big[(e^{\imath(2\bar{k})}-2e^{\imath\bar{k}}+1)(e^{\imath(3\omega\Delta t)}+e^{\imath(2\omega\Delta t)}-e^{\imath\omega\Delta t}-1)\Big] \\ -\chi(\Delta t)^2\Big[(e^{\imath(2\bar{k})}+2e^{\imath\bar{k}}+1)(e^{\imath(3\omega\Delta t)}+e^{\imath(2\omega\Delta t)}-e^{\imath\omega\Delta t}-1)\Big] \;=\; 0 \end{aligned} \tag{5.37}$$

with λ given by (4.31).

Define $c_1 = 12\sigma - 4\lambda^2\tau + \chi(\Delta t)^2\sigma$ and let d be given by (5.25b). The solution to the equation

$$\rho^3 - \frac{c_1}{d}\rho^2 + \frac{c_1}{d}\rho - 1 = 0$$

is a symbol of the MS–2 scheme.

For further analysis note first that the equation above can be factored

$$(\rho-1)\Big[\rho^2 + \Big(1-\frac{c_1}{d}\Big)\rho + 1\Big] = 0$$

That is, either $e^{\imath\omega\Delta t} = e^{-\bar{\omega}_I}e^{\imath\bar{\omega}_R} = 1$, so $\omega_R = \bar{\omega}_I = 0$ or

$$\rho^2 + \Big(1-\frac{c_1}{d}\Big)\rho + 1 = 0$$

which has the solution

$$\rho = \frac{(c_1-d) \pm \sqrt{c_1^2 - 2dc_1 - 3d^2}}{2d}$$

The discriminant is equal to

$$c_1^2 - 2dc_1 - 3d^2 = 64\sigma^2\Big(\chi(\Delta t)^2 - 4\lambda^2\tan(\bar{k}/2)\Big)$$

and is negative for $\bar{k}$ satisfying (5.28) and (5.29). Therefore

$$|\rho|^2 = e^{-2b\Delta t} = \frac{(c_1 - d)^2}{4d^2} + \frac{-(c_1^2 - 2dc_1 - 3d^2)}{4d^2} = 1$$

thus $\bar{\omega}_I = 0$ (stable, nondissipative scheme) and

$$\tan^2(\bar{\omega}_R) = \frac{3d^2 + 2dc_1 - c_1^2}{(c_1 - d)^2} = \frac{64\sigma^2\Big(4\lambda^2 \tan^2(\bar{k}/2) - \chi(\Delta t)^2\Big)}{4\sigma^2\Big(4 + \chi(\Delta t)^2 - 4\lambda^2 \tan^2(\bar{k}/2)\Big)^2}$$

which we recognize to be (5.32). We thus conclude, that for the MS–2 formulation the dispersion curve is the union of curves described by (5.35) and the curve given by $e^{\imath\omega\Delta t} = e^{-\bar{\omega}_I} e^{\imath\bar{\omega}_R} = 1$, that is $\omega_R \equiv 0$.

5.2.2 Leap–frog (MS–3)

For the linearized equation the leap–frog scheme takes the form

$$(u_{j+1}^{n+2} - 2u_{j+1}^{n+1} + u_{j+1}^{n}) - \lambda^2(u_{j+2}^{n+1} - 2u_{j+1}^{n+1} + u_{j}^{n+1}) - \chi(\Delta t)^2 u_{j+1}^{n+1} = 0 \tag{5.38}$$

Substituting the ansatz solution (5.2) and simplifying one arrives at

$$\Big(e^{2\imath\omega\Delta t} - 2e^{\imath\omega\Delta t} + 1\Big) - 2\lambda^2 e^{\imath\omega\Delta t}\Big(\cos(\bar{k}) - 1\Big) - \chi(\Delta t)^2 e^{\imath\omega\Delta t} = 0 \tag{5.39}$$

There are two possible approaches. The first one is similar to the one presented in [6] and will be described in Section 5.4. The symbol approach will provide us with more information and thus we consider (5.39) and let ρ, σ and τ to be as defined in (5.22), (5.23) so that

$$\rho^2 - \Big(2 - 2\lambda^2\tau + \chi(\Delta t)^2\Big)\rho + 1 = 0$$

Denote $c_2 = 2 + \chi(\Delta t)^2 - 2\lambda^2\tau$. The quadratic equation above has the solution

$$\rho = \frac{c_2 \pm \sqrt{c_2^2 - 4}}{2}$$

Clearly $\tau \in [0,2]$ is a monotonically increasing function of $\bar{k}$ and since the discriminant

$$c_2^2 - 4 = 4\lambda^4\tau^2 - 4\lambda^2(2+\chi(\Delta t)^2)\tau + \chi\Big(4(\Delta t)^2 + (\Delta t)^4\Big) \tag{5.40}$$

is a quadratic form in τ with the discriminant

$$16\lambda^4(2+\chi(\Delta t)^2)^2 - 16\chi\lambda^4\Big(4(\Delta t)^2 + (\Delta t)^4\Big) = 2^6\lambda^4 > 0$$

so there are two roots of (5.40)

$$\tau = \frac{4\lambda^2(2+\chi(\Delta t)^2) \pm 8\lambda^2}{8\lambda^4} = \frac{(2+\chi(\Delta t)^2) \pm 2}{2\lambda^2} > 0$$

Notice that for $\lambda < 1$ (CFL condition)

$$\tau_+ = \frac{(4+\chi(\Delta t)^2)}{2\lambda^2} > 2$$

and since $\tau_- = \chi(\Delta x)^2/2 > 0$ we have that $c_2^2 - 4 > 0$ for all $\tau < \tau_-$, i.e. for all $\bar{k}$ satisfying

$$2\sin^2(\bar{k}/2) < \chi(\Delta x)^2/2$$

that is for $\bar{k}$ satisfying (5.28) with

$$\bar{k}_0 = \bar{k}_0(\Delta x) = 2\arcsin(\chi(\Delta x)/2) \tag{5.41}$$

Clearly if $\Delta x < 2$ than $\tau_- < 2$ as well.

Assuming (5.30) we arrive at the conclusion that the scheme is unconditionally stable

$$|\rho|^2 = e^{-2b\Delta t} = \frac{c_2^2}{4} + \frac{4-c_2^2}{4} = 1$$

and the dispersion relation is given by

$$\begin{aligned}
\tan^2(\bar{\omega}_R) &= \frac{4-c_2^2}{c_2^2} \\
&= \frac{-16\lambda^4\sin^4(\bar{k}/2) + 8\lambda^2(2+\chi(\Delta t)^2)\sin^2(\bar{k}/2) - \chi\Big(4(\Delta t)^2 + (\Delta t)^4\Big)}{\Big(2+\chi(\Delta t)^2 - 4\lambda^2\sin^2(\bar{k}/2)\Big)^2}
\end{aligned}$$

The standard perturbation analysis yields that $\omega_R^2 \approx k^2 - \chi$. Clearly $c_2 = 0$ for

$$\bar{k}_S = \arcsin\Big(\frac{\sqrt{2+\chi(\Delta t)^2}}{2\lambda}\Big) \tag{5.42}$$

and thus, for the purpose of inverting the tangent function, its domain has to be restricted to $(0, \pi/2) \cup (\pi/2, \pi)$.

Moreover, since

$$\begin{aligned} |\tan(\bar{\omega}_R)| &= \frac{\sqrt{-16\lambda^4 \sin^4(\bar{k}/2) + 8\lambda^2(2+\chi(\Delta t)^2)\sin^2(\bar{k}/2) - \chi\Big(4(\Delta t)^2 + (\Delta t)^4\Big)}}{\Big|2 + \chi(\Delta t)^2 - 4\lambda^2 \sin^2(\bar{k}/2)\Big|} \\ &\stackrel{\text{df}}{=} \Upsilon_2(\bar{k}; \Delta x, \Delta t) \end{aligned}$$

the dispersion relation takes the form (5.35) with $\Upsilon = \Upsilon_2$.

5.2.3 Implicit Runge – Kutta (MS–4)

The linearized sine–Gordon equation (5.5) with the notation introduced for (3.12) yields the following discretization

$$\dot{p}_j = \frac{1}{(\Delta x)^2}(q_{j-1} - 2q_j + q_{j+1}) + \chi q_j \tag{5.43a}$$

$$\dot{q}_j = p_j \tag{5.43b}$$

The system (5.43) is a hamiltonian system of ODEs with Hamiltonian function

$$\widetilde{H}_L(\mathbf{p}, \mathbf{q}) = \sum_j \Big[\frac{1}{2}(p_j^2 + \chi q_j^2) + \frac{1}{2(\Delta x)^2}(q_{j+1} - q_j)^2\Big] \tag{5.44}$$

Using an implicit midpoint rule we can write the MS–4 scheme as

$$\begin{aligned} p_j^{n+1} - p_j^n &= \frac{\Delta t}{2(\Delta x)^2}\Big[(q_{j-1}^{n+1} - 2q_j^{n+1} + q_{j+1}^{n+1}) + (q_{j-1}^n - 2q_j^n + q_{j+1}^n)\Big] + \frac{\chi \Delta t}{2}(q_j^{n+1} + q_j^n) \\ q_j^{n+1} &= q_j^n + \frac{\Delta t}{2}(p_j^{n+1} + p_j^n) \end{aligned}$$

for $j \in \{1, \ldots, J\}$ and for any $n \in \mathbb{N}$. Solving for p_j^{n+1} and p_j^n and substituting back we have that

$$\begin{aligned} & 4(q_j^{n+2} - 2q_j^{n+1} + q_j^n) - \chi(\Delta t)^2(q_j^{n+2} + 2q_j^{n+1} + q_j^n) \\ -\lambda^2\Big[(q_{j-1}^{n+2} - 2q_j^{n+2} + q_{j+1}^{n+2}) + 2(q_{j-1}^{n+1} - 2q_j^{n+1} + q_{j+1}^{n+1}) + (q_{j-1}^n - 2q_j^n + q_{j+1}^n)\Big] &= 0 \end{aligned}$$

Using for q_j^n the right hand side of the ansatz solution (5.2) and notation (4.31) one can write

$$4(\rho^2 - 2\rho + 1) - \chi(\Delta t)^2(\rho^2 + 2\rho + 1) + 2\lambda^2\tau(\rho^2 + 2\rho + 1) = 0$$

where ρ is given in (5.22). Combining like–terms we have

$$d_3\rho^2 - 2c_3\rho + d_3 = 0$$

where

$$\begin{aligned} c_3 &= 4 + \chi(\Delta t)^2 - 2\lambda^2\tau \\ d_3 &= 4 - \chi(\Delta t)^2 + 2\lambda^2\tau \end{aligned}$$

The solution is

$$\rho = \frac{1}{d_3}\Big[c_3 \pm \sqrt{c_3^2 - d_3^2}\Big]$$

where

$$c_3^2 - d_3^2 = 16\lambda^2\Big(\chi(\Delta x)^2 - 2\tau\Big)$$

Notice that $0 \leq \Delta x \leq 2$ the discriminant $c_3^2 - d_3^2 \geq 0$ iff

$$\chi(\Delta x)^2 - 4\sin^2(\bar{k}/2) \geq 0$$

that is for $\bar{k}$ satisfying (5.28) with $\bar{k}_0$ given by (5.41).

For all $\bar{k}$ for which $c_3^2 - d_3^2 < 0$ the scheme under consideration is nondissipative and stable, since if we assume (5.30) and (5.31) we arrive at

$$\rho = \frac{c_3}{d_3} \pm \imath \frac{\sqrt{d_3^2 - c_3^2}}{d_3}$$

and so

$$|\rho|^2 = e^{-2b\Delta t} = \frac{c_3^2}{d_3^2} + \frac{d_3^2 - c_3^2}{d_3^2} = 1$$

that implies $\bar{\omega}_I = 0$. Moreover

$$\tan^2(\bar{\omega}_R) = \frac{d_3^2 - c_3^2}{c_3^2} = \frac{16\Big(4\lambda^2 \sin^2(\bar{k}/2) - \chi(\Delta t)^2\Big)}{\Big(4 + \chi(\Delta t)^2 - 4\lambda^2 \sin^2(\bar{k}/2)\Big)^2} \tag{5.45}$$

that is, to leading order, consistent with the analytic dispersion relation.

In order to obtain correct plots notice first that for

$$\bar{k} = \bar{k}_S = \arcsin\Big(\frac{\sqrt{4 + \chi(\Delta t)^2}}{2\lambda}\Big)$$

the denominator in (5.45) is zero. Moreover, since

$$|\tan(\bar{\omega}_R)| = \frac{4\sqrt{4\lambda^2 \sin^2(\bar{k}/2) - \chi(\Delta t)^2}}{|4 + \chi(\Delta t)^2 - 4\lambda^2 \sin^2(\bar{k}/2)|} \stackrel{\text{df}}{=} \Upsilon_3(\bar{k}; \Delta x, \Delta t)$$

the dispersion relation has the form (5.35) with $\Upsilon = \Upsilon_3$.

Since, by the virtue of the Viete's formulas, $\rho_+ \rho_- = c/a = 1$, there always will be an unstable solution for $k \leq k_0$.

5.2.4 Explicit Runge–Kutta (ERK)

A nonsymplectic discretization of (5.43) obtained by the explicit Runge–Kutta method (ERK) can be written as

$$\begin{aligned} P_j^n &= p_j^n + \frac{\Delta t}{2}\Big[\frac{1}{(\Delta x)^2}(q_{j-1}^n - 2q_j^n + q_{j+1}^n) + \chi q_j^n\Big] \\ Q_j^n &= q_j^n + \frac{\Delta t}{2} p_j^n \end{aligned}$$

and

$$\begin{aligned} p_j^{n+1} &= p_j^n + \Delta t\Big[\frac{1}{(\Delta x)^2}(Q_{j-1}^n - 2Q_j^n + Q_{j+1}^n) + \chi Q_j^n\Big] \\ q_j^{n+1} &= q_j^n + \Delta t P_j^n \end{aligned}$$

Clearly

$$Q_{j-1}^n - 2Q_j^n + Q_{j+1}^n = (q_{j-1}^n - 2q_j^n + q_{j+1}^n) + \frac{\Delta t}{2}(p_{j-1}^n - 2p_j^n + p_{j+1}^n)$$

thus

$$\begin{aligned} p_j^{n+1} &= p_j^n + \Delta t\Big[\frac{1}{(\Delta x)^2}\Big((q_{j-1}^n - 2q_j^n + q_{j+1}^n) + \frac{\Delta t}{2}(p_{j-1}^n - 2p_j^n + p_{j+1}^n)\Big) \\ &\qquad +\chi\Big(q_j^n + \frac{\Delta t}{2} p_j^n\Big)\Big] \qquad (5.46a) \\ q_j^{n+1} &= q_j^n + \Delta t\Big[p_j^n + \frac{\Delta t}{2}\Big(\frac{1}{(\Delta x)^2}(q_{j-1}^n - 2q_j^n + q_{j+1}^n) + \chi q_j^n\Big)\Big] \qquad (5.46b) \end{aligned}$$

and from the equation (5.46b)

$$(\Delta t) p_j^n = (q_j^{n+1} - q_j^n) - \frac{(\Delta t)^2}{2}\Big(\frac{1}{(\Delta x)^2}(q_{j-1}^n - 2q_j^n + q_{j+1}^n) + \chi q_j^n\Big),$$

that is

$$(\Delta t) p_j^n = (q_j^{n+1} - q_j^n) - \frac{1}{2}\lambda^2 S_j^n - \frac{\chi}{2}(\Delta t)^2 q_j^n,$$

where $S_j^n = q_{j-1}^n - 2q_j^n + q_{j+1}^n$ and λ is given by (4.31). Clearly then

$$(\Delta t)(p_{j-1}^n - 2p_j^n + p_{j+1}^n) = S_j^{n+1} - S_j^n - \frac{\lambda^2}{2}(S_{j-1}^n - 2S_j^n + S_{j+1}^n) - \frac{\chi}{2}(\Delta t)^2 S_j^n$$

and

$$\begin{aligned}(\Delta t)(p_j^{n+1} - p_j^n) &= (q_j^{n+2} - 2q_j^{n+1} + q_j^n) \\ &\quad -\frac{1}{2}\lambda^2(S_j^{n+1} - S_j^n) - \frac{\chi(\Delta t)^2}{2}(q_j^{n+1} - q_j^n) \qquad (5.47)\end{aligned}$$

on the other hand side, from (5.46a) one obtains

$$\begin{aligned}(\Delta t)(p_j^{n+1} - p_j^n) &= \frac{\lambda^2}{2}(S_j^{n+1} - S_j^n) + \frac{\chi(\Delta t)^2}{2}(q_j^{n+1} - q_j^n) + \lambda^2 S_j^n + \chi(\Delta t)^2 q_j^n \\ &\quad -\frac{\lambda^4}{4}(S_{j-1}^n - 2S_j^n + S_{j+1}^n) - \frac{\chi(\Delta t)^2}{2}\lambda^2 S_j^n - \frac{\chi^2(\Delta t)^4}{4}q_j^n \qquad (5.48)\end{aligned}$$

It is now clear, by equating right-hand sides of (5.47) and (5.48) and simplifying, that

$$\begin{aligned}&(q_j^{n+2} - 2q_j^{n+1} + q_j^n) - \chi(\Delta t)^2 q_j^{n+1} - \lambda^2 S_j^{n+1} \\ &+\frac{\lambda^4}{4}(S_{j-1}^n - 2S_j^n + S_{j+1}^n) + \frac{\chi(\Delta t)^2}{2}\lambda^2 S_j^n + \frac{\chi^2(\Delta t)^4}{4}q_j^n &= 0.\end{aligned}$$

If we assume that q_j^n is equal to the right hand side of (5.2) we will obtain

$$\begin{aligned}S_j^n &= -4\sin^2(\bar{k}/2)q_j^n \\ S_j^{n+1} &= -4e^{\imath\omega\Delta t}\sin^2(\bar{k}/2)q_j^n \\ S_{j+1}^n - 2S_j^n + S_{j-1}^n &= 16\sin^4(\bar{k}/2)q_j^n\end{aligned}$$

and upon division by q_j^n and simplification

$$e^{\imath 2\omega\Delta t} - [2 + \chi(\Delta t)^2 - 4\lambda^2\tau]e^{\imath\omega\Delta t} + 4\lambda^4\sin^4(\bar{k}/2) - 2\chi\lambda^2(\Delta t)^2\tau + \frac{\chi(\Delta t)^4}{4} + 1 = 0,$$

where we used notation (5.23). Let now ρ be as in (5.22) and

$$\begin{aligned} c_4 &= 2+\chi(\Delta t)^2-4\lambda^2\tau \\ d_4 &= 4\lambda^4\tau^2-2\chi\lambda^2(\Delta t)^2\tau+\frac{\chi(\Delta t)^4}{4}+1 \end{aligned}$$

The equation takes the form

$$\rho^2-c_4\rho+d_4=0$$

and its discriminant is equal to

$$c_4^2-4d_4=4\chi(\Delta t)^2-16\lambda^2\tau$$

The discriminant is negative for

$$\chi(\Delta t)^2-4\lambda^2\sin^2(\bar{k}/2)<0$$

that is for $\bar{k}$ satisfying (5.28) with $\bar{k}_0$ given by (5.41).

The scheme has the dispersion–dissipation relation obtained as follows. First, assume (5.30) and (5.31) so that

$$\rho=\frac{c_4}{2}\pm\frac{\sqrt{c_4^2-4d_4}}{2}$$

and we have that

$$|\rho|^2=e^{-2b\Delta t}=\frac{c_4^2}{4}+\frac{4d_4-c_4^2}{4}=d_4=4\lambda^4\tau^2-2\chi\lambda^2(\Delta t)^2\tau+\frac{\chi(\Delta t)^4}{4}+1 \tag{5.49}$$

and

$$\begin{aligned} \tan^2(\bar{\omega}_R)=\frac{4d_4-c_4^2}{c_4^2} &= \frac{-4(\Delta t)^2}{(2+\chi(\Delta t)^2)^2}\frac{\chi-\frac{2}{(\Delta x)^2}\sin^2(\bar{k}/2)}{\Big(1-\frac{2\lambda^2}{2+\chi(\Delta t)^2}\sin^2(\bar{k}/2)\Big)^2} \\ &\approx \frac{-4(\Delta t)^2}{(2+\chi(\Delta t)^2)^2}(\chi-\bar{k}^2)\Big(1+2\frac{(\Delta t)^2\bar{k}^2}{2+\chi(\Delta t)^2}\Big) \end{aligned}$$

Now

$$\omega_R^2 \approx \frac{-4}{(2+\chi(\Delta t)^2)^2}(\chi - \bar{k}^2)\Big(1 + 2\frac{(\Delta t)^2\bar{k}^2}{2+\chi(\Delta t)^2}\Big)$$

and as $\Delta t \to 0$ we have that

$$\omega_R^2 \approx k^2 - \chi$$

that is the analytic dispersion relation.

Observe also that $|\rho|^2 \geq 1$ since

$$|\rho|^2 - 1 = e^{-2b\Delta t} = \frac{c_4^2}{4} + \frac{4d_4 - c_4^2}{4} = d_4 = 4\lambda^4\tau^2 - 2\chi\lambda^2(\Delta t)^2\tau + \frac{\chi(\Delta t)^4}{4} \tag{5.50}$$

is a quadratic form in τ and its discriminant

$$4\chi\lambda^4(\Delta t)^4 - 16\lambda^4\frac{\chi(\Delta t)^4}{4} \equiv 0$$

and $\lambda^4 > 0$. The only stable Fourier mode is for $|\rho|^2 = 1$ that is then

$$|\rho|^2 = \lambda^4\Big(\tau - \frac{\chi(\Delta t)^2}{2\lambda^2}\Big)^2$$

i.e. for $\bar{k} = \bar{k}_0$ given by (5.41).

Finally, since the dispersion relationship has the form

$$\tan^2(\bar{\omega}_R) \;=\; \frac{4c - c_4^2}{c_4^2} = \frac{4\Big(4\lambda^2\sin^2(\bar{k}/2) - \chi(\Delta t)^2\Big)}{\Big(2 + \chi(\Delta t)^2 - 4\lambda^2\sin^2(\bar{k}/2)\Big)^2}$$

with the denominator having singularity for

$$\sin^2(\bar{k}/2) = \frac{2+\chi(\Delta t)^2}{4\lambda^2}$$

that is for $\bar{k} = \bar{k}_S$ given by (5.42) one can restrict the domain of the arctan to $(0, \pi/2) \cup (\pi/2, \pi)$ obtain

$$|\tan(\bar{\omega}_R)| = \frac{2\sqrt{4\lambda^2 \sin^2(\bar{k}/2) - \chi(\Delta t)^2}}{\left|2 + \chi(\Delta t)^2 - 4\lambda^2 \sin^2(\bar{k}/2)\right|} \stackrel{\text{df}}{=} \Upsilon_4(\bar{k}; \Delta x, \Delta t)$$

so the dispersion relation has the form (5.35) with $\Upsilon = \Upsilon_4$.

5.2.5 Preservation of the Dispersion Relation

A very informative quantity related to numerical dispersion relationship is the error in the propagation speed, defined as

$$R_c = \frac{\omega}{k} - c, \tag{5.51}$$

which in the particular case of the linearized sine–Gordon equation and discrete dispersion relations describer in this section takes the form

$$R_c = \frac{\bar{\omega}_R - \sqrt{\bar{k}^2 - \chi}}{\bar{k}}. \tag{5.52}$$

It is important to note that the residual in the phase velocity has the form $R_c = c_N - c_A$, i.e. it is the difference between the discrete phase velocity and the continuous one. What is important in propagation error analysis is the sign of the $R_c = R_c(\bar{k})$. Figure 5.4 represents the error in the propagation speed. One notes that the MS schemes have R_c is positive and thus the higher is the wave number is the faster that mode travels. Exactly opposite is the effect of other integrators. For all the non–MS schemes, except for ERK all numerical modes travel slower that analytic ones since $R_c < 0$. One observes that the error in the propagation speed curve for the ERK scheme changes sign, and is only negative for higher

wave numbers. The behavior of the solution although is qualitatively the same as for MS–3 and MS–4 schemes. Qualitatively, this behavior persists for all the choices of $(\Delta t, \Delta x)$, as long as $\lambda < 1$.

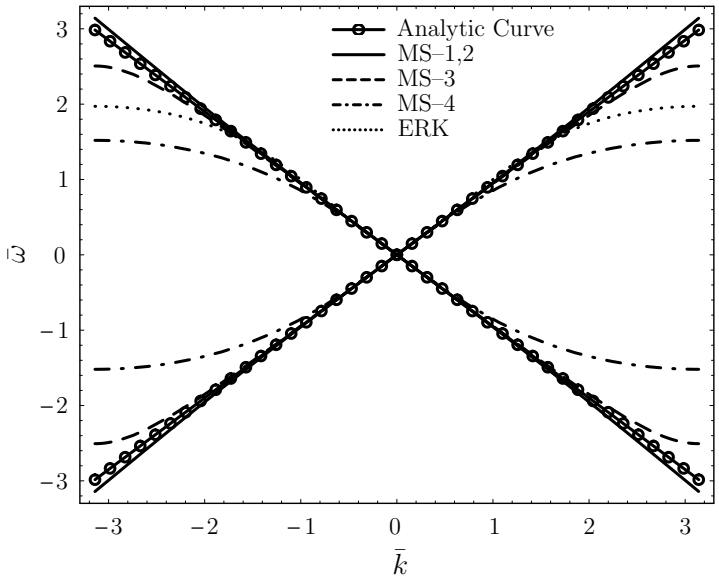

Figure 5.1: Dispersion curves for $\lambda = 0.95$.

The only curve that we could not derive from the simplified approach was the dispersion curve for the ERK. This is the first benefit of using the symbol approach. The second benefit of (a more complicated) symbol approach is the ability of the method to give the information about the linear stability. This information is obtained by considering a (general) complex–valued $\bar{\omega}$ and at the end splitting it onto the real and imaginary part. As we have seen the imaginary part gives rise to the dispersion curve and the real part occurs in the exponent of the growth factor e^{ω_I}. We observed that for all symplectic and multisymplectic schemes the growth factor if identically equal to 1 (indicating no growth and lack of energy dissipation).

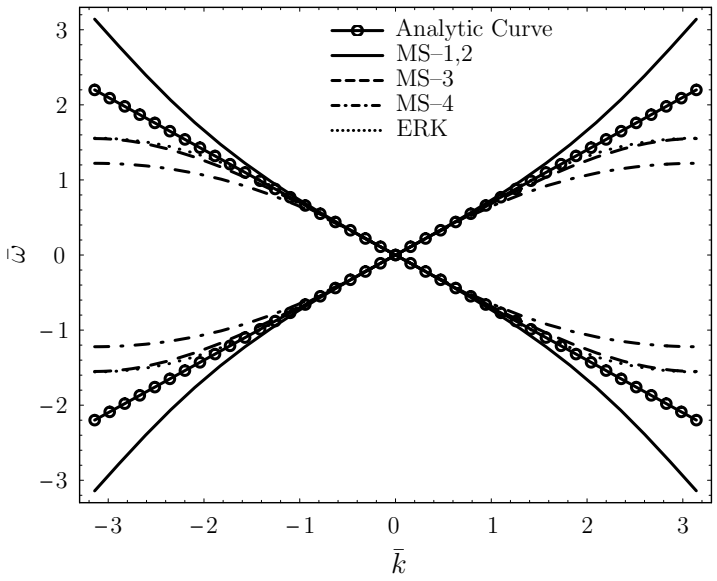

Figure 5.2: Dispersion curves for $\lambda = 0.70$.

It turned out that for the non–symplectic scheme (ERK) the growth factor is greater that 1 (indicating growth, instability) which is further confirmed by numerical simulations (Figure 6.4).

5.2.6 Group Velocity Disperssion

Recollect (cf. [4, 40]) that the problem is *dispersive* if

$$\frac{\mathrm{d}^2\omega}{\mathrm{d}k^2} \not\equiv 0.$$

In t he case of dispersive equation different waves have different phase speeds, and the behavior of the solution depends on how the waves reinforce or interfere with each other. The important propagation velocity here is the group velocity

$$c_g(k) = \frac{\mathrm{d}\omega}{\mathrm{d}k}.$$

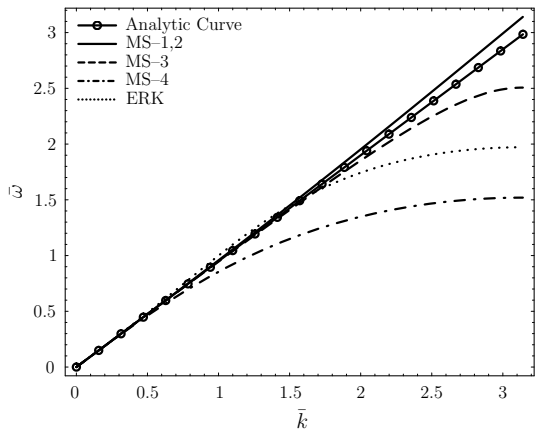

(a) $\lambda = 0.95$.

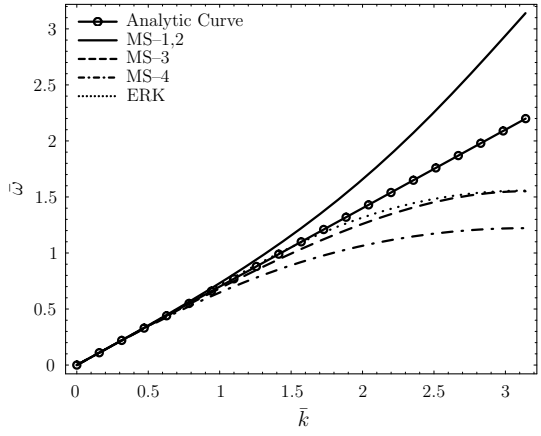

(b) $\lambda = 0.70$.

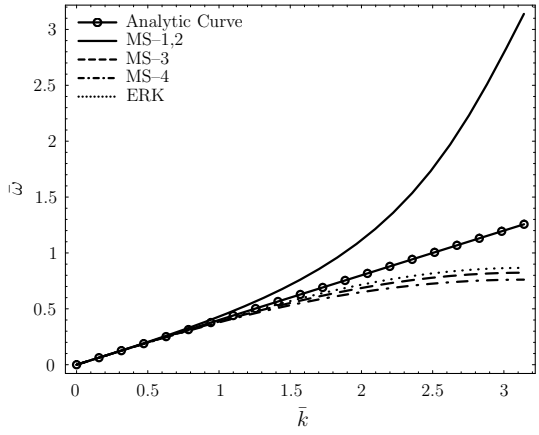

(c) $\lambda = 0.40$.

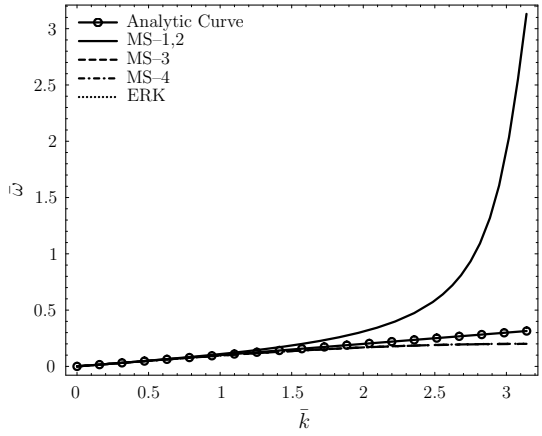

(d) $\lambda = 0.10$.

Figure 5.3: Dispersion curves for different values of λ. Plots show only the first quadrant due to symmetries with respect to both coordinate axes.

We observe that numerical group velocity for the discretizations, although different from the analytic one ($c = 1$) if well preserved. There exists diffeomorphisms mapping the analytic dispersion curve onto the numerical one for all the discretizations. As a consequence the sign of the numerical group velocity is constant in $\bar{k}$ thus indicating that the numerical solution will not have spurious modes.

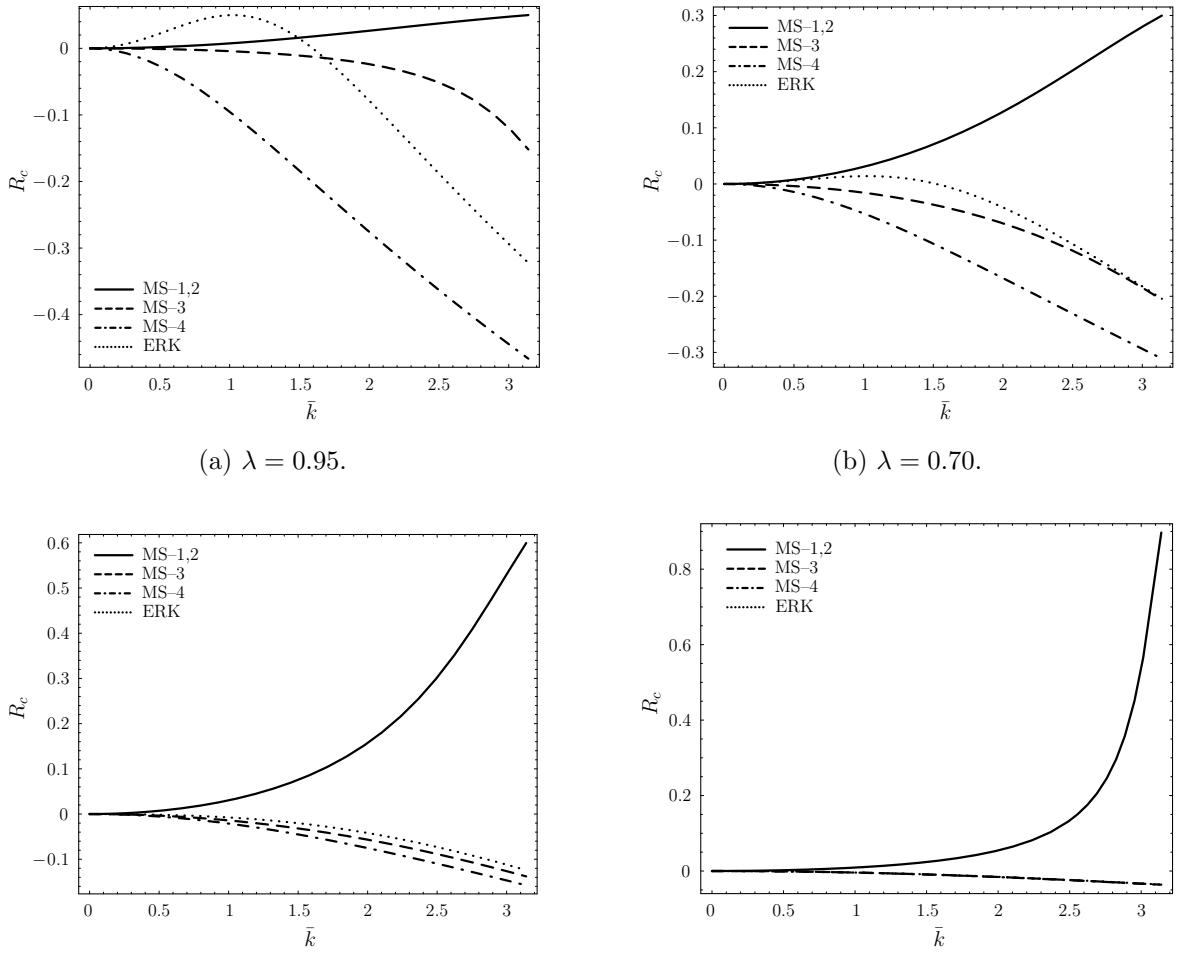

(a) $\lambda = 0.95$.

(b) $\lambda = 0.70$.

(c) $\lambda = 0.40$.

(d) $\lambda = 0.10$.

Figure 5.4: Error in the propagation speed for different values of λ.

We supplement dispersion analysis by discussing the significance of the second derivative of dispersion curves for the dispersion analysis. We first observe that $\bar{\omega}'' \not\equiv 0$ indicting that the discretization introduced artificial dispersion. Furthermore, we can divide schemes under investigation into two classes. The first class contains methods designated MS–1,2 and is described by the condition that $\forall_{\bar{k}}\ \bar{\omega}''(\bar{k}) > 0$. For these methods the higher the wave number $\bar{k}$ of a mode the faster the mode travels. The second class contains methods

designated MS–3,4 (and, for most cases – for sufficiently small λ, ERK belongs to this class). Here $\forall_{\bar{k}}\ \bar{\omega}''(\bar{k}) < 0$ and the higher the wave number $\bar{k}$ of a mode the slower the mode travels.

For the presentation we have chosen dispersion curves obtained for the discretizations of the linear wave equation $u_{tt} - u_{xx} = 0$. In this case discrete dispersion relation depends only on the parameter $\lambda = (\Delta t)/(\Delta x)$, which on the finite interval of the length ℓ can be written as $\lambda = J(\Delta t)/\ell$. One should not that the dispersion analysis does not take into account neither the initial nor boundary conditions imposed on the problem and therefore it suffices to present the dependence of the $\bar{\omega}''$ on the parameter λ in order to indicate independence of the $\mathrm{sgn}(\bar{\omega}'')$ on the mesh, i.e. its independence on λ. Values for λ are relatively large since, otherwise, curves designated MS–3,4 and ERK became indistinguishable.

5.3 Linearization of the NLS Equation

5.3.1 Box Scheme for the Linearized NLS

In order to supplement our discussion on dispersive properties of the box scheme we decided to present reduced box scheme discretization of the linearized NLS equation (5.15). Clearly, box scheme operators (4.6) applied to equation (5.16) yield

$$\begin{aligned}
D_t M_x v_j^n + D_x M_t (q_j^n + 4a^2 w_j^n) &= 0, \\
-D_t M_x u_j^n &= -M_t M_x v_j^n, \\
-D_x M_t (4a^2 u_j^n + p_j^n) &= -M_t M_x (q_j^n + 4a^2 w_j^n), \\
D_x M_t w_j^n &= M_t M_x p_j^n, \\
-D_x M_t u_j^n &= -M_t M_x w_j^n.
\end{aligned}$$

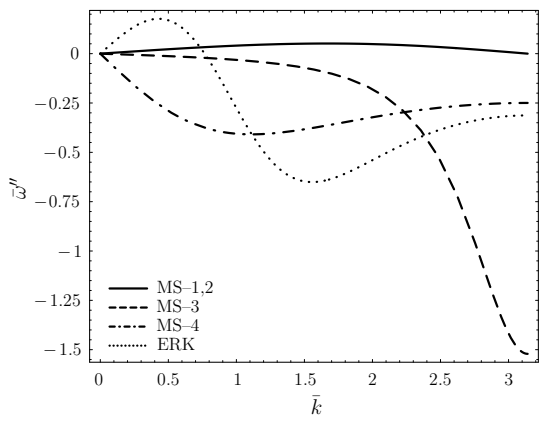

(a) $\lambda = 0.95$.

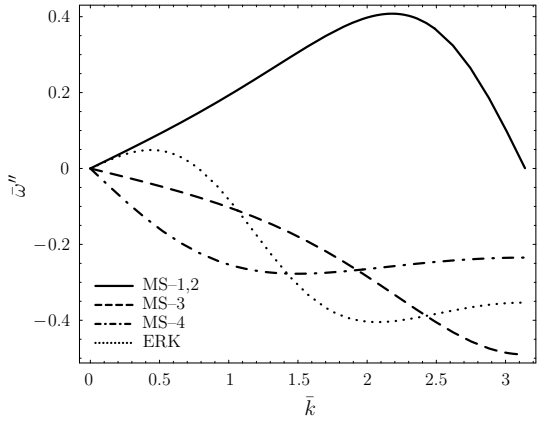

(b) $\lambda = 0.70$.

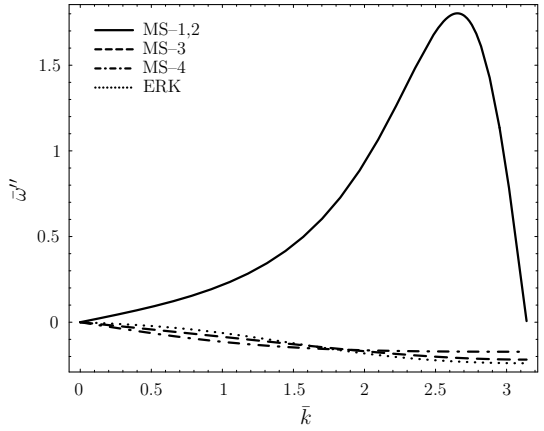

(c) $\lambda = 0.40$.

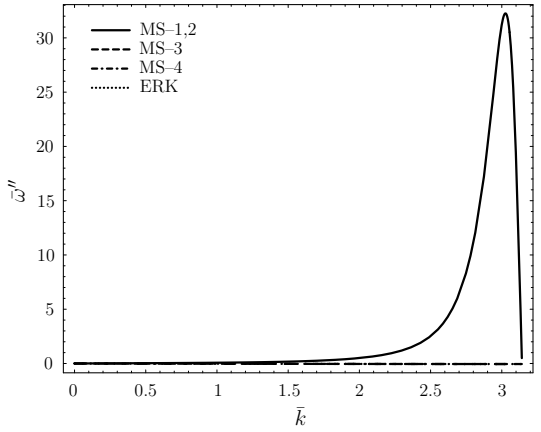

(d) $\lambda = 0.10$.

Figure 5.5: Group velocity dispersion ($\bar{\omega}''$) for different values of λ.

A reduced form is obtained by first applying M_x operator to the first equation and D_x to the third

$$\begin{aligned} D_t M_x^2 v_j^n + D_x M_t M_x (q_j^n + 4a^2 w_j^n) &= 0, \\ D_x^2 M_t (p_j^n + 4a^2 u_j^n) &= D_x M_t M_x (q_j^n + 4a^2 w_j^n), \end{aligned}$$

i.e., after applying $D_t M_x$ operator to the second equation,

$$\begin{aligned} D_t M_x^2 M_t v_j^n + D_x^2 M_t (p_j^n + 4a^2 u_j^n) &= 0, \\ -D_t^2 M_x^2 u_j^n &= -D_t M_x^2 M_t v_j^n. \end{aligned}$$

Moreover, applying M_x operator to the first equation gives

$$D_t^2 M_x^3 u_j^n + D_x^2 M_t^2 M_x (p_j^n + 4a^2 u_j^n) = 0.$$

From the fourth and fifth equation we can obtain

$$\begin{aligned} M_t M_x^2 p_j^n &= D_x M_t M_x w_j^n, \\ D_x^2 M_t u_j^n &= D_x M_t M_x w_j^n, \end{aligned}$$

i.e.

$$D_x^2 M_t^2 M_x^2 p_j^n = D_x^4 M_t^2 u_j^n,$$

and finally

$$D_t^2 M_x^4 u_j^n + D_x^4 M_t^2 u_j^n + 4a^2 D_x^2 M_t^2 M_x^2 u_j^n = 0. \tag{5.53}$$

Implementation For further use in Section 5.3 it would be convenient to express equation (5.53) explicitly in indices j and n. To achieve this we use notation (4.19) and (4.20) to obtain

the following

$$
\begin{aligned}
D_x^4 M_t^2 u_j^n &= \frac{1}{4(\Delta x)^4}\Bigg[\Big(u_{j+4}^{n+2} - 4u_{j+3}^{n+2} + 6u_{j+2}^{n+2} - 4u_{j+1}^{n+2} + u_j^{n+2}\Big) \\
&\quad +2\Big(u_{j+4}^{n+1} - 4u_{j+3}^{n+1} + 6u_{j+2}^{n+1} - 4u_{j+1}^{n+1} + u_j^{n+1}\Big) \\
&\quad +\Big(u_{j+4}^{n} - 4u_{j+3}^{n} + 6u_{j+2}^{n} - 4u_{j+1}^{n} + u_j^{n}\Big)\Bigg], \qquad (5.54a) \\
D_x^2 M_t^2 M_x^2 u_j^n &= \frac{1}{16(\Delta x)^2}\Bigg[\Big(u_{j+4}^{n+2} - 2u_{j+2}^{n+2} + u_j^{n+2}\Big) \\
&\quad +2\Big(u_{j+4}^{n+1} - 2u_{j+2}^{n+1} + u_j^{n+1}\Big) + \Big(u_{j+4}^{n} - 2u_{j+2}^{n} + u_j^{n}\Big)\Bigg], \qquad (5.54b) \\
D_t^2 M_x^4 u_j^n &= \frac{1}{16(\Delta t)^2}\Bigg[\Big(u_{j+4}^{n+2} + 4u_{j+3}^{n+2} + 6u_{j+2}^{n+2} + 4u_{j+1}^{n+2} + u_j^{n+2}\Big) \\
&\quad -2\Big(u_{j+4}^{n+1} + 4u_{j+3}^{n+1} + 6u_{j+2}^{n+1} + 4u_{j+1}^{n+1} + u_j^{n+1}\Big) \\
&\quad +\Big(u_{j+4}^{n} + 4u_{j+3}^{n} + 6u_{j+2}^{n} + 4u_{j+1}^{n} + u_j^{n}\Big)\Bigg]. \qquad (5.54c)
\end{aligned}
$$

5.3.2 Discrete Dispersion Relationship for the NLS

Consider now (5.53) and assume that u_j^n takes the form (5.2). Simple calculations yield

$$
\begin{aligned}
&(\Delta x)^2 \cos^4(\bar{k}/2)(\rho^2 - 2\rho + 1) + 4\lambda^2 \sin^4(\bar{k}/2)(\rho^2 + 2\rho + 1) \\
&\qquad -4a^2\lambda^2(\Delta x)^2 \sin^2(\bar{k}/2)\cos^2(\bar{k}/2)(\rho^2 + 2\rho + 1) \;=\; 0
\end{aligned}
$$

where ρ is given by (5.22) and $\lambda = \Delta t/\Delta x$. Dividing by $\cos^4(\bar{k}/2)$ we have

$$
d_5\rho^2 - 2c_5\rho + d_5 = 0
$$

where

$$
\begin{aligned}
d_5 &= (\Delta x)^2 + 4\lambda^2 \tan^4(\bar{k}/2) - 4a^2(\Delta t)^2 \tan^2(\bar{k}/2) \\
c_5 &= (\Delta x)^2 - 4\lambda^2 \tan^4(\bar{k}/2) + 4a^2(\Delta t)^2 \tan^2(\bar{k}/2)
\end{aligned}
$$

We observe that $d_5 > 0$ when $a^2(\Delta t) - 4 < 0$. Thus for numerical meshes satisfying $\Delta t < 4/a^2$ one has to solve

$$\rho^2 - 2\frac{c_5}{d_5}\rho + 1 = 0$$

The solution is

$$\rho = \frac{c_5 \pm \sqrt{c_5^2 - d_5^2}}{d_5}$$

and since $c_5^2 - d_5^2 = (c_5 + d_5)(c_5 - d_5) = 16(\Delta x)^2(a^2(\Delta t)^2 \tan^2(\bar{k}/2) - \lambda^2 \tan^4(\bar{k}/2))$ the solution ρ has nonzero imaginary part if $a(\Delta t) - \lambda \tan(\bar{k}/2) < 0$ i.e. if

$$\bar{k} > 2 \arctan\Big(a(\Delta x)\Big)$$

Then the solution can be written as

$$\rho = \frac{c_5}{d_5} \pm \imath \frac{\sqrt{d_5^2 - c_5^2}}{d_5}$$

so that, assuming that $\omega = \omega_R + \imath b$,

$$e^{-2b\Delta t} = |\rho|^2 = \frac{c_5^2}{d_5^2} + \frac{d_5^2 - c_5^2}{d_5^2} = 1$$

so $b = 0$ and the scheme is unconditionally stable and moreover

$$\begin{aligned} \tan^2(\bar{\omega}_R) &= \frac{d_5^2 - c_5^2}{c_5^2} \\ &= \frac{16(\Delta t)^2 \tan^2(\bar{k}/2)\Big(\tan^2(\bar{k}/2) - a^2(\Delta x)^2\Big)}{\Big((\Delta x)^2 - 4\lambda^2 \tan^4(\bar{k}/2) + 4a^2(\Delta t)^2 \tan^2(\bar{k}/2)\Big)^2} \stackrel{\text{df}}{=} \Upsilon_{NLS}(\bar{k}; \Delta x, \Delta t) \end{aligned}$$

Note, that the denominator vanishes at

$$\tan^2(\bar{k}/2) = (\Delta x)^2 \frac{a^2(\Delta t) \pm \sqrt{a^4(\Delta t)^2 + 1}}{2(\Delta t)}$$

and since we are interested in real solutions we have to choose $\bar{k}_S$ such that

$$\tan^2(\bar{k}_S/2) = (\Delta x)^2 \frac{a^2(\Delta t) + \sqrt{a^4(\Delta t)^2 + 1}}{2(\Delta t)}$$

Similarly as before, discrete dispersion relationship for the multisymplectic box discretization of the NLS equation is of the form (5.35) with $\Upsilon = \Upsilon_{NLS}$.

Standard perturbation techniques gives the following approximation

$$\omega_R^2 \approx \frac{4\bar{k}^2}{(\Delta x)^4}\Big((\bar{k}/2)^2 - a^2(\Delta x)^2\Big) = k^2(k^2 - 4a^2),$$

which, to the leading order, is equal to the analytic result (5.18).

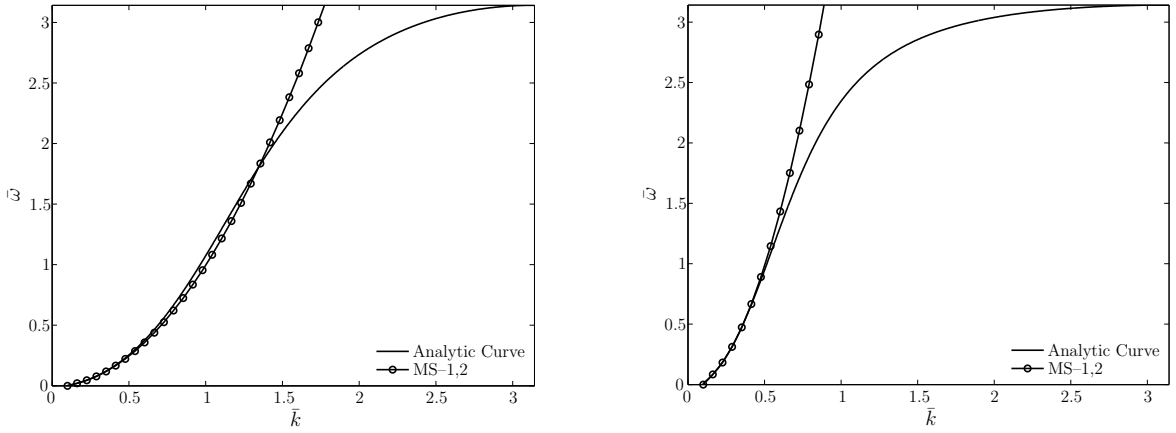

(a) $a = 0.5$, $\Delta x = 0.1$, $\Delta t = 0.01$.

(b) $a = 1$, $\Delta x = 0.05$, $\Delta t = 0.01$.

Figure 5.6: Dispersion Curves for the linearized NLS. The plot depicting dispersion curves shows only the first quadrant due to natural symmetries with respect to the origin.

5.4 Alternative Derivation of Dispersion Relationships

Following the approach of McLachlan and Ascher presented in [6] one can derive dispersion relations in a way simpler than what was presented before. The assumption underlying the

process is that $\bar{\omega}$ is a real quantity and has to be made in the initial stages of the derivation to enable conversion to the trigonometric form. Results, dispersion curves for schemes MS–1, MS–2, MS–3 and MS–4 are presented below. This approach produces identical results as previously discussed method, when applicable. However, there are two major drawbacks of this method. Firstly, one does not have access to information about possible growth/decay in the amplitude and secondly, for ERK, this method fails to produce correct dispersion curve. In the text that follows we use λ as defined in (4.31).

5.4.1 MS–1

Substituting the discrete Fourier mode (5.2) to the discretization (5.19) and simplifying one obtains

$$\begin{aligned} 4(e^{\imath 2\bar{k}} + 2e^{\imath\bar{k}} + 1)(e^{\imath 2\bar{\omega}} - 2e^{\imath\bar{\omega}} + 1) - 4\lambda^2(e^{\imath 2\bar{k}} - 2e^{\imath\bar{k}} + 1)(e^{\imath 2\bar{\omega}} + 2e^{\imath\bar{\omega}} + 1) & \\ -\chi(\Delta t)^2(e^{\imath 2\bar{k}} + 2e^{\imath\bar{k}} + 1)(e^{\imath 2\bar{\omega}} + 2e^{\imath\bar{\omega}} + 1) &= 0 \end{aligned} \quad (5.55)$$

Dividing both sides of (5.55) by $4(e^{\imath 2\bar{k}} + 2e^{\imath\bar{k}} + 1)(e^{\imath 2\bar{\omega}} + 2e^{\imath\bar{\omega}} + 1)$ one has

$$\frac{(e^{\imath\bar{\omega}} - 1)^2}{(e^{\imath\bar{\omega}} + 1)^2} - \lambda^2\frac{(e^{\imath\bar{k}} - 1)^2}{(e^{\imath\bar{k}} + 1)^2} - \chi\frac{(\Delta t)^2}{4} = 0$$

i.e. in trigonometric form

$$\left(\frac{2}{\Delta t}\tan\frac{\bar{\omega}}{2}\right)^2 - \left(\frac{2}{\Delta x}\tan\frac{\bar{k}}{2}\right)^2 + \chi = 0 \quad (5.56)$$

5.4.2 MS–2

For the MS–2 formulation (5.36) one has

$$\begin{aligned} & 4(e^{\imath 2\bar{k}} + 2e^{\imath\bar{k}} + 1)(e^{\imath 3\bar{\omega}} - 3e^{\imath 2\bar{\omega}} + 3e^{\imath\bar{\omega}} - 1) \\ & -4\lambda^2(e^{\imath 2\bar{k}} - 2e^{\imath\bar{k}} + 1)(e^{\imath 3\bar{\omega}} + e^{\imath 2\bar{\omega}} - e^{\imath\bar{\omega}} - 1) \\ & -\chi(\Delta t)^2(e^{\imath 2\bar{k}} + 2e^{\imath\bar{k}} + 1)(e^{\imath 3\bar{\omega}} + e^{\imath 2\bar{\omega}} - e^{\imath\bar{\omega}} - 1) \;\; = \;\; 0 \end{aligned} \tag{5.57}$$

Notice first that $e^{\imath 3\bar{\omega}} + e^{\imath 2\bar{\omega}} - e^{\imath\bar{\omega}} - 1 = (e^{\imath\bar{\omega}} - 1)(e^{\imath\bar{\omega}} + 1)^2$ and $e^{\imath 3\bar{\omega}} - 3e^{\imath 2\bar{\omega}} + 3e^{\imath\bar{\omega}} - 1 = (e^{\imath\bar{\omega}} - 1)^3$. Dividing (5.57) by $4(e^{\imath 2\bar{k}} + 2e^{\imath\bar{k}} + 1)$ one obtains

$$(e^{\imath\bar{\omega}} - 1)^3 - \lambda^2 \frac{(e^{\imath\bar{k}} - 1)^2}{(e^{\imath\bar{k}} + 1)^2}(e^{\imath\bar{\omega}} - 1)(e^{\imath\bar{\omega}} + 1)^2 - \chi \frac{(\Delta t)^2}{4}(e^{\imath\bar{\omega}} - 1)(e^{\imath\bar{\omega}} + 1)^2 = 0$$

Two cases are now possible. Either $e^{\imath\bar{\omega}} - 1 = 0$, i.e. $\bar{\omega} \equiv 0$, or $e^{\imath\bar{\omega}} - 1 \neq 0$ in which case, one can divide by $(e^{\imath\bar{\omega}} - 1)(e^{\imath\bar{\omega}} + 1)^2$ and use definitions of trigonometric functions to obtain (5.56). Clearly in the case of MS–2 method the discrete dispersion relationship is a union of two curves, but is mostly identical to the discrete dispersion relation obtained for MS–1 scheme.

In order to show that this approach, when applicable produces the same result as symbol approach we assume that $\bar{\omega}$ satisfies equation (5.56), i.e. that

$$4\tan^2\frac{\bar{\omega}}{2} = 4\lambda^2\tan^2\frac{\bar{k}}{2} - \chi(\Delta t)^2$$

Clearly, since

$$\tan 2\theta = \frac{2\tan\theta}{1 - \tan^2\theta}$$

we can write that

$$\tan^2 \bar{\omega}_R = \frac{16\Big(4\lambda^2 \tan^2 \frac{\bar{k}}{2} - \chi(\Delta t)^2\Big)}{\Big(4 - (4\lambda^2 \tan^2 \frac{\bar{k}}{2} - \chi(\Delta t))\Big)^2}$$

which is exactly the result of the symbol approach for MS–1 and MS–2. Results so far are summarized by the following

Theorem 12 (McLachlan & Ascher, 2004) *The box scheme qualitatively preserves the dispersion relation of any linear, first order PDEs of the form (3.2). Specifically, there are diffeomorphisms ψ_1 and ψ_2 which conjugate the exact and numerical dispersion relations such that to each pair (k, ω) satisfying the numerical dispersion relation there corresponds a pair $(\psi_1(k), \psi_2(\omega))$ satisfying the exact dispersion relation.*

The required diffeomorphisms are

$$\psi_1 : (-\pi, \pi) \to \mathbb{R}, \qquad \psi_1(k) = 2\tan(k/2) \tag{5.58a}$$

$$\psi_2 : (-\pi, \pi) \to \mathbb{R}, \qquad \psi_1(\omega) = 2\tan(\omega/2) \tag{5.58b}$$

5.4.3 MS–3

For the leap–frog scheme (5.38) one derives discrete dispersion relationship by substituting discrete Fourier ansatz which yields

$$e^{\imath\bar{k}}(e^{\imath 2\bar{\omega}} - 2e^{\imath\bar{\omega}} + 1) - \lambda^2 e^{\imath\bar{\omega}}(e^{\imath 2\bar{k}} - 2e^{\imath\bar{k}} + 1) - \chi(\Delta t)^2 e^{\imath\bar{k}} e^{\imath\bar{\omega}} = 0$$

or equivalently

$$e^{\imath\bar{k}}(e^{\imath\bar{\omega}} - 1)^2 - \lambda^2 e^{\imath\bar{\omega}}(e^{\imath\bar{k}} - 1)^2 - \chi(\Delta t)^2 e^{\imath\bar{k}} e^{\imath\bar{\omega}} = 0$$

Upon division by $-4e^{\imath\bar{k}}e^{\imath\bar{\omega}}$ one can write a trigonometric form of the dispersion relation as

$$\Big(\frac{2}{\Delta t}\sin\frac{\bar{\omega}}{2}\Big)^2-\Big(\frac{2}{\Delta x}\sin\frac{\bar{k}}{2}\Big)^2+\chi=0 \tag{5.59}$$

Noticing that (5.59) can be written as

$$4\sin^2\frac{\bar{\omega}}{2}=4\lambda^2\sin^2\frac{\bar{k}}{2}-\chi(\Delta t)^2$$

and since

$$\tan^2 2\theta=\frac{4\sin^2\theta(1-\sin^2\theta)}{(1-2\sin^2\theta)^2}$$

we have that

$$\tan^2\bar{\omega}_R=\frac{\Big(4\lambda^2\sin^2\frac{\bar{k}}{2}-\chi(\Delta t)^2\Big)\Big(4-(4\lambda^2\sin^2\frac{\bar{k}}{2}-\chi(\Delta t)^2)\Big)}{\Big(2-(4\lambda^2\sin^2\frac{\bar{k}}{2}-\chi(\Delta t)^2)\Big)^2},$$

which simplifies to be exactly the result obtained for MS–3 via symbol approach.

5.4.4 MS–4

We can now discus the dispersive properties of integrators applied to the Hamiltonian spatial semidiscretization. Linearized sine–Gordon equation (5.4) with $\bar{u}\equiv\pi$ and notation introduced for (3.12) yields the following discretization (5.43). The system (5.43) is a Hamiltonian system of ODEs with Hamiltonian function being a modification of (4.46).

Implicit Runge–Kutta method for Hamiltonian semidiscretization (5.43), after eliminating all the variables related to p, takes the form

$$\begin{aligned}&4(q_{j+1}^{n+2}-2q_{j+1}^{n+1}+q_{j+1}^{n})\\ -\lambda^2\Big[&(q_{j+2}^{n+2}-2q_{j+1}^{n+2}+q_{j}^{n+2})+2(q_{j+2}^{n+1}-2q_{j+1}^{n+1}+q_{j}^{n+1})\\ &+(q_{j+2}^{n}-2q_{j+1}^{n}+q_{j}^{n})\Big]-\chi(\Delta t)^2(q_{j+1}^{n+2}+2q_{j+1}^{n+1}+q_{j+1}^{n}) \;=\; 0\end{aligned} \tag{5.60}$$

which upon substitution of the discrete ansatz takes the form

$$\begin{aligned} & 4(e^{\imath 2\bar{\omega}} - 2e^{\imath\bar{\omega}} + 1)e^{\imath\bar{k}} - \chi(\Delta t)^2(e^{\imath 2\bar{\omega}} + 2e^{\imath\bar{\omega}} + 1)e^{\imath\bar{k}} \\ -\lambda^2\Big[e^{\imath 2\bar{\omega}}(e^{\imath 2\bar{k}} - 2e^{\imath\bar{k}} + 1) + 2e^{\imath\bar{\omega}}(e^{\imath 2\bar{k}} - 2e^{\imath\bar{k}} + 1) + (e^{\imath 2\bar{k}} - 2e^{\imath\bar{k}} + 1)\Big] &= 0 \end{aligned}$$

Dividing by $(e^{\imath 2\bar{\omega}} + 2e^{\imath\bar{\omega}} + 1)$ one has

$$4\frac{(e^{\imath\bar{\omega}} - 1)^2}{(e^{\imath\bar{\omega}} + 1)^2}e^{\imath\bar{k}} - \lambda^2(e^{\imath\bar{k}} - 1)^2 - \chi(\Delta t)^2 e^{\imath\bar{k}} = 0$$

that in trigonometric form is

$$\Big(\frac{2}{\Delta t}\tan\frac{\bar{\omega}}{2}\Big)^2 - \Big(\frac{2}{\Delta x}\sin\frac{\bar{k}}{2}\Big)^2 + \chi = 0 \tag{5.61}$$

Clearly for (5.61) we have that

$$4\tan^2\frac{\bar{\omega}}{2} = 4\lambda^2\sin^2\frac{\bar{k}}{2} - \chi(\Delta t)^2,$$

which gives

$$\tan^2\bar{\omega}_R = \frac{16\Big(4\lambda^2\sin^2\frac{\bar{k}}{2} - \chi(\Delta t)^2\Big)}{\Big(4 - (4\lambda^2\sin^2\frac{\bar{k}}{2} - \chi(\Delta t)^2)\Big)^2},$$

showing the equivalence with the symbol approach.

The results of the Theorem 12 can easily be generalized onto MS–3 and MS–4 (with different diffeomorphisms). Note that these schemes are both multisymplectic. Similar conclusions can be obtained for discrete dispersion relations related to the linearization of the NLS equation. All the results are consistent with the dispersion curves in continuous case.

5.4.5 Summary

Results of our work on the preservation of discrete dispersion relationship can be summarized in the following

Proposition 1 *Numerical schemes (5.19), (5.36), (5.38) and (5.60) qualitatively preserve the dispersion relation of linear PDEs. Specifically, there exist diffeomorphisms ψ_1 and ψ_2 which conjugate the exact and numerical dispersion relations such that to each pair (k, ω) satisfying the numerical dispersion relation there corresponds a pair $(\psi_1(k), \psi_2(\omega))$ satisfying the exact dispersion relation.*

Required diffeomorphisms are:

1. for MS box scheme [6] given by (5.58)

2. for MS–3:

$$\psi_1 : (-2, 2) \to \mathbb{R}, \qquad \psi_1(k) = 2\sin(k/2) \tag{5.62a}$$

$$\psi_2 : (-2, 2) \to \mathbb{R}, \qquad \psi_1(\omega) = 2\sin(\omega/2) \tag{5.62b}$$

3. and for MS–4:

$$\psi_1 : (-2, 2) \to \mathbb{R}, \qquad \psi_1(k) = 2\sin(k/2) \tag{5.63a}$$

$$\psi_2 : (-\pi, \pi) \to \mathbb{R}, \qquad \psi_1(\omega) = 2\tan(\omega/2) \tag{5.63b}$$

Proposition 1 generalizes the result of [6] in three directions. Firstly, it shows that their theorem applies to the reduced box scheme (i.e. a box scheme solved for the unknown

function, with all the other variables eliminated). Secondly, it indicated existence of diffeomorphisms ψ_1 and ψ_2 for other symplectic schemes analyzed in this paper (i.e. for MS–3 and MS–4 schemes), as well as for other equation (i.e. linearized NLS equation). This property indicates that existence of diffeomorhisms is not a special feature of the box scheme. Dispersion curve for the ERK, although qualitatively similar to the analytic one, does not have such a representation in terms of diffeomorphisms from Proposition 1. Since dispersion curve (5.35) has an inflection point in the interval $[0, \pi]$, is is a nontrivial task to find diffeomorphisms of Theorem 1.

CHAPTER SIX: RESULTS OF NUMERICAL SIMULATIONS

In the first part of this chapter we want to discuss results of simulation performed on the linear wave equation with initial data characterized by a broad Fourier spectrum. Integrating linear wave equation with such an initial data will permit us to understand dispersive error better and present how error in preservation of the dispersion relationship causes destruction of qualitative properties of the initial data. From that experiment we concluded that the most informative quantity for that purpose is the error in the propagation speed. We have also observed that the formation mechanism for discrete solitons in analogous to the mechanism of formation of solitons in continuous systems, i.e. dispersion cancellation introduced by nonlinear terms.

In the second part of this chapter we present a representative selection of results from our extensive numerical simulations of the sine–Gordon equations. For various initial data we tested five different second order finite difference integrators using the following spatial and temporal resolutions: $\Delta t \in \{128, 64, 32, 16, 8, 4, 2, 1\} \cdot 10^{-3}$ and $J \in \{64, 128, 256, 512, 1024\}$. Solutions were computed for every pair $(\ell/J, \Delta t)$ and for $\ell = 2\pi\sqrt{2}$ in the periodic case and $\ell = 40$ in the soliton regime. We will present and discuss different phenomena we encountered during our tests. We use these results to conclude that, although in most practical cases classical notion of order and convergence of the methods are good measure of quality of integration, is some, selected cases where initial data were chosen in special regions of the phase space the classical definition of error fails to address the convergence issues and one has to resort to more sophisticated tools related to qualitative analysis of differential equations.

In such cases discrete dynamical systems behavior is of decisive nature and has to be taken into account in order to understand error in numerical solution of Hamiltonian PDEs.

In the numerical experiment periodic boundary conditions are used as they are "reflective" and energy is not lost in the simulations. Typically the time frame for the numerical experiments is $T = 100$.

6.1 Discrete Dispersion and Linear Stability

Dispersive error, associated with error in the phase velocity, is responsible for destroying qualitative features of the initial data for the linear wave equation. Here one would expect two wave forms of the same shape as initial data

$$u(x,0) = \exp(-3200 \cdot x^2), \qquad u_t(x,0) = 0, \tag{6.1}$$

traveling in opposite directions, but retaining original shape with the amplitude decreased, but constant in time. Initial data of the form (6.1) were used as illustration in [37], where one can also find analysis of the importance of the preservation of the group velocity by the discretization and examples of simulation results obtained by schemes with non-monotone dispersion relations.

In numerical simulations one notices a periodic wave–train instead that can be readily observed on Figure 6.1 and Figure 6.2. This phenomenon is explained by the error in the propagation speed as a function of the wave number $\bar{k}$. On Figure 5.3(d), the error in the propagation speed for MS schemes is positive indicating that the higher the wave–number is the faster the modes with this wave–number will travel, while for the non–MS schemes the error is negative indicating the opposite. In numerical simulations, see Figure 6.1, we

observe that the wave–front travels faster than the low–amplitude oscillations which was predicted the analysis. Opposite phenomenon is observed for all the non–MS schemes, which is illustrated by the example of the MS–3 scheme on Figure 6.2.

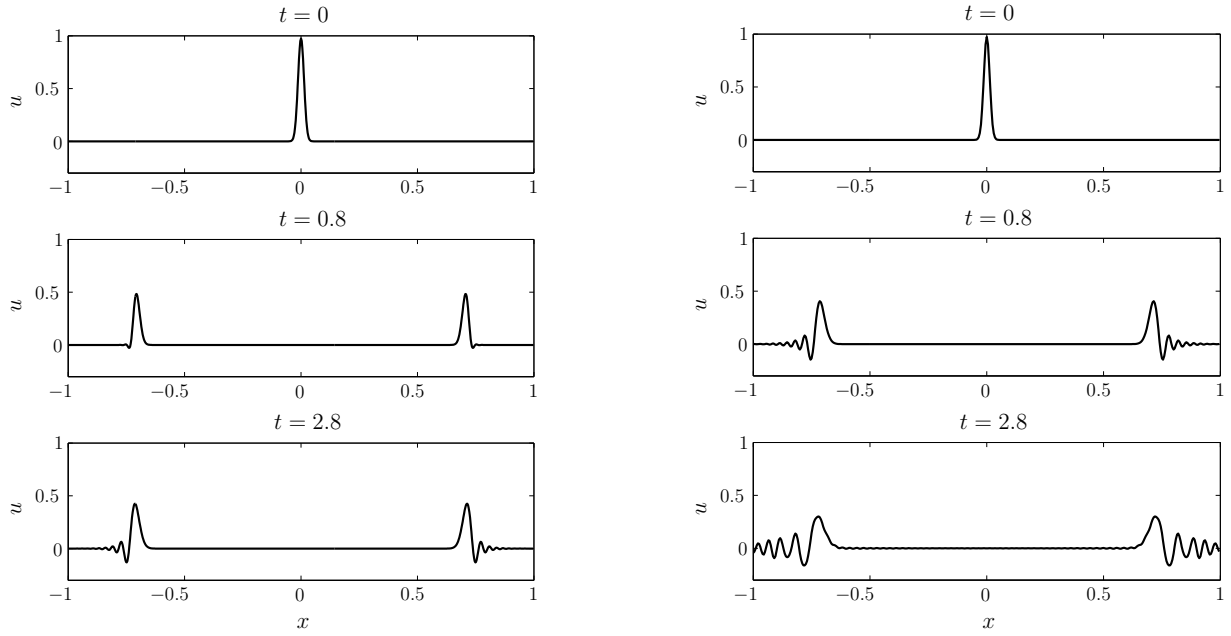

(a) $J = 700$, i.e. $\lambda = 0.70$.

(b) $J = 400$, i.e. $\lambda = 0.40$.

Figure 6.1: Evolution of the initial Gaussian wave form (6.1) for different values of λ under the MS–2 discretization. Times for snapshots were chosen in such a way, that disturbances are traveling outbound. We observe elongation of the envelope in the direction of propagation (positive GVD). For $\lambda = 0.1$ one notes an instability. Remaining mesh parameters are: $\ell = 2$ and $\Delta t = 2 \cdot 10^{-3}$.

Identical phenomenon is responsible for occurrence of wiggles in numerical simulations of the (nonlinear) sine–Gordon equation with initial data

$$u(x,0) = 0, \qquad u_t(x,0) = (4/\gamma)\,\mathrm{sech}(x/\gamma), \tag{6.2}$$

corresponding, for $\gamma < 1$, to the kink–antikink two–soliton wave–form. For the illustration see Figures 6.3(a) and (b) for which we have chosen $\gamma = 1/2$. In the nonlinear case the

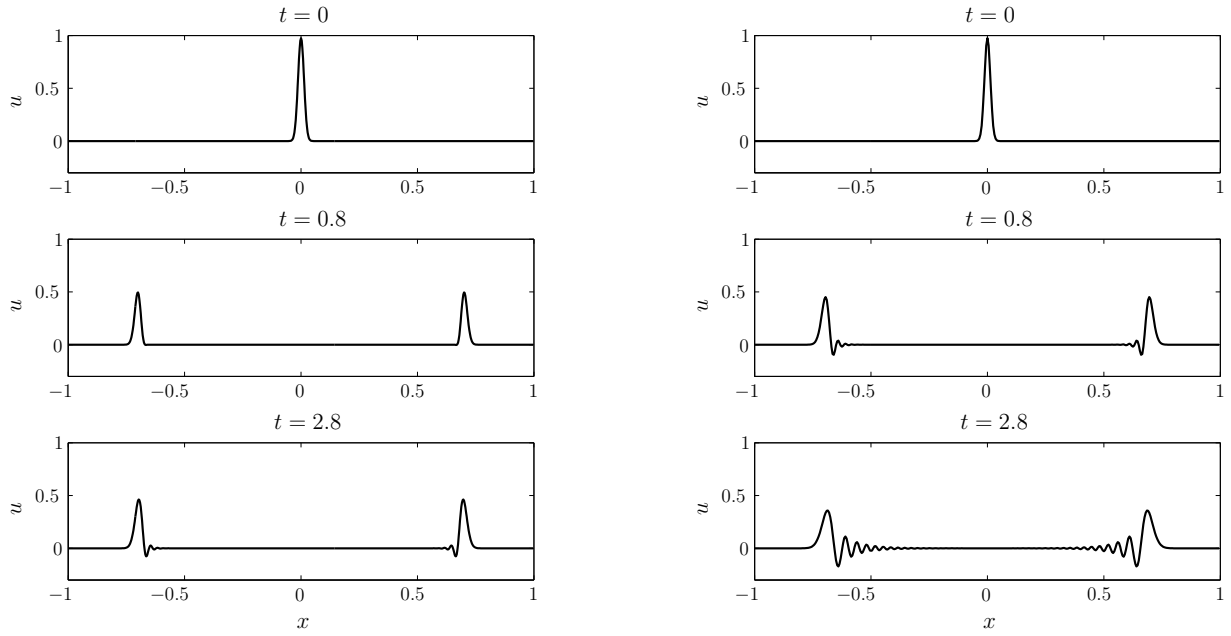

(a) $J = 700$, i.e. $\lambda = 0.70$.

(b) $J = 400$, i.e. $\lambda = 0.40$.

Figure 6.2: Evolution of the initial Gaussian wave form (6.1) for different values of λ under the MS–3 discretization. Times for snapshots were chosen in such a way, that disturbances are traveling outbound. We observe elongation of the envelope in the direction opposite to the direction of propagation (negative GVD). The wave form is completely destroyed for $\lambda = 0.1$. Remaining mesh parameters are: $\ell = 2$ and $\Delta t = 2 \cdot 10^{-3}$.

qualitative features are not destroyed which indicates that discrete solitons, analogically to its continuous counterpart, are formed when nonlinear term cancels out dispersive effects of maps. Wiggles are only observed for very rough mesh sizes and vanish with the sufficient increase of mesh resolution. The velocity in which wiggles propagate can again be explained by linear dispersion analysis presented earlier.

From the dispersion/dissipation analysis for the ERK discretization one also obtains that there is a growth in the amplitude of every discrete mode, thus suggesting an increase of energy in time. Figure 6.4 presents a time evolution of the error in the 4th order approximation

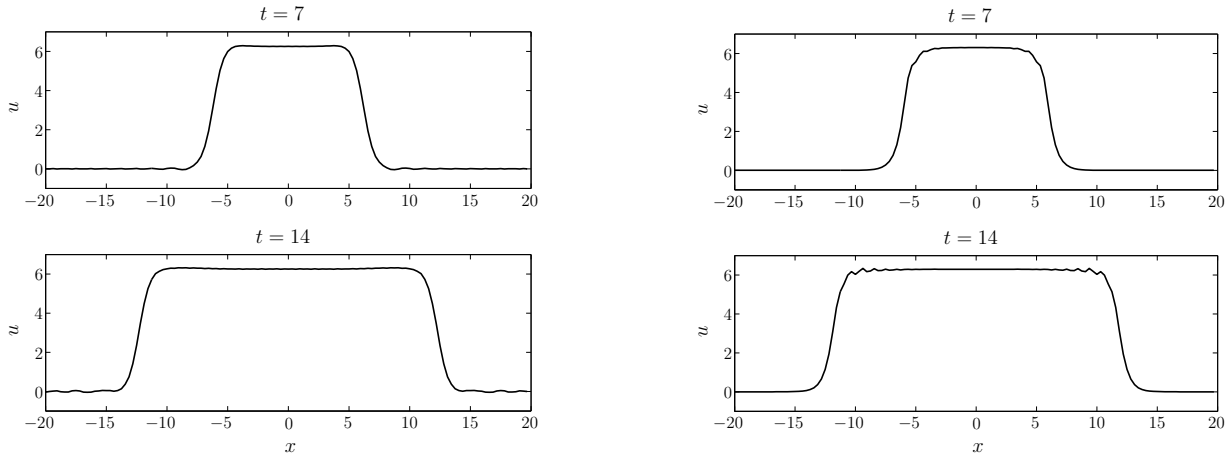

(a) MS–2. (b) MS–3.

Figure 6.3: Dispersive Error in Solitons. Figure presents wave form evolution for the kink–antikink initial data (6.2) for $\gamma = 1/2$. Top plots are snapshots of the wave form at time $t = 7$ and bottom ones at time $t = 14$. Simulation parameters are: $\ell = 40$, $J = 128$ and $\Delta t = 32 \cdot 10^{-3}$.

of the Hamiltonian functional (3.12)

$$\begin{aligned}\mathscr{H}(t) &= \int_0^\ell h(t,x)\mathrm{d}x \approx \frac{\Delta x}{3}\Big(h(t,x_1) + 4h(t,x_2) + 2h(t,x_3) + \cdots \\ &\quad +4h(t,x_{J-2}) + 2h(t,x_{J-1}) + 4h(t,x_J) + h(t,x_1)\Big) - \frac{L}{3\Delta x}\frac{(\Delta x)^5}{90}\frac{\partial^4}{\partial x^4}h(t,\xi)\end{aligned}$$

where $\xi \in (0,\ell)$, which is the Simpson's rule [12]. Fourth order approximation is used in computing diagnostics in order to avoid introducing other significant error to them. As a matter of fact, for our experiments, any approximation of order higher than two would be appropriate. Using forth order, centered cell approximation to derivative we can write the integrand in vector form

$$\mathbf{h}(t_n) = \mathbf{h}^n = \frac{1}{2}\Big[\Big(\mathbf{u}^{n-2} - 8\mathbf{u}^{n-1} + 8\mathbf{u}^{n+1} - \mathbf{u}^{n+2}\Big)^2 + (W\mathbf{u}^n)^2\Big] + \mathbf{1} - \cos(\mathbf{u}^n) \qquad (6.3)$$

where $\mathbf{h}^n = [h_1^n, \ldots, h_J^n]^T$, $n \in \{2, \ldots, N-2\}$ and $\mathbf{1} = [1, \ldots, 1]^T \in \mathcal{M}_{J\times 1}(\mathbb{R})$ so that

$$\begin{aligned} \mathscr{H}^n &= \frac{\Delta x}{3}\Big(h_1^n + 4h_2^n + 2h_3^n + \cdots + 4h_{J-2}^n + 2h_{J-1}^n + 4h_J^n + h_1^n\Big) \\ &= \frac{\Delta x}{3}\Big(2h_1^n + 4h_J^n + \sum_{k=1}^{J/2-1}(4h_{2k}^n + 2h_{2k+1}^n)\Big) \end{aligned} \tag{6.4}$$

The error in the discrete Hamiltonian is defined as $R_H^n = |\mathscr{H}^n - \mathscr{H}^2|$. Long time numerical simulations, $T = 1000$, for the breather initial data (6.2), for $\gamma = 2$, presented in Figure 6.4) confirm the energy growth induced by a non-symplectic time discretization.

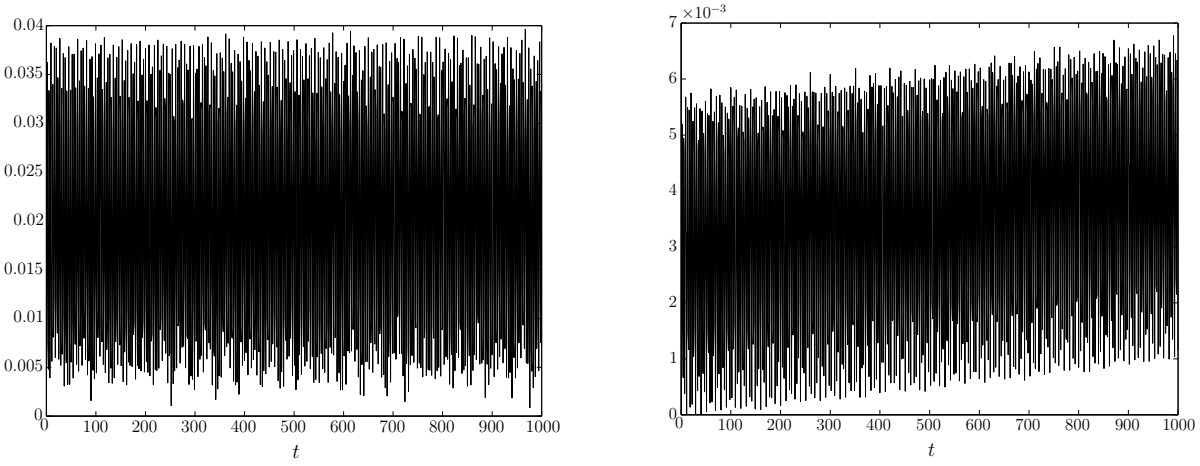

(a) MS–2.

(b) ERK.

Figure 6.4: Time evolution of $R_H^n = |\mathscr{H}^n - \mathscr{H}^2|$, i.e. the error in the 4th order discretization of the Hamiltonian functional as a function of discrete time. Conservative (MS–2) vs. nonconservative (ERK) discretization for the breather initial data (6.2), $\gamma = 2$, simulated to $T = 1000$. ERK is the only scheme for which the dispersion–dissipation analysis indicates growth. Simulation parameters are: $\ell = 40$, $J = 64$ and $\Delta t = 10^{-2}$.

Similarly to (6.3), for the momentum functional we have

$$\mathscr{M}^n = \frac{\Delta x}{3}\Big(2m_1^n + 4m_J^n + \sum_{k=1}^{J/2-1}(4m_{2k}^n + 2m_{2k+1}^n)\Big), \tag{6.5}$$

where

$$\mathbf{m}^n = [v_j^n \cdot w_j^n]_{j\in\{1,\ldots,J\}}^T. \tag{6.6}$$

Figure 6.5 provides a comparison of the maximal error in time of the Hamiltonian and the momentum for the different integrators using the breather soliton initial data. We computed discrete momentum as a 4th order approximation to the momentum functional $\mathscr{C}_1$. It is given by equation (6.5). The period is chosen sufficiently large so that the solution is not significantly affected by the boundary conditions. For the Hamiltonian we observe the error to saturate at the level of 10^{-4}. This indicates that an increase of the temporal accuracy will have no affect on the solution and, for the error to decrease further, one has to increase the spatial accuracy. Since the solution schemes are second order we note the correct second order behavior of this quantity. There is no visible superiority of the box scheme. On the second plot, the plot of the momentum, we note that the error for both box schemes is higher than other schemes and follows expected second order behavior (dashed lines). For all the other integrators the error is at the level of the accuracy of the iterative solver which was chosen to be 10^{-12}.

6.2 Preservation of Phase Space Structures

Preservation of the multisymplectic structure by the numerical scheme does not imply preservation of other dynamical invariants of the system such as the local conservation laws or other global invariants which determine the phase space structure. A question then arises about the extent to which those invariants are preserved by the numerical scheme. We use local and global conserved quantities to assess the performance of the numerical schemes. We also

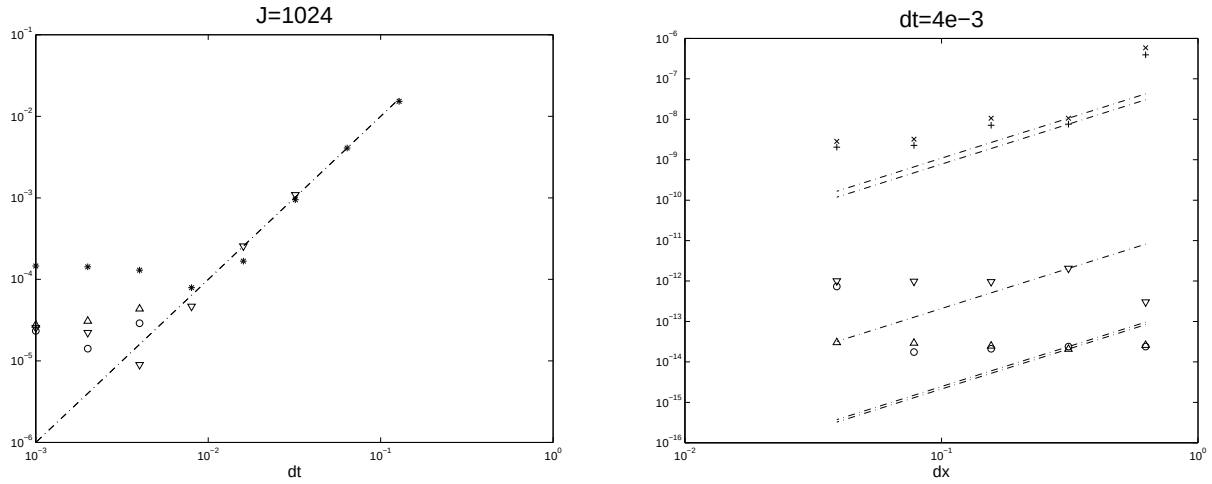

(a) Hamiltonian, $J = 1024$.

(b) Momentum, $\Delta t = 4 \cdot 10^{-3}$.

Figure 6.5: Order plots (log–log) for Hamiltonian and momentum. Comparison between MS–1 (+), MS–2 ($\times$), MS–3 ($\triangledown$), MS–4 ($\triangle$) and ERK ($\circ$) methods. Asterisk (overlapping + and $\times$) and hexagram (overlapping $\triangledown$ and $\triangle$) signs indicate that corresponding schemes produced identical error. Dashed lines have slope 2 indicating the expected (second) order behavior. Simulation horizon $T = 100$.

show the rate of convergence plots for those invariants and observe that homoclinic crossings can introduce a disturbance, in otherwise very clear, convergence patterns.

This section will be devoted to a more thorough analysis of behavior of discrete, nonlinear maps arising from different discretization of the sine–Gordon equation. We will begin presenting preservation of local and global momentum and energy in the form of their time evolution plots as well as order plots of the maximal error as a function of the mesh resolution. These quantities are good indicators for solutions that are away from "difficult" regions of the phase space, like neighborhoods of homoclinic, or other separatrix, solutions. Later we will show, that for numerical solutions close to such special regions the change of geometry the phase space is a dominating source of error. We will present numerical evidence

that different integrators changes the geometry of the phase space in different ways. This behavior is independent of the resolution of numerical mesh and therefore we will have to consider other than absolute error measures of closeness to analytic solution.

6.2.1 Discrete Local Conservation Laws

Consider a system of local conservation laws (3.18) and (3.20). It is a system of the first order PDE, so we can directly apply the box–scheme obtaining

$$D_t M_x \tilde{\mathscr{E}}_j^n + D_x M_t \tilde{\mathscr{F}}_j^n = 0 \tag{6.7a}$$

$$D_t M_x \tilde{\mathscr{I}}_j^n + D_x M_t \tilde{\mathscr{G}}_j^n = 0 \tag{6.7b}$$

where

$$\tilde{\mathscr{E}}_j^n = \frac{1}{2}\Big((v_j^n)^2 + (w_j^n)^2\Big) - \cos(u_j^n), \qquad \tilde{\mathscr{F}}_j^n = (v_j^n)(w_j^n), \tag{6.8a}$$

$$\tilde{\mathscr{I}}_j^n = (v_j^n)(w_j^n), \qquad \tilde{\mathscr{G}}_j^n = \frac{1}{2}\Big((v_j^n)^2 + (w_j^n)^2\Big) + \cos(u_j^n). \tag{6.8b}$$

In general, due to the numerical error we can not expect equations (6.7) to be satisfied exactly, so we want to use the residuals

$$\begin{aligned}(R_{LECL})_j^n &= 2(\Delta x \Delta t)\Big(D_t M_x \tilde{\mathscr{E}}_j^n + D_x M_t \tilde{\mathscr{F}}_j^n\Big) \\ &= \Delta x\Big(\tilde{\mathscr{E}}_{j+1}^{n+1} + \tilde{\mathscr{E}}_j^{n+1} - \tilde{\mathscr{E}}_{j+1}^n - \tilde{\mathscr{E}}_j^n\Big) \\ &\quad + \Delta t\Big(\tilde{\mathscr{F}}_{j+1}^{n+1} - \tilde{\mathscr{F}}_j^{n+1} + \tilde{\mathscr{F}}_{j+1}^n - \tilde{\mathscr{F}}_j^n\Big)\end{aligned} \tag{6.9a}$$

$$\begin{aligned}(R_{LMCL})_j^n &= 2(\Delta x \Delta t)\Big(D_t M_x \tilde{\mathscr{I}}_j^n + \Delta t D_x M_t \tilde{\mathscr{G}}_j^n\Big) \\ &= \Delta x\Big(\tilde{\mathscr{I}}_{j+1}^{n+1} + \tilde{\mathscr{I}}_j^{n+1} - \tilde{\mathscr{I}}_{j+1}^n - \tilde{\mathscr{I}}_j^n\Big) \\ &\quad + \Delta t\Big(\tilde{\mathscr{G}}_{j+1}^{n+1} - \tilde{\mathscr{G}}_j^{n+1} + \tilde{\mathscr{G}}_{j+1}^n - \tilde{\mathscr{G}}_j^n\Big)\end{aligned} \tag{6.9b}$$

as a measure of the performance of the scheme. Since we are using a modified box scheme (yields only approximation of u, but does not give a direct approximation of its derivatives v and w) we have to approximate derivatives by some higher (than 2) order method. In this project we have chosen to do so by the fourth order, finite difference method

$$\begin{aligned}(u_t)_j^n = v_j^n &= \frac{1}{12\Delta t}(u_j^{n-2} - 8u_j^{n-1} + 8u_j^{n+1} - u_j^{n+2}) \\ (u_x)_j^n = w_j^n &= \frac{1}{12\Delta x}(u_{j-2}^n - 8u_{j-1}^n + 8u_{j+1}^n - u_{j+2}^n)\end{aligned}$$

For the periodic boundary condition case, it is very natural to represent that approximation in a matrix form. This will be useful especially for approximating $\mathbf{w}^n$. Denote

$$W = \begin{bmatrix} 0 & 8 & -1 & & & 1 & -8 \\ -8 & 0 & 8 & -1 & & & 1 \\ 1 & -8 & 0 & 8 & -1 & & \\ & \ddots & \ddots & \ddots & \ddots & \ddots & \\ & & 1 & -8 & 0 & 8 & -1 \\ -1 & & & 1 & -8 & 0 & 8 \\ 8 & -1 & & & 1 & -8 & 0 \end{bmatrix} \tag{6.10}$$

so that

$$\mathbf{w}^n = (\mathbf{u}_x)^n = W(\mathbf{u}^n)^T$$

This approach can be interpreted as approximating an (infinite dimensional) linear (differential) operator by a finite dimensional (matrix) one. Also

$$\mathbf{v}^n = \mathbf{u}^{n-2} - 8\mathbf{u}^{n-1} + 8\mathbf{u}^{n+1} - \mathbf{u}^{n+2}$$

In order to assess quality of discretizations based on the multisymplectic form of the equation we also computed residuals in local momentum and local energy conservation laws. These residuals are define by equations (6.9). As can be notices in Figure 6.6, and according to our expectations, there is no growth neither decrease in maximal values of the residuals. This indicates that there is no gain nor loss of the energy in the discrete system.

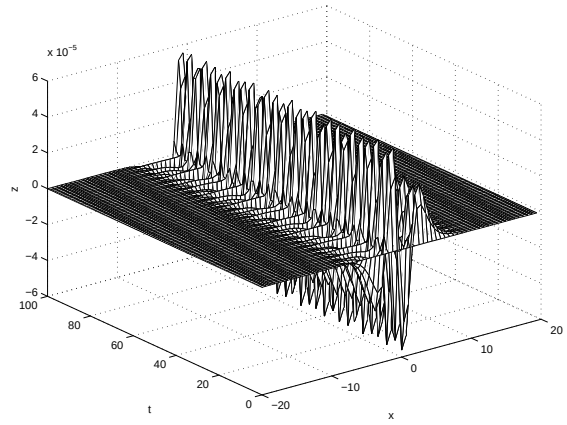

(a) LMCL. MS–2, $J = 1024$, $\Delta t = 4 \cdot 10^{-3}$, $\max R_{LMCL} = 6 \cdot 10^{-5}$.

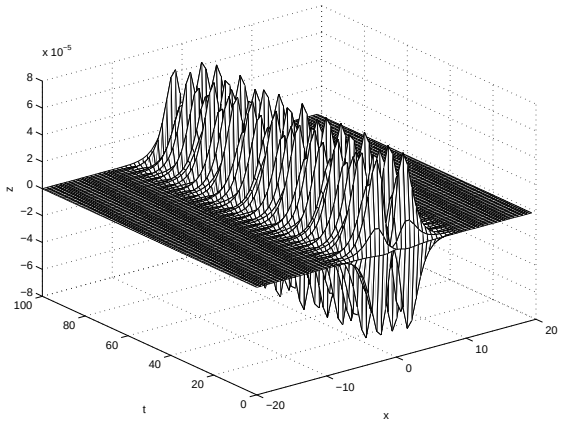

(b) LECL. MS–2, $J = 1024$, $\Delta t = 4 \cdot 10^{-3}$, $\max R_{LECL} = 8 \cdot 10^{-5}$.

Figure 6.6: Local Momentum (LM) and Local Energy (LE) Conservation Laws.

Nonlinear wave equations, such as the sine–Gordon equation, can have a complicated phase space structure, depending on the type of the boundary conditions considered. In this paper we worked with the periodic boundary conditions exclusively, even though the soliton solutions require the infinite–line boundary conditions. Finite–difference schemes can have difficulty in resolving spatial structures in very sensitive regimes, for instance homoclinic manifolds. One observes homoclinic crossings occurring after relatively short time. We find that the local conservation laws are important indicators of spatial discretization errors which can corrupt the solution, as such, provide additional insight into the qualitative behavior of

the numerical schemes. Last part of this section will be devoted to fully periodic problem on the interval $x \in [-\ell/2, \ell/2)$ for $\ell = 2\pi\sqrt{2}$. We present wave forms computed for initial data

$$u(x,0) = \pi + 0.1\cos(\mu x), \qquad u_t(x,0) = 0 \tag{6.11}$$

with $\mu = 2\pi/\ell$. In this case our initial data are located within a vicinity of a homoclinic orbit and the perturbation induced by the discretization leads to the phenomenon called homoclinic crossings (intersections). This phenomenon is the main source of error in simulation for that type of initial data. Homoclinic intercections are known in the theory of Hamiltonian ODEs and are the source of near–homoclinic chaos [1]. Figure 6.7 presents results of simulations for initial data given by (6.11). Here, additionally to the wave form plot, we present a sample of results for computing other quantities closely related to LM and LE conservation laws, namely global momentum (GM) and energy (GE) obtained by summing over the spatial index, as well as spatial global momentum (spatial GM) and spatial global energy (spatial GE) obtained by summing over temporal index.

At the time when the wave form is distorted one can observe a peak in the error of the momentum (GM) and a small irregularity in the energy (GE). This behavior is universal in the sense of mesh–independence and also observed in the behavior of momentum and energy diagnostics based on the 4th order discretization of integrals of motion. Neither of these quantities can be used to fully explain the phenomenon of homoclinic intersections and they can not be used to measure the magnitude of this error. One should use the nonlinear spectrum of the Lax's pair to fully understand what happens to the phase space structures under the discretization. A more detailed account can be found in [22].

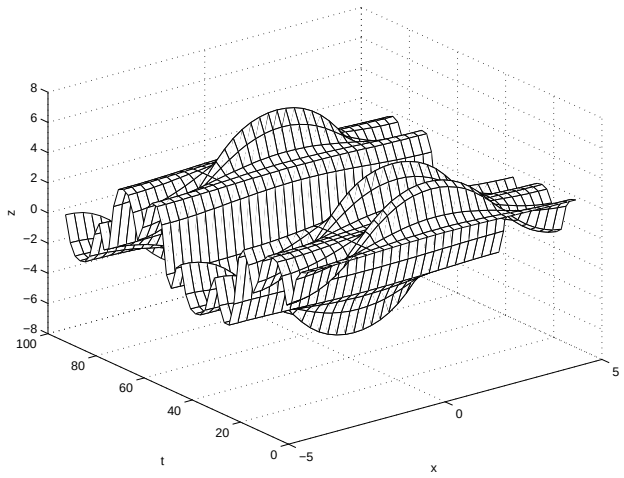

(a) Wave profile

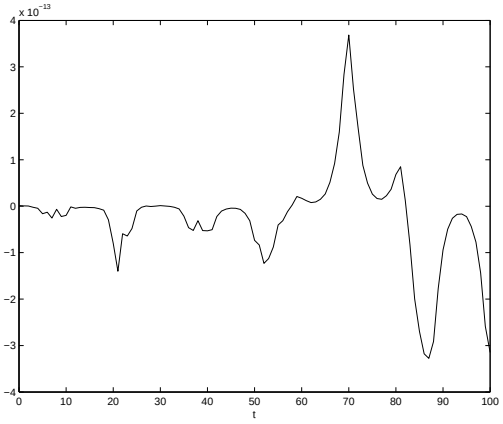

(b) GM. Magnitude of order 10^{-13}.

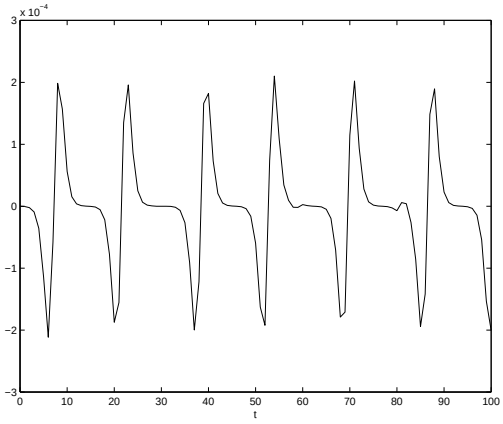

(c) GE. Magnitude of order 10^{-4}.

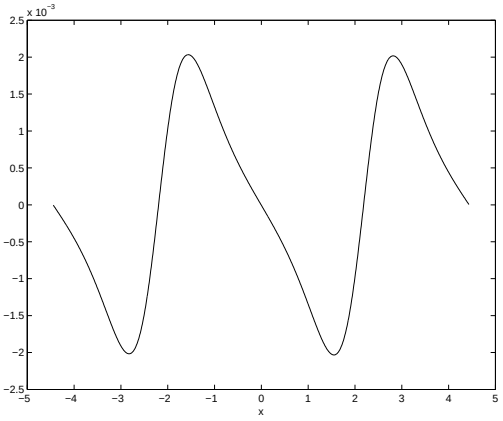

(d) Spatial GM. Magnitude of order 10^{-3}.

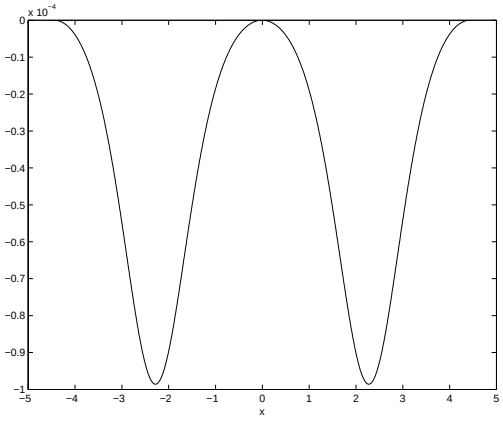

(e) Spatial GE. Magnitude of order 10^{-4}.

Figure 6.7: Periodic Case. MS–2. $J = 1024$, $\Delta t = 10^{-3}$.

6.3 Nonlinear Stability

Typically in numerically solving differential equations one tries to achieve mesh independence of the solution, i.e. a series of simulations is performed, with increasing mesh resolution, as long as, within a given simulation horizon, there is a change in the solution. Once convergence is achieved, other mesh resolutions are disregarded. In this section we will analyze different convergence patterns. For Hamiltonian PDEs symplectic time integrators are the most natural choice, but spatial discretization is also of high importance and, in many cases, determines the type of the solution we obtain (which is also independent of temporal discretization and the resolution).

For the sine–Gordon equations on can analytically construct a one–parameter family of two–solitons. Initial data that correspond to this family is given by (6.2). In that equation, for $0 < \gamma < 1$ we have so called kink-antikinks and for $\gamma > 1$ we have so called breathers. Breathers are stationary waves (localized in space) that are periodic in time, while kink–antikinks are two–solitons that are wave fronts traveling in opposite directions in space. Parameter $\gamma = 1$ corresponds to a special, separatrix–like solution, called the double–pole soliton. One can show that that the energy functional is an decreasing function of γ, i.e. that breathers are of lower energy that double–pole soliton which in turn has lower energy than kink–antikinks.

The fact that the double–pole soliton corresponds to an orbit dividing the phases space onto two regions carries important numerical consequences. It is an infinite–dimensional analog of the result obtained by McLachlan, Perlmutter and Quispel [27]. The numerical

experiment that shows this analogy was performed for initial data

$$u(x,0) = 0, \qquad u_t(x,0) = 4\,\mathrm{sech}(x), \qquad x \in [-20, 20) \tag{6.12}$$

with periodic boundary conditions, corresponds to the double pole soliton. In this experiment we numerically solved the sine–Gordon equation using different integrators and various mesh resolutions. We observer proper convergence of numerical solutions, but also noticed a significant change in the qualitative features of the solution depending upon the numerical method applied. These changes were independent of the choice of both Δx and Δt. An example from this experiment is presented on Figure 6.8, where for both MS box schemes and initial data (6.12) we have breather–like behavior, while for all the other integrators we obtained kink–antikink type solution. With the increase of the resolution of numerical mesh we observed convergence to the correct, analytical solution, nevertheless the qualitative features of the discrete solutions were preserved.

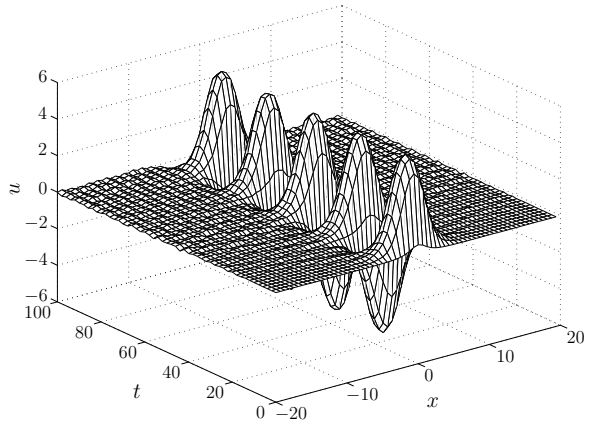

(a) MS–1, $J = 64$, $\Delta t = 64 \cdot 10^{-3}$.

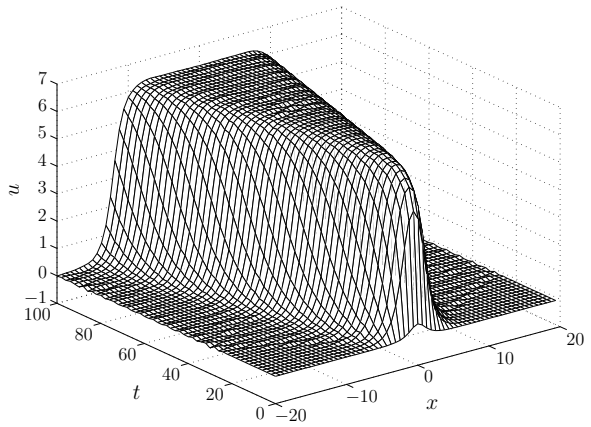

(b) MS–3, $J = 64$, $\Delta t = 64 \cdot 10^{-3}$.

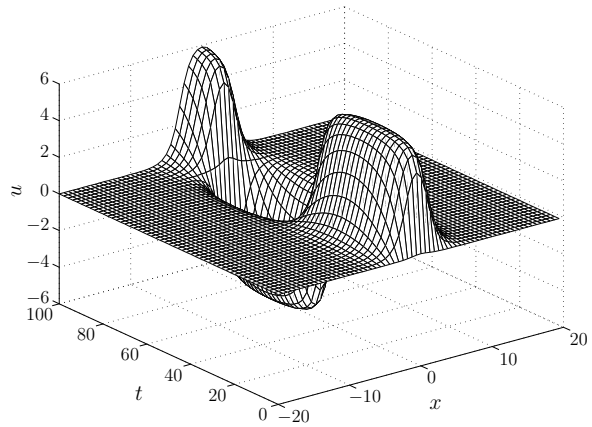

(c) MS–1, $J = 256$, $\Delta t = 16 \cdot 10^{-3}$.

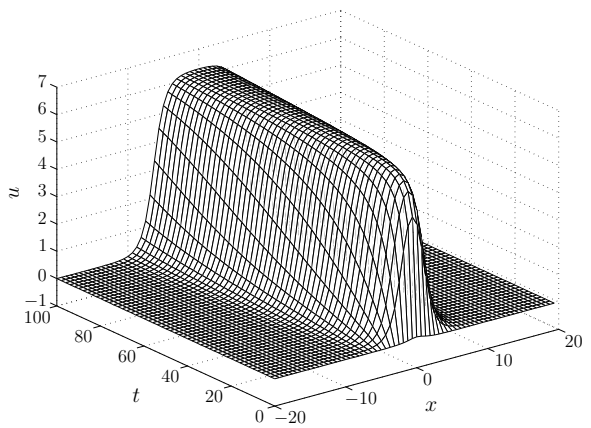

(d) MS–3, $J = 256$, $\Delta t = 16 \cdot 10^{-3}$.

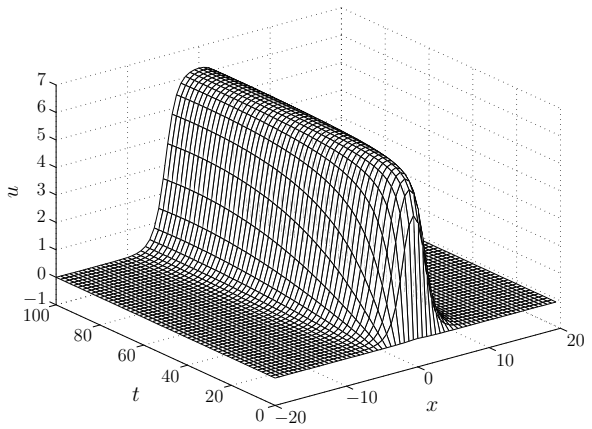

(e) MS–1, $J = 1024$, $\Delta t = 4 \cdot 10^{-3}$.

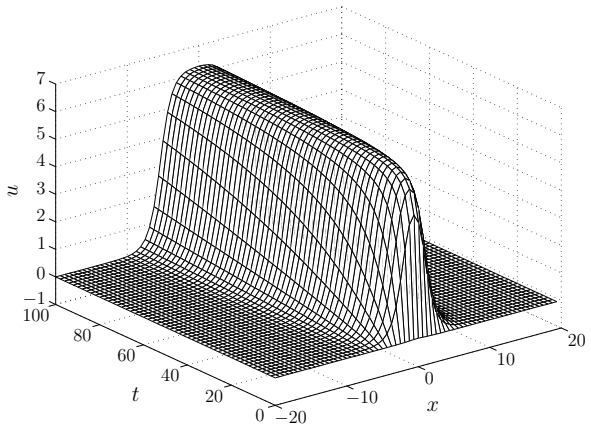

(f) MS–3, $J = 1024$, $\Delta t = 4 \cdot 10^{-3}$.

Figure 6.8: Convergence. Wave form of the double-pole soliton, $\ell = 40$.

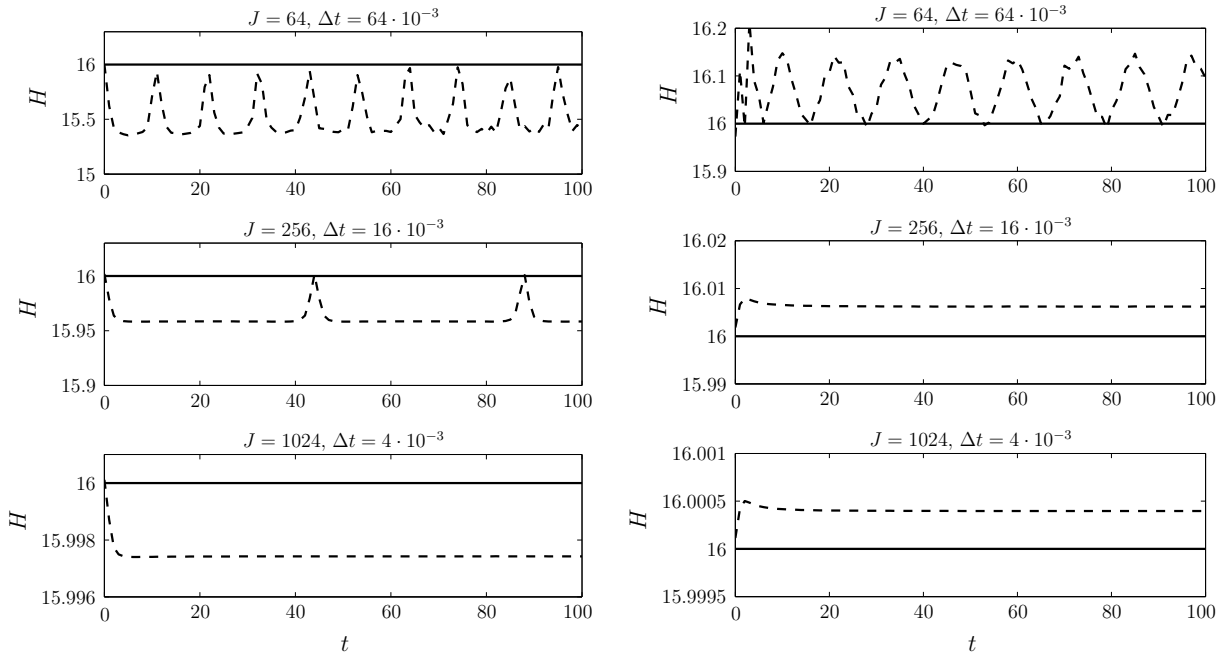

(a) MS–1. (b) MS–3.

Figure 6.9: Energy of the double-pole soliton, $\ell = 40$.

Conclusions drawn from observation of the wave form can further be confirmed by analysing time evolution of the energy functional. On Figures 6.9 presented is a result of calculating Hamiltonian functional discretized to 4th order accuracy. For MS box scheme Figures 6.9(a) shows that numerical energy (dashed line) is lower than analytical (black line) for almost all times, while for all the other schemes tested numerical energy is higher. Again, this feature is independent on the mesh size and therefore confirms, that the perturbation introduced by the map pushes the numerical solutions to live in the region of the phase space that corresponds to breather (lower energy state) or toward kink–antikink (higher energy state) depending solely upon the discretization.

Error in discrete Hamiltonian (6.4) is in this section to explain a concept of nonlinear

stability and connect it to the analysis performed by McLachlan, Perlmutter and Quispel [27].This quantity is a universal comparison tool since it relates solution of the discrete problem to the solution of the continuous one and enables to compare not only stability properties but also gives clues on how original infinite–dimensional phase space structures are distorted under the truncation to finite number of dimensions introduced by the discretization.

One should note that for initial data (6.12) classical notion of absolute error will not indicate convergence of the numerical solution. In sufficiently long time, the absolute error will be of order of unity regardless of the numerical mesh resolution. Another words as $(\Delta t, \Delta x) \to (0, 0)$ the absolute error $|u - u_{\text{num}}|$ remains constant, different than 0. One could claim than that numerical solution is invalid, and that disretizations failed to resolve the correct wave form. As a matter of fact this is not the case, since the convergence for this wave form should be considered with respect to the closeness of numerical solution to analytic one in the phase space, that is in qualitative manner. An appropriate quantitative tool to measure the distance of the numerical solution of analytic one in this case would be a splitting distance in the nonlinear spectrum of the pair of Lax operators. This quantity reflects qualitative differences between phase space structures.

6.4 Supplementary Figures

This last section we would like to devote to graphical presentation of our simulations. All the important phenomena were described and illustrated in earlier sections, so in what follows we only show a sequence of plots for different initial data and various mesh resolutions.

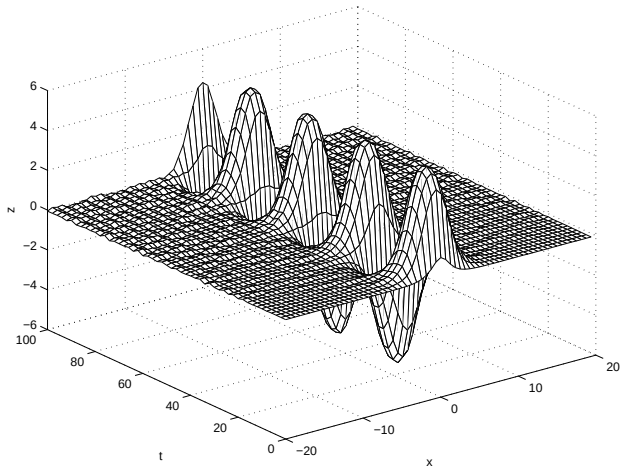

(a) Wave profile.

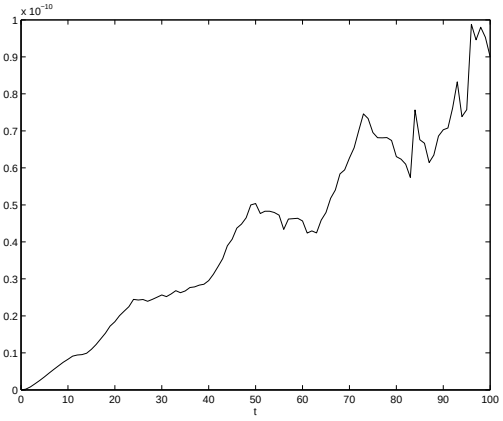

(b) Momentum. Magnitude of order 10^{-10}.

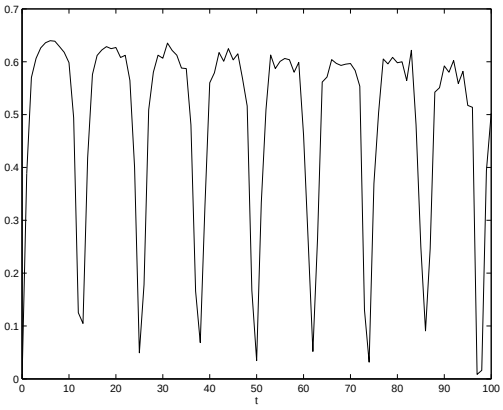

(c) Hamiltonian. Magnitude of order 10^{-1}.

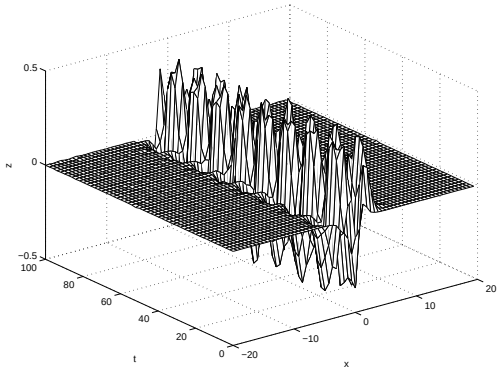

(d) LMCL. Magnitude of order 10^{-1}.

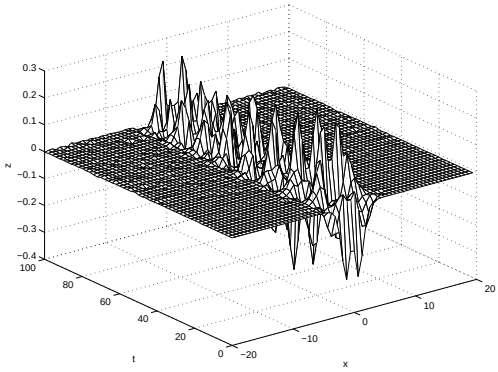

(e) LECL. Magnitude of order 10^{-1}.

Figure 6.10: Double–Pole Soliton. MS–2. $J = 64$, $\Delta t = 128 \cdot 10^{-3}$.

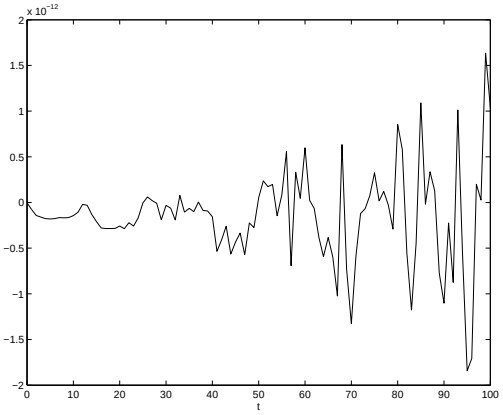

(a) GM. Magnitude of order 10^{-12}.

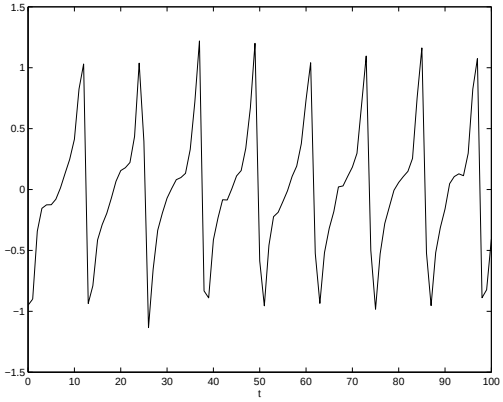

(b) GE. Magnitude of order 1.

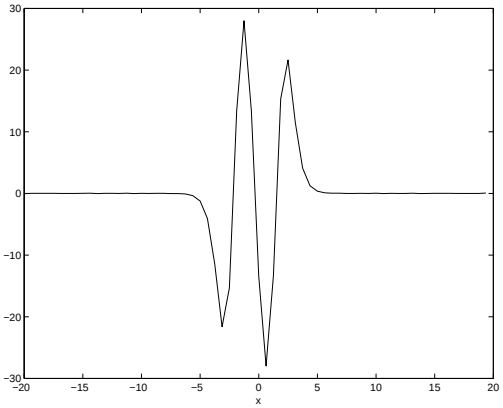

(c) Spatial GM. Magnitude of order 10.

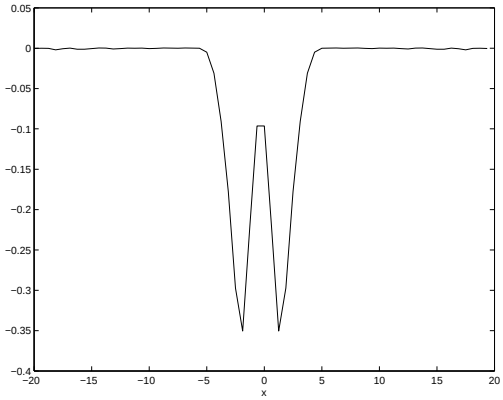

(d) Spatial GE. Magnitude of order 10^{-2}.

Figure 6.11: Double–Pole Soliton. MS–2. $J = 64$, $\Delta t = 128 \cdot 10^{-3}$.

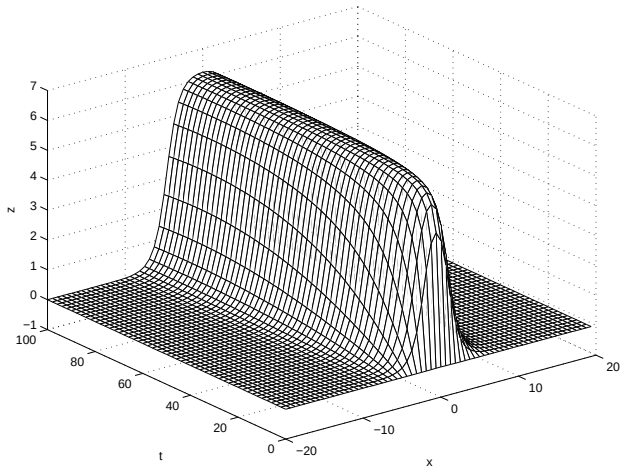

(a) Wave profile.

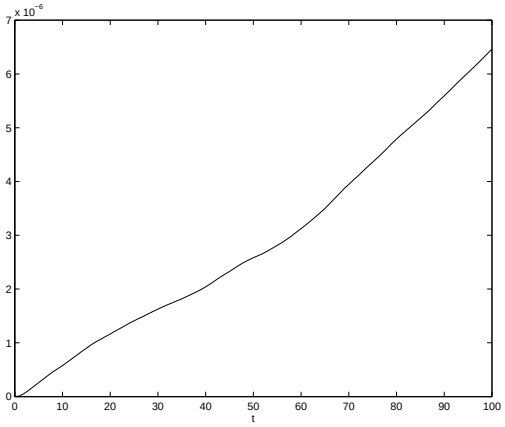

(b) Momentum. Magnitude of order 10^{-6}.

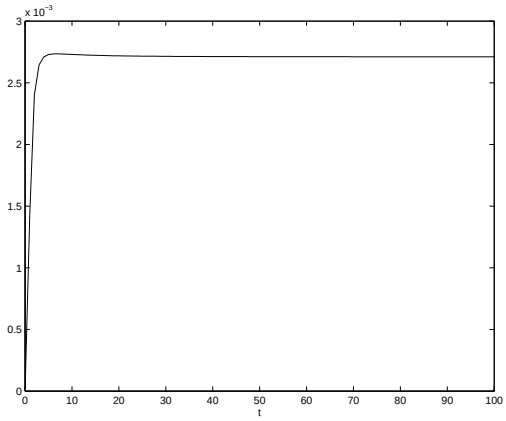

(c) Hamiltonian. Magnitude of order 10^{-3}.

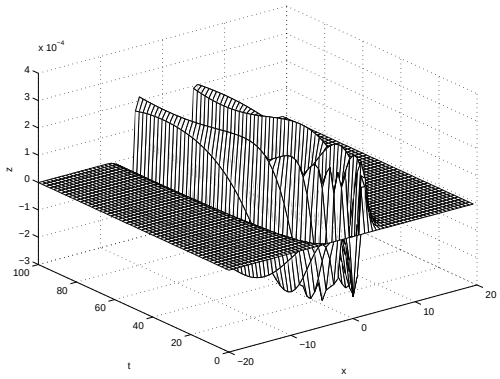

(d) LMCL. Magnitude of order 10^{-4}.

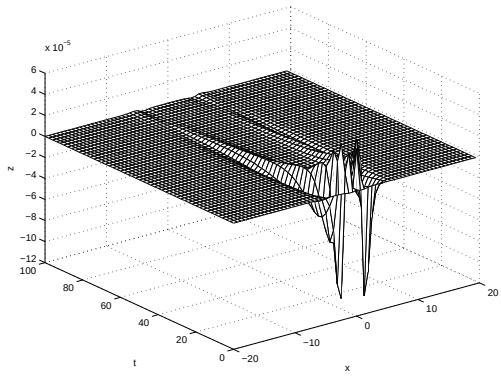

(e) LECL. Magnitude of order 10^{-5}.

Figure 6.12: Double–Pole Soliton. MS–2. $J = 1024$, $\Delta t = 10^{-3}$.

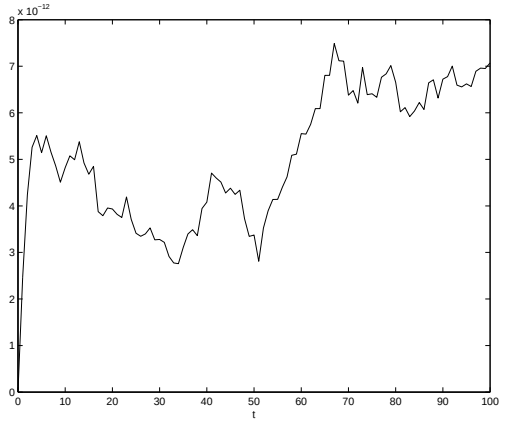

(a) GM. Magnitude of order 10^{-12}.

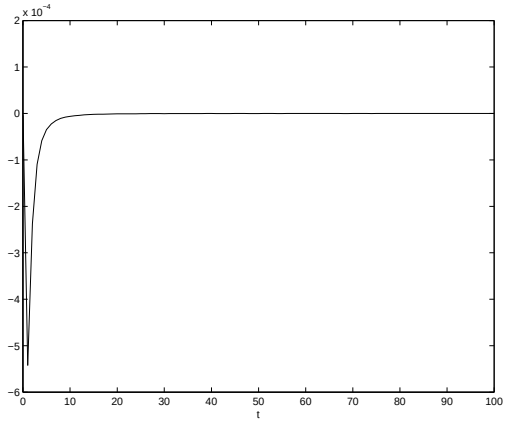

(b) GE. Magnitude of order 10^{-4}.

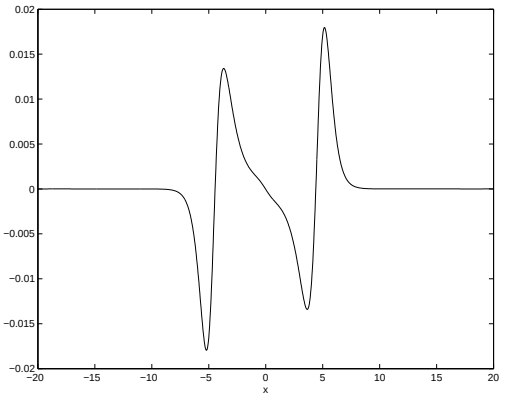

(c) Spatial GM. Magnitude of order 10^{-2}.

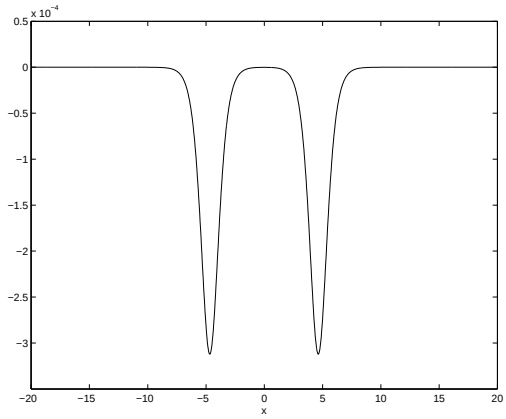

(d) Spatial GE. Magnitude of order 10^{-4}.

Figure 6.13: Double–Pole Soliton. MS–2. $J = 1024$, $\Delta t = 10^{-3}$.

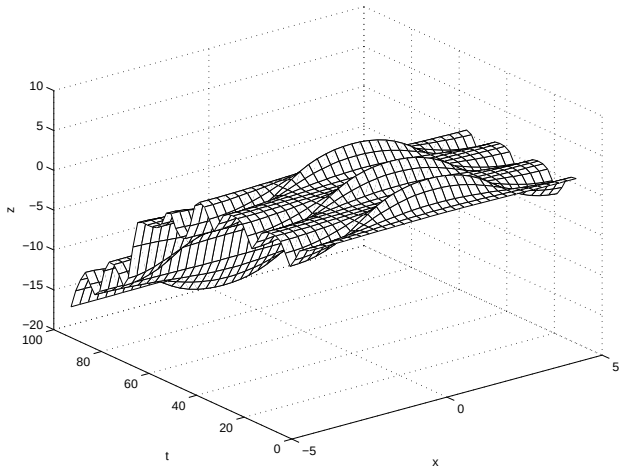

(a) Wave profile

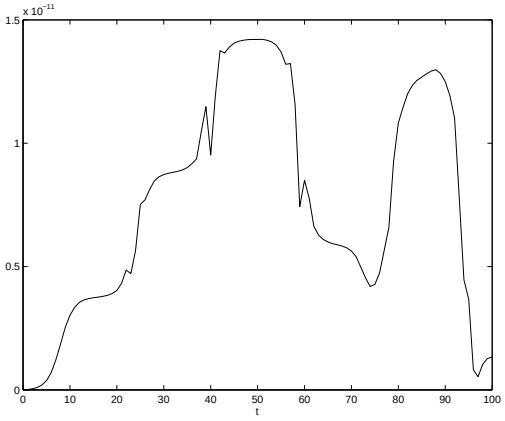

(b) Momentum. Magnitude of order 10^{-11}.

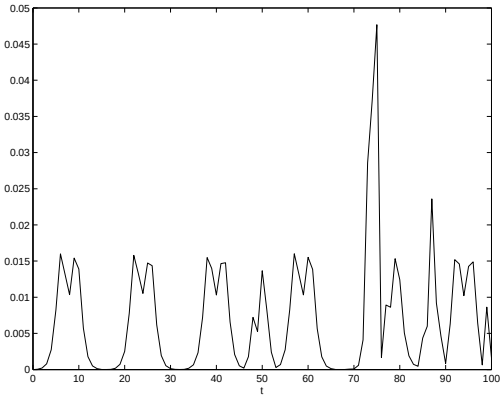

(c) Hamiltonian. Magnitude of order 10^{-2}.

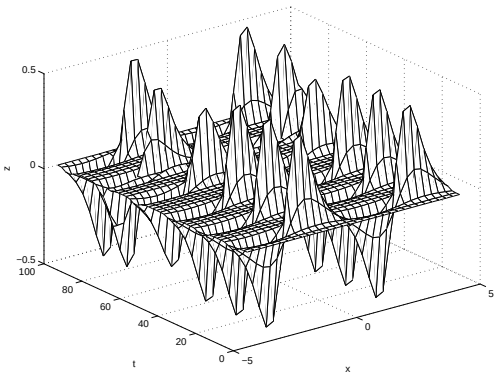

(d) LMCL. Magnitude of order 10^{-1}.

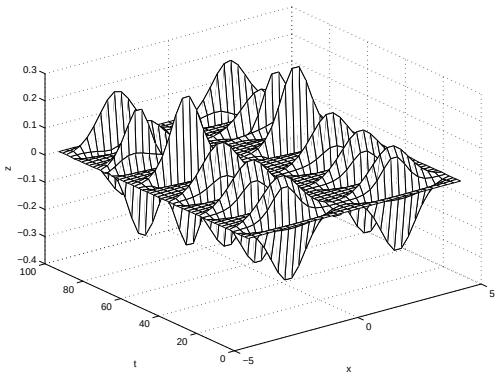

(e) LECL. Magnitude of order 10^{-1}.

Figure 6.14: Periodic Case. MS–2. $J = 32$, $\Delta t = 128 \cdot 10^{-3}$.

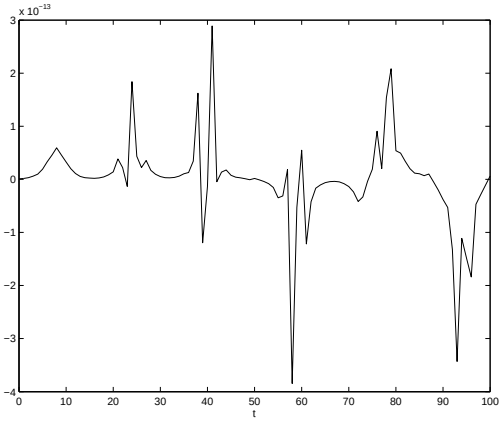

(a) GM. Magnitude of order 10^{-13}.

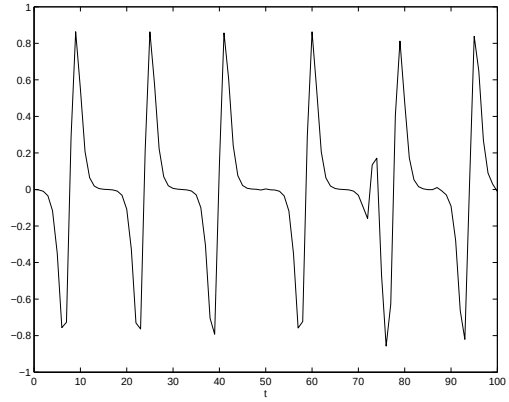

(b) GE. Magnitude of order 1.

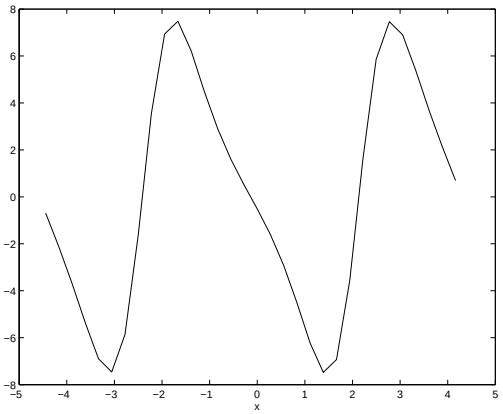

(c) Spatial GM. Magnitude of order 1.

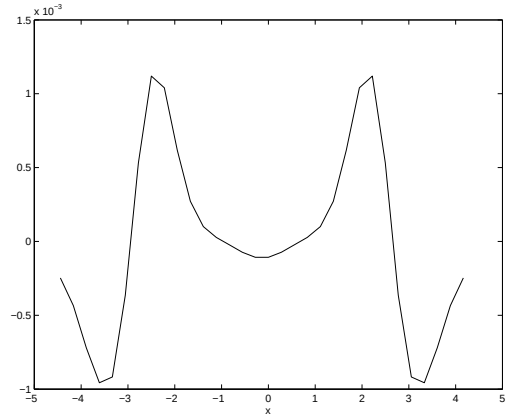

(d) Spatial GE. Magnitude of order 10^{-3}.

Figure 6.15: Periodic Case. MS–2. $J = 32$, $\Delta t = 128 \cdot 10^{-3}$.

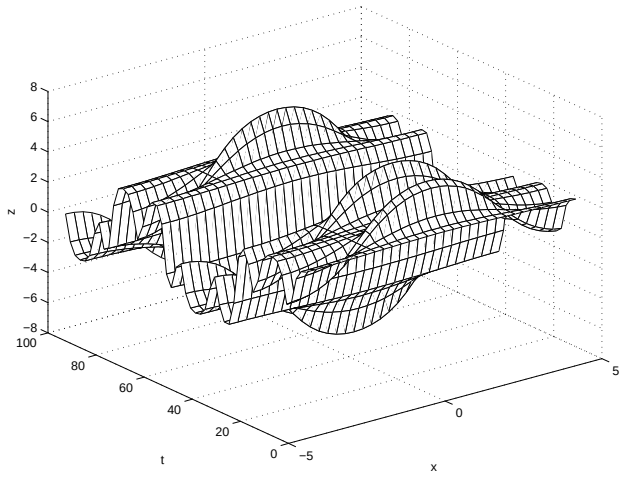

(a) Wave profile

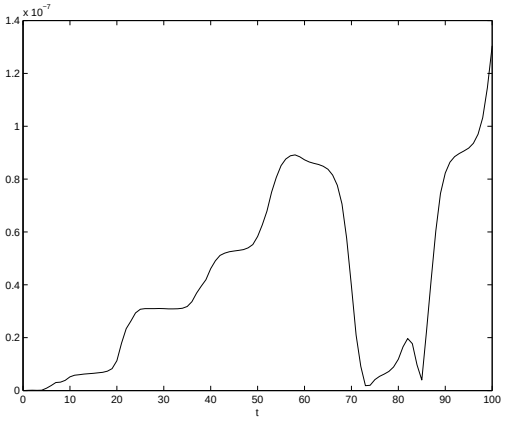

(b) Momentum. Magnitude of order 10^{-7}.

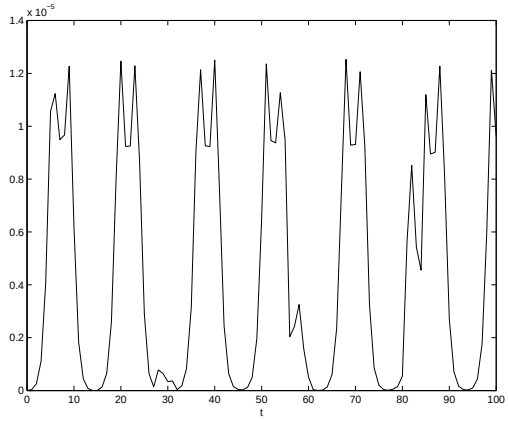

(c) Hamiltonian. Magnitude of order 10^{-5}.

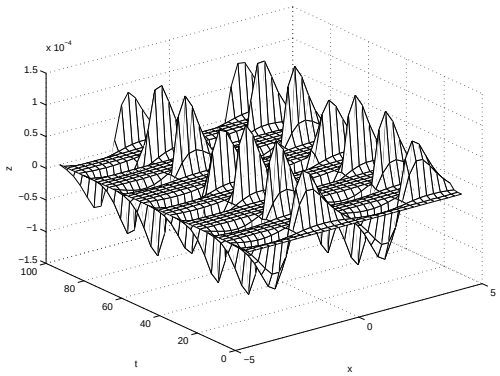

(d) LMCL. Magnitude of order 10^{-4}.

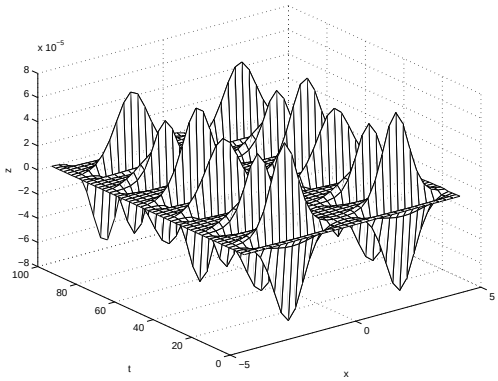

(e) LECL. Magnitude of order 10^{-5}.

Figure 6.16: Periodic Case. MS–2. $J = 1024$, $\Delta t = 10^{-3}$.

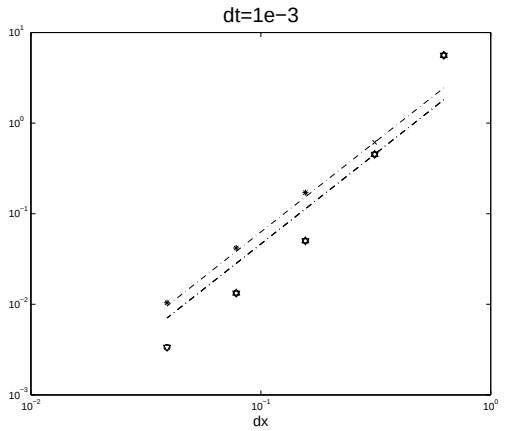

(a) Hamiltonian. Order 2 in Δx. $\Delta t = 10^{-3}$.

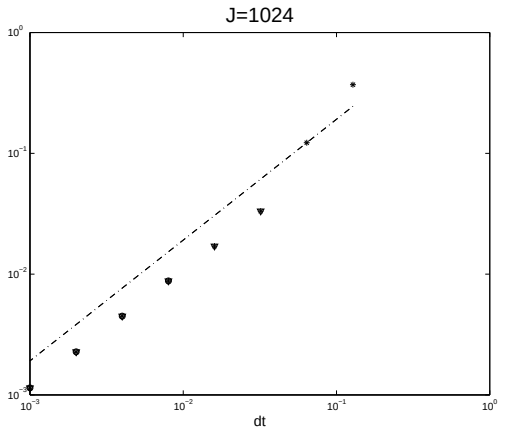

(b) GE. Order 1 in Δt. $J = 1024$.

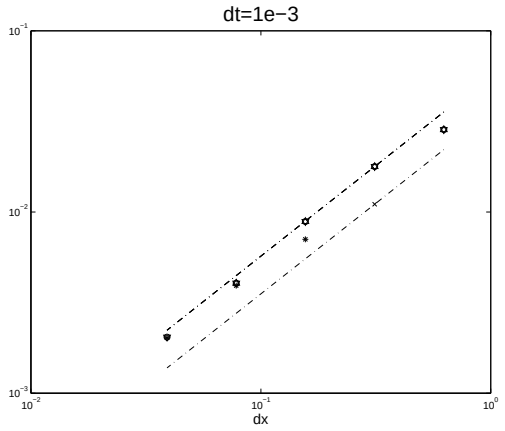

(c) LMCL. Order 1 in J. $\Delta t = 10^{-3}$.

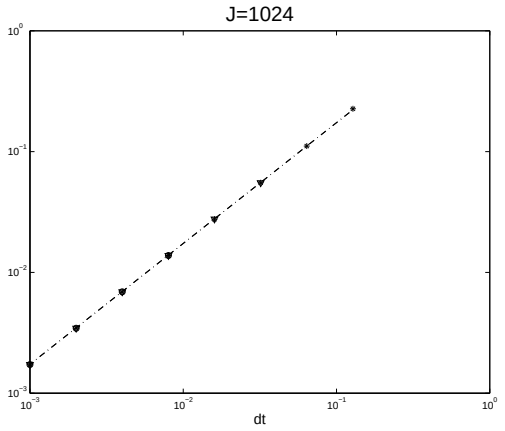

(d) spatial GM. Order 1 in Δt. $J = 1024$.

Figure 6.17: Comparison (log–log plots) of schemes for the kink–antikink initial data. For the large values of the Δt the non-multisymplectic schemes ceased to produce the result due to the nonconconvergence of the algebraic solver (implicit schemes) or growth in the wave amplitude (explicit). This in an indication of the the robustness of the box scheme.

Figure 6.17 presents a summary of convergence analysis of various discretizations of the sine–Gordon equation presented in this work. Dashed lines present an expected order of convergence and we note that all the diagnostics are in accordance with the expectations. A comparison of Figure 6.17(a) with Figure 6.5(a) suggests that the solution depends stronger

on the spatial resolution, than on the temporal one, but this is only true for the Hamiltonian. None of the other diagnostic tools used in this work possess similar properties. A final remark should concern with the momentum plot (like Figure 6.17(b)). Maxima in the momentum residual are on the order of either solver accuracy, or the round–off so the convergence pattern is, in most cases, not present.

CHAPER SEVEN: CONSERVATION OF WAVE ACTION

In this chapter we discuss conservation of the wave action under multisymplectic discretization. The first two sections summarize existing results on the wave action in Lagrangian formulation and its relations to adiabatic invariants, i.e. quantities that remain constant to the leading order in the slow-time. Average Lagrangian formulation for slowly varying linear waves gives a common ground for both the dispersion relationship and the wave action conservation law. This interesting property of average Lagrangian for linear wave equations, after proper generalization, might provide a connection between seemingly different areas discussed in this dissertation. In sections that follow we will discuss the wave action conservation for the multisymplectic formulation of continuous problems in physical as well as in Fourier spectral spaces, thus providing methods of addressing the issue of preservation of the wave action under various discretizations, with special emphasis on multisymplectic ones. Novel results concerning existence and the form of spectral wave action conservation law and its discrete analog for the midpoint rule time discretization are presented. Some numerical results illustrating the method of computing the wave action from the multisymplectic discretization are presented. The material of this chapter presents an ongoing work. It establishes theoretical foundations for the numerical simulations that will be presented somewhere else.

7.1 Lagrangian Wave Action

Let's begin with a short review of results from [18, 40]. Assume that the physical system obeys a variational principle with a Lagrangian density function $L(\dot{\phi}, \phi', \phi, x, t)$, where $\dot{\phi} = \partial\phi/\partial t$ and $\phi' = \partial\phi/\partial x$. The variational principle yields the Euler–Lagrange equation

$$\frac{\partial}{\partial t}L_{\dot{\phi}} + \frac{\partial}{\partial x}L_{\phi'} - L_{\phi} = 0 \tag{7.1}$$

and, if the quantity $\Lambda(\phi, \psi)$ defined by

$$\Lambda(\phi, \psi) = L_{\dot{\phi}}\dot{\psi} + L_{\phi'}\psi' + L_{\phi}\psi$$

is introduced, by the Euler–Lagrange equation (7.1), the following holds

$$\begin{aligned}
\frac{\partial}{\partial t}(L_{\dot{\phi}}\psi) + \frac{\partial}{\partial x}(L_{\phi'}\psi) &= \frac{\partial}{\partial t}(L_{\dot{\phi}})\psi + L_{\dot{\phi}}\dot{\psi} + \frac{\partial}{\partial x}(L_{\phi'})\psi + L_{\phi'}\psi' \\
&= \Big(\frac{\partial}{\partial t}(L_{\dot{\phi}}) + \frac{\partial}{\partial x}(L_{\phi'})\Big)\psi + L_{\dot{\phi}}\dot{\psi} + L_{\phi'}\psi' \\
&= L_{\phi}\psi + L_{\dot{\phi}}\dot{\psi} + L_{\phi'}\psi',
\end{aligned}$$

and therefore

$$\Lambda(\phi, \psi) = \frac{\partial}{\partial t}(L_{\dot{\phi}}\psi) + \frac{\partial}{\partial x}(L_{\phi'}\psi).$$

Assume now that ϕ is periodic in θ_0 with period 2π, i.e. that $\phi(x, t; \theta_0 + 2\pi) = \phi(x, t; \theta_0)$ and choose $\psi = \phi_{\theta_0}$. Clearly

$$\Lambda(\phi, \phi_{\theta_0}) = \frac{\partial L}{\partial \theta_0}$$

and one has

$$\frac{\partial}{\partial t}(L_{\dot{\phi}}\phi_{\theta_0}) + \frac{\partial}{\partial x}(L_{\phi'}\phi_{\theta_0}) = \frac{\partial L}{\partial \theta_0}.$$

Integrating with respect to θ_0 over a single period one obtains the following

$$\int_0^{2\pi} \frac{\partial}{\partial t}(L_{\dot\phi}\phi_{\theta_0})\ \mathrm{d}\theta_0 + \int_0^{2\pi} \frac{\partial}{\partial x}(L_{\phi'}\phi_{\theta_0})\ \mathrm{d}\theta_0 = \int_0^{2\pi} \frac{\partial L}{\partial \theta_0}\ \mathrm{d}\theta_0. \tag{7.2}$$

Equation (7.2) reduces to the conservation law of the wave action

$$\partial_t \mathscr{A} + \partial_x \mathscr{B} = 0, \tag{7.3}$$

where

$$\mathscr{A} = \frac{1}{2\pi}\int_0^{2\pi} L_{\dot\phi}\phi_{\theta_0}\ \mathrm{d}\theta_0 = \frac{1}{2\pi}\oint L_{\dot\phi}\ \mathrm{d}\phi, \tag{7.4a}$$

$$\mathscr{B} = \frac{1}{2\pi}\int_0^{2\pi} L_{\phi'}\phi_{\theta_0}\ \mathrm{d}\theta_0 = \frac{1}{2\pi}\oint L_{\phi'}\ \mathrm{d}\phi. \tag{7.4b}$$

Example: The Klein–Gordon Equation As an example consider the Klein–Gordon equation ([40]/p.366)

$$\phi_{tt} - \alpha^2\phi_{xx} + \beta^2\phi = 0. \tag{7.5}$$

For the Klein–Gordon equation (7.5) the Lagrangian has the form ([40]/p.392)

$$L = \frac{1}{2}(\dot\phi)^2 - \frac{1}{2}\alpha^2(\phi')^2 - \frac{1}{2}\beta^2\phi^2$$

and therefore the wave action density and flux are

$$\mathscr{A} = \frac{1}{2\pi}\int_0^{2\pi} \dot\phi\phi_{\theta_0}\ \mathrm{d}\theta_0 \quad \text{and} \quad \mathscr{B} = \frac{1}{2\pi}\int_0^{2\pi} -\alpha^2\phi'\phi_{\theta_0}\ \mathrm{d}\theta_0. \tag{7.6}$$

Additionally, an assumption about periodicity of ϕ in the space variable x leads, upon integration with respect to x to the conservation of total action

$$\frac{\partial}{\partial t}\int \mathscr{A}\ \mathrm{d}x = 0.$$

7.2 Approximate Approach of Whitham

To study slowly varying wave trains in which

$$\phi \sim a\cos(\eta + \theta_0) \tag{7.7}$$

one substitutes (7.7) to L and neglects derivatives of a, θ_0, ω and k, as from the assumption that the wave train is slowly varying, these are small quantities. The result is a function $\mathscr{L}$ for which Whitham [40] proposes the following "average variational principle",

$$\delta \iint \mathscr{L}(\eta_t, \eta_x, a)\ \mathrm{d}t\mathrm{d}x = 0$$

for the functions $a(t,x)$ and $\eta(t,x)$. Now, Euler–Lagrange equations for average variational principle above are:

$$\begin{aligned} \delta a: &\quad \mathscr{L}_a = 0, \\ \delta \eta: &\quad \frac{\partial}{\partial t}\mathscr{L}_{\dot\eta} + \frac{\partial}{\partial x}\mathscr{L}_{\eta'} = 0. \end{aligned}$$

In terms of wave number $k = \eta_x$ and frequency $\omega = \eta_t$ the variational equations take the form

$$\delta a: \quad \mathscr{L}_a = 0, \tag{7.8a}$$

$$\delta \eta: \quad \frac{\partial}{\partial t}\mathscr{L}_\omega + \frac{\partial}{\partial x}\mathscr{L}_k = 0. \tag{7.8b}$$

with additional consistency condition that

$$\frac{\partial k}{\partial t} + \frac{\partial \omega}{\partial x} = 0,$$

ensureing existence of η. Relation (7.8a) is the dispersion relation associated with the problem and thus, for linear problems, one has

$$\mathscr{L} = G(\omega, k)a^2$$

where $G(\omega, k) = 0$ is the dispersion relation [40]. Equation (7.8b) is a conservation law exact to the leading order in slow-time and, as such, should be more properly called an adiabatic conservation law. This equation is referred to, in [40], as the "wave action conservation law" with the time-like adiabatic quantity $\mathscr{L}_\omega$, called the wave action density and the space-like adiabatic quantity $\mathscr{L}_k$, called the wave action flux.

7.3 Multisymplectic Wave Action Conservation Law

Following [8, 13], consider a wave equation in the multisymplectic form (3.2) and assume that the solution $\mathbf{z}$ depends smoothly on a parameter θ_0. In other words, consider a one-parameter family (ensemble) of solutions $\mathbf{z}(x, t; \theta_0)$ to (3.2) smoothly parametrized by θ_0. Taking the standard real vector inner product $\langle \mathbf{u}, \mathbf{v} \rangle = \mathbf{v}^T \mathbf{u}$ of (3.2) with $\mathbf{z}_{\theta_0} = \partial_{\theta_0} \mathbf{z}$ one obtains

$$\langle L\mathbf{z}_t, \mathbf{z}_{\theta_0} \rangle + \langle K\mathbf{z}_x, \mathbf{z}_{\theta_0} \rangle = \langle \nabla_{\mathbf{z}} S, \mathbf{z}_{\theta_0} \rangle,$$

or equivalently

$$\mathbf{z}_{\theta_0}^T L\mathbf{z}_t + \mathbf{z}_{\theta_0}^T K\mathbf{z}_x = \mathbf{z}_{\theta_0}^T \nabla_{\mathbf{z}} S. \tag{7.9}$$

It is not difficult to note that $\mathbf{z}_{\theta_0}^T \nabla_{\mathbf{z}} S(\mathbf{z}) = \partial_{\theta_0} S(\mathbf{z})$ and the transposition of the equation (7.9) takes the form

$$-\mathbf{z}_t^T L\mathbf{z}_{\theta_0} - \mathbf{z}_x^T K\mathbf{z}_{\theta_0} = \partial_{\theta_0} S(\mathbf{z}),$$

since $\partial_{\theta_0} S(\mathbf{z})$ is a scalar function and both L and K are skew-symmetric. Adding these equations we obtain

$$2\partial_{\theta_0} S(\mathbf{z}) = \left(\mathbf{z}_{\theta_0}^T L\mathbf{z}_t - \mathbf{z}_t^T L\mathbf{z}_{\theta_0} \right) + \left(\mathbf{z}_{\theta_0}^T K\mathbf{z}_x - \mathbf{z}_x^T K\mathbf{z}_{\theta_0} \right)$$

Clearly, by the product rule, we can rewrite this equation as

$$2\partial_{\theta_0} S(\mathbf{z}) = \Big(\partial_t(\mathbf{z}_{\theta_0}^T L\mathbf{z}) - \partial_{\theta_0}(\mathbf{z}_t^T L\mathbf{z})\Big) + \Big(\partial_x(\mathbf{z}_{\theta_0}^T K\mathbf{z}) - \partial_{\theta_0}(\mathbf{z}_x^T K\mathbf{z})\Big). \tag{7.10}$$

If we now assume that parameter θ_0 represents a closed loop in the phase space, upon integrating (7.10) with respect to $\theta_0 \in [0, 2\pi]$ and normalizing, one obtains the wave action conservation law

$$\partial_t \mathscr{A} + \partial_x \mathscr{B} = 0 \tag{7.11}$$

with the wave action density $\mathscr{A}$ and the wave action flux $\mathscr{B}$ giben by

$$\mathscr{A} = \frac{1}{2\pi}\int_0^{2\pi} \frac{1}{2}(\mathbf{z}_{\theta_0}^T L\mathbf{z})\ \mathrm{d}\theta_0 \tag{7.12a}$$

$$\mathscr{B} = \frac{1}{2\pi}\int_0^{2\pi} \frac{1}{2}(\mathbf{z}_{\theta_0}^T K\mathbf{z})\ \mathrm{d}\theta_0 \tag{7.12b}$$

An assumption about periodicity of $\mathbf{z}$ with respect to θ_0, i.e. the fact that $\mathbf{z}(t, x; \theta_0 + 2\pi) = \mathbf{z}(t, x; \theta_0)$, is necessary to eliminate ∂_{θ_0} terms of $\mathbf{z}$ in θ_0.

Integrating (7.11) with respect to x with periodic boundary conditions (3.7) one obtains conservation of total action

$$\frac{\partial}{\partial t}\int \mathscr{A}\ \mathrm{d}x = 0.$$

It turns out that the wave action conservation law (7.11) is equivalent, via the Stokes theorem (see also remarks preceding the statement of the Theorem 4) for differential forms [5], to the

conservation of multisymplecticness (3.3). The equivalence is shown as follows

$$\begin{aligned}\mathscr{A} &= \frac{1}{4\pi}\int_0^{2\pi} L\mathbf{z}\cdot\mathbf{z}_{\theta_0}\mathrm{d}\theta_0 = \frac{1}{4\pi}\oint_{\partial D}(L\mathbf{z})\cdot\mathrm{d}\mathbf{z} = \frac{1}{4\pi}\iint_D \mathrm{d}(L\mathbf{z})\wedge\mathrm{d}\mathbf{z}\\ &= -\frac{1}{4\pi}\iint_D \mathrm{d}\mathbf{z}\wedge L\mathrm{d}\mathbf{z} = -\frac{1}{2\pi}\iint_D \Omega^{(t)}, \qquad (7.13a)\\ \mathscr{B} &= \frac{1}{4\pi}\int_0^{2\pi} K\mathbf{z}\cdot\mathbf{z}_{\theta_0}\mathrm{d}\theta_0 = \frac{1}{4\pi}\oint_{\partial D}(K\mathbf{z})\cdot\mathrm{d}\mathbf{z} = \frac{1}{4\pi}\iint_D \mathrm{d}(K\mathbf{z})\wedge\mathrm{d}\mathbf{z}\\ &= -\frac{1}{4\pi}\iint_D \mathrm{d}\mathbf{z}\wedge K\mathrm{d}\mathbf{z} = -\frac{1}{2\pi}\iint_D \Omega^{(x)} \qquad (7.13b)\end{aligned}$$

and $D\subset\mathcal{H}$ is a subset of the phase space $\mathcal{H}$ with ∂D is its boundary Now, following [8], the conservation of multisymplecticness (3.3) follows immediately since

$$0 = -\frac{1}{2\pi}\Big(\partial_t\iint_D \Omega^{(t)} + \partial_x\iint_D \Omega^{(x)}\Big) = -\frac{1}{2\pi}\iint_D\Big(\partial_t\Omega^{(t)} + \partial_x\Omega^{(x)}\Big)$$

and the exchange of integration with differentiation is permissible because integration is performed with respect to the phase space variables $\mathbf{z}$. The assumption that $\mathrm{d}(L\mathbf{z}) = L\mathrm{d}\mathbf{z}$ and $\mathrm{d}(K\mathbf{z}) = K\mathrm{d}\mathbf{z}$ is needed, but from the by definition we have that pre-symplectic matrices L, K are independent of x, t and $\mathbf{z}$ (constant matrices).

Example: Variable Coefficient Klein–Gordon Equation As an example of the conservation of the wave action let's consider a variable coefficient Klein–Gordon equation (3.11) in a multisymplectic form (3.2) with matrices L_1 and K_1 given by (3.15) and the energy function

$$S = S(u,v,w) = \frac{1}{2}(v^2 - \alpha^{-2}w^2 + \beta^2u^2).$$

Wave action density and flux are

$$\begin{aligned}\mathscr{A} &= \frac{1}{4\pi}\int_0^{2\pi}(\mathbf{z}_{\theta_0}^T L\mathbf{z})\ \mathrm{d}\theta_0 = \frac{1}{4\pi}\int_0^{2\pi} u_{\theta_0}v - uv_{\theta_0}\ \mathrm{d}\theta_0, \qquad (7.14a)\\ \mathscr{B} &= \frac{1}{4\pi}\int_0^{2\pi}(\mathbf{z}_{\theta_0}^T K\mathbf{z})\ \mathrm{d}\theta_0 = \frac{1}{4\pi}\int_0^{2\pi} u_{\theta_0}w - uw_{\theta_0}\ \mathrm{d}\theta_0. \qquad (7.14b)\end{aligned}$$

It is not difficult to notice that (7.14) are exactly the wave action density and flux (7.6) derived in the Lagrangian formulation with $u = \phi$, $v = u_t = \dot{\phi}$ and $w = -\alpha^2 u_x = -\alpha^2 \phi'$. Indeed, integration by parts yields

$$\int_0^{2\pi} u v_{\theta_0} \, \mathrm{d}\theta_0 = uv\Big|_0^{2\pi} - \int_0^{2\pi} u_{\theta_0} v \, \mathrm{d}\theta_0$$

and

$$\int_0^{2\pi} u w_{\theta_0} \, \mathrm{d}\theta_0 = uw\Big|_0^{2\pi} - \int_0^{2\pi} u_{\theta_0} w \, \mathrm{d}\theta_0,$$

and thus the conclusion holds by periodicity of u, v and w with respect to θ_0.

7.3.1 Local Energy and Momentum Conservation Laws Revisited

Formalism presented in the previous section used in deriving the wave action conservation law enables derivation of local energy and momentum conservation laws. Assuming that S is independent of θ_0 and choosing θ_0 in the equation (7.10) to be either $\theta_0 = x$ or $\theta_0 = t$ one obtains local conservation of momentum (3.6b) and local conservation of energy (3.6a) laws, respectively. For the proof, notice first that the local energy an momentum conservation laws have the form (3.6). More specifically, choosing θ_0 in equation (7.10) to be equal to t, for S explicitly independent of t, one has

$$2\partial_t S(\mathbf{z}) - \Big(\partial_x(\mathbf{z}_t^T K \mathbf{z}) - \partial_t(\mathbf{z}_x^T K \mathbf{z})\Big) = \partial_t(\mathbf{z}_t^T L \mathbf{z}) - \partial_t(\mathbf{z}_t^T L \mathbf{z}),$$

which is a local energy conservation law (3.6a):

$$\partial_t\Big(S(\mathbf{z}) + \frac{1}{2}(\mathbf{z}_x^T K \mathbf{z})\Big) + \partial_x\Big(-\frac{1}{2}(\mathbf{z}_t^T K \mathbf{z})\Big) = 0.$$

Identical argumentation, for S explicitly independent of x with $\theta_0 = x$, yields

$$2\partial_x S(\mathbf{z}) - \Big(\partial_t(\mathbf{z}_x^T L\mathbf{z}) - \partial_x(\mathbf{z}_t^T L\mathbf{z})\Big) = \Big(\partial_x(\mathbf{z}_x^T K\mathbf{z}) - \partial_x(\mathbf{z}_x^T K\mathbf{z})\Big),$$

which is a local momentum conservation law (3.6b):

$$\partial_t\Big(-\frac{1}{2}(\mathbf{z}_x^T L\mathbf{z})\Big) + \partial_x\Big(S(\mathbf{z}) + \frac{1}{2}(\mathbf{z}_t^T L\mathbf{z})\Big) = 0.$$

7.3.2 Alternate Formulation via Operator Splitting

For alternate form of the multisymplectic equation given by splitting (3.22) there exists conservation laws of energy and momentum in the form (3.6), as shown in [29], with L and K replaced by $2L^+$ and $2K^+$, respectively. Moreover, wave action conservation law (7.11) also holds with

$$\mathscr{A} = \frac{1}{2\pi}\int_0^{2\pi} (\mathbf{z}_{\theta_0}^T L^+\mathbf{z})\ \mathrm{d}\theta_0, \tag{7.15a}$$

$$\mathscr{B} = \frac{1}{2\pi}\int_0^{2\pi} (\mathbf{z}_{\theta_0}^T K^+\mathbf{z})\ \mathrm{d}\theta_0. \tag{7.15b}$$

7.4 Multisymplectic Spectral Wave Action

It turns out that a procedure analogous to the one used in deriving conservation law of wave action in physical space, applied to the multisymplectic spectral PDE (3.29) yields a new conservation law that we will be calling the spectral wave action conservation law. It is yet unclear whether the spectral wave action conservation lwa can be shown to be equivalent to the multisymplectic spectral conservation law (3.30). One would expect that an analog of the Stokes' theorem would be true in Fourier space thus permitting establishing such a relation.

In order to dervive spectral wave action conservation law, let's assume that $\hat{\mathbf{Z}}$, a solution to (3.29), smoothly depends on a parameter θ_0 and taking a dot product with $\hat{\mathbf{Z}}_{\theta_0}$ on has

$$\langle \mathbf{L}\partial_t\hat{\mathbf{Z}}, \hat{\mathbf{Z}}_{\theta_0}\rangle + \langle \mathbf{K}\boldsymbol{\Theta}\hat{\mathbf{Z}}, \hat{\mathbf{Z}}_{\theta_0}\rangle = \langle \nabla_{\hat{\mathbf{Z}}}\hat{S}(\hat{\mathbf{Z}}), \hat{\mathbf{Z}}_{\theta_0}\rangle,$$

and the conjugated and transposed ("starred") equation

$$-\hat{\mathbf{Z}}_t^*\mathbf{L}\hat{\mathbf{Z}}_{\theta_0} - (\boldsymbol{\Theta}\hat{\mathbf{Z}})^*\mathbf{K}\hat{\mathbf{Z}}_{\theta_0} = \partial_{\theta_0}\hat{S}(\hat{\mathbf{Z}}).$$

Adding these equations one obtains

$$2\partial_{\theta_0}\hat{S}(\hat{\mathbf{Z}}) = \hat{\mathbf{Z}}_{\theta_0}^*\mathbf{L}\hat{\mathbf{Z}}_t + \hat{\mathbf{Z}}_{\theta_0}^*\mathbf{K}(\boldsymbol{\Theta}\hat{\mathbf{Z}}) - \hat{\mathbf{Z}}_t^*\mathbf{L}\hat{\mathbf{Z}}_{\theta_0} - (\boldsymbol{\Theta}\hat{\mathbf{Z}})^*\mathbf{K}\hat{\mathbf{Z}}_{\theta_0}$$

or equivalently, that

$$2\partial_{\theta_0}\hat{S}(\hat{\mathbf{Z}}) = \Big(\hat{\mathbf{Z}}_{\theta_0}^*\mathbf{L}\hat{\mathbf{Z}}_t - \hat{\mathbf{Z}}_t^*\mathbf{L}\hat{\mathbf{Z}}_{\theta_0}\Big) + \Big(\hat{\mathbf{Z}}_{\theta_0}^*\mathbf{K}(\boldsymbol{\Theta}\hat{\mathbf{Z}}) - (\boldsymbol{\Theta}\hat{\mathbf{Z}})^*\mathbf{K}\hat{\mathbf{Z}}_{\theta_0}\Big)$$

It is not difficult to note that

$$\begin{aligned} 0 \;=\; & \partial_t\Big(\frac{1}{2}\hat{\mathbf{Z}}_{\theta_0}^*\mathbf{L}\hat{\mathbf{Z}}\Big) + \frac{1}{2}\Big(\hat{\mathbf{Z}}_{\theta_0}^*\mathbf{K}(\boldsymbol{\Theta}\hat{\mathbf{Z}}) + (\boldsymbol{\Theta}\hat{\mathbf{Z}})_{\theta_0}^*\mathbf{K}\hat{\mathbf{Z}}\Big) \\ & -\frac{\partial}{\partial\theta_0}\Big(\frac{1}{2}\hat{\mathbf{Z}}_t^*\mathbf{L}\hat{\mathbf{Z}} + \frac{1}{2}(\boldsymbol{\Theta}\hat{\mathbf{Z}})^*\mathbf{L}\hat{\mathbf{Z}} + \hat{S}(\hat{\mathbf{Z}})\Big) \end{aligned} \tag{7.16}$$

and thus, upon integration, one obtains a WACL

$$\partial_t\int_0^{2\pi}\frac{1}{2}\langle \mathbf{L}\hat{\mathbf{Z}}, \hat{\mathbf{Z}}_{\theta_0}\rangle\;\mathrm{d}\theta_0 + \int_0^{2\pi}\frac{1}{2}\Big(\langle \mathbf{K}(\boldsymbol{\Theta}\hat{\mathbf{Z}}), \hat{\mathbf{Z}}_{\theta_0}\rangle + \langle \mathbf{K}\hat{\mathbf{Z}}, (\boldsymbol{\Theta}\hat{\mathbf{Z}})_{\theta_0}\rangle\Big)\;\mathrm{d}\theta_0 = 0 \tag{7.17}$$

Now, if there exists an analog of the Stokes' theorem one could show that equation (7.17) is a multisymplectic spectral conservation law established in [9].

7.4.1 Spectral Local Energy Conservation Law

Spectral form of multisymplectic PDE can be though of as a spatial semi-discretization and as such does not have momentum conservation law. In this section we use formalism of (7.16) to derive local energy conservation law in Fourier space. In order to obtain spectral LECL [11, 22] consider first equation (7.16) and assume $\theta_0 = t$.

$$\begin{aligned} 0 &= \partial_t\Big(\frac{1}{2}\hat{\mathbf{Z}}_t^*\mathbf{L}\hat{\mathbf{Z}}\Big) + \frac{1}{2}\Big(\hat{\mathbf{Z}}_t^*\mathbf{K}(\boldsymbol{\Theta}\hat{\mathbf{Z}}) + (\boldsymbol{\Theta}\hat{\mathbf{Z}})_t^*\mathbf{K}\hat{\mathbf{Z}}\Big) \\ &\quad -\frac{\partial}{\partial t}\Big(\frac{1}{2}\hat{\mathbf{Z}}_t^*\mathbf{L}\hat{\mathbf{Z}} + \frac{1}{2}(\boldsymbol{\Theta}\hat{\mathbf{Z}})^*\mathbf{L}\hat{\mathbf{Z}} + \hat{S}(\hat{\mathbf{Z}})\Big). \end{aligned} \tag{7.18}$$

Equivalently

$$\frac{\partial}{\partial t}\Big(\frac{1}{2}(\hat{S}(\hat{\mathbf{Z}}) + \boldsymbol{\Theta}\hat{\mathbf{Z}})^*\mathbf{L}\hat{\mathbf{Z}}\Big) + \frac{1}{2}\Big(\hat{\mathbf{Z}}_t^*\mathbf{K}(\boldsymbol{\Theta}\hat{\mathbf{Z}}) + (\boldsymbol{\Theta}\hat{\mathbf{Z}})_t^*\mathbf{K}\hat{\mathbf{Z}}\Big) = 0 \tag{7.19}$$

which is called spectral local energy conservation law and can be written in the form given by equation (3.33). Therefore we have just proved Theorem 10 stated in Chapter 3.

7.5 Discrete Wave Action Conservation Law

It should be clear by now that the wave action conservation law is somewhat a more primitive and fundamental property than multisymplectic conservation law. In previous sections we discussed wave action in continuous systems. Following the development of multisymplectic discretizations, we would like to attempt deriving discrete analogs of the wave action conservation law. Material contained in this section can be divided onto two parts. The firs part is a derivation of an exact, discrete conservation law of wave action of the MS box scheme while the second contains a brief discussion of previous work of Frank [13], where an

exact, discrete wave action conservation law for a sub-class of Runge–Kutta, multisymplectic box schemes was derived. We will attempt to generalize this result and investigate discrete analog of wave action conservation laws for spectral semi-discretizations. Last part of this section will contain supporting numerical evidence.

7.5.1 Multisymplectic Box Scheme

We begin by presenting an example, related to [13], where we show derivation of a variant of an exact, discrete wave action conservation law for the Preissmann–Keller (multisymplectic) box scheme (4.7) discretization of the MS form, i.e.

$$LD_tM_x\mathbf{z}_j^n + KD_xM_t\mathbf{z}_j^n = \nabla_{\mathbf{z}}S(M_tM_x\mathbf{z}_j^n)$$

and take a standard inner product with $M_tM_x(\mathbf{z}_{\theta_0})_j^n$ to obtain

$$\langle LD_tM_x\mathbf{z}_j^n, M_tM_x(\mathbf{z}_{\theta_0})_j^n\rangle + \langle KD_xM_t\mathbf{z}_j^n, M_tM_x(\mathbf{z}_{\theta_0})_j^n\rangle = \langle \nabla_{\mathbf{z}}S(M_tM_x\mathbf{z}_j^n), M_tM_x(\mathbf{z}_{\theta_0})_j^n\rangle. \quad (7.20)$$

Observing that $\langle \nabla_{\mathbf{z}}S(M_tM_x\mathbf{z}_j^n), M_tM_x(\mathbf{z}_{\theta_0})_j^n\rangle = \partial_{\theta_0}S(M_tM_x\mathbf{z}_j^n)$ we can transpose the above equation to obtain

$$-(D_tM_x\mathbf{z}_j^n)^TL(M_tM_x(\mathbf{z}_{\theta_0})_j^n) - (D_xM_t\mathbf{z}_j^n)^TK(M_tM_x(\mathbf{z}_{\theta_0})_j^n) = \partial_{\theta_0}S(M_tM_x\mathbf{z}_j^n).$$

Adding we have

$$\begin{aligned} 2\partial_{\theta_0}S(M_tM_x\mathbf{z}_j^n) &= (M_tM_x(\mathbf{z}_{\theta_0})_j^n)^TL(D_tM_x\mathbf{z}_j^n) - (D_tM_x\mathbf{z}_j^n)^TL(M_tM_x(\mathbf{z}_{\theta_0})_j^n) \\ &\quad + (M_tM_x(\mathbf{z}_{\theta_0})_j^n)^TK(D_xM_t\mathbf{z}_j^n) - (D_xM_t\mathbf{z}_j^n)^TK(M_tM_x(\mathbf{z}_{\theta_0})_j^n) \end{aligned}$$

or equivalently

$$\begin{aligned} 2\partial_{\theta_0} S(M_t M_x \mathbf{z}_j^n) &= (M_t M_x (\mathbf{z}_{\theta_0})_j^n)^T L(D_t M_x \mathbf{z}_j^n) + (D_t M_x (\mathbf{z}_{\theta_0})_j^n)^T L(M_t M_x \mathbf{z}_j^n) \\ &\quad + (M_t M_x (\mathbf{z}_{\theta_0})_j^n)^T K(D_x M_t \mathbf{z}_j^n) + (D_x M_t (\mathbf{z}_{\theta_0})_j^n)^T K(M_t M_x \mathbf{z}_j^n) \\ &\quad - \partial_{\theta_0}(D_t M_x \mathbf{z}_j^n)^T L(M_t M_x \mathbf{z}_j^n) - \partial_{\theta_0}(D_x M_t \mathbf{z}_j^n)^T K(M_t M_x \mathbf{z}_j^n) \end{aligned}$$

Now since

$$\begin{aligned} &(M_t M_x (\mathbf{z}_{\theta_0})_j^n)^T L(D_t M_x \mathbf{z}_j^n) + (D_t M_x (\mathbf{z}_{\theta_0})_j^n)^T L(M_t M_x \mathbf{z}_j^n) \\ &= \frac{1}{2(\Delta t)}((M_x \mathbf{z}_{\theta_0})_j^{n+1} + (M_x \mathbf{z}_{\theta_0})_j^n)^T L((M_x \mathbf{z}_{\theta_0})_j^{n+1} - (M_x \mathbf{z}_{\theta_0})_j^n) \\ &+ \frac{1}{2(\Delta t)}((M_x \mathbf{z}_{\theta_0})_j^{n+1} - (M_x \mathbf{z}_{\theta_0})_j^n)^T L((M_x \mathbf{z}_{\theta_0})_j^{n+1} + (M_x \mathbf{z}_{\theta_0})_j^n) \\ &= D_t((\mathbf{z}_{\theta_0})_j^n)^T L(\mathbf{z}_j^n) \end{aligned} \tag{7.21}$$

and symmetrical argument holds for terms containing matrix K, we have that

$$\begin{aligned} 2\partial_{\theta_0} S(M_t M_x \mathbf{z}_j^n) &= D_t((M_x \mathbf{z}_{\theta_0})_j^n)^T L(M_x \mathbf{z}_j^n) + D_x((M_t \mathbf{z}_{\theta_0})_j^n)^T K(M_t \mathbf{z}_j^n) \\ &\quad - \partial_{\theta_0}(D_t M_x \mathbf{z}_j^n)^T L(M_t M_x \mathbf{z}_j^n) - \partial_{\theta_0}(D_x M_t \mathbf{z}_j^n)^T K(M_t M_x \mathbf{z}_j^n). \end{aligned}$$

Assuming that $\mathbf{z}_j^n$ is periodic with respect to θ_0 with period 2π, i.e. that for every n, j one has $\mathbf{z}_j^n(\theta_0 + 2\pi) = \mathbf{z}_j^n(\theta_0)$ and integrating with respect to θ_0 over the entire period we arrive at the discrete wave action conservation law

$$D_t \int_0^{2\pi} \frac{1}{2}\langle L M_x \mathbf{z}_j^n, M_x (\mathbf{z}_{\theta_0})_j^n \rangle \, \mathrm{d}\theta_0 + D_x \int_0^{2\pi} \frac{1}{2}\langle K M_t \mathbf{z}_j^n, M_t (\mathbf{z}_{\theta_0})_j^n \rangle \, \mathrm{d}\theta_0 = 0 \tag{7.22}$$

Using notation $\mathbf{z}_{1/2}^n = M_x \mathbf{z}_j^n$ and $\mathbf{z}_j^{1/2} = M_t \mathbf{z}_j^n$ we can rewrite above equation as

$$D_t \int_0^{2\pi} \frac{1}{2}\langle L \mathbf{z}_{1/2}^n, (\mathbf{z}_{\theta_0})_{1/2}^n \rangle \, \mathrm{d}\theta_0 + D_x \int_0^{2\pi} \frac{1}{2}\langle K \mathbf{z}_j^{1/2}, (\mathbf{z}_{\theta_0})_j^{1/2} \rangle \, \mathrm{d}\theta_0 = 0 \tag{7.23}$$

Equation (7.23) is called wave action conservation law and, upon normalization, written as

$$D_t \mathscr{A}_{1/2}^n + D_x \mathscr{B}_j^{1/2} = 0, \tag{7.24}$$

where

$$\mathscr{A}_{1/2}^n = \frac{1}{2\pi}\int_0^{2\pi} \frac{1}{2}\langle L\mathbf{z}_{1/2}^n, (\mathbf{z}_{\theta_0})_{1/2}^n\rangle \, \mathrm{d}\theta_0, \tag{7.25a}$$

$$\mathscr{B}_j^{1/2} = \frac{1}{2\pi}\int_0^{2\pi} \frac{1}{2}\langle K\mathbf{z}_j^{1/2}, (\mathbf{z}_{\theta_0})_j^{1/2}\rangle \, \mathrm{d}\theta_0. \tag{7.25b}$$

Alternative Form Consider again (7.20) written as

$$\begin{aligned}\partial_{\theta_0} S(M_t M_x \mathbf{z}_j^n) = {} & \langle L D_t M_x \mathbf{z}_j^n, M_t M_x (\mathbf{z}_{\theta_0})_j^n\rangle + \langle L M_t M_x \mathbf{z}_j^n, D_t M_x (\mathbf{z}_{\theta_0})_j^n\rangle \\ & -\partial_{\theta_0}\langle L M_t M_x \mathbf{z}_j^n, D_t M_x \mathbf{z}_j^n\rangle + \langle L M_t M_x (\mathbf{z}_{\theta_0})_j^n, D_t M_x \mathbf{z}_j^n\rangle \\ & +\langle K D_x M_t \mathbf{z}_j^n, M_t M_x (\mathbf{z}_{\theta_0})_j^n\rangle + \langle K M_t M_x \mathbf{z}_j^n, D_x M_t (\mathbf{z}_{\theta_0})_j^n\rangle \\ & -\partial_{\theta_0}\langle K M_t M_x \mathbf{z}_j^n, D_x M_t \mathbf{z}_j^n\rangle + \langle K M_t M_x (\mathbf{z}_{\theta_0})_j^n, D_x M_t \mathbf{z}_j^n\rangle \end{aligned} \tag{7.26}$$

Using skew-symmetry of matrices L and K and the fact that $\langle A\mathbf{u}, \mathbf{v}\rangle = \langle \mathbf{u}, A^*\mathbf{v}\rangle$ we have that

$$\begin{aligned}&\langle L M_t M_x (\mathbf{z}_{\theta_0})_j^n, D_t M_x \mathbf{z}_j^n\rangle + \langle K M_t M_x (\mathbf{z}_{\theta_0})_j^n, D_x M_t \mathbf{z}_j^n\rangle \\ &\quad = -\langle M_t M_x (\mathbf{z}_{\theta_0})_j^n, (L D_t M_x \mathbf{z}_j^n + K D_x M_t \mathbf{z}_j^n)\rangle = -\partial_{\theta_0} S(M_t M_x \mathbf{z}_j^n)\end{aligned}$$

by equation (7.20). Integration with respect to θ_0 yields an alternative form of the discrete WACL

$$\mathscr{A}_j^n + \mathscr{B}_j^n = 0 \tag{7.27}$$

with

$$\begin{aligned}\mathscr{A}_j^n &= \frac{1}{2\pi}\int_0^{2\pi}\frac{1}{2}\langle LD_tM_x\mathbf{z}_j^n, M_tM_x(\mathbf{z}_{\theta_0})_j^n\rangle + \frac{1}{2}\langle LM_tM_x\mathbf{z}_j^n, D_tM_x(\mathbf{z}_{\theta_0})_j^n\rangle\ \mathrm{d}\theta_0\\ \mathscr{B}_j^n &= \frac{1}{2\pi}\int_0^{2\pi}\frac{1}{2}\langle KD_xM_t\mathbf{z}_j^n, M_tM_x(\mathbf{z}_{\theta_0})_j^n\rangle + \frac{1}{2}\langle KM_tM_x\mathbf{z}_j^n, D_xM_t(\mathbf{z}_{\theta_0})_j^n\rangle\ \mathrm{d}\theta_0\end{aligned}$$

One observes that the two forms of discrete wave action conservation law (7.24) and (7.27) are equivalent, since

$$\langle LD_t\mathbf{u}^n, M_t(\mathbf{u}_{\theta_0})^n\rangle + \langle LM_t\mathbf{u}^n, D_t(\mathbf{u}_{\theta_0})^n\rangle = D_t\langle L\mathbf{u}^n, (\mathbf{u}_{\theta_0})^n\rangle,$$

and symmetrical property holds for terms with matrix K with operators D_x and M_x.

7.5.2 Discrete Spectral WA for the Midpoint Time-Discretization

Taking an inner product of the equation (4.62) with $M_t\hat{\mathbf{Z}}_{\theta_0}^n$ we obtain

$$\langle LD_t\hat{\mathbf{Z}}^n, M_t\hat{\mathbf{Z}}_{\theta_0}^n\rangle + \langle K\bar{\Theta}(M_t\hat{\mathbf{Z}}^n), M_t\hat{\mathbf{Z}}_{\theta_0}^n\rangle = \langle\nabla_{\hat{\mathbf{Z}}}\hat{S}(M_t\hat{\mathbf{Z}}^n), M_t\hat{\mathbf{Z}}_{\theta_0}^n\rangle \tag{7.28}$$

and its conjugate transpose

$$-(D_t\hat{\mathbf{Z}}^n)^*L(M_t\hat{\mathbf{Z}}_{\theta_0}^n) - (\bar{\Theta}M_t\hat{\mathbf{Z}}^n)^*K(M_t\hat{\mathbf{Z}}_{\theta_0}^n) = \partial_{\theta_0}\hat{S}(M_t\hat{\mathbf{Z}}^n)$$

Adding

$$\begin{aligned}&(M_t\hat{\mathbf{Z}}_{\theta_0}^n)^*L(D_t\hat{\mathbf{Z}}^n) - (D_t\hat{\mathbf{Z}}^n)^*L(M_t\hat{\mathbf{Z}}_{\theta_0}^n)\\ +(M_t\hat{\mathbf{Z}}_{\theta_0}^n)^*K\bar{\Theta}(M_t\hat{\mathbf{Z}}^n) - (\bar{\Theta}M_t\hat{\mathbf{Z}}^n)^*K(M_t\hat{\mathbf{Z}}_{\theta_0}^n) &= 2\partial_{\theta_0}\hat{S}(M_t\hat{\mathbf{Z}}^n)\end{aligned}$$

and it is not difficult to note that is is equivalently

$$\begin{aligned}&(M_t\hat{\mathbf{Z}}_{\theta_0}^n)^*L(D_t\hat{\mathbf{Z}}^n) + (D_t\hat{\mathbf{Z}}_{\theta_0}^n)^*L(M_t\hat{\mathbf{Z}}^n) - \partial_{\theta_0}\Big((D_t\hat{\mathbf{Z}}^n)^*L(M_t\hat{\mathbf{Z}}^n)\Big)\\ +(M_t\hat{\mathbf{Z}}_{\theta_0}^n)^*K\bar{\Theta}(M_t\hat{\mathbf{Z}}^n) + (\bar{\Theta}M_t\hat{\mathbf{Z}}_{\theta_0}^n)^*K(M_t\hat{\mathbf{Z}}^n) - \partial_{\theta_0}\Big((\bar{\Theta}M_t\hat{\mathbf{Z}}^n)^*K(M_t\hat{\mathbf{Z}}^n)\Big)&\\ = 2\partial_{\theta_0}\hat{S}(M_t\hat{\mathbf{Z}}^n)&\end{aligned}$$

We first observe that

$$
\begin{aligned}
&(M_t\hat{\mathbf{Z}}^n_{\theta_0})^* L(D_t\hat{\mathbf{Z}}^n) + (D_t\hat{\mathbf{Z}}^n_{\theta_0})^* L(M_t\hat{\mathbf{Z}}^n)\\
&= \frac{1}{2(\Delta t)}\Big[(\hat{\mathbf{Z}}^{n+1}_{\theta_0} + \hat{\mathbf{Z}}^n_{\theta_0})^* L(\hat{\mathbf{Z}}^{n+1} - \hat{\mathbf{Z}}^n) + (\hat{\mathbf{Z}}^{n+1}_{\theta_0} - \hat{\mathbf{Z}}^n_{\theta_0})^* L(\hat{\mathbf{Z}}^{n+1} + \hat{\mathbf{Z}}^n)\Big]\\
&= \frac{1}{2(\Delta t)}\Big[(\hat{\mathbf{Z}}^{n+1}_{\theta_0})^* L\hat{\mathbf{Z}}^{n+1} - (\hat{\mathbf{Z}}^{n+1}_{\theta_0})^* L\hat{\mathbf{Z}}^n + (\hat{\mathbf{Z}}^n_{\theta_0})^* L\hat{\mathbf{Z}}^{n+1} - (\hat{\mathbf{Z}}^{n+1}_{\theta_0})^* L\hat{\mathbf{Z}}^n\Big]\\
&\quad + \frac{1}{2(\Delta t)}\Big[(\hat{\mathbf{Z}}^{n+1}_{\theta_0})^* L\hat{\mathbf{Z}}^{n+1} + (\hat{\mathbf{Z}}^{n+1}_{\theta_0})^* L\hat{\mathbf{Z}}^n - (\hat{\mathbf{Z}}^n_{\theta_0})^* L\hat{\mathbf{Z}}^{n+1} - (\hat{\mathbf{Z}}^n_{\theta_0})^* L\hat{\mathbf{Z}}^n\Big]\\
&= D_t\langle L\hat{\mathbf{Z}}^n, (\hat{\mathbf{Z}}^n_{\theta_0})\rangle.
\end{aligned}
$$

It is now an immediate conclusion, that the discrete spectral WACL has the form

$$
\begin{aligned}
&D_t \int_0^{2\pi} \frac{1}{2}\langle L\hat{\mathbf{Z}}^n, (\hat{\mathbf{Z}}^n_{\theta_0})\rangle \, \mathrm{d}\theta_0\\
+\int_0^{2\pi} \frac{1}{2}\Big(\langle K(\bar{\Theta}M_t\hat{\mathbf{Z}}^n), M_t\hat{\mathbf{Z}}^n_{\theta_0}\rangle + \langle KM_t\hat{\mathbf{Z}}^n, (\bar{\Theta}M_t\hat{\mathbf{Z}}^n)_{\theta_0}\rangle\Big) \, \mathrm{d}\theta_0 &= 0.
\end{aligned} \tag{7.29}
$$

Alternative Form Consider again equation (7.28) written as

$$
\begin{aligned}
\partial_{\theta_0}\hat{S}(M_t\hat{\mathbf{Z}}^n) &= \langle LD_t\hat{\mathbf{Z}}^n, M_t\hat{\mathbf{Z}}^n_{\theta_0}\rangle + \langle LM_t\hat{\mathbf{Z}}^n, D_t\hat{\mathbf{Z}}^n_{\theta_0}\rangle\\
&\quad -\partial_{\theta_0}\langle LM_t\hat{\mathbf{Z}}^n, D_t\hat{\mathbf{Z}}^n\rangle + \langle LM_t\hat{\mathbf{Z}}^n_{\theta_0}, D_t\hat{\mathbf{Z}}^n\rangle\\
&\quad +\langle KM_t\bar{\Theta}\hat{\mathbf{Z}}^n, M_t\hat{\mathbf{Z}}^n_{\theta_0}\rangle + \langle KM_t\hat{\mathbf{Z}}^n, M_t\bar{\Theta}\hat{\mathbf{Z}}^n_{\theta_0}\rangle\\
&\quad -\partial_{\theta_0}\langle KM_t\hat{\mathbf{Z}}^n, M_t\bar{\Theta}\hat{\mathbf{Z}}^n\rangle + \langle KM_t\hat{\mathbf{Z}}^n_{\theta_0}, M_t\bar{\Theta}\hat{\mathbf{Z}}^n\rangle
\end{aligned} \tag{7.30}
$$

Skew-symmetry of matrices L and K, and equation (4.62) yields

$$
\begin{aligned}
&\langle LM_t\hat{\mathbf{Z}}^n_{\theta_0}, D_t\hat{\mathbf{Z}}^n\rangle + \langle KM_t\hat{\mathbf{Z}}^n_{\theta_0}, M_t\bar{\Theta}\hat{\mathbf{Z}}^n\rangle\\
&\quad = -\langle M_t\hat{\mathbf{Z}}^n_{\theta_0}, LD_t\hat{\mathbf{Z}}^n + KM_t\bar{\Theta}\hat{\mathbf{Z}}^n\rangle = \partial_{\theta_0}\hat{S}(M_t\hat{\mathbf{Z}}^n)
\end{aligned}
$$

Integrating in θ_0 one obtains the following discrete spectral WACL

$$
\hat{\mathscr{A}}^n + \hat{\mathscr{B}}^n = 0,
$$

where

$$\begin{aligned}\hat{\mathscr{A}}^n &= \frac{1}{2\pi}\int_0^{2\pi}\frac{1}{2}\langle LD_t\hat{\mathbf{Z}}^n, M_t\hat{\mathbf{Z}}^n_{\theta_0}\rangle + \langle LM_t\hat{\mathbf{Z}}^n, D_t\hat{\mathbf{Z}}^n_{\theta_0}\rangle\ \mathrm{d}\theta_0\\ \hat{\mathscr{B}}^n &= \frac{1}{2\pi}\int_0^{2\pi}\frac{1}{2}\langle KM_t\bar{\Theta}\hat{\mathbf{Z}}^n, M_t\hat{\mathbf{Z}}^n_{\theta_0}\rangle + \frac{1}{2}\langle KM_t\hat{\mathbf{Z}}^n, M_t\bar{\Theta}\hat{\mathbf{Z}}^n_{\theta_0}\rangle\ \mathrm{d}\theta_0\end{aligned}$$

which is equivalent to the equation (7.29).

7.6 Numerical Experiments

We illustrate the wave action conservation by multisymplectic discretization by first presenting an experiment described in [13]. Multisymplectic Euler's method for the Klein–Gordon equation takes the form (4.42). Assuming that $u_j^n = u_j^n(\theta_0)$ is a differentiable function of a parameter θ_0 and differentiating with respect to it one obtains

$$\begin{aligned} -\tfrac{1}{\Delta t}((v_{\theta_0})_j^{n+1} - (v_{\theta_0})_j^n) \quad -\tfrac{1}{\Delta x}((w_{\theta_0})_{j+1}^n - (w_{\theta_0})_j^n) &= (\beta_j^n)^2(u_{\theta_0})_j^n \\ \tfrac{1}{\Delta t}((u_{\theta_0})_j^n - (u_{\theta_0})_j^{n-1}) &= (v_{\theta_0})_j^n \\ \tfrac{1}{\Delta x}((u_{\theta_0})_j^n - (u_{\theta_0})_{j-1}^n) &= -(\alpha_j^n)^{-2}(w_{\theta_0})_j^n \end{aligned} \tag{7.31}$$

Initial conditions for slowly modulated wave train

$$u(t,x;\theta_0) = A\sin(\eta+\theta_0), \qquad A = A(t,x),\ \eta = \eta(t,x) = kx+\omega t$$

are obtained by setting $t=0$ in the following equations

$$\begin{aligned} v(t,x;\theta_0) = u_t(t,x;\theta_0) &= A\omega\cos(\eta+\theta_0)\\ w(t,x;\theta_0) = u_x(t,x;\theta_0) &= Ak\cos(\eta+\theta_0)\\ u_{\theta_0}(t,x;\theta_0) &= A\cos(\eta+\theta_0)\\ v_{\theta_0}(t,x;\theta_0) = (u_{\theta_0})_t(t,x;\theta_0) &= -A\omega\sin(\eta+\theta_0)\\ w_{\theta_0}(t,x;\theta_0) = (u_{\theta_0})_x(t,x;\theta_0) &= -Ak\sin(\eta+\theta_0)\end{aligned}$$

and in [13] those are $A \equiv 1$

$$u(0,x;\theta_0) = \sin(kx+\theta_0) \qquad u_{\theta_0}(0,x;\theta_0) = \cos(kx+\theta_0)$$

$$v(0,x;\theta_0) = \omega\cos(kx+\theta_0) \qquad v_{\theta_0}(0,x;\theta_0) = -\omega\sin(kx+\theta_0)$$

$$w(0,x;\theta_0) = k\cos(kx+\theta_0) \qquad w_{\theta_0}(0,x;\theta_0) = -k\sin(kx+\theta_0)$$

7.6.1 Implementation

Equations (4.42) and (7.31) in a vector are

$$\begin{aligned}
\mathbf{v}^{n+1} &= \mathbf{v}^n - (\Delta t)(\boldsymbol{\beta}^n)^2\mathbf{u}^n + \lambda U\mathbf{w}^n \\
\mathbf{u}^{n+1} &= \mathbf{u}^n + (\Delta t)\mathbf{v}^{n+1} \\
\mathbf{w}^{n+1} &= -\frac{1}{\Delta x}(\boldsymbol{\alpha}^{n+1})^2(U^T)\mathbf{u}^{n+1}
\end{aligned}$$

and

$$\begin{aligned}
(\mathbf{v}_{\theta_0})^{n+1} &= (\mathbf{v}_{\theta_0})^n - (\Delta t)(\boldsymbol{\beta}^n)^2(\mathbf{u}_{\theta_0})^n + \lambda U(\mathbf{w}_{\theta_0})^n \\
(\mathbf{u}_{\theta_0})^{n+1} &= (\mathbf{u}_{\theta_0})^n + (\Delta t)(\mathbf{v}_{\theta_0})^{n+1} \\
(\mathbf{w}_{\theta_0})^{n+1} &= -\frac{1}{\Delta x}(\boldsymbol{\alpha}^{n+1})^2(U^T)(\mathbf{u}_{\theta_0})^{n+1}
\end{aligned}$$

where $U \in \mathcal{M}_{J\times J}(\mathbb{R})$ has the form

$$U = \begin{bmatrix}
1 & -1 & & & \\
 & 1 & -1 & & \\
 & & \ddots & \ddots & \\
 & & & 1 & -1 \\
-1 & & & & 1
\end{bmatrix}$$

and bolded letters, like $\mathbf{u} = [u_j]_{j\in\{1,\ldots,J\}}$, etc., denote vectors in $\mathcal{M}_{J\times 1}(\mathbb{R})$.

7.7 Simulation Results

The results of simulation are presented on Figure 7.1. Shown is an actual wave profile (blue) at $n = 100$ and its amplitude (red) calculated from

$$A_j^n = \sqrt{(u_j^n)^2 + ((u_{\theta_0})_j^n)^2} \tag{7.32}$$

The parameters were set to be $\epsilon = 0.02$, $\ell = 2\pi/\epsilon$, $\omega = 4\pi/(\epsilon\ell)$, $k = \omega$, $J = 30/\epsilon$, $\Delta t = \epsilon\ell/J$, $t_0 = 0$, $T = 10/\epsilon$, $\Delta x = \ell/J$. Moreover

$$\begin{aligned} \alpha &= 1 + \frac{1}{5}\sin\left(\frac{\pi}{27}\epsilon t\right)\exp\left(-25\left(\frac{x}{\ell} - \frac{1}{2}\right)^2\right) \\ \beta &= 1 - \cos\left(\frac{\pi}{20}\epsilon t\right)\exp\left(-25\left(\frac{x}{\ell} - \frac{1}{2}\right)^2\right) \end{aligned}$$

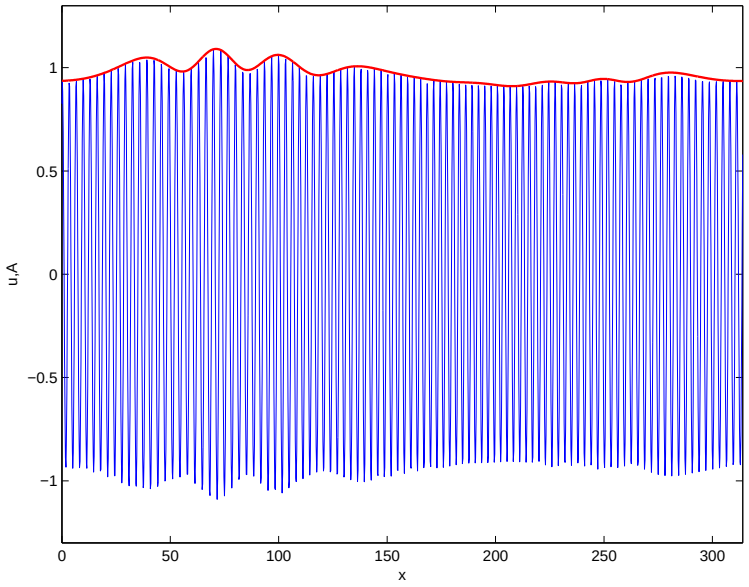

Figure 7.1: Wave-train (blue) and its amplitude (red) at $T = 10/\epsilon$.

For the simulations one has to consider a family of initial data parametrized with $\theta_0 \in [0, 2\pi]$ discretized with some step $\Delta\theta_0 = 2\pi/M$, M is a number of numerical experiments

to be performed indexed by $m \in \{1, \ldots, M\}$. One can compute the discrete action density and action flux and than approximate the loop integral to some higher–than–2 order. For discretizations of nonlinear systems one needs to solve

$$L\partial_t^{j,n}(\mathbf{z}_{\theta_0})_j^n + K\partial_x^{j,n}(\mathbf{z}_{\theta_0})_j^n = \frac{\partial}{\partial\theta_0}\Big(\nabla_{\mathbf{z}} S\Big)_j^n$$

For instance the sine–Gordon becomes

$$\begin{aligned}
\partial_t^{j,n}(v_{\theta_0})_j^n \;+\; \partial_x^{j,n}(w_{\theta_0})_j^n \;&=\; -((u_{\theta_0})_j^n)\cos(u_j^n) \\
-\;\partial_t^{j,n}(u_{\theta_0})_j^n \;&=\; -(v_{\theta_0})_j^n \\
-\;\partial_x^{j,n}(u_{\theta_0})_j^n \;&=\; (w_{\theta_0})_j^n
\end{aligned}$$

where u_j^n is the solution of the original system of equations.

7.7.1 Slow-variation Approximation – Discrete Case

Following [13], for Lagrangian integrators in the case of slow-variation approximation, we consider a set of two equations

$$\begin{aligned}
0 \;=\; & -\frac{1}{2(\Delta t)^2}\Big(A_j^{n+1}\sin(\theta_j^{n+1}-\theta_j^n) - A_j^{n-1}\sin(\theta_j^n-\theta_j^{n-1})\Big) \\
& +\frac{1}{2(\Delta x)^2}\Big((\alpha_{j+1/2}^n)^2 A_{j+1}^n\sin(\theta_{j+1}^n-\theta_j^n) - (\alpha_{j-1/2}^n)^2 A_{j-1}^n\sin(\theta_j^n-\theta_{j-1}^n)\Big) \qquad (7.33a) \\
0 \;=\; & \frac{1}{(\Delta t)^2}\Big(A_j^n - \frac{1}{2}A_j^{n+1}\cos(\theta_j^{n+1}-\theta_j^n) - \frac{1}{2}A_j^{n-1}\cos(\theta_j^n-\theta_j^{n-1})\Big) \\
& -\frac{1}{(\Delta x)^2}\Big(\frac{1}{2}((\alpha_{j+1/2}^n)^2 + (\alpha_{j-1/2}^n)^2)A_j^n - \frac{1}{2}(\alpha_{j+1/2}^n)^2 A_{j+1}^n\cos(\theta_{j+1}^n-\theta_j^n) \\
& \qquad -\frac{1}{2}(\alpha_{j-1/2}^n)^2 A_{j-1}^n\cos(\theta_j^n-\theta_{j-1}^n)\Big) - \frac{1}{2}(\beta_j^n)^2 A_j^n \qquad (7.33b)
\end{aligned}$$

Note also that applying summation over index j with periodic boundary conditions $A_0 = A_J$, $\theta_0 = \theta_J$, $A_{J+1} = A_1$ and $\theta_{J+1} = \theta_1$ we can write the following discrete conservation

$$0 = \sum_{j=1}^{J}\Big(\frac{1}{2}A_j^{n+1}A_j^n\sin(\theta_j^{n+1}-\theta_j^n) - \frac{1}{2}A_j^{n-1}A_j^n\sin(\theta_j^n-\theta_j^{n-1})\Big)$$

which can also be written as

$$\mathscr{A}^{n+1} - \mathscr{A}^n = 0 \tag{7.34}$$

with

$$\mathscr{A}^n = \sum_{j=1}^{J} \frac{1}{2} A_j^{n-1} A_j^n \sin(\theta_j^n - \theta_j^{n-1}). \tag{7.35}$$

The proof follows immediately from the fact that

$$\begin{aligned}
&\sum_{j=1}^{J} (\alpha_{j+1/2}^n)^2 A_j^n A_{j+1}^n \sin(\theta_{j+1}^n - \theta_j^n) \\
&= \Big(\sum_{j=1}^{J-1} (\alpha_{j+1/2}^n)^2 A_j^n A_{j+1}^n \sin(\theta_{j+1}^n - \theta_j^n) \Big) + (\alpha_{J+1/2}^n)^2 A_J^n A_{J+1}^n \sin(\theta_{J+1}^n - \theta_J^n)
\end{aligned}$$

and

$$\begin{aligned}
&\sum_{j=1}^{J} (\alpha_{j-1/2}^n)^2 A_j^n A_{j-1}^n \sin(\theta_j^n - \theta_{j-1}^n) = \sum_{j=0}^{J-1} (\alpha_{j+1/2}^n)^2 A_j^n A_{j+1}^n \sin(\theta_{j+1}^n - \theta_j^n) \\
&= (\alpha_{1/2}^n)^2 A_0^n A_1^n \sin(\theta_1^n - \theta_0^n) + \Big(\sum_{j=1}^{J-1} (\alpha_{j+1/2}^n)^2 A_j^n A_{j+1}^n \sin(\theta_{j+1}^n - \theta_j^n) \Big)
\end{aligned}$$

We are now at the position to numerically test conservation of total wave action. Time evolution of (7.35) can be easily computed from solutions of (7.31), since the amplitude is obtained from (7.32) and the phase is computed as

$$\theta^n = \arctan \frac{u^n}{(u_{\theta_0})^n} - \theta_0. \tag{7.36}$$

Figure 7.2 shows time evolution of a normalized error of the total wave action computed using equation (7.35). Normalized error R_{WA} is obtained as

$$R_{WA} = \frac{\mathscr{A}^n}{\mathscr{A}^0} - 1.$$

We note that, after initial burst in the error, magnitude of R_{WA} becomes of order 10^{-2}. Simulation parameters were identical as these used to obtain Figure 7.1.

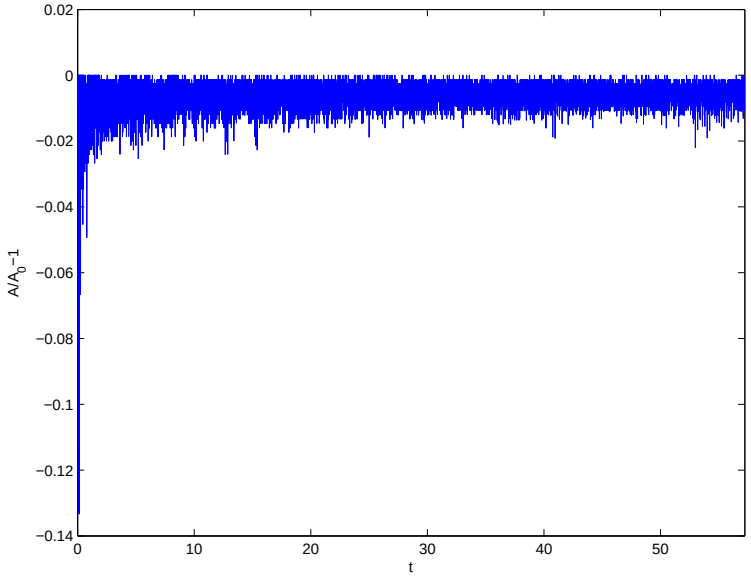

Figure 7.2: Normalized error in the total wave action for slowly varying solutions of the Klein–Gordon equation.

APPENDIX A: IMPLICIT RUNGE – KUTTA METHODS

A.1 Basic theorems

Let $\Omega \subset \mathbb{R}^D$ be a domain (open, simply connected set), and $I \subset \mathbb{R}$ be an interval and consider a system of ODEs of the form

$$\frac{\mathrm{d}\mathbf{x}}{\mathrm{d}t} = \mathbf{f}(t, \mathbf{x})$$

where $\mathbf{x} \in \mathbb{R}^D$ and $\mathbf{f} : \Omega \times I \to \mathbb{R}^D$.

Definition 7 *Let $b_i, a_{ij} \in \mathbb{R}$, $i, j \in \{1, \ldots, s\}$ and*

$$c_i = \sum_{j=1}^{s} a_{ij}.$$

The following iterative process

$$\mathbf{k}_i = \mathbf{f}(t_0 + hc_i, \mathbf{x}_0 + h\sum_{j=1}^{s} a_{ij}\mathbf{k}_j) \tag{A.1a}$$

$$\mathbf{x}_1 = \mathbf{x}_0 + h\sum_{i=1}^{s} b_i\mathbf{k}_i, \tag{A.1b}$$

$n \in N \subset \mathbb{N}$ is called s–stage implicit Runge–Kutta method.

Theorem 13 *Let $\mathbf{f} \in \mathcal{C}(I \times \mathbb{R}^n)$ and assume there exists L such that*

$$\forall_{t\in I}\ \forall_{\mathbf{x},\mathbf{y}\in\mathbb{R}^n} \quad |\mathbf{f}(t, \mathbf{x}) - \mathbf{f}(t, \mathbf{y})| \leq L|\mathbf{x} - \mathbf{y}|.$$

If

$$h < \frac{1}{L \cdot \max_i \sum_j |a_{ij}|}$$

then there exists unique solution to (A.1a), which can be obtained by iteration

$$\mathbf{k}_i^{[0]} = \mathbf{x}_0$$

$$\mathbf{k}_i^{[\nu+1]} = \mathbf{f}(t_0 + hc_i, \mathbf{x}_0 + h\sum_{j=1}^{s} a_{ij}\mathbf{k}_j^{[\nu]}).$$

Moreover, if $\mathbf{f}(t, \mathbf{x}) \in \mathcal{C}^p(\mathbb{R} \times \mathbb{R}^n)$ then $k_i = k_i(h) \in \mathcal{C}^p(\mathbb{R})$.

Proof can be found in [15].

The above functional iteration for $\mathbf{k}_i$ can be modified in the following way. First of all we can redefine IRK method as

$$\mathbf{Y}_i = \mathbf{x}_0 + h\sum_{j=1}^{s} a_{ij}\mathbf{f}(t_0 + hc_j, \mathbf{Y}_j) \tag{A.2a}$$

$$\mathbf{x}_1 = \mathbf{x}_0 + h\sum_{i=1}^{s} b_i\mathbf{f}(t_0 + hc_i, \mathbf{Y}_i), \tag{A.2b}$$

We can now introduce $\mathbf{g}_i = \mathbf{Y}_i - \mathbf{x}_0$. Clearly $\mathbf{Y}_i = \mathbf{g}_i + \mathbf{x}_0$ and we may consider

$$\begin{aligned} \mathbf{g}_i^{[0]} &= 0 \\ \mathbf{g}_i^{[\nu+1]} &= h\sum_{j=1}^{s} a_{ij}\mathbf{f}(t_0 + hc_i, \mathbf{x}_0 + \mathbf{g}_j^{[\nu]}). \end{aligned}$$

For stopping conditions see [32] p.64.

A.2 Gaussian Collocation

Theorem 14 *Let q be a nontrivial polynomial of degree $n+1$ such that*

$$\forall_{k\in\{0,\ldots,n\}} \quad \int_a^b x^k q(x)\mathrm{d}x = 0.$$

Let c_i be such a points that $q(c_i) = 0$ for every $i \in \{0,\ldots,n\}$, then for every polynomial p of degree at most $2n+1$

$$\int_a^b p(x)\mathrm{d}x = \sum_{i=0}^{n} A_i p(c_i),$$

with

$$A_i = \int_a^b \ell_i(x)\mathrm{d}x,$$

where $\ell_i(x)$ denotes i–th Lagrange polynomial.

$$\ell_i(x) = \prod_{j=0, j\neq i}^{n} \frac{x - c_j}{c_i - c_j}$$

Lemma 5 *The set*

$$SL = \left\{ \frac{\mathrm{d}^s}{\mathrm{d}x^s}(x^s(1-x)^s) \right\}_{s\in\mathbb{N}_0}$$

of all shifted Legendre polynomials form an orthogonal set with respect to the weight function $w(x) \equiv 1$ on $[0, 1]$.

Gaussian nodes on $[t_0, t_1]$ are given by $\{t_0 + h \cdot c_i\}_i$, with c_i being zeros of i–th shifted Legendre polynomial. Note that

$$\int_{t_0}^{t_1} g(x)\mathrm{d}x = (t_1 - t_0) \int_0^1 g(\xi)\mathrm{d}\xi$$

where $\xi = \frac{x-t_0}{t_1-t_0}$. Inverse variable transformation is given by $x = t_0 + h\xi$ with $h = t_1 - t_0$.

Definition 8 *Let $c_1, \ldots, c_n \in \mathbb{R}$ are distinct (and usually $0 < c_i < 1$). The collocation polynomial $u(t)$ is a polynomial of degree at most s satisfying*

$$\begin{aligned} u(t_0) &= x_0 \\ \dot{u}(t_0 + h \cdot c_i) &= f(t_0 + h \cdot c_i, u(t_0 + h \cdot c_i)) \end{aligned} \tag{A.3}$$

the numerical solution of the collocation method is defined to be

$$x_1 = u(t_0 + h)$$

Theorem 15 (Gillou & Soulé (1969), Wright (1970)) *Collocation method defined by (A.3) is equivalent to the s–stage Runge–Kutta method (A.1a), (A.1b) with coefficients*

$$a_{ij} = \int_0^{c_i} \ell_j(x)\mathrm{d}x; \qquad b_i = \int_0^1 \ell_i(x)\mathrm{d}x,$$

where $\ell_i(x)$ is the $(i-1)$–st Lagrange polynomial.

PROOF: Let $g(x) = \dot{u}(t_0 + hx)$. Lagrange interpolation formula for g with nodes $c_1, \ldots, c_s$ is given by

$$g(x) = \sum_{i=1}^{s} g(c_i)\ell_i(x)$$

Therefore

$$\dot{u}(t_0 + hx) = \sum_{i=1}^{s} \dot{u}(t_0 + h \cdot c_i)\ell_i(x)$$

Define $k_i = \dot{u}(t_0 + h \cdot c_i)$ to get

$$\dot{u}(t_0 + hx) = \sum_{i=1}^{s} k_i \ell_i(x) \tag{A.4}$$

Integrating (A.4) with respect to x from 0 to c_i we have

$$\begin{aligned} \int_0^{c_i} \dot{u}(t_0 + hx)\mathrm{d}x &= \sum_{j=1}^{s} k_j \int_0^{c_i} \ell_j(x)\mathrm{d}x \\ u(t_0 + h \cdot c_i) - u(t_0) &= \sum_{j=1}^{s} k_j a_{ij} \end{aligned}$$

so

$$k_i = x_0 + \sum_{j=1}^{s} a_{ij} k_j$$

Similarly, integrating (A.4) from 0 to 1, we get

$$\begin{aligned}\int_0^1 \dot{u}(t_0+hx)\mathrm{d}x &= \sum_{j=1}^{s} k_j \int_0^1 \ell_j(x)\mathrm{d}x \\ u(t_0+h)-u(t_0) &= \sum_{i=1}^{s} k_i b_i\end{aligned}$$

Finally we have

$$x_1 = x_0 + \sum_{i=1}^{s} b_i k_i$$

■

A.2.1 Example

Consider 2–nd shifted Legendre polynomial

$$\begin{aligned}\frac{\mathrm{d}^2}{\mathrm{d}x^2}(x^2(1-x)^2) &= \frac{\mathrm{d}}{\mathrm{d}x}(2x(1-x)^2+2x^2(1-x)) = 2(x-1)^2+8x(x-1)+2x^2 \\ &= (x-1)(2x+2+8x)+2x^2 = 2(6x^2-6x+1)\end{aligned}$$

We can easily find that Gaussian nodes (zeros of the above polynomial) are

$$c_i = \frac{1}{2} \pm \frac{\sqrt{3}}{6}$$

Further examples of application of Theorem 15 can be found in Tables A.1 and A.2.

A.3 Symplecticness Conditions for R–K methods

Consider a Hamiltonian system of ODEs

$$\begin{aligned}\dot{p}_i &= -\frac{\partial H}{\partial q_i} \\ \dot{q}_i &= \frac{\partial H}{\partial p_i}\end{aligned}$$

or in another words

$$\begin{aligned}\dot{\mathbf{p}} &= \mathbf{f}(t, \mathbf{p}, \mathbf{q}) \\ \dot{\mathbf{q}} &= \mathbf{g}(t, \mathbf{p}, \mathbf{q})\end{aligned}$$

with $\mathbf{p} = [p_1, \ldots, p_J]^T$ and $\mathbf{q} = [q_1, \ldots, q_J]^T$. The Runge–Kutta method for the above system can be written as

$$\mathbf{P}_i = \mathbf{p}_0 + h \sum_{j=1}^{s} a_{ij} \mathbf{f}(t_0 + hc_j, \mathbf{P}_j, \mathbf{Q}_j) \tag{A.5a}$$

$$\mathbf{Q}_i = \mathbf{q}_0 + h \sum_{j=1}^{s} a_{ij} \mathbf{g}(t_0 + hc_j, \mathbf{P}_j, \mathbf{Q}_j) \tag{A.5b}$$

$$\mathbf{p}_1 = \mathbf{p}_0 + h \sum_{i=1}^{s} b_i \mathbf{f}(t_0 + hc_i, \mathbf{P}_i, \mathbf{Q}_i) \tag{A.5c}$$

$$\mathbf{q}_1 = \mathbf{q}_0 + h \sum_{i=1}^{s} b_i \mathbf{g}(t_0 + hc_i, \mathbf{P}_i, \mathbf{Q}_i) \tag{A.5d}$$

Let's introduce some notation. Let

$$\begin{aligned}\mathbf{k}_j &= \mathbf{f}(t_0 + hc_j, \mathbf{P}_j, \mathbf{Q}_j) \\ \mathbf{l}_j &= \mathbf{g}(t_0 + hc_j, \mathbf{P}_j, \mathbf{Q}_j)\end{aligned}$$

are the "slopes" at the intermediate stges.

Theorem 16 (Sanz–Serna, Suris, Lasagne (1988)) *If $M \in \mathcal{M}_{s\times s}(\mathbb{R})$ with entries*

$$m_{ij} = b_i a_{ij} + b_j a_{ji} - b_i b_j, \qquad i, j \in \{1, \ldots, s\}$$

satisfies

$$M = 0$$

then Runge–Kutta method is symplectic.

PROOF: Differentiating (total derivative) (A.5c) and (A.5d) we have

$$\begin{aligned} \mathrm{d}\mathbf{p}_1 &= \mathrm{d}\mathbf{p}_0 + h\sum_{i=1}^{s} b_i \mathrm{d}\mathbf{k}_i \\ \mathrm{d}\mathbf{q}_1 &= \mathrm{d}\mathbf{q}_0 + h\sum_{i=1}^{s} b_i \mathrm{d}\mathbf{l}_i \end{aligned}$$

Differentating (A.5a) and (A.5b) we have

$$\mathrm{d}\mathbf{P}_i = \mathrm{d}\mathbf{p}_0 + h\sum_{j=1}^{s} a_{ij} \mathrm{d}\mathbf{k}_i \tag{A.6a}$$

$$\mathrm{d}\mathbf{Q}_i = \mathrm{d}\mathbf{q}_0 + h\sum_{j=1}^{s} a_{ij} \mathrm{d}\mathbf{l}_i \tag{A.6b}$$

No we have

$$\begin{aligned} \mathrm{d}\mathbf{p}_1 \wedge \mathrm{d}\mathbf{q}_1 &= \mathrm{d}\mathbf{p}_0 \wedge \mathrm{d}\mathbf{q}_0 + h\sum_{j=1}^{s} b_i \mathrm{d}\mathbf{p}_0 \wedge \mathrm{d}\mathbf{l}_i + h\sum_{j=1}^{s} b_i \mathrm{d}\mathbf{k}_i \wedge \mathrm{d}\mathbf{q}_0 \\ &\quad + h^2 \left(\sum_{i=1}^{s} b_i \mathrm{d}\mathbf{k}_i\right) \wedge \left(\sum_{i=1}^{s} b_i \mathrm{d}\mathbf{l}_i\right) \end{aligned}$$

note that

$$\begin{aligned} \left(\sum_{i=1}^{s} b_i \mathrm{d}\mathbf{k}_i\right) \wedge \left(\sum_{i=1}^{s} b_i \mathrm{d}\mathbf{l}_i\right) &= \sum_{j=1}^{s} b_j \left(\sum_{i=1}^{s} b_i \mathrm{d}\mathbf{k}_i\right) \wedge \mathrm{d}\mathbf{l}_j \\ &= \sum_{j=1}^{s} b_j \left(\sum_{i=1}^{s} b_i \mathrm{d}\mathbf{k}_i \wedge \mathrm{d}\mathbf{l}_j\right) = \sum_{i=1}^{s}\sum_{j=1}^{s} b_i b_j \mathrm{d}\mathbf{k}_i \wedge \mathrm{d}\mathbf{l}_j \end{aligned}$$

Moreover, form (A.6a) and (A.6b) we have

$$\begin{aligned} \mathrm{d}\mathbf{P}_i \wedge \mathrm{d}\mathbf{l}_i &= \mathrm{d}\mathbf{p}_0 \wedge \mathrm{d}\mathbf{l}_i + h\sum_{j=1}^{s} a_{ij} \mathrm{d}\mathbf{k}_j \wedge \mathrm{d}\mathbf{l}_i \\ \mathrm{d}\mathbf{k}_i \wedge \mathrm{d}\mathbf{Q}_i &= \mathrm{d}\mathbf{k}_i \wedge \mathrm{d}\mathbf{q}_0 + h\sum_{j=1}^{s} a_{ij} \mathrm{d}\mathbf{k}_i \wedge \mathrm{d}\mathbf{l}_j \end{aligned}$$

and from here

$$\begin{aligned} \mathrm{d}\mathbf{p}_0 \wedge \mathrm{d}\mathbf{l}_i + \mathrm{d}\mathbf{k}_i \wedge \mathrm{d}\mathbf{q}_0 &= \mathrm{d}\mathbf{P}_i \wedge \mathrm{d}\mathbf{l}_i + \mathrm{d}\mathbf{k}_i \wedge \mathrm{d}\mathbf{Q}_i \\ &\quad - h\left(\sum_{j=1}^{s} a_{ij} \mathrm{d}\mathbf{k}_j \wedge \mathrm{d}\mathbf{l}_i + \sum_{i=1}^{s} a_{ji} \mathrm{d}\mathbf{k}_j \wedge \mathrm{d}\mathbf{l}_i\right), \end{aligned}$$

as well as,

$$\begin{aligned}
\mathrm{d}\mathbf{p}_1 \wedge \mathrm{d}\mathbf{q}_1 &= \mathrm{d}\mathbf{p}_0 \wedge \mathrm{d}\mathbf{q}_0 + h\sum_{i=1}^{s} b_i(\mathrm{d}\mathbf{p}_0 \wedge \mathrm{d}\mathbf{l}_i + \mathrm{d}\mathbf{k}_i \wedge \mathrm{d}\mathbf{q}_0) \\
&\quad + h^2 \sum_{i=1}^{s}\sum_{j=1}^{s} b_i b_j \mathrm{d}\mathbf{k}_i \wedge \mathrm{d}\mathbf{l}_j \\
&= \mathrm{d}\mathbf{p}_0 \wedge \mathrm{d}\mathbf{q}_0 + h\sum_{i=1}^{s} b_i(\mathrm{d}\mathbf{P}_i \wedge \mathrm{d}\mathbf{l}_i + \mathrm{d}\mathbf{k}_i \wedge \mathrm{d}\mathbf{Q}_i) \\
&\quad - h^2 \sum_{i=1}^{s} b_i \left(\sum_{j=1}^{s} a_{ij} \mathrm{d}\mathbf{k}_j \wedge \mathrm{d}\mathbf{l}_i + \sum_{j=1}^{s} a_{ij} \mathrm{d}\mathbf{k}_i \wedge \mathrm{d}\mathbf{l}_j \right) \\
&\quad + h^2 \sum_{i=1}^{s}\sum_{j=1}^{s} b_i b_j \mathrm{d}\mathbf{k}_i \wedge \mathrm{d}\mathbf{l}_j .
\end{aligned}$$

We can rename summation indices, to obtain that

$$\begin{aligned}
&\sum_{i=1}^{s} b_i \left(\sum_{j=1}^{s} a_{ij} \mathrm{d}\mathbf{k}_j \wedge \mathrm{d}\mathbf{l}_i + \sum_{j=1}^{s} a_{ij} \mathrm{d}\mathbf{k}_i \wedge \mathrm{d}\mathbf{l}_j \right) = \sum_{i=1}^{s} b_i \sum_{j=1}^{s} a_{ij} \mathrm{d}\mathbf{k}_j \wedge \mathrm{d}\mathbf{l}_i \\
&\quad + \sum_{i=1}^{s} b_i \sum_{j=1}^{s} a_{ij} \mathrm{d}\mathbf{k}_i \wedge \mathrm{d}\mathbf{l}_j = \sum_{j=1}^{s} b_j \sum_{i=1}^{s} a_{ji} \mathrm{d}\mathbf{k}_i \wedge \mathrm{d}\mathbf{l}_j + \sum_{i=1}^{s} b_i \sum_{j=1}^{s} a_{ij} \mathrm{d}\mathbf{k}_i \wedge \mathrm{d}\mathbf{l}_j \\
&= \sum_{i=1}^{s}\sum_{j=1}^{s} (b_j a_{ji} + b_i a_{ij}) \mathrm{d}\mathbf{k}_i \wedge \mathrm{d}\mathbf{l}_j
\end{aligned}$$

Now we have

$$\begin{aligned}
\mathrm{d}\mathbf{p}_1 \wedge \mathrm{d}\mathbf{q}_1 &= \mathrm{d}\mathbf{p}_0 \wedge \mathrm{d}\mathbf{q}_0 + h\sum_{i=1}^{s} b_i(\mathrm{d}\mathbf{P}_i \wedge \mathrm{d}\mathbf{l}_i + \mathrm{d}\mathbf{k}_i \wedge \mathrm{d}\mathbf{Q}_i) \\
&\quad - h^2 \sum_{i=1}^{s}\sum_{j=1}^{s} (b_i a_{ij} + b_j a_{ji} - b_i b_j) \mathrm{d}\mathbf{k}_i \wedge \mathrm{d}\mathbf{l}_j
\end{aligned}$$

The theorem will be proved if we can show, that

$$\sum_{j=1}^{s} b_i(\mathrm{d}\mathbf{P}_i \wedge \mathrm{d}\mathbf{l}_i + \mathrm{d}\mathbf{k}_i \wedge \mathrm{d}\mathbf{Q}_i) = 0$$

Following [32] p. 73, it is enough to show that

$$\forall_i \qquad \mathrm{d}\mathbf{P}_i \wedge \mathrm{d}\mathbf{l}_i + \mathrm{d}\mathbf{k}_i \wedge \mathrm{d}\mathbf{Q}_i = 0$$

dropping index i that indicates number of stage (the following computations are independent of i) we may write

$$\mathrm{d}\mathbf{P} \wedge \mathrm{d}\mathbf{l} + \mathrm{d}\mathbf{k} \wedge \mathrm{d}\mathbf{Q} = \sum_{\nu=1}^{d} \mathrm{d}P_\nu \wedge \mathrm{d}l_\nu + \mathrm{d}k_\nu \wedge \mathrm{d}Q_\nu$$

where summation is over the elements of the respective vectors. Moreover, note that

$$\begin{aligned}
\mathrm{d}k_\nu &= \sum_{\mu=1}^{d} \frac{\partial f_\nu}{\partial p_\mu}\mathrm{d}P_\mu + \frac{\partial f_\nu}{\partial q_\mu}\mathrm{d}Q_\mu \\
\mathrm{d}l_\nu &= \sum_{\mu=1}^{d} \frac{\partial g_\nu}{\partial p_\mu}\mathrm{d}P_\mu + \frac{\partial g_\nu}{\partial q_\mu}\mathrm{d}Q_\mu
\end{aligned}$$

Thus

$$\begin{aligned}
\mathrm{d}P_\nu \wedge \mathrm{d}l_\nu &= \sum_{\mu=1}^{d} \frac{\partial g_\nu}{\partial p_\mu}\mathrm{d}P_\nu \wedge \mathrm{d}P_\mu + \frac{\partial g_\nu}{\partial q_\mu}\mathrm{d}P_\nu \wedge \mathrm{d}Q_\mu \\
\mathrm{d}k_\nu \wedge \mathrm{d}Q_\nu &= \sum_{\mu=1}^{d} \frac{\partial f_\nu}{\partial p_\mu}\mathrm{d}P_\mu \wedge \mathrm{d}Q_\nu + \frac{\partial f_\nu}{\partial q_\mu}\mathrm{d}Q_\mu \wedge \mathrm{d}Q_\nu
\end{aligned}$$

Notice that

$$\begin{aligned}
\frac{\partial f_\nu}{\partial p_\mu} &= \frac{\partial}{\partial p_\mu}\left(-\frac{\partial H}{\partial q_\nu}\right) & \frac{\partial f_\nu}{\partial q_\mu} &= \frac{\partial}{\partial q_\mu}\left(-\frac{\partial H}{\partial q_\nu}\right) \\
\frac{\partial g_\nu}{\partial p_\mu} &= \frac{\partial}{\partial p_\mu}\left(\frac{\partial H}{\partial p_\nu}\right) & \frac{\partial g_\nu}{\partial q_\mu} &= \frac{\partial}{\partial q_\mu}\left(\frac{\partial H}{\partial p_\nu}\right)
\end{aligned}$$

Finally we have that

$$\begin{aligned}
\mathrm{d}\mathbf{P} \wedge \mathrm{d}\mathbf{l} + \mathrm{d}\mathbf{k} \wedge \mathrm{d}\mathbf{Q} &= \sum_{\nu=1}^{d}\sum_{\mu=1}^{d}\left(-\frac{\partial^2 H}{\partial p_\mu \partial q_\nu}\mathrm{d}P_\mu \wedge \mathrm{d}Q_\nu - \frac{\partial^2 H}{\partial q_\mu \partial q_\nu}\mathrm{d}Q_\mu \wedge \mathrm{d}Q_\nu\right) \\
&\qquad + \sum_{\nu=1}^{d}\sum_{\mu=1}^{d}\left(\frac{\partial^2 H}{\partial p_\mu \partial p_\nu}\mathrm{d}P_\nu \wedge \mathrm{d}P_\mu + \frac{\partial^2 H}{\partial q_\mu \partial p_\nu}\mathrm{d}P_\nu \wedge \mathrm{d}Q_\nu\right) \\
&= \sum_{\nu=1}^{d}\sum_{\mu=1}^{d} -\frac{\partial^2 H}{\partial p_\mu \partial q_\nu}\mathrm{d}P_\mu \wedge \mathrm{d}Q_\nu + \sum_{\mu=1}^{d}\sum_{\nu=1}^{d}\frac{\partial^2 H}{\partial q_\nu \partial p_\mu}\mathrm{d}P_\mu \wedge \mathrm{d}Q_\nu \\
&\qquad - \sum_{\nu=1}^{d}\sum_{\mu=1}^{d}\frac{\partial^2 H}{\partial q_\mu \partial q_\nu}\mathrm{d}Q_\mu \wedge \mathrm{d}Q_\nu + \sum_{\nu=1}^{d}\sum_{\mu=1}^{d}\frac{\partial^2 H}{\partial p_\mu \partial p_\nu}\mathrm{d}P_\nu \wedge \mathrm{d}P_\mu \\
&= 0
\end{aligned}$$

by skew–symmerticity of wedge product (assuming that we can change the order of differentiation in partial derivatives). ■

Remark 2 *Necessary conditions require the RK method to be irreducible. See [32] Thm. 6.6 p.84.*

Remark 3 *If* $\forall_{i \leq j} \quad a_{ij} = 0$ *(explicit RK) and* $M = 0$*, then we must have*

$$m_{ii} = b_i a_{ii} + b_j a_{ii} - b_i b_i = b_i^2 = 0$$

thus $\forall_i b_i = 0$*.*

This means no consistent ($\sum_{i=1}^{s} b_i = 1$) explicit RK method is symplectic.

Theorem 17 *The implicit s–stage Gauss (collocation) method of order* $2s$ *(Kuntzman & Butcher) is symplectic for all* s*.*

Proof: By the fundamental theorem of calculus

$$\begin{aligned} \int_{t_n}^{t_{n+1}} \frac{\mathrm{d}}{\mathrm{d}t}(\mathrm{d}p \wedge \mathrm{d}q)(t)\mathrm{d}t &= (\mathrm{d}p \wedge \mathrm{d}q)(t)\Big|_{t_n}^{t_{n+1}} = \mathrm{d}p(t_{n+1}) \wedge \mathrm{d}q(t_{n+1}) - \mathrm{d}p(t_n) \wedge \mathrm{d}q(t_n) \\ &= \mathrm{d}p^{n+1} \wedge \mathrm{d}q^{n+1} - \mathrm{d}p^n \wedge \mathrm{d}q^n \end{aligned}$$

where we are assuming $p(t)$ and $q(t)$ are polynomials of degree at most s. Moreover, by exterior differentiation formula, we have that

$$\frac{\mathrm{d}}{\mathrm{d}t}(\mathrm{d}p \wedge \mathrm{d}q) = \mathrm{d}\dot{p} \wedge \mathrm{d}q + \mathrm{d}p \wedge \mathrm{d}\dot{q}$$

now, since

$$\deg\left(\frac{\mathrm{d}}{\mathrm{d}t}(\mathrm{d}p \wedge \mathrm{d}q)\right) \leq 2s - 1$$

we have, by the Gaussian quadrature theorem, that there exist c_i, $i \in \{1, \ldots, s\}$ such that

$$\begin{aligned}\int_{t_n}^{t_{n+1}} \frac{\mathrm{d}}{\mathrm{d}t}(\mathrm{d}p \wedge \mathrm{d}q)(t)\mathrm{d}t &= (t_{n+1} - t_n) \int_0^1 \frac{\mathrm{d}}{\mathrm{d}t}(\mathrm{d}p \wedge \mathrm{d}q)(t)\mathrm{d}t \\ &= h \sum_{i=1}^{s} b_i \left.\frac{\mathrm{d}}{\mathrm{d}t}(\mathrm{d}p \wedge \mathrm{d}q)(t)\right|_{t=t_n+hc_i}\end{aligned}$$

Notice that $p(t_n + hc_i) = P_i$, $q(t_n + hc_i) = Q_i$ and $\dot{p}(t_n + hc_i) = k_i$, $\dot{q}(t_n + hc_i) = l_i$, therefore $\mathrm{d}p = \mathrm{d}P_i$, $\mathrm{d}q = \mathrm{d}Q_i$, $\mathrm{d}\dot{p} = \mathrm{d}k_i$, $\mathrm{d}\dot{q} = \mathrm{d}l_i$ which means, that for every i

$$\left.\frac{\mathrm{d}}{\mathrm{d}t}(\mathrm{d}p \wedge \mathrm{d}q)(t)\right|_{t=t_n+hc_i} = \left.\mathrm{d}\dot{p} \wedge \mathrm{d}q + \mathrm{d}p \wedge \mathrm{d}\dot{q}\right|_{t=t_n+hc_i} = \mathrm{d}k_i \wedge \mathrm{d}Q_i + \mathrm{d}P_i \wedge \mathrm{d}l_i = 0$$

and proves symplecticness. ■

Table A.1: Tableau for the Hammer & Hollingsworth method of order 4.

$$\begin{array}{c|cc} \frac{1}{2} - \frac{\sqrt{3}}{6} & \frac{1}{4} & \frac{1}{4} - \frac{\sqrt{3}}{6} \\ \frac{1}{2} + \frac{\sqrt{3}}{6} & \frac{1}{4} + \frac{\sqrt{3}}{6} & \frac{1}{4} \\ \hline & \frac{1}{2} & \frac{1}{2} \end{array}$$

Table A.2: Tableau for the Kuntzmann & Butcher method of order 8.

$\frac{1}{2}-\omega_2$	ω_1	$\omega_1'-\omega_3+\omega_4'$	$\omega_1'-\omega_3-\omega_4'$	$\omega_1-\omega_5$
$\frac{1}{2}-\omega_2'$	$\omega_1-\omega_3'+\omega_4$	ω_1'	$\omega_1'-\omega_5'$	$\omega_1-\omega_3'-\omega_4$
$\frac{1}{2}+\omega_2'$	$\omega_1+\omega_3'+\omega_4$	$\omega_1'+\omega_5'$	ω_1'	$\omega_1+\omega_3'-\omega_4$
$\frac{1}{2}+\omega_2$	$\omega_1+\omega_5$	$\omega_1'+\omega_3+\omega_4'$	$\omega_1'+\omega_3-\omega_4'$	ω_1
	$2\omega_1$	$2\omega_1'$	$2\omega_1'$	$2\omega_1$

$$\omega_1 = \frac{1}{8} - \frac{\sqrt{30}}{144} \qquad \omega_1' = \frac{1}{8} + \frac{\sqrt{30}}{144}$$

$$\omega_2 = \frac{1}{2}\sqrt{\frac{15+2\sqrt{30}}{35}} \qquad \omega_2' = \frac{1}{2}\sqrt{\frac{15-2\sqrt{30}}{35}}$$

$$\omega_3 = \omega_2\left(\frac{1}{6} + \frac{\sqrt{30}}{24}\right) \qquad \omega_3' = \omega_2'\left(\frac{1}{6} - \frac{\sqrt{30}}{24}\right)$$

$$\omega_4 = \omega_2\left(\frac{1}{21} + \frac{5\sqrt{30}}{168}\right) \qquad \omega_4' = \omega_2'\left(\frac{1}{21} - \frac{5\sqrt{30}}{168}\right)$$

$$\omega_5 = \omega_2 - 2\omega_3 \qquad \omega_5' = \omega_2' - 2\omega_3'$$

APPENDIX B: SOLITONS FOR THE SINE–GORDON EQUATION

In numerical analysis, and especially for new schemes, it is always advisable to conduct a preliminary test of algorithms and codes on known solutions for which one can obtain analytic formulas. In this project, we have chosen some classical solutions to the benchmark equation – solitons. Following [4] we have that, for $-\infty < x < \infty$, the following are the soliton solutions to the sine–Gordon equation:

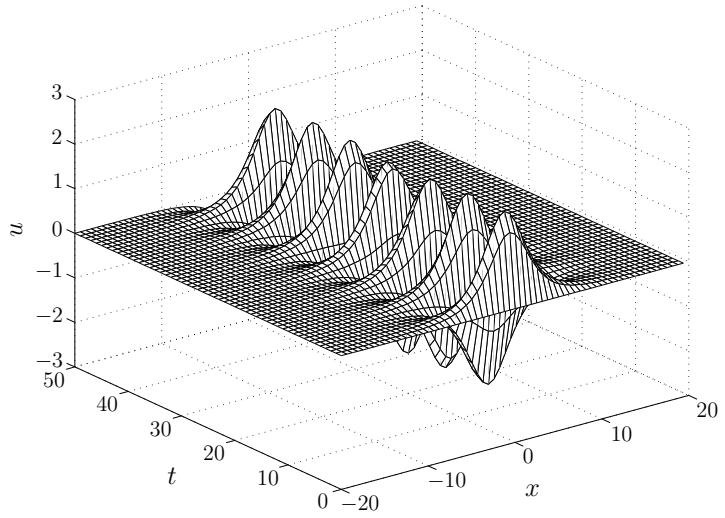

Figure B.1: Breather. Analytic solution for $\sqrt{1-\tilde{\gamma}^2} = 1/2$.

Breather is a stationary, periodic wave of the form

$$u(t,x) = 4\arctan\Big(\frac{\sqrt{1-\tilde{\gamma}^2}}{\tilde{\gamma}}\sin(\tilde{\gamma}t)\ \mathrm{sech}(x\sqrt{1-\tilde{\gamma}^2})\Big)$$

One finds the following initial conditions correspond to the breather soliton

$$u(0,x) = 0, \qquad u_t(0,x) = 4\sqrt{1-\tilde{\gamma}^2}\ \mathrm{sech}(x\sqrt{1-\tilde{\gamma}^2}).$$

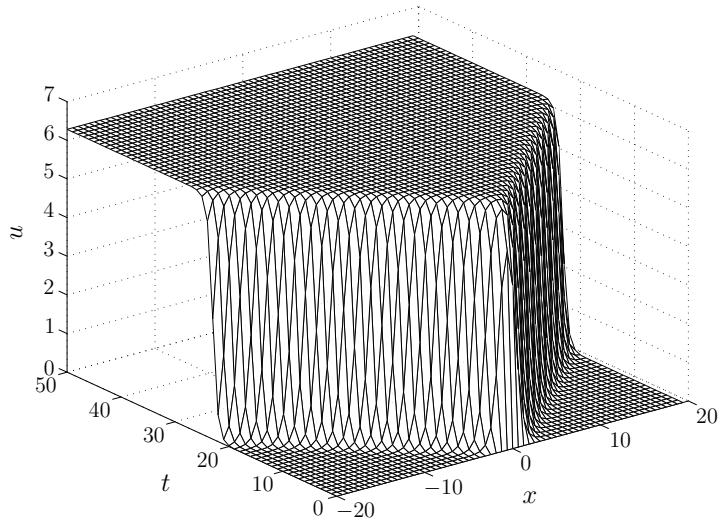

Figure B.2: Kink–antikink. Analytic solution for $1/\sqrt{1-\tilde{\gamma}^2} = 2$.

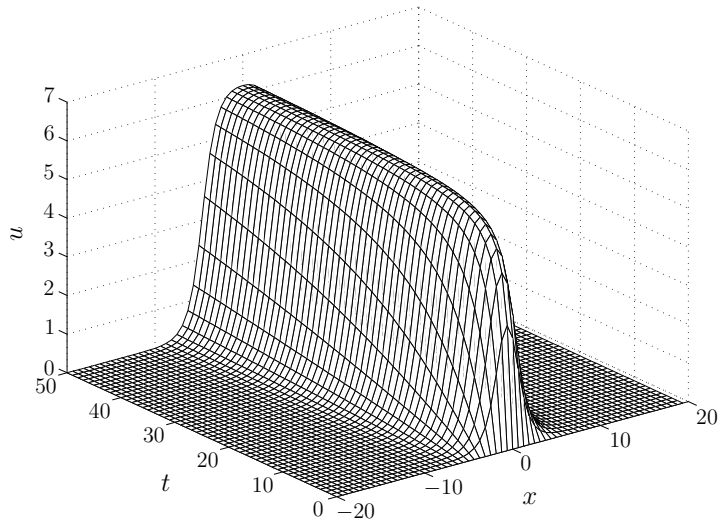

Figure B.3: Limiting case between breather and kink – antikink. Analytic solution.

Kink–antikink is a superposition of two, traveling in opposite directions, waves of the form

$$u(t,x) = 4\arctan\Big(\frac{1}{\tilde{\gamma}}\sinh\Big(\frac{\tilde{\gamma}t}{\sqrt{1-\tilde{\gamma}^2}}\Big)\ \mathrm{sech}\Big(\frac{x}{\sqrt{1-\tilde{\gamma}^2}}\Big)\Big)$$

One can find that

$$u(0,x) = 0, \qquad u_t(0,x) = \frac{4}{\sqrt{1-\tilde{\gamma}^2}}\ \mathrm{sech}(\frac{x}{\sqrt{1-\tilde{\gamma}^2}}).$$

Double pole solution is a limit as $\tilde{\gamma} \to 0$ in the above cases

$$u(x,t) = 4\arctan(t \cdot \mathrm{sech}(x)),$$

i.e. by the following initial conditions:

$$u(x,0) = 0, \qquad u_t(0,x) = 4\ \mathrm{sech}(x)$$

LIST OF REFERENCES

[1] M. J. Ablowitz, B. M. Herbst, and C. M. Schober. Numerical simulation of quasi–periodic solutions of the sine–Gordon Equation. *Physica D*, 87:37–47, 1995.

[2] M. J. Ablowitz, B. M. Herbst, and C. M. Schober. On the Numerical Solution of the Sine–Gordon Equation. I. Integrable Discretizations and Homoclinic Manifolds. *Journal of Computational Physics*, 126:299–314, 1996.

[3] M. J. Ablowitz, B. M. Herbst, and C. M. Schober. On the Numerical Solution of the Sine–Gordon Equation. II. Performance of Numerical Schemes. *Journal of Computational Physics*, 131:354–367, 1997.

[4] Mark J. Ablowitz and Harvey Segur. *Solitons and the Inverse Scattering Transform*. SIAM, Philadelphia, 1981.

[5] Vladimir. I. Arnold. *Mathematical Methods of Classical Mechanics*. Springer–Verlag, New York, 1989.

[6] Uri M. Ascher and Robert I. McLachlan. Multisymplectic box scheme and the Kortweg–de Vries equation. *Applied Numerical Mathematics*, 48:255–269, 2004.

[7] T. J. Bridges and G. Derks. Unstable eigenvalues and the linearization about solitary waves and fronts with symmetry. *R. Soc. Lond. Proc. Ser. A Math. Phys. Eng. Sci.*, 455(1987):2427–2469, 1999.

[8] Thomas J. Bridges. A Geometric Formulation of the Conservation of Wave Action and Its Implications for Signature and the Classification of Instabilities. *Proc.R.Soc.Lond.A.*, 453:1365–1395, 1997.

[9] Thomas J. Bridges and Sebastian Reich. Multi-symplectic spectral discretizations for the Zakharov–Kuznetsov and shallow water equations. *Physica D*, 152-153:491–504, 2001.

[10] T.J. Bridges. Multisymplectic structures and wave propagation. *Math. Proc. Cambridge Philos. Soc.*, 121:147–190, 1997.

[11] T.J. Bridges and S. Reich. Multi–symplectic integrators: numerical schemes for Hamiltonian PDEs that conserve symplecticity. *Physics Letters A*, 284:184–193, 2001.

[12] Richard L. Burden and J. Douglas Faires. *Numerical Analysis*. Brooks/Cole. Thompson Learning, Pacific Grove, seventh edition, 2001.

[13] Jason Frank. Conservation of wave action under multisymplectic discretizations. *J.Phys.A:Math.Gen.*, 39:5479–5493, 2006.

[14] Jason Frank, Brian E. Moore, and Sebastian Reich. Linear PDEs and Numerical Methods that Preserve a Multisymplectic Conservation Law. *SIAM J. Sci. Comput.*, 28:260–277, 2006.

[15] E. Hairer, S. P. Nørset, and G. Wanner. *Solving Ordinary Differential Equations I. Nonstiff Problems*. Springer–Verlag, Berlin, 1993.

[16] E. Hairer and G. Wanner. *Solving Ordinary Differential Equations II. Stiff and Differential–Algebraic Problems*. Springer–Verlag, Berlin, 1996.

[17] Ernst Hairer, Christian Lubich, and Gerhard Wanner. *Geometric Numerical Integration. Structure–Preserving Algorithms for Ordinary Differential Equations*. Springer, Berlin, 2002.

[18] W. D. Hayes. Conservation of action and modal wave action. *Proc.Roy.Soc.Lond.A.*, 320:187–208, 1970.

[19] F. Q. Hu, M. Y. Hussaini, and J. L. Manthey. Low–Dissipation and Low–Dispersion Runge–Kutta Schemes for Computational Acoustics. *Journal of Computational Physics*, 124:177–191, 1996.

[20] Eugene Isaacson and Herbert Bishop Keller. *Analysis of the Numerical Methods*. John Wiley & Sons, Inc., New York, London, Sydney, 1966.

[21] A. L. Islas, D. A. Karpeev, and C. M. Schober. Geometric Integrators for the Nonlinear Schorödinger Equation. *Journal of COmputational Physics*, 173:116–148, 2001.

[22] A. L. Islas and C. M. Schober. On the preservation of phase space structure under multisymplectic discretization. *Journal of Computational Physics*, 197 no. 2:585–609, 2004.

[23] A. L. Islas and C. M. Schober. Backward error analysis for multisymplectic discretizations of Hamiltonian PDEs. *Mathematic and Computers in Simulation*, 69:290–303, 2005.

[24] Alvaro L. Islas. *Multi-Symplectic Integrators for Nonlinear Wave Equations*. PhD thesis, Old Dominion University, 2003.

[25] Herbert B. Keller. A New Difference Scheme for Parabolic Problems. In *Numerical Solution of Partial Differential Equations – II. SYNSPADE 1970*, pages 327–350, New York, 1971. Academic Press.

[26] J. E. Marsden, G. P. Patrick, and S. Shkoller. Multi-symplectic geometry, variational integrators, and nonlinear PDEs. *Communications in Mathematical Physics*, 199:351–395, 1999.

[27] Robert I. McLachlan, Matthew Perlmutter, and G. R. W. Quispel. On the Nonlinear Stability of Symplectic Integrators. *BIT Numerical Mathematics*, 44:99–117, 2004.

[28] Brian E. Moore. *A Modified Equations Approach for Multi-Symplectic Integration Methods*. PhD thesis, University of Surrey, 2003.

[29] Brian E. Moore and Sebastian Reich. Backward error analysis for multi–symplectic integration methods. *Numer.Math.*, 95:625–652, 2003.

[30] A. Portillo and J. M. Sanz-Serna. Lack of dissipativity is not symplecticness. *BIT*, 35:269–276, 1995.

[31] A. Preissmann. Propagation des intumescensec dans les canaux et rivieres. *First Conagress of the French Assoc. for Computation*, pages 433 – 442, 1961.

[32] J. M. Sanz-Serna and M. P. Calvo. *Numerical Hamiltonian Problems*. Chapman & Hall, London, 1994.

[33] Michael Spivak. *Calculus on manifolds: a modern approach to classical theorems of advanced calculus.* Addison–Wesley, Reading, 1993.

[34] A. M. Stuart and A. R. Humphries. *Dynamical Systems and Numerical Analysis*. Cambridge University Press, New York, 1996.

[35] Jian-Qiang Sun and Meng-Zhao Qin. Multi-symplectic methods for the coupled 1D nonlinear Schrdinger system. *Computer Physics Communication*, 155:221–235, 2003.

[36] James William Thomas. *Numerical Partial Differential Equations. Volume 1: Finite Difference Methods*. Springer, New York, 1995.

[37] Lloyd N. Trefethen. Group Velocities in Finite Difference Schemes. *SIAM Review*, 24:113–136, 1982.

[38] Yu Shun Wang and Meng-Zhao Qin. Multisymplectic schemes for the nonlinear Klein-Gordon equation. *Math. Comput. Modelling*, 36:963–977, 2002.

[39] Yu Shun Wang, Bin Wang, and Meng-Zhao Qin. Numerical implementation of the multisymplectic Preissman scheme and its equivalent schemes. *Appl. Math. Comput.*, 149:299–326, 2004.

[40] G. B. Whitham. *Linear and Nonlinear Waves*. John Wiley & Sons, New York, 1974.

[41] Ping Fu Zhao and Meng Zhao Qin. Multisymplectic geometry and multisymplectic Priessmann scheme for the KdV equation. *J. Phys. A: Math. Gen.*, 33:3613–3626, 2000.